Quantum Mechanical Continuum Solvation Models

Jacopo Tomasi,*,† Benedetta Mennucci,† and Roberto Cammi‡

Dipartimento di Chimica e Chimica Industriale, Università di Pisa, Via Risorgimento 35, 56126 Pisa, Italy, and Dipartimento di Chimica, Università di Parma, Viale delle Scienze 17/A, 43100 Parma, Italy

Contents

* Author to whom correspondence should be addressed (e-mail tomasi@dcci.unipi.it).
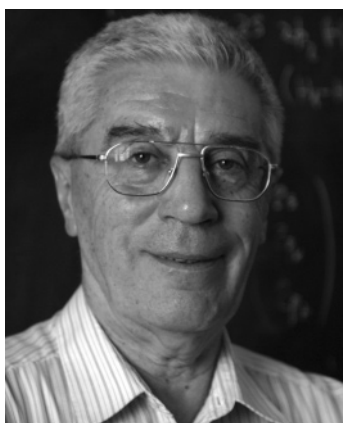† Università di Pisa.
‡ Università di Parma.

1. Introduction

1.1. Generalities about This Review

This review on continuum solvation models has been preceded in *Chemical Reviews* by others addressing the same subject. They are due to Tomasi and Persico[1] (published in 1994), Cramer and Truhlar[2] (published in 1999), and Luque and Orozco[3] (published in 2000). These three reviews on the same topic in a journal covering all of the aspects of chemical research indicate the interest this topic has for a sizable portion of the chemical community.

Liquid solutions play in fact a fundamental role in chemistry, and this role has been amply acknowledged by *Chemical Reviews* since its very beginning. In the abundant number of reviews addressing different aspects of chemistry in the liquid phase, the number of those centered on the theoretical and computational aspects of the study of liquid systems has considerably increased in the past two decades. This reflects the increasing importance of computational approaches in chemistry, an aspect of the evolution of scientific research chemistry shares with physics, biology, engineering, geology, and all of the other branches of sciences, an evolution that is ultimately due to the widespread availability of efficient computers.

Computers have permitted the activation of many approaches in sciences that were dormant, or limited in their applications to the level of simple model, for the lack of appropriate computational tools; an example in chemistry is given by the activation of methods based on quantum mechanics for the description of isolated molecules, which have now

Benedetta Mennucci was born in Lucca, Italy, in 1969. She received her "Laurea" degree in chemistry in 1994 and her Ph.D. degree in chemistry from the University of Pisa in 1998 discussing a thesis on theoretical models and computational applications of molecular phenomena involving the environment effect. In the same year she became assistant professor in the Department of Chemistry of the University of Pisa. Since 2002 she has been associate professor of physical chemistry at the same institution. Her research interests focus on the elaboration of theoretical models and computational algorithms to describe molecular systems in condensed phase with particular attention to molecular properties and time-dependent phenomena. She has authored, or coauthored, more than 80 publications.
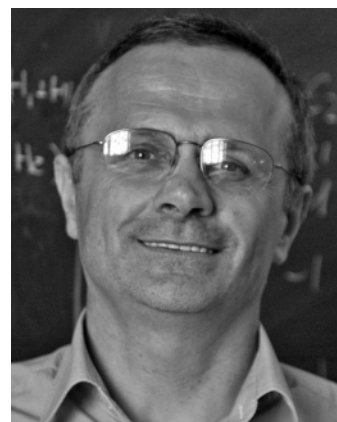
Roberto Cammi was born in Busseto, Italy, in 1954. In 1979, he was awarded the degree of "Dottore in Chimica" at the University of Parma, discussing a thesis in theoretical chemistry. Since 1983 he has been a researcher with the Institute of Physical Chemistry of the University f Parma. In 2000 he became an associate professor in the Department of General and Inorganic Chemistry, Analytical Chemistry, Physical Chemistry of the University of Parma, and since 2002 he has been a full professor of theoretical chemistry of the University of Parma. He teaches physical chemistry and theoretical chemistry. His research field is theoretical and computational chemistry, mainly the developments and applications of quantum mechanical continuum methods to the study of solvent effects on molecular processes and properties. He has published more than 80 research papers and 8 chapters of collective books.

Jacopo Tomasi received his "Laurea" degree in chemistry in 1958 (University of Pisa) discussing a thesis on the theoretical determination of the intensities of vibrational overtones. Since 1980 he has been a full professor of physical chemistry at the University of Pisa. His research interests cover several aspects of theoretical chemistry with propensity to the formulation and elaboration of models based on ab initio quantum chemistry with a special emphasis on the exploitation of the interpretation of the phenomenon to obtain computational codes of easy use. This approach has been applied to molecular interactions, chemical reaction mechanisms, photochemical processes, solvent effects on molecular response properties, and other related subjects. He has authored, or coauthored, more than 300 scientific papers.

reached the degree of accuracy in the description of molecular structures that chemists require.

Computers have also completely modified the ways of doing theoretical and computational studies of liquid systems, permitting the introduction of new approaches, new concepts, and new ideas. The most important innovations in this field are related to the use of computer simulations that directly, or indirectly, are the basis of our present understanding of condensed systems. Simulations, initiated about 50 years ago, have greatly evolved in the past 20 years and proceed now in covering all of the fields in which condensed matter occurs. One aspect of this evolution

is of direct interest here: the merging of simulations with quantum mechanical (QM) descriptions of molecular structures. This merging, in progress for several years, has to overcome computational difficulties, due to the computationally quite intensive numerical procedures.

At this point of our rapid exposition we may introduce what we consider the second important innovation in the field of condensed systems made possible by the use of computers: the continuum models.

Continuum models were introduced more than a century ago, in very simplified versions, giving results of remarkable importance using computational instruments no more complex than a slide rule. These models have been used for more than 50 years, and in more detailed versions they are still in use, but the essential step, opening new perspectives for the study of solvent effects, has been its merging with the QM descriptions of molecules. Continuum models are in fact the ideal conceptual framework to describe solvent effects within the QM approach, as will be shown in section 2.

This merging was initiated more than 30 years ago by a small group of young researchers (Claverie, Rivail, Tapia, and Tomasi), working in French and Italian laboratories gravitating around Paris and Pisa. The initial stimulus was provided by the recognition that the QM description of the electrostatic potential generated by the charge distribution of a molecule could represent a valid analytic and interpretative tool to study intermolecular interactions.[4]

The perspectives opened by these findings were elaborated independently by the various laboratories and led to the alternative theoretical methods[5−8] that have been examined in detail in the preceding reviews. In the present one we abandon the historical perspective used in the first review[1] to present and analyze the methodological issues of the "modern" continuum solvation theory (modern in the sense that is essentially based on the QM description of the solute). The second[2] and third[3] reviews give considerable space to methodological issues, but also pay attention to applications: detailed surveys on the results on chemical equilibria, spectra, and dynamics of reactions are reported in the former, whereas, in the latter, attention is centered on biomolecular systems, also including in the survey simulation methods with QM description of the solute.

The present review is again centered on methodological issues, with a perspective focused on the most recent developments. The body of the theory developed in the first 30 years of the "modern" solvation methods is summarized, giving emphasis to those aspects that are at the basis of all recent extensions and reformulations of the model. Some among them were already considered in the previous reviews, reflecting, however, the provisional state of the methodological elaboration, now accomplished; others correspond to new entries in the theory.

With respect to all of the previous reviews, here a much larger space is devoted to three aspects that we consider to be important in future applications of continuum models, namely, their use in studying phenomena involving time-dependent solvation, on the one hand, and molecular properties, on the other hand, and their coupling to discrete models. None of these three aspects is completely new, but only in the past few years have they acquired the necessary reliability and accuracy. In parallel, the extension of the continuum models to treat complex condensed phases (ionic solutions, anisotropic dielectrics, heterogeneous systems, liquid−gas and liquid−liquid interfaces, crystals, etc.) has allowed us to enlarge the range of possible applications and to consider phenomena and processes that have been until now the exclusive property of computer simulations. The table of contents should give a schematic but clear proof of this new trend in continuum solvation methods.

Throughout the text, we have also added remarks indicating other extensions of the continuum methods that are still in their infancy, or even in an earlier stage, but which seem to us to be possible and to promise a satisfactory reward. A further analysis of future prospects will be done in the last section dedicated to comments and conclusions.

We conclude this introductory section with a short exposition of the main features of the computational strategies based on continuum distributions. The considerations reported here do not claim originality, but we find it convenient to report them to put continuum approaches in the right perspective.

1.2. Generalities about Continuum, Focused, and Layered Models

A continuum model in computational molecular sciences can be defined as a model in which a number of the degrees of freedom of the constituent particles (a large number, indeed) are described in a continuous way, usually by means of a distribution function.

Continuum distributions are a very general concept. In the standard quantum mechanical description of a single molecule M based on the usual Born−Oppenheimer (BO) approximation (the cornerstone of the theory for molecular sciences), the electronic wave function, Ψ, is expressed in terms of one-electron wave functions, each depending on the coordinates of a single electron. From this single-particle description a one-particle distribution function is easily derived with an averaging operation, the one-electron density function $\rho_M^e(r)$, which contains a good deal of the information conveyed by the original wave function. According to the formal theory, one-electron $\rho_M^e(r)$ and two-electron $\rho_M^e(r,r')$ density functions collect all of the elements necessary for a full exploitation of the QM basic calculation. Electron density functions are endowed with many important formal properties, as they represent the kernels of integral equations from which properties can be derived. Actually, the formalism of the density matrices is completely equivalent to (and even more powerful than) the usual wave function formalism.

By tradition, in basic quantum mechanics, the emphasis is not placed on the continuity of the electronic distribution but on the discreteness of the molecular assembly. We are here interested in the

application of the concept of continuum distribution functions to particles of different physical types, including electrons and nuclei as well. Continuum distributions of this kind, often supplemented by constraints acknowledging the existence of molecules, are of current use in statistical mechanics and find application, among others, in computer simulations of pure liquids and solutions.

The continuum models we shall consider are intermediate between the two extremes we have mentioned, a continuum model for the electrons of a single molecule, and a continuum model for a very large assembly of molecules. Our aim is to preserve the accuracy of the former in describing details of the molecule and the capability of the latter in strongly reducing the degrees of freedom of large molecular assemblies. To do it in a proper way it is convenient to introduce another concept, that of focused models.

In focused models the interest of the enquirer falls on a limited portion of the whole system. There is a large variety of systems and properties for which the focusing approach can be profitably exploited. A single solute molecule in a dilute solution is just an example, but many other examples can be cited: a defect inside a crystal, the superficial layer of a solid, the active part of an enzyme, the proton or energy transfer unit in a larger molecular assembly, and even a single component of a homogeneous system, as a single molecule in a pure liquid or in a gas.

The definition of a focused model presents specific problems for each different case; here, we shall highlight some general aspects referring to solvation models.

The concept of a focused model can be translated into a simple formal expression. The whole system is partitioned into two parts, which we define as the focused part F, and the remainder R. The Hamiltonian of the whole system may be written as

$$\hat{H}^{FR}(\mathbf{f,r}) = \hat{H}^F(\mathbf{f}) + \hat{H}^R(\mathbf{r}) + \hat{H}^{int}(\mathbf{f,r}) \qquad (1)$$

where $\{\mathbf{f}\}$ and $\{\mathbf{r}\}$ indicate the degrees of freedom of the F and R parts, respectively. To focus the model means to treat the F part at a more detailed level than the R part. An important parameter in focused models is the number of the degrees of freedom of R, which are not explicitly taken into account. In continuum solvation models the whole $\hat{H}^R(\mathbf{r})$ term is eliminated and the total Hamiltonian is reduced to an effective Hamiltonian (EH) for the solute in the form

$$\hat{H}^{FR}_{eff}(\mathbf{f,r}) = \hat{H}^F(\mathbf{f}) + \hat{H}^{int}(\mathbf{f,r}) \qquad (2)$$

In this approach in fact, there is no need to get a detailed description of the solvent, it being sufficient to have a good description of the interaction. This is surely a considerable simplification. In other solvation models $\hat{H}^R(\mathbf{r})$ is maintained and the focusing simplifications involve the number of freedom degrees within R. This is the case of the QM/MM methods, in which a limited number of the degrees of freedom for each molecule within R are explicitly considered, at least those involving position and orientation.

The elimination of the solvent Hamiltonian is not sufficient to eliminate the $\{\mathbf{r}\}$ degrees of freedom, because they appear in the interaction Hamiltonian. An almost complete elimination can be obtained by introducing an appropriate solvent response function that we indicate here with the symbol $Q(\vec{r},\vec{r}')$, where $(\vec{r})$ is no more the whole set of solvent coordinates, but just a position vector.

$$\hat{H}^{FR}_{eff}(\mathbf{f,r}) = \hat{H}^F(\mathbf{f}) + \hat{V}^{int}[\mathbf{f}, Q(\vec{r},\vec{r}')] \qquad (3)$$

The solvent response function is similar in nature to the response functions that can be derived from the electron density function in the case of a molecule. The density here is that of the liquid system R, and $Q(\vec{r},\vec{r}')$ is, in the more complete formulations, expressed as a sum of separate terms each related to a different component of the solute−solvent interaction.

We shall be more specific in section 3, but for this general discussion we limit ourselves to the electrostatic contribution. The response to be considered in this term is that with respect to an external electric field. As in classical electrostatics, the polarization function $\vec{P}$ of the medium is proportional to the external field

$$\vec{P} = \frac{\epsilon - 1}{4\pi} \vec{E} \qquad (4)$$

and the kernel response function we have to use is related to the function we have here introduced, namely, the permittivity, ϵ. The expression of ϵ may be quite simple, just a numerical constant, or more complex, according to the model one uses. This point will be fully developed in section 4, in which also the basic assumption of linearity introduced with eq 4 will be reconsidered, but here it is sufficient to remark that the whole set of solvent coordinates $\{\mathbf{r}\}$ is replaced by a function depending only on one parameter, the position vector $\vec{r}$, or by a couple of position vectors $(\vec{r},\vec{r}')$.

The quest for the accuracy requested in chemical applications of such focused models suggests the introduction of additional features, different according to the various cases. Within this very large variety of proposals a third concept emerges for its generality, the concept of layering.

Layering can be considered a generalization of focusing. The material components of the models are partitioned into several parts, or layers, because often these parts are defined in a concentric way, encircling the part of main interest. Each layer is defined at a given level of accuracy in the description of the material system and with the appropriate reduction of the degrees of freedom. There is a large variety of layering; for simplicity, they can be denoted with abbreviations, as, for example, QM/QM/Cont or QM/MM/Cont for a couple of three-layer models in which the inner layer is treated at a given QM level, the second at a lower QM or at a molecular mechanics level, respectively, and the third using a continuum approach. Some type of layering involving as chain end the continuum description will be examined in section 7.

2. Methodological Outlines of the Basic QM Continuum Model

This topic has been amply presented in the first review on the argument,[1] complemented in a second review,[2] and summarized in many other places, including textbooks.[9-12] For this reason we shall avoid an exhaustive presentation of the whole literature but shall only present the essential elements. By contrast, we shall pay attention to all topics that have been the subject of discussion in recent years and/or new methodological proposals.

In the next subsection we shall identify the characteristics that define the "basic QM continuum model": these in principle completely determine the model we are interested in but, in practice, they are seldom completely fulfilled. We thus suggest that the reader consider this definition more as a "literal" convenience and a research of formal clarity rather than as a description of a real methodology. As a matter of fact, in this section, there will be many occasions to present models that do not completely conform to this basic definition.

2.1. Definition of the Basic Model

For the basic QM model we intend models with the following characteristics:

(1) The solute is described at a homogeneous QM level. Computational procedures based on semiclassical or classical descriptions of the solute will be considered as derivation of the basic QM model and briefly examined. Other models based on layered QM descriptions of the solute (including layers treated all at a QM level or mixed QM and semiclassical descriptions) will be considered in section 7.

(2) The solute−solvent interactions are limited to those of electrostatic origin. Other interaction terms exist, and they must be taken into account to have a well-balanced description of solvent effects (see section 3). This point has to be emphasized; our choice of paying attention first to the electrostatic model, dictated by convenience of exposition, should not lead the reader to the false conclusion that only electrostatics is important in solvation. Often the opposite happens, and in addition some problems arising in treating the electrostatic term are greatly alleviated by the consideration of other solute−solvent interactions.

(3) The model system is a very dilute solution. In other words, it is composed of a single solute molecule (including, when convenient, some solvent molecules, the whole being treated as a supermolecule at a homogeneous QM level) immersed in an infinite solvent reservoir.

(4) The solvent is isotropic, at equilibrium at a given temperature (and pressure). Possible extensions beyond the isotropic approximation will be considered mainly to show new potentialities of the most recent solvation models.

(5) Only the electronic ground state of the solute will be considered. Extensions to other electronic states will be considered in section 5.

(6) No dynamic effects will be considered in the basic model. Under the heading of "dynamic effects" there is so large a variety of important phenomena that it would require a separate review. The main aspects of these phenomena will be considered in sections 5 and 6.

Once we have better defined what we intend with the expression "basic QM continuum model", we can consider some of its essential elements.

2.2. Cavity

The cavity is a basic concept in all continuum models. The model in fact is composed of a molecule (or a few molecules), the solute, put into a void cavity within a continuous dielectric medium mimicking the solvent. The shape and size of the cavity are differently defined in the various versions of the continuum models. As a general rule, a cavity should have a physical meaning, such as that introduced by Onsager,[13] and not be only a mathematical artifice as often happens in other descriptions of solvent effects. On the physical meaning of Onsager's cavity, see also the comments in ref 14. In particular, the cavity should exclude the solvent and contain within its boundaries the largest possible part of the solute charge distribution. Here, for convenience, we divide it into its electronic and nuclear components:

$$\rho_M = \rho_M^e + \rho_M^n \tag{5}$$

Obviously these requirements are in contrast with the description of the whole system given by any QM level. The electronic charge distribution of an isolated molecule, in fact, persists to infinity. In a condensed medium the conditions on ρ_M^e at large distances are less well-defined, but in any case there will be an overlap with the charge distribution of the medium, not explicitly described in continuum models but existing in real systems.

In continuum models, much attention has been paid to the portion of solute electronic charge outside the boundaries of the cavity; the terms "escaped charge" and "outlying charge" are often used to indicate this portion of charge. This subject will be treated in due detail in section 2.4.3. Here we will assume that all of the solute charge distribution lies inside the cavity, which in turn has a size not so large as to be in contrast with the solvent exclusion postulate.

The optimal size of the cavity has thus been a subject of debate, and several definitions have been proposed. The adopted definitions are the result of a tradeoff between conflicting physical requirements.

The shape of the cavity has also been the object of many proposals. It is universally accepted that the cavity shape should reproduce as well as possible the molecular shape. Cavities not respecting this condition may lead to deformations in the charge distribution after solvent polarization, with large unrealistic effects on the results, especially for properties. Here, once again, there is a tradeoff between computational exigencies and the desire for better accuracy.

Computations are far simpler and faster when simple shapes are used, such as spheres and ellipsoids, but molecules are often far from having a spherical or ellipsoidal shape.

Quantum mechanical calculations of the molecular surface can give a direct ab initio definition of the cavity.

An accurate description is based on the use of a surface of constant electronic density (isodensity surface).[15,16] Within this framework, one only needs to specify the isodensity level (typically in the range of 0.0004–0.001 au) and, thus, the cavity will be derived uniquely from the real electronic environment. Such a cavity has been inserted into the Gaussian computational package.[17] Even if not largely used at the moment, in our opinion the isodensity surface represents an important definition of the cavity for continuum solvation models, and it will surely receive a renewed interest in the coming years.

A different technique pioneered by Amovilli and McWeeny[18] and employed by Bentley and others[19–24] is based on the calculation of the interaction energy between a given molecule and an atomic probe (typically a rare gas atom, from He to Ar) placed at opportune positions in the outer molecular space. From these calculations, a set of three-dimensional isoenergy surfaces is determined. As described below, two kinds of surfaces are of interest, the solvent-accessible surface (SAS) and the solvent-excluded surface (SES). The first can be directly obtained from these calculations, whereas the second requires an additional assumption. According to Bentley the SES can be determined from the electronic density function of the system constituted by the molecule and the probe. Following the AIM topological analysis,[25] the points of the surfaces can be identified in the saddle points [also indicated as $(3,-1)$ bond critical points] of such a function.

A connection of these surfaces with the thermal energy kT allows one to define T-dependent molecular surfaces and cavities. This technique is of potential interest as a benchmark for solvent calculations far from the ambient temperature; otherwise, the approach is too costly to be used in standard applications.

The generally adopted compromise between analytical but too simple and realistic but computationally expensive cavities is based on the definition of the cavity as an interlocked superposition of atomic spheres with radii near the van der Waals (vdW) values (the precise determination of such radii is related to the problem of the cavity size).

The most used set of vdW radii in the chemical literature is that defined by Bondi[26] ($\sim$5000 citations in the past 15 years). This set was confirmed as the recommended one some years ago,[27] after the examination of a quite large number of intermolecular contact distances drawn from the Cambridge Structural Database. For his tabulation, Bondi used data of other origin, mainly addressing the hard volume of the molecule and not the non-covalent contact distances. The data drawn from 28403 crystal structures confirm the Bondi values, with the only exception the hydrogen radius, set by Bondi at 1.2 Å, which is probably too high by 0.1 Å.

Another tabulation of vdW radii frequently used is that of Pauling,[28] available in many tabulations of

physicochemical data, for example, in the *CRC Handbook*.[29]

A third set of values has been inserted in the latest versions of the Gaussian package.[17] It is drawn from the compilation of data for the universal force field (UFF),[30] and it covers the whole periodic table including groups not present in Bondi's or Pauling's tabulations.

The presence of small differences in the radius values currently used in continuum models and the consequent effect on the solvation energies deserve a few words of comment. Chemical applications of molecular calculations generally involve trends, in particular, comparisons of selected properties computed for different systems. In the particular case of solvation calculations, the comparisons may involve properties of different solutes in the same solvent or of the same solute in different solvents. Absolute values at a precision comparable with that of very accurate experiments are rarely requested. For this reason, the selection of the hard radii to use among the recommended tabulations seems to us to be not a critical issue. Attention has to be paid, however, to maintain a coherent choice for all of the calculations and to avoid comparisons among results obtained with different definitions of the radii.

Molecules often have an irregular shape, and the occurrence of small portions of space on their periphery where solvent molecules cannot penetrate is not a rare event. This intuitive consideration is at the basis of two definitions, those of solvent-excluding and solvent-accessible surface (SES and SAS, respectively).[31–35]

Both introduce in the surface (and in the volume) changes to the vdW description related, in a different way, to the finite size of the solvent molecules. In both cases, the solvent molecule is reduced to a sphere, with a volume equal to the vdW volume (other definitions of this radius have been used, but this seems to be the most consistent definition). The positions assumed by the center of a solvent sphere rolling on the vdW surface of the solute define the SA surface, that is, the surface enclosing the volume in which the solvent center cannot enter. The same sphere used as a contact probe on the solute surface defines the SE surface, that is, the surface enclosing the volume in which the whole solvent molecule cannot penetrate (see Figure 1 for a schematic drawing of the different surfaces for the same molecule).

In the literature, the SES is also called "smooth molecular surface" or "Connolly surface", due to Connolly's fundamental work in this field. Indeed, the SE surface developed by Connolly[32,36] can be considered to be the prototype for the computational study of molecular surfaces. Visualization and handling of surfaces have given origin to a very large literature that cannot be reviewed here. The reader can be referred to Connolly's website[37] for a clear and concise review accompanied by a sizable selection of references, adjourned at 1996 (430 entries). Connolly's surfaces have been applied to a very large variety of problems, and they have been also used to compute
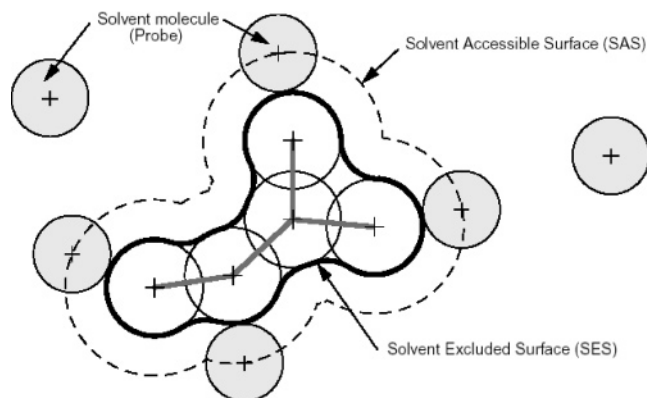
Figure 1. Solvent accessible surface (SAS) traced out by the center of the probe representing a solvent molecule. The solvent excluded surface (SES) is the topological boundary of the union of all possible probes that do not overlap with the molecule.

solvation energies with continuum models (generally of classical type). The probe sphere divides the whole SE surface into pieces of three types: the convex patches in which the probe touches just one sphere of the hard vdW shape function, the toroidal patches in which the probe touches two spheres of the hard body, and the concave (reentrant) patches in which the probe touches three spheres. An analytical expression for this shape, easy to visualize on a computer screen with a probe provided with markers that put dots on the SES, has been given by Connolly within a short time from the first computer implementation of the procedure (1979−1981), and it is still in use, with some modifications. The analytical description presents some problems, among which we mention a few: the intersection between a torus and a sphere is described by a fourth-degree equation, for which the available solvers are not sufficiently robust; the SES may present singularities and cusps; these last problems are better treated with methods developed by Gogonea[38,39] and by Sanner et al.[40] The latter have developed a computational code called MSMS,[41] standing for Michael Sanner's Molecular Surface, which has received much attention, especially among biochemistry-oriented computational researchers. MSMS computes, for a given set of spheres and a probe radius, the reduced surface and the analytical model of the SES. The MSMS algorithm can also compute a triangulation of the SES with a user-specified density of vertices.

Besides Connolly's SES, another SES-like surface will be reviewed here as of current use in QM continuum solvation methods. This alternative surface is defined following a different strategy, originally conceived in Pisa around 1984 and finalized in 1986 by Pascual-Ahuir in his Ph.D. research.[42] This surface-building method, known as GEPOL,[43−45] is based on a sequential examination of the distance among the centers of each couple of hard vdW spheres and comparison of it with the solvent probe diameter. If the distance is such that the probe cannot pass between the two hard spheres, additional spheres are added. Only three cases are possible, each corresponding to a different positioning of the additional spheres, each with the opportune radius (position and radius are determined with very simple

and unambiguous algorithms). The whole set of spheres, the original vdW spheres and those added, is subjected again to the same sequential examination to add new spheres (second-generation spheres) to smooth the surface. The program originally written by Pascual-Ahuir introduced thresholds and options to keep the number of additional spheres within reasonable limits.

In GEPOL, the final surface is thus always the result of the intersections of spheres and, in this sense, it can be seen as an alternative version of the SES made only by convex elements.

To complete the section on the definition of the cavity, we recall an alternative strategy to define van der Waals, solvent-accessible, and solvent-excluding molecular surfaces originally formulated by Pomelli in 1994−1995 for his master's thesis. This strategy, known as DEFPOL,[46,47] has never been implemented in publicly released computational packages, and thus its use is limited to a few examples; however, it still presents some aspects that are worth recalling here. The basic strategy consists of progressive deformations of a regular polyhedron with the desired number of faces (triangular faces are preferred) inscribed into a sphere centered on the mass center of the molecule. The sphere is deformed into the inertial ellipsoid and enlarged so as to have all shape functions of the molecule within it. Each vertex of the deformed polyhedron is then shifted along the line connecting the initial position with the origin of the coordinates until it lies on the surface of the shape function. The polyhedron is so transformed into a corrugated polyhedron topologically equivalent to the initial one, with faces still defined as triangles. The center of each triangle is then shifted along the axis orthogonal to the triangle until it touches the surface of the shape function. In the cases in which the volume of the tetrahedron defined by the three displaced vertices and the displaced center is larger than a given threshold, the procedure is repeated on a finer scale on the three triangles having as vertices the original ones and the triangle center. The final step consists of transforming the flat triangles into spherical triangles, each with the appropriate curvature.

2.3. Solution of the Electrostatic Problem

The physics of the electrostatic solute−solvent interaction is simple. The charge distribution ρ_M of the solute, inside the cavity, polarizes the dielectric continuum, which in turn polarizes the solute charge distribution. This definition of the interaction corresponds to a self-consistent process, which is numerically solved following an iterative procedure. It is important to remark that the corresponding interaction potential is the one we shall put in the Hamiltonian of the model. As this potential depends on the final value of ρ_M reached at the end of this iterative procedure, the Hamiltonian (previously introduced as an "effective Hamiltonian", see eq 2) thus turns out to be nonlinear. This formal aspect has important consequences in the elaboration and use of the computational results (see section 2.4.4).

Reference is often made to the *solvent reaction field* for the interaction potential obtained with continuum models (and also with models using explicit solvent molecules). This label has a historical reason, being related to Onsager's seminal paper[13] in which the solute was reduced to a polarizable point dipole and the electrostatic interaction between a polarizable medium and a dipole was expressed in terms of an electrostatic field, having its origin in the polarization of the dielectric. Actually, it is now convenient to speak in terms of the *solvent reaction potential*, because a potential is the term we have to introduce into the Hamiltonian.

The basic model requires the solution of a classical electrostatic problem (Poisson problem) nested within a QM framework. Let us consider the electrostatic problem first.

In our simplified model the general Poisson equation

$$-\vec{\nabla}[\epsilon(\vec{r})\nabla\vec{V}(\vec{r})] = 4\pi\rho_M(\vec{r}) \quad (6)$$

can be noticeably simplified to

$$-\nabla^2 V(\vec{r}) = 4\pi\rho_M(\vec{r}) \quad \text{within } C \quad (7)$$

$$-\epsilon\nabla^2 V(\vec{r}) = 0 \quad \text{outside } C \quad (8)$$

where C is the portion of space occupied by the cavity, ϵ is the dielectric function (actually a constant) within the medium, and V is the sum of the electrostatic potential V_M generated by the charge distribution ρ_M and the reaction potential V_R generated by the polarization of the dielectric medium:

$$V(\vec{r}) = V_M(\vec{r}) + V_R(\vec{r}) \quad (9)$$

Observe that we have assumed that all of the real charges of the system (i.e., those described by ρ_M) are inside the cavity. Therefore, this basic model is not formally valid for liquid systems having real charges in the bulk of the medium (as is the case, e.g., for ionic solutions) and also, strictly speaking, for the tiny portions of the electronic component of ρ_M lying out of the cavity (see section 2.4.4 for a more detailed analysis). It is valid, however, for systems having a multiplicity of cavities $C_1, C_2, ..., C_n$, each containing a different $\rho_{M1}, \rho_{M2}, ..., \rho_{Mn}$ charge distribution.

Equations 7 and 8 are accompanied by two sets of boundary conditions, the first at infinity and the second on the cavity surface. At infinity we have

$$\lim_{r\to\infty} rV(r) = \alpha \quad (10)$$

$$\lim_{r\to\infty} r^2 V(r) = \beta \quad (11)$$

with finite values for α and β. These conditions ensure the harmonic behavior of the solution, but they have to be specifically invoked in just one of the methods we shall examine; in the other cases, the conditions are automatically satisfied in our basic QM model.

More important, from a practical point of view, are the conditions at the cavity surface Γ. They may be concisely expressed as jump conditions:

$$[V] = 0 \quad \text{on } \Gamma \quad (12)$$

$$[\partial V] = 0 \quad \text{on } \Gamma \quad (13)$$

The jump condition (eq 12) expresses the continuity of the potential across the surface, a condition valid also for other dielectric systems we shall consider later:

$$[V] = V_{in} - V_{out} = 0 \quad (14)$$

The second jump condition (eq 13) involves the discontinuity of the component of the field (expressed as a gradient of V) that is perpendicular to the cavity surface. In the model we are considering here, a cavity with a dielectric constant equal to 1 and an external medium with ϵ (a finite value >1), this condition leads to

$$[\partial V] = \left(\frac{\partial V}{\partial n}\right)_{in} - \epsilon\left(\frac{\partial V}{\partial n}\right)_{out} = 0 \quad (15)$$

where $\vec{n}$ is the outward-pointing vector perpendicular to the cavity surface.

Equations 7−15 are the basic elements to use in the elaboration of solvation methods according to standard electrostatics. In the first review[1] the approaches in use were classified into six categories, namely, (1) the apparent surface charge (ASC) methods, (2) the multipole expansion (MPE) methods, (3) the generalized Born approximation (GBA), (4) the image charge (IMC) methods, (5) the finite element methods (FEM), and (6) the finite difference methods (FDM).

We maintain here this classification, but with the required modifications due to the important developments achieved in the past years in almost all of the categories. Only in the category of the IMC methods are no new important developments to be found, at least within the framework of molecular calculations, and thus this category of methods will be not considered in the present review: the interested reader is referred to our previous review.[1]

2.3.1. ASC Methods

From the jump condition (eq 15) one may derive an auxiliary quantity that defines all of the ASC methods: an apparent surface charge $\sigma(s)$ spread on the cavity surface. We are using the symbol s for the position variable, to emphasize that this charge distribution is limited to the surface Γ.

The definition of the ASC is not unequivocal but changes in alternative versions of the model. In all cases, however, the ASC defines a potential over the whole space:

$$V_\sigma(\vec{r}) = \int_\Gamma \frac{\sigma(\vec{s})}{|\vec{r} - \vec{s}|} d^2 s \quad (16)$$

This potential is exactly the reaction potential V_R of eq 9. There are no approximations in this elaboration: the definition of V_R given with eq 16 is exact

when $\sigma(s)$ is defined according to the proper electrostatic equations.

The reduction of the source of the reaction potential to a charge distribution limited to a closed surface greatly simplifies the electrostatic problem with respect to other formulations in which the whole dielectric medium is considered as the source of the reaction potential. Despite this remarkable simplification, the integration of eq 16 over a surface of complex shape is computationally challenging. The solutions are generally based on a discretization of the integral into a finite number of elements. This technique may be profitably linked to the boundary element method (BEM), a numerical technique widely used in physics and engineering to solve complex differential equations via numerical integration of integral equations (see the Website http://www.boundary-element-method.com/ for a global view on literature and applications of this method).

The cavity surface Γ is approximated in terms of a set of finite elements (called tesserae) small enough to consider $\sigma(s)$ almost constant within each tessera. With $\sigma(s)$ completely defined point-by-point, it is possible to define a set of point charges, q_k, in terms of the local value of $\sigma(s)$ on each of these tesserae times the corresponding area A_k. The integral of eq 16 is thus transformed in the following finite sum:

$$V_\sigma(\vec{r}) \simeq \sum_k \frac{\sigma(\vec{s}_k) A_k}{|\vec{r} - \vec{s}_k|} = \sum_k \frac{q_k}{|\vec{r} - \vec{s}_k|} \qquad (17)$$

Actually the local value of the potential necessary to define q_k also depends on the whole set of the surface charges, and so the correct values of the surface charges, and the correct expression of the reaction potential, are to be obtained through an iterative procedure. These aspects will be examined in section 2.3.1.5; now we present the most important ASC models. In this presentation we shall not make use of the BEM version of the ASC equations involving the point charges q_k but instead the original ones in terms of a continuous surface charge $\sigma(s)$. A description of the formal and practical aspects related to the use of the BEM approach for ASC methods will be given in section 2.3.1.5.

2.3.1.1. Polarizable Continuum Model (PCM): Original Formulation. PCM, the oldest ASC method, at present is no more a single code, but rather a set of codes, all based on the same philosophy and sharing many features, some specialized for some specific purposes, others of general use, but with differences deserving mention.

The original PCM version was published in 1981, after some years of elaboration,[8] and subsequently implemented in local and official versions of various QM computational packages.[48] More recently, PCM was renamed D-PCM (D stands for dielectric)[49] to distinguish it from the two successive reformulations (CPCM and IEFPCM) that we shall present in the next sections. This acronym is not completely correct as also the other reformulations refer to dielectric media (directly or indirectly); however, we cannot forget that it has become of common use in these years, and, thus, in the present review, we will adopt

DPCM to refer to the first version of the model, whereas PCM will be used to refer to the entire family of models.

DPCM, like all members of the PCM family, is able to describe an unlimited number of solutes, each equipped with its own cavity and ASC, interacting among them through the dielectric. In this way, DPCM permits an extension of the basic model to association−dissociation phenomena, molecular clustering, etc., and it can account for a continuous shift from a single cavity to two cavities during a dissociation and the merging of two or more cavities during association. In parallel, it permits an extension to models in which the medium is composed by a set of nonoverlapping dielectric regions at different permittivity, constant within each region.

The reason for this versatility is in the use of the ASC approach in an unsophisticated version. To better appreciate this point, let us look again at the basic electrostatics from a different viewpoint.

For systems composed by regions at constant isotropic permittivity (including systems composed of a single isotropic solvent with multiple cavities), the polarization vector is given by the gradient of the total potential $V(r)$ (including also that deriving from apparent charges)

$$\vec{P}_i(\vec{r}) = - \frac{\epsilon_i - 1}{4\pi} \nabla \vec{V}(\vec{r}) \qquad (18)$$

where ϵ_i is the dielectric constant of the region i.

At the boundary of two regions i and j, there is an ASC distribution given by

$$\sigma_{ij} = - (\vec{P}_j - \vec{P}_i) \cdot \vec{n}_{ij} \qquad (19)$$

where $\vec{n}_{ij}$ is the unit vector at the boundary surface pointing from medium i to medium j. The basic ASC model is so transformed into a similar system, with several ASCs that must be treated all on the same footing.

The basic PCM definition may be derived from the general expression 18 by taking into account the facts that in the basic case $\epsilon_i = 1$ and $\epsilon_j = 1$ and that we have computed the gradient on the internal (in) part of the surface, namely

$$\sigma(s) = \frac{\epsilon - 1}{4\pi\epsilon} \frac{\partial}{\partial \vec{n}} (V_M + V_\sigma)_{in} \qquad (20)$$

where $\vec{n}$ indicates the unit vector perpendicular to the cavity surface and pointing outward.

After its first formulation, the DPCM was revised many times both in its theoretical aspects and in its numerical implementation; among all of these revisions, a fundamental one was proposed in 1995 by Cammi and Tomasi[50] when a new, and more efficient, computational strategy was defined to solve the BEM equivalent of eq 20 (see section 2.3.1.5 for more details and comments on this strategy).

Since its first presentation in 1981, DPCM has been "adopted" by many groups, which have thus largely contributed to its diffusion and its development. Some of these extensions will be examined in following sections of this review, but here we cannot

forget to cite the work of three groups that have given, and continue to give, important contributions to show potentialities of DPCM.

First we cite the extensive and systematic work done in Barcelona by Luque, Orozco, and co-workers. The work of this group has to be here mentioned for several reasons. Their reformulation of DPCM, known by the acronym MST from the names of the three authors of the first PCM paper, has been applied to almost all aspects of solvation problems, with special attention to organic and biological systems; the amount of results of remarkable quality is the largest given by a single group. The papers of this vast literature devoted to methodological innovations (the main theme of this review) are abundant, all deserving attention. For obvious reasons, only a few[51-54] are cited here, and the reader is referred to a recent review[3] for many others. Barcelona's group has spent efforts during the past 10 years to analyze the performances of the method in many ways and to validate it by comparisons with other procedures: simulations of different type, other continuum models. Among them we cite a comparison with two methods we shall examine in the following pages, the MPE method of Nancy (section 2.3.2) and the GB method of Minneapolis (section 2.3.3), performed in collaboration with the authors of such methods.[55] In the following, we shall cite other papers by Luque and Orozco, but what stimulated us here is to manifest the appreciation for the considerable work in developing solvation methods, through the example of numerous impeccable applications, the work of analysis and validation, the suggestion of methodological innovations improving or extending the potentialities of the approach, and the activity of popularizing it by means of several short (or long) review papers.

Another important contribution to the development of the DPCM has been done by Basilevsky and co-workers; in their numerous works on solvation phenomena they started from the original definition of DPCM to develop a parallel model known by the acronym BKO,[56] standing for Born−Kirkwood−Onsager. During the years, this model has been applied to many different problems. Here it is not possible to report the vast literature, but in the following sections we shall analyze in detail the main developments introduced by Basilevsky and co-workers, namely, the reformulation of continuum models to nonlocal dielectrics, their application to studies of solvation dynamics, and their extension to mixed continuum/discrete approaches. In these sections, we shall also report all correspondent references.

A last contribution we quote here is that of the research team of the Gaussian computational package.[17] This team soon realized the potentialities and computational interest of the ASC approach to solvation, in the form given by DPCM. A version of the original model was rewritten by Gaussian and inserted in some releases around 1990, but the official collaboration between the PCM group and Gaussian started only at the end of 1996, and it has continued since then: more details on the results of this collaboration will be given in the following sections.

The Gaussian team has also independently elaborated a different PCM-like model based upon the previously mentioned isodensity surfaces (see section 2.2). This version of PCM is generally known as the isodensity-PCM (IPCM) model.[16] The same model has been further extended to allow the isodensity surface at each SCF iteration to be varied; that is, the cavity is not fixed, even once the geometry is fixed (as is the case in the standard PCM model), but it is relaxed to the isodensity of the solvated molecule at each SCF iteration. This further development is generally known as self-consistent isodensity (SCI-PCM).[57] Both IPCM and SCIPM models are available in the Gaussian computational package.[17]

2.3.1.2. Conductor-like Screening Model (COS-MO). In this method, originally devised by Klamt and Schüürmann,[58] the dielectric constant of the medium is changed from the specific finite value ϵ, characteristic of each solvent, to $\epsilon = \infty$. This value corresponds to that of a conductor, and this change strongly modifies the boundary conditions of the electrostatic problem. The most important effect is that the total potential $V(r)$ of eq 9 cancels out on the cavity surface. From this condition it follows that the ASC is determined by the local value of the electrostatic potential instead of the normal component of its gradient (as in eq 20). To recover the effects of the finite value of the dielectric constant of the medium, the ideal unscreened charge density, σ^*, corresponding to $\epsilon = \infty$, is finally scaled by a proper function of ϵ, namely

$$\sigma(s) = f(\epsilon)\sigma^*(s) \qquad (21)$$

The scaling function, $f(\epsilon)$, has been empirically determined by comparing COSMO (unscaled) and correct electrostatic solute−solvent energies. The suggested formula is of the type

$$f(\epsilon) = \frac{\epsilon - 1}{\epsilon + k} \qquad (22)$$

with k small.

In the original paper about COSMO, Klamt suggested $k = 0.5$,[58] with the remark that k seems to depend on the cavity shape and on the distribution of charges in the solute. Other versions of COSMO proposed in the following years adopted other values for k. Truong and Stefanovic, in their GCOSMO,[59,60] and Cossi and Barone, in their C-PCM[61] (this program is a part of the PCM suite of programs), proposed $k = 0$ on the basis of an analogy with the Gauss law. Subsequently, Cossi et al.[62] compared the solvation free energies for neutral and charged solutes in water and in CCl_4, and they found that the choice of k is irrelevant for water but important in CCl_4: for neutral solutes the best agreement is obtained for $k = 0.5$, whereas for charged molecules it is preferable to use $k = 0$. Pye and Ziegler[63] in their implementation of COSMO in the ADF computational package[64,65] use $k = 0$ as default, but leave the users free to select the value they prefer. Chipman, in a recent comparison of several continuum models,[66] gives results for both $k = 0$ and 0.5, remarking that $k = 0$ seems to be somewhat better.

We note that the corrections introduced by this factor are quite small for solvents with high dielectric constant, and the final output of the energy is almost insensitive to changes in the k parameter. Things are a bit more critical for solvents of low ϵ and, in particular, for the cases in which one has to separately compute the inertial and the electronic component of the polarization vector $\vec{P}$ (see sections 5.1 and 5.2); in these cases attention has to be paid in the use of solvation codes of the COSMO family.

An extension of the COSMO model, called COSMO-RS (conductor-like screening model for real solvents), has been proposed by Klamt,[67] starting from the analysis that solvents do not behave linearly when we consider strong electric fields on the molecular surfaces of fairly polar solutes. COSMO-RS is a theory that describes the interactions in a fluid as local contact interactions of molecular surfaces, the interaction energies being quantified by the values of the two screening charge densities that form a molecular contact. Having reduced all interactions to local interactions of pairs of molecular surface pieces, one can consider the ensemble of interacting molecules as an ensemble of independently interacting surface segments. COSMO-RS has become a predictive method for the thermodynamic properties of pure and mixed fluids. In contrast to group contribution methods, which depend on an extremely large number of experimental data, COSMO-RS calculates the thermodynamic data from molecular surface polarity distributions, which result from quantum chemical calculations of the individual compounds in the mixture. The different interactions of molecules in a liquid, that is, electrostatic interactions, hydrogen bonding, and dispersion, are represented as functions of surface polarities of the partners. Using an efficient thermodynamic solution for such pairwise surface interactions, COSMO-RS finally converts the molecular polarity information into standard thermodynamic data of fluids, that is, vapor pressures, activity coefficients, excess properties, etc.;[68−72] the corresponding computational code is called COSMOtherm.[73]

2.3.1.3. Integral Equation Formalism (IEF). With the IEF method[74−76] originally formulated by Cancès and Mennucci in 1997, we come back again to methods involving solutes in a liquid phase and using the characterization of the solvent given by macroscopic properties of the specific liquid (such as the permittivity, ϵ). Actually, IEF is a method more general than DPCM, or COSMO, and the case of an isotropic dielectric is nothing more than one of its possible applications, as we shall show below. Together with the previously mentioned DPCM and CPCM, IEF is a member of the PCM suite of solvation codes implemented in Gaussian since its 1998 version and, in the latest G03 version,[17] it has become the default PCM formulation.

As in the two other ASC methods we have described in the previous sections, also for IEF we start from the electrostatic system (eq 6) and we introduce the decomposition (eq 9) of the potential V in the sum of the electrostatic potential generated by the charge

distribution ρ_M in vacuo, V_M, and the "reaction potential", V_R.

In the IEF, however, the potentials are redefined in terms of the proper Green functions; we recall that the Green function of an electrostatic problem $G(x,y)$ is the potential produced in x by a unit point charge located in y (here with x and y we indicate two general positions in the space, but for simplicity's sake we drop the vector symbol).

If we indicate by $G(x,y) = 1/|x - y|$ the Green function corresponding to the operator $-\nabla^2$ (namely, its kernel), by $G^s(x,y)$ the Green kernel of the operator $-\nabla(\epsilon\nabla)$, and $G^R(x,y) = G^s(x,y) - G(x,y)$, the following relationships arise:

$$V(x) = \int_{R^3} G^s(x,y)\rho_M(y)\,dy$$

$$V_M(x) = \int_{R^3} G(x,y)\rho_M(y)\,dy \qquad (23)$$

$$V_R(x) = \int_{R^3} G^R(x,y)\rho_M(y)\,dy$$

Exploiting some basic results of the theory of integral equations (see ref 76 for details), it can be proved that the reaction potential, V_R, which satisfies

$$-\nabla^2 V_R = 0 \text{ in } C \text{ and outside } C$$

$$[V_R] = 0 \text{ on } \Gamma \qquad (24)$$

$$V_R \rightarrow 0 \text{ at infinity}$$

can be represented as a *single layer potential*

$$V_R(x) = \int_\Gamma \frac{\sigma(y)}{|x - y|}\,dy \;\forall\; x \in R^3 \qquad (25)$$

where the surface charge σ is the unique solution to the equation

$$A\sigma = -g \qquad (26)$$

with A and g being two integral operators defined as

$$A = (2\pi - D_e)S_i + S_e(2\pi + D_i^*)$$
$$g = (2\pi - D_e)V_M + S_e(\partial V_M/\partial n) \qquad (27)$$

In the two last relationships we have introduced the operators S_a, D_a, and D_a^* with $a =$ e or i standing for *external* (i.e., outside the cavity) and *internal* (i.e., inside the cavity), respectively. These operators are formally defined for σ by

$$(S_a\sigma)(x) = \int_\Gamma G_a(x,y)\sigma(y)\,dy$$

$$(D_a\sigma)(x) = \int_\Gamma [(\epsilon_a\vec{\nabla}_y G_a(x,y))\cdot\vec{n}(y)]\sigma(y)\,dy \quad (28)$$

$$(D_a^*\sigma)(x) = \int_\Gamma [(\epsilon_a\vec{\nabla}_x G_a(x,y))\cdot\vec{n}(x)]\sigma(y)\,dy$$

where $\epsilon_a = 1$ for $a =$ i and $\epsilon_a = \epsilon$ (the solvent permittivity) for $a =$ e.

We note that eq 27 is different with respect to that reported in the original papers[74,76] because here we

have used a different form of the Poisson eq 6 including a 4π factor on the right-hand side. This is reflected in the Green functions, G_a, and thus in the corresponding operators S_a and D_a, which now do not include the $1/4\pi$ factor.

The operators defined in eq 28 are well-known in the theory of integral equations: they are three of the four components of the Calderon projector.[77] We recall some of their properties: the operator S_i is self-adjoint, and D_i^* is the adjoint of D_i for the scalar product. Besides, $S_i D_i^* = D_i S_i$.

Equation 26 may be further simplified using the equality $(2\pi - D_i)V_M + S_i(\partial V_M/\partial n) = 0$; in this way the expression for g in eq 27 can be rewritten as[78]

$$g = [(2\pi - D_e) - S_e S_i^{-1}(2\pi - D_i)]V_M \quad (29)$$

and thus the surface charge σ depends only on the potential V_M (and no longer on a normal component of the field) exactly as in the COSMO approach. This simplification is important from both numerical and formal points of view.

Numerically, it is advantageous not only because the calculation of a single scalar function (the potential) is computationally less demanding than the parallel calculation of both the potential and the vectorial electric field, but also because the potential is less sensitive than the field to numerical instabilities that can appear when we introduce a BEM approach to solve the electrostatic equations. From a formal point of view, the reformulation of the IEF ASC in terms of only the potential is important because it represents an implicit correction of the error due to the fraction of solute electric charge diffusing outside the cavity (namely, the previously defined outlying charge). The details on this issue will be given in section 2.4.3. Here it is worth reporting the final equations for the IEF ASC in the case of isotropic solvents; these, in fact, will be useful in the following when we shall compare IEF to other ASC methods. Namely, using the relations, $S_e = S_i/\epsilon$, $D_i = D_e$, we can transform the IEF operators A of eq 27 and g of eq 29 in

$$A = (1 - 1/\epsilon)[2\pi(\epsilon + 1)/(\epsilon - 1) - D_i]S_i$$
$$g = (1 - 1/\epsilon)(2\pi - D_i)V_M \quad (30)$$

and thus eq 26, defining the ASC, reduces to[78]

$$\left[2\pi\left(\frac{\epsilon + 1}{\epsilon - 1}\right) - D_i\right]S_i\sigma = -(2\pi - D_i)V_M \quad (31)$$

where, once again, we have used the relationship $S_i D_i^* = D_i S_i$. In the following, this version of IEF will be denoted IEF(V) to indicate that only the solute electrostatic potential (V_M) is required to determine the ASCs.

From eqs 24−29 it can be seen that the IEF approach is completely general, in the sense that it can be applied without the need of modifying either the basic aspects of the model or the basic equations (26−29) to all of those systems for which the Green functions inside and outside the cavity are known. As a matter of fact, as the interior form of G is always

known, $G_i(x,y) = 1/4\pi|x - y|$, the problem is shifted to the evaluation of the exterior, $G_e(x,y)$. Analytical expressions of this function are available for standard isotropic solvents characterized by a constant and scalar permittivity ϵ [namely $G_e(x,y) = 1/(\epsilon|x - y|)$], but also for anisotropic environments characterized by a tensorial but constant permittivity ϵ for ionic solutions described in terms of the linearized Poisson−Boltzmann equation (see section 2.3.1.6 for further details) and for sharp planar liquid−metal interfaces.[79] Obviously, it is not always possible to have analytical Green functions. However, in several cases the Green function can be effectively built numerically, and thus the IEF approach can be generalized to many other environments as, for example, a diffuse interface with an electric permittivity depending on the position.[80]

As a final comment it is worth noting that IEF contains as subcases both the DPCM and the COSMO models. In the first case we have to consider an isotropic solvent with a scalar permittivity and use the electrostatic equation already introduced above to rewrite the IEF ASC eq 29 in terms of the potential, in the opposite way so as to keep $(\partial V^M/\partial n)$ instead. To recover COSMO ASC, on the other hand, we have to consider that $\epsilon \rightarrow \infty$, and thus all of the terms in eqs 27 and 29 involving the S_e operator can be neglected (S_e is in fact proportional to $1/\epsilon$).

2.3.1.4. Surface and Volume Polarization for Electrostatic [SVPE and SS(V)PE]. From 1997 to date, Chipman and co-workers have developed a series of continuum models[81−85] that have, as a starting point, the consideration that unconstrained quantum mechanical calculation of solute charge density generally produces a tail that penetrates outside the cavity into the solvent region (the "outlying charge" mentioned in the previous sections). Exact solution of Poisson's equation in this situation would require invocation of an apparent volume polarization charge density lying outside the cavity in addition to the apparent surface polarization charge density lying on the cavity.[86] As a consequence, also the reaction potential heretofore written in terms of an apparent surface charge has to be supplemented with a term due to the apparent volume charge, namely, following the notation used by Chipman

$$V_R(x) = V_o(x) + V_\beta(x)$$

$$V_\beta(x) = \int_{ext} \frac{\beta(y)}{|x - y|}\,dy = -\left(\frac{\epsilon - 1}{\epsilon}\right)\int_{ext} \frac{\rho_M(y)}{|x - y|}\,dy \quad (32)$$

where the integration is over the whole volume excluding the molecular cavity.

The acronym used to indicate this formulation was SVPE, meaning that both surface and volume polarization for electrostatic interactions were included. Contrary to the previous ASC models, this method requires a discretization of both the cavity surface and the exterior volume; in particular, the volume polarization charge density β was approximated by a collection of point charges located at various nodes

on a series of layers covering the exterior region, as described in detail in ref 82.

The exact SVPE method is laborious to implement and time-consuming, because it utilizes a volume polarization potential arising from a discontinuous volume charge density. With a cavity surface that is adapted to the detailed nonspherical shape of a general molecular solute, this leads to difficult integrations over just part of the full three-dimensional space.

To avoid this large complexity a simpler approximate solution that involves only apparent surface charge distributions was subsequently introduced. Here, we limit ourselves to summarize the main aspects of this method denoted "surface and simulation of volume polarization for electrostatics", SS(V)PE.

The SS(V)PE method originated with the demonstration[81] that all direct and indirect effects of the volume polarization charge density on the exact SVPE reaction potential can be exactly represented at all points inside the cavity (which is the most important region) by simulating the explicit volume charge density in terms of an additional surface charge density so that the total apparent surface charge satisfies the equation[84]

$$T\sigma^{\text{SS(V)PE}} = \left(\frac{\epsilon - 1}{\epsilon + 1}\right)\left[\frac{D_{\text{i}}}{2\pi} - I\right]V_{\text{M}}$$

$$T = S_i - \left(\frac{\epsilon - 1}{\epsilon + 1}\right)\frac{1}{4\pi}(D_{\text{i}}S_{\text{i}} + S_{\text{i}}D_{\text{i}}^*) \tag{33}$$

where we have used the same notation introduced for IEF in the previous section.

The correspondence between SS(V)PE and IEF is not only of notation: the two methods in fact coincide when the isotropic IEF(V) eq 31 is considered; to show this, it is sufficient to multiply both sides of eq 33 by $2\pi(\epsilon + 1)/(\epsilon - 1)$ and to use the relationship $S_{\text{i}}D_{\text{i}}^* = D_{\text{i}}S_{\text{i}}$. The formal equivalence of the two methods was published[87] only one year after the publication of the SS(V)PE original paper,[84] and thus the two methods are often considered as two alternative ASC methods. As a matter of fact, when the whole solute charge is contained within the cavity, SS(V)-PE is equivalent also to DPCM (besides IEF), but when a part of this charge lies outside this, equivalence with DPCM is no longer valid; on the contrary, the equivalence with IEF(V) (see the end of section 2.3.1.3) remains in all cases. The late recognition of the equivalence of the two approaches is also reflected in a further PCM approach proposed by Cossi et al.[88] In fact, this model, indicated as implicit volume charges PCM (or IVCPCM), was presented by the authors as the PCM reformulation of the SS(V)PE by Chipman but, in practice, it exactly coincides with the IEF version of PCM. Unfortunately, also in papers that appeared later, the authors never clarified this point, and thus the two methods continued to be described as different approaches.[89]

2.3.1.5. Discretization of the Cavity Surface and the ASC-BEM Equations. In the presentation of the ASC models we have adopted the original formalism using a continuous surface charge σ. Here, we go a step farther and present a description of the formal and practical aspects related to the use of the BEM version of the ASC equations involving the point charges q_k. It is interesting to note that BEM is a relatively young technique (the acronym was first used in 1977[90]), but now a very large literature, including books and dedicated international conferences (the principal conference on BEM conducts its 27th meeting in 2005[91]), can be found on this very powerful mathematical approach.

As introduced at the beginning of section 2.3.1, the definition of ASC elements uses the discretization of the surface into a finite number of elements (usually called tesserae), which is the cornerstone of BEM, and for this reason it may be considered an application of a BEM procedure (or, better, of the indirect BEM procedure; see also section 2.3.1.6). Actually it is not a trivial application, because the original BEM was limited to cases without internal sources, that is, based on the Laplace equation $\nabla^2 V(r) = 0$ instead of the Poisson equation (7). Other features of BEM have been considered in more recent versions of ASC methods, but it must be said that the large wealth of suggestions available in the BEM literature has not yet been fully exploited in the continuum solvation methods.

The necessary preliminary step in BEM-ASC strategy is the generation of the surface finite elements. This step can be achieved in many different ways; here, in particular, we shall focus on the algorithm developed for the GEPOL cavity (see section 2.2).

In the original formulation, the GEPOL tesserae were generated by inscribing a polyhedron with 60 faces within each sphere, projecting the faces onto the spherical surface, and discarding those that were fully inside an intersecting sphere. If a polyhedron face happened to be partially inside a neighboring sphere, the tessera was cut into smaller triangles, and only those triangles that were completely exposed were kept; in this way the final tessera was represented by a complex polygon.

GEPOL has been considerably improved during the years; we mention here an improved scheme to fill the solvent-excluded space[92] and the algorithm through which the exposed portion of a tessera partially inside other spheres is analytically cut by adding edges to the tessera being generated.[93] In this way, all of the tesserae are defined in terms of connected arc segments, and their surface areas can be analytically computed using the Gauss−Bonnet formula so that the analytical derivatives of all the tesserae can be computed. Another important improvement is the introduction of flexible tessellation[94] and symmetry-adapted tessellations.[95,96] This advanced version of GEPOL is available in GAMESS[97,98] and Gaussian[17] computational codes. The last revision of Gaussian (Gaussian 03) includes an even more advanced version of GEPOL; this recent re-implementation has been realized by Scalmani et al.[99] and, among different important numerical improvements, it presents also a linear scaling computational cost, thus extending the range of applicability to very large molecular systems.

Table 1. Matrices To Be Used in Equation 34 To Get the Apparent Charges in Various ASC Methods

	K	f
DPCM	$\left(2\pi\dfrac{\epsilon+1}{\epsilon-1}\mathbf{A}^{-1} - \mathbf{D}^*\right)^{-1}$ with $D_{ij} = \dfrac{(\vec{s}_i - \vec{s}_j)\cdot\vec{n}_j}{|\vec{s}_i - \vec{s}_j|^3} \xrightarrow{i\rightarrow j} D^*_{ij}$	E_n
COSMO [CPCM]	$\mathbf{S}^{-1}$ with $S_{ij} = \dfrac{1}{|\vec{s}_i - \vec{s}_j|}$	V
IEFPCM(iso) [IVPCM]	$\left\{\left[2\pi\left(\dfrac{\epsilon+1}{\epsilon-1}\right)\mathbf{A}^{-1} - \mathbf{D}\right]\mathbf{S}\right\}^{-1}[2\pi\mathbf{A}^{-1} - \mathbf{D}]$	V
SS(V)PE	$\left\{\left[2\pi\left(\dfrac{\epsilon+1}{\epsilon-1}\right)\mathbf{A}^{-1}\mathbf{S} - \mathbf{A}^{-1}\dfrac{(\mathbf{DAS}+\mathbf{SAD}^*)}{2}\right]\right\}^{-1}[2\pi\mathbf{A}^{-1} - \mathbf{D}]$	
IEFPCM	$\{[2\pi\mathbf{A}^{-1} - \mathbf{D}_e]\mathbf{S} + \mathbf{S}_e[2\pi\mathbf{A}^{-1} + \mathbf{D}^*]\}^{-1}\{[2\pi\mathbf{A}^{-1} - \mathbf{D}_e] - \mathbf{S}_e\mathbf{S}^{-1}[2\pi\mathbf{A}^{-1} - \mathbf{D}]\}$	V
aniso	$[D_e]_{ij} = \dfrac{(\vec{s}_i - \vec{s}_j)\cdot\vec{n}_j}{\sqrt{\det\epsilon}[(\epsilon^{-1}\cdot(\vec{s}_i - \vec{s}_j))\cdot(\vec{s}_i - \vec{s}_j)]^{3/2}}$ $[S_e]_{ij} = \dfrac{1}{\sqrt{\det\epsilon}[(\epsilon^{-1}\cdot(\vec{s}_i - \vec{s}_j))\cdot(\vec{s}_i - \vec{s}_j)]^{1/2}}$	
ionic	$[D_e]_{ij} = \dfrac{\exp[-k|\vec{s}_i - \vec{s}_j|][1 + k|\vec{s}_i - \vec{s}_j|](\vec{s}_i - \vec{s}_j)\cdot\vec{n}_j}{|\vec{s}_i - \vec{s}_j|^3}$ $[S_e]_{ij} = \dfrac{\exp[-k|\vec{s}_i - \vec{s}_j|]}{\epsilon|\vec{s}_i - \vec{s}_j|}$	

Recently, two independent novel schemes have been proposed[100,101] to sample the GEPOL molecular surface without an explicit discretization of the cavity surface, which may lead to unphysical discontinuities. In both of these schemes the sampling of the surface is done on each original sphere, and it is not changed after all of the spheres have been combined to construct the final cavity. Each sampling point is then associated with a "weight" (which in the simple scheme coincides with the area of the tessera) and to a switching function, the definitions of which are different in the two methods. In both cases, however, the main result is that no sampling points and weights will be discarded; their number remains constant also during a geometry optimization when changes in the solute geometry induce changes in the relative position of the atom-centered spheres.

Once the cavity surface has been partitioned in tesserae small enough to consider $\sigma(s)$ almost constant within each tessera, it is possible to define a set of point charges q_k in terms of the local value of $\sigma(s)$ on each of these tesserae times the corresponding area. In doing this the electrostatic equation presented in sections 2.3.1.1−2.3.1.4 for $\sigma(s)$ within the various ASC methods can be rewritten as a set of T (with T equal to the number of tesserae) coupled equations, which can be recast in a matrix form of the type

$$\mathbf{q} = -\mathbf{Kf} \qquad (34)$$

where $\mathbf{K}$ is a square matrix $T \times T$ collecting the cavity geometrical factors (the tesserae representative points s_k and the corresponding areas) and the dielectric constant of the medium and $\mathbf{q}$ and $\mathbf{f}$ are column matrices, the first containing the unknown charges and the second the values of the proper electrostatic quantity, namely, the normal component of the electric field E_n or the electrostatic potential V, calculated at the tesserae. Equation 34 represents the electrostatic BEM problem we have to solve.

The elaboration of the problem giving origin to an equation of type 34 has been done in a large number of ways, in practice one for each ASC method, and also in several different ways for the same method. There is no need to repeat here the various elaborations; instead, we provide a table with the expressions of the elements of the $\mathbf{K}$ and $\mathbf{f}$ matrices for the most important variants of ASC methods, namely, DPCM, CPCM, IEFPCM, and SS(V)PE. As far as concerns IEFPCM, two different sets of expressions are given, the first referring to standard isotropic solvents (characterized by a constant scalar permittivity ϵ) and the second for anisotropic solvents (i.e., characterized by a constant but tensorial permittivity ϵ) and for ionic solutions (in the limit of a linearized PB scheme, see eq 43). We also note that in all cases, IEFPCM equations have been rewritten in the IEF-(V) form, that is, using only $\mathbf{f} = \mathbf{V}$ and not the combination of $\mathbf{V}$ and E_n as in the first formulation of the method; this reformulation was originally proposed for the isotropic case only, but recently it has been generalized to anisotropic dielectrics;[102] here, we present for the first time the parallel version for the linearized Poisson−Boltzmann scheme (see also section 2.3.1.6).

In Table 1 we have reported only the off-diagonal elements of the $\mathbf{D}$ and $\mathbf{S}$ matrices involved in the different versions, because different numerical solutions have been proposed for the diagonal elements. In particular, for $\mathbf{S}$ the following approximation is

generally used

$$S_{ii} = k \sqrt{\frac{4\pi}{a_i}} \qquad (35)$$

where a_i indicates the area of tessera i and k is a numerical parameter. This equation derives from the exact formula of a small circular cap section of a sphere or a flat circular element of any size for which $k = 1$. To improve the approximation in the case of a spherical element such as those used in ASC methods, a different value of k is used. The constant k was originally determined[58] to have the value 1.07 on the basis of the numerical evaluation for a sphere divided into various numbers of equivalent finite segments, but then, after a more accurate fitting, this value was revised to 1.0694, and this is the value implemented, for example, in the latest version of CPCM and IEFPCM in Gaussian code.[103] For the **D** matrix, it can be shown that, if the tessera is placed on a sphere, then[75]

$$D_{ii} = k \frac{\sqrt{4\pi a_i}}{2R_I} \qquad (36)$$

where R_I is the radius of such a sphere.

An alternative expression for D_{ii} has been adopted by Foresman et al.,[16] by Chipman,[83,104,105] and by Cossi et al.[88] following the original proposal by Purisima;[106,107] this expression uses the sum of the off-diagonal elements, namely

$$D_{ii} = -\left(2\pi + \sum_{j \neq i} D_{ij} a_j\right) \frac{1}{a_i} \qquad (37)$$

In the case of IEFPCM for anisotropic dielectrics and ionic solutions, no analytical expressions can be given for the diagonal elements of the $\mathbf{D_e}$ and $\mathbf{S_e}$ matrices, and thus the procedure that has been implemented is based on a Gaussian integration scheme.[74]

The linear system (eq 34) can be solved either by matrix inversion or iteratively.[50] The cost of computing the ASC terms used to be usually negligible if compared to other steps in an ab initio calculation (e.g., Fock matrix building and diagonalization). Nowadays, this is no longer true as, in the field of ab initio methods, fast algorithms for which the cost grows linearly with the system size [e.g., the fast multipole method (FMM)] are beginning to be widely available and applied.[108−111] On the other hand, the significant research effort being devoted to hybrid quantum/classical approaches (see section 7) is driving toward the handling of large (partly) classical solutes, which could easily involve thousands of atoms.

Given these methodological and algorithmic advances, the cost of calculating the ASCs could easily become the computational bottleneck. Indeed, whenever fast and linear scaling algorithms, such as the FMM, are used to compute the electrostatic potential/ field on the tesserae, the cost of evaluating the interaction of the polarization charges among themselves will grow more steeply and will rapidly become dominant as the number of tesserae increases.

Recently, an efficient linearly scaling procedure has been formulated[112] (and implemented in the latest revision of Gaussian) by exploiting the FMM for computing electrostatic interactions. Such a procedure has been formulated for DPCM, CPCM, and IEFPCM models, and it is based on an iterative solution of the linear system (eq 34). Here, we present the basic equations just for the DPCM case as more intuitive, but we refer the interested reader to the reference paper for the corresponding equations for CPCM and IEFPCM. By properly rewriting the system (eq 34), the iterative equation defining the apparent charges becomes

$$q_i^{(n)} = \left[\frac{1}{a_i}\left(\frac{4\pi}{\epsilon - 1} + z_i[a_j]\right)\right]^{-1} [-(E_n)_i + z_i^*[q_j^{(n-1)}]] \quad (38)$$

where

$$z_i^*[x_j] = \sum_{j \neq i} D_{ij}^* x_j$$

$$z_i[x_j] = \sum_{j \neq i} D_{ij} x_j \qquad (39)$$

and $q^{(n-1)}$ and $q^{(n)}$ are the charges at the $(n-1)$th and nth iteration, respectively. The definitions of $z_i^*[x_j]$ and $z[x]$ (eqs 39) state that these "kernels" cost formally as the square of the number of tesserae T. However, taking a closer look at those expressions, it is easy to realize that both quantities can be computed in the framework of the FMM algorithm, thus achieving linear-scaling computational cost. In particular, $z_i^*[x_j]$ is the normal component of the electric field at the ith tessera generated by the (pseudo)charges x_j located at the other $T-1$ tesserae, and $z[x]$ is the sum of the "normal fields" generated by the (pseudo)charges x_j at the other $T-1$ tesserae. The performances of different iterative solvers and preconditioning strategies have been assessed for the different PCM models.

We conclude this section by mentioning an alternative approach to define the apparent charges formulated by York and Karplus[113] within the COSMO formalism. The method uses smooth Gaussian basis functions of the form

$$\phi_k(|\vec{r} - \vec{r}_k|) = \left(\frac{\zeta_k^2}{\pi}\right)^{3/2} e^{-\zeta_k/2|\vec{r} - \vec{r}_k|^2} \qquad (40)$$

to represent the electrostatic potential and surface element interaction matrices and circumvents the Coulomb singularity problem due to overlapping surface elements represented by point charges. Here, r_k is the coordinate of the surface element k, and ζ_k is the Gaussian exponent that is adjusted to obtain the exact Born ion solvation energy.

For the appearance and disappearance of surface elements to occur smoothly as a function of geometrical changes, a switching layer around each atom is introduced. The switching layer serves to "turn off" or "turn on" the surface elements associated with other atoms as they pass into or out of the layer.

Very recently, this approach has been extended to the PCM suite of models by Scalmani and Frisch[114]

within the Gaussian code. In this new formalism the **S** and **D** matrices reported in Table 1 can be expressed in terms of two-center, two-electron integrals and their derivatives, for example

$$S_{ij} = \langle \phi_i | \phi_j \rangle = \frac{\mathrm{erf}(\zeta_{ij}|\vec{s}_i - \vec{s}_j|)}{|\vec{s}_i - \vec{s}_j|}$$

$$D_{ij} = \frac{\partial S_{ij}}{\partial \vec{s}_j} \hat{n}_j = \frac{(\vec{s}_i - \vec{s}_j)\hat{n}_j}{|\vec{s}_i - \vec{s}_j|^3} \left[\mathrm{erf}(\zeta_{ij}|\vec{s}_i - \vec{s}_j|) - \frac{2}{\sqrt{\pi}} \zeta_{ij} \left| \vec{s}_i - \vec{s}_j \right| e^{-(\zeta_{ij}|\vec{s}_i - \vec{s}_j|)^2} \right]$$

(41)

where

$$\zeta_{ij} = \zeta_i \zeta_j / \sqrt{\zeta_i^2 + \zeta_j^2}$$

2.3.1.6. More on the BEM. When one wants to extend the basic model to solutions with nonzero ionic strength (i.e., to salt solutions), additional problems appear. One way to treat these problems consists of adopting other formulations of the BEM approach such as those reported here below. These methods can be applied also to zero ionic strength, and for this reason they are considered here, in a section of the review dedicated to isotropic liquids without dispersed ions. The basic electrostatic equations modify as

$$-\nabla^2 V(\vec{r}) = 4\pi \rho_{\mathrm{M}}(\vec{r}) \text{ within } C \quad (42)$$

$$-\epsilon(\nabla^2 - k^2)V(\vec{r}) = 0 \text{ outside } C \quad (43)$$

where k accounts for the ion screening: its inverse is known as the Debye screening length $(1/k)$, namely, $k^2 = 8\pi e^2 I/\epsilon kT$ (I is the ionic strength $\sum_i z_i^2 c_i/2$ for a dissolved salt containing two or more types of ion i, each having charge $z_i e$ and an average bulk concentration c_i).

Equation 43, generally known as the linearized Poisson–Boltzmann (LPB) equation, is the result of the Debye–Huckel approximation applicable in the case of low potentials, a condition approached at low concentrations. The LPB equation is obtained by taking the linear term of the Taylor expansion of the hyperbolic sine function which, according to a treatment of statistical physics in the thermodynamic equilibrium approximation, represents the distribution of the mobile ions in the field of the electrostatic potential V.

The LPB equation can be solved analytically for simple cavity shapes such as a sphere.[115] However, for a general cavity of more complicated shape (such as that adapted to the molecular solute), it must be solved numerically. Many different models have been developed so far. In this section, we are interested in the specific class of approaches, which determines the total electrostatic potential indirectly by using BEM techniques. To better analyze this class of approaches it is useful to introduce some further information about BEM that has not been presented yet.

To derive the BEM, one must replace the partial differential equation that governs the solution in a domain by an equation that governs the solution on the boundary alone. There are two fundamental approaches to the derivation of an integral equation formulation of a partial differential equation. The first is often termed the *direct method*, and the integral equations are derived through the application of Green's second theorem. The other method is called the *indirect method* and is based on the assumption that the solution can be expressed in terms of a source density function defined on the boundary.

Among the indirect methods, we can, for example, mention the IEF and the parallel SS(V)PE approaches described in the previous sections. Both of these two methods have been generalized to treat the LPB problem,[75,116,117] and, as for the basic isotropic solvent, only a single-layer (charge) distribution $\sigma(s)$ is exploited. We note here that, for problems involving ionic effects, the use of indirect approaches is new and thus not largely used until now (to the best of our knowledge the original implementation of IEF in 1997 is the first example). A far more used BEM method is the direct one. To explain this method let us consider the electrostatic equations (42 and 43) governing the domain C bounded by the surface Γ. By applying Green's second theorem, these equations can be replaced by integral equations; for example, eq 43 becomes

$$\int_{\Gamma} \frac{\partial G(x,y)}{\partial n_y} V(y) \, \mathrm{d}y + \frac{1}{2} V(y) = \int_{\Gamma} G(x,y) \frac{\partial V(x,y)}{\partial n_y} \, \mathrm{d}y$$

(44)

where the function G is the Green function $\exp(-k|x - y|)/|x - y|$.

The surface integral on the right-hand side of eq 44 is called the single-layer potential, whereas the one on the left is called the double-layer potential. For this reason, the direct BEM approaches are also indicated as models employing both single-layer and double-layer distributions over the surface cavity.

The power of this formulation lies in the fact that it relates the potential V and its derivative on the boundary alone; no reference is made to V at points in the domain. To numerically solve the integral equations of the type of eq 44, the first step is to partition the surface into surface elements (i.e., to define an N-point grid on the surface).[118–124] Triangular and quadrilateral elements are commonly used for this purpose. As a second step, the unknown functions $V(r)$ and $\partial V(r)/\partial n$ are approximated by continuous trial functions over each boundary element. Generally, polynomials determined by their values at the N grid points (the *nodes*) are used. In this way, the integrals become sums of integrals over elements, which results in a set of linear equations for the polynomial coefficients. This set of equations can then be written as a single matrix equation of dimension $2N$.[125,126] A fast multipole algorithm can be used to reduce computational costs,[107,127,128] or one can apply an iterative procedure on a pair of coupled $N \times N$ finite matrix linear equations in every iteration.[129]

2.3.2. MPE Methods

The seminal papers of Kirkwood[115,130] and Onsager[131] have provided inspiration for various continuum solvation models based on a multipole expansion (MPE) of the solute charge distribution. Here, we present these models starting from the simplest one (a dipole inside a sphere) and passing to those using multipole expansions and/or cavities of more complex form.

Appreciable popularity was gained in past years by the Onsager−SCRF code, elaborated by Wiberg and co-workers[132,133] for the Gaussian computational code.[103] The Onsager model is the simplest version of the MPE approach. Solvation is described in terms of a dipole moment, drawn in an iterative way from QM calculations on the molecule. The appealing feature of Onsager−SCRF was that it permitted one to directly exploit almost all of the computational facilities of the Gaussian packages. For this reason, and for its very limited computational cost, it is still in use by people not requiring an accurate description of solvation effects but just a guess or a qualitative correction to the values obtained for the isolated molecule. Users must be aware of the limitations of the approach, of the unphysical deformation of the solute charge distribution it may induce, and of other shortcomings specific of the approach, such as the lack of solvation for solutes with zero permanent dipole.

A more general model going beyond the dipole approximation is that developed by Mikkelsen and co-workers.[134] This model starts from the idea proposed by Kirkwood to describe the interaction between a set of classical charges (described in terms of a multipole expansion) enclosed in a spherical cavity embedded in a structureless polarizable dielectric medium described by the macroscopic dielectric constant ϵ. Mikkelsen applies the model to QM charge distributions instead of classical point charges, as in the original Kirkwood paper, and the effects of the solvent polarization are described in terms of proper QM operators to be added to the Hamiltonian of the isolated system (i.e., adopting the same strategy introduced in section 2.3 to define the "effective Hamiltonians").

Even if the model is limited to spherical cavities, it presents very advanced features especially as far as concerns the QM aspects. The model has been implemented in the Dalton quantum chemistry program,[135] and it has been used to study solvent effects on a large number of molecular response properties; it has also been generalized to several QM approaches including multiconfigurational self-consistent field and coupled cluster methods[136−143] (see also section 2.4.6 and section 6).

The most complete, and also the most largely used MPE method, is that developed in Nancy by Rivail and co-workers.[6,144] Historically, this method represents the first example of QM continuum solvation methods, but over the years it has been continuously developed, and it continues its evolution.[145] In some cases the acronym SCRF (self-consistent reaction field) is also used to indicate this specific method, even if it also identifies the larger class of solvation

methods implying the use of a reaction potential to be self-consistently solved together with the solute charge.

Here, we shall consider three steps in the evolution of this MPE method: (i) a one-center expansion for a spherical cavity (in this case it coincides with that developed by Mikkelsen); (ii) its extension to ellipsoid cavities; and, finally, (iii) its extension to multicenter expansion and to cavities of general shape.

(i) The expression of the multipole expansion for the potential of a charge distribution placed into a sphere of radius a, immersed into a continuum with dielectric constant ϵ, has been known for a long time and can be found in numerous textbooks. We report the expression given by Böttcher[146] for the potential inside the cavity, namely

$$V(r) = V_{\mathrm{M}} + V_r = \sum_{l=0}^{\infty} \frac{1}{r^{l+1}} \sum_{m=-l}^{l} M_l^m \, Y_l^m(\theta,\varphi) +$$
$$\sum_{l=0}^{\infty} f_l r^l \sum_{m=-l}^{l} M_l^m \, Y_l^m(\theta,\varphi) \quad (45)$$

where the coefficients f_l, called reaction field coefficients, have the following form:

$$f_l = -\frac{(l+1)(\epsilon - 1)}{l + (l+1)\epsilon} \frac{1}{a^{2l+1}} \quad (46)$$

$Y_l^m(\theta,\varphi)$ are the spherical harmonic functions, whereas M_l^m is a multipole moment of the solute charge distribution. Note that an explicit use of the boundary conditions at $r \rightarrow \infty$ (eqs 10 and 11) has been made here. The second term of eq 45 represents the solvent reaction potential acting on the portion of space occupied by the solute.

The QM reformulation of the problem given by Rivail consists of using quantum mechanical approaches to compute the elements of the multipole expansion of ρ_{M} and in introducing the corresponding V_r terms in the Hamiltonian to get a new solvent-modified ρ_{M}, until convergence. This process, as in the ASC methods, is of iterative nature.

(ii) Rivail and co-workers rapidly abandoned the spherical cavity of the first formulation of the model to pass to ellipsoids. The shape of the cavity is a critical factor in continuum methods, and surely an ellipsoidal cavity, with its variable parameters, is more suited than a sphere to describe solvent effects on molecules. To do this extension, Rivail's group was compelled to develop a part of the mathematical theory on multipole expansions (in terms of ellipsoidal harmonics), which was almost completely neglected before. We shall use now the simplified notation introduced by Rivail and valid for both ellipsoids and spheres.

The solute−solvent interaction energy can be written in the form

$$W_{\mathrm{MS}} = \sum_l \sum_m M_l^m \, R_l^m \quad (47)$$

where R_l^m is the component of the reaction field corresponding to multipole moment M_l^m. There is a

linear relationship between each (lm) element of the charge distribution expansion and the corresponding element of the reaction potential, namely

$$R_l^m = \sum_{l'} \sum_{m'} f_{ll'}^{mm'} M_{l'}^{m'} = f_{ll'}^{mm'} M_{l'}^{m'} \qquad (48)$$

where we have introduced the Einstein convention of summation over the repeated indices. The coefficients $f_{ll'}^{mm'}$ are the generalization of the reaction field coefficients f_l defined in eq 46; we note, in fact, that for a sphere values of $f_{ll'}^{mm'}$ are no longer dependent on m and are nonzero only when $l' = l$. Also, in the more general case of an ellipsoid the coefficients $f_{ll'}^{mm'}$ have an analytical expression depending only on the geometrical parameters of the cavity and on the dielectric constant. The Nancy MPE codes now in use truncate the multipole expansion to l_{max} = 6. Only recently have results with a larger l_{max} been published.[55]

(iii) The reaction field components, expanded over a set of centers I, J, ... have the following expression

$$R_l^m(I) = \sum_J f_{ll'}^{mm'}(I,J) M_{l'}^{m'}(J) \qquad (49)$$

whereas the analogue of eq 47 is

$$W_{MS} = \sum_{I,J} M_l^m(I) f_{ll'}^{mm'}(I,J) M_{l'}^{m'}(J) \qquad (50)$$

In this more general case of a multicenter expansion, the reaction factors $f_{ll'}^{mm'}$ do not have an analytical form and have to be computed numerically using the classical electrostatic conditions at the boundary of the cavity.

In the latest version of the Nancy MPE method,[145] the ellipsoidal cavity has been abandoned, shifting to a molecular-shaped cavity such as that used in PCM. For this cavity, the number of points selected to fix the reaction factors is relatively large (usually of the order of 1500 or more), but this large amount of numerical values (quite simply individually computed, however) is efficiently compacted into linear equations, put into a matrix form, and solved with standard methods. The large number of points ensures rotational stability with respect to the selection of sampling points, a problem that disturbs other similar fitting procedures, such as the definition of the ESP atomic charges, that is, the charges fitted on the electrostatic potential, and some early versions of PCM.

Another point of general methodological interest in this latest version of the Nancy MPE code involves the selection of the multipole multicenter distribution. Because the partition is arbitrary, there is an infinite number of ways of defining the distribution, but they are not equivalent from a computational viewpoint. The literature on intermolecular interaction is rich with proposals and debates about the choice of the multipole distribution. Rivail and co-workers have selected and tested three different distributions. In the first, called GAD (Gaussian averaged distribution), each multipole is distributed

over the N centers (the number of centers corresponds to the number of nuclei) with a Gaussian weight, with the translation expressed in terms of solid harmonics. In the second, called MSP (Mulliken−Sokalski−Poirier), use is made, for the electronic component, of the one-electron integrals of the pertinent $\chi_\mu^* \chi_v$ elementary charge distribution for the multipole moment operator, namely

$$M_l^m(I) = \sum_{\mu \in I} \sum_{v \in I} P_{\mu v} \langle \mu | \hat{M}_l^m | v \rangle \qquad (51)$$

This expression is similar to that used in preceding one-center versions of the method. The zeroth order moment is taken equal to the Mulliken charge of the atom.

In the last expansion, called LSP, use is made of the Lowdin orthogonalization procedure applied to expression 51.

All three expansions are convergent, but GAD and MSP have a better convergence, MSP being the less time-consuming. The solvation code is accompanied by analytical derivatives with respect to the nuclear coordinates,[145,147] a feature essential for the performance of geometry optimizations in solution (see section 6.1.1).

We conclude this section by noting that this recent re-elaboration of the Nancy MPE code shows that previous criticisms about the unreliability of MPE codes for large molecules are not justified. Indeed, results are obtained that are of comparable quality to those of ASC codes and still with comparable computational times.

2.3.3. Generalized Born (GB) Approaches

The GB methods can be considered as an extreme case of multicenter MPE, with multipoles truncated at the first term, the charge, and the centers of expansion placed on all of the nuclei.

The name comes from an affiliation with the old Born model, which gives the interaction free energy of a spherical ion inside a dielectric[148]

$$\Delta G = -\frac{q^2}{2a} \left(\frac{\epsilon - 1}{\epsilon} \right) \qquad (52)$$

where a is the sphere radius.

The passage from a single sphere to a multiplicity of interacting spheres, each with a charge at its center, required a considerable amount of ingenuity. Earlier versions of the GB approach were described in the 1994 review, and we start here from the definition given by Still and co-workers[149] of an empirical Coulomb operator $1/f_{GB}$ that has to be applied to all pairs q_i and q_j of atomic solute charges, namely, by generalizing the free energy (eq 52) to

$$\Delta G = -\left(\frac{\epsilon - 1}{\epsilon} \right) \sum_{i,j=1} \frac{q_i q_j}{2 f_{GB}} \qquad (53)$$

The expression of f_{GB} was not defined uniquely in this

seminal paper, but a simple effective expression was given

$$f_{GB} = \sqrt{r_{ij}^2 + \alpha_{ij}^2 \, e^{-D_{ij}}} \qquad (54)$$

where $\alpha_{ij} = (\alpha_j \alpha_i)^{0.5}$ is the geometrical mean of the pertinent pair of the so-called generalized Born radii α_i (which may be interpreted roughly as the distance from each atom to the dielectric boundary). The exponent $r_{ij}^2/2\alpha_{ij})^2$ is a damping factor between the charges placed on atoms i and j, leading smoothly to the Born formula, when the spheres are separated and placed at very large distances among them, and to the normal Coulomb operator, when two spheres merge.[150]

We note that when eq 53 is applied to a two-dielectric system in which the set of charges occupies a molecular cavity with a dielectric constant ϵ_p surrounded by a uniform high-dielectric continuum environment with a dielectric constant ϵ_w, the prefactor becomes $(1/\epsilon_p - 1/\epsilon_w)$. An internal dielectric of $\epsilon_p = 1$ is appropriate for simulations when dipole fluctuations occur explicitly as part of the model. A larger internal dielectric constant is more appropriate when the energies of minimized or averaged structures are evaluated.

A fundamental problem arising in the GB approach, and present in all of its successive formulations, is the definition of the appropriate Born radii α_i.[151−155]

For every charged atom i, the effective Born radius α_i is related to the effective Born free energy of solvation, ΔG_i, of a reference system through the Born formula (eq 52), where the reference system is, by definition, the same as the original solute/continuum solvent system, except that in the reference system atom i bears unit charge and all other atoms are neutral. Exact calculation of α_i for every charged atom in a macromolecule through numerical solution of the Poisson−Boltzmann equation is time-consuming and of little practical use. The potential of GB models has come from the progress in the formulation of approximate methods to compute α_i with sufficient accuracy and efficiency. An analytical formula proposed by Qiu et al.[156] forms the basis of several recent parametrizations and applications of the GB model for protein systems.[150,157−160] In Qiu's work, the parameters contained in the formula have been optimized to minimize the differences between the effective Born radii calculated by the finite difference Poisson−Boltzmann (FDPB) method (see section 2.3.5) and by formula 53. Besides the approach of Qiu et al., Hawkins et al. have proposed another approximate pairwise method to compute the effective Born radius analytically.[161,162]

There are many different GB models, and still they are the subject of active research, especially in the simulation of macromolecules[150,163−165] such as nucleic acids and proteins. Here, we obviously cannot mention all of them and analyze their specificities. Moreover, most of these models are formulated within classical descriptions and thus are beyond the scope of the present section (see section 7.1 instead).

GB methods have been also successfully applied to QM descriptions of the solute.

The best known and more widely used QM GB method is that developed by Cramer and Truhlar in Minneapolis.[166] This method has been elaborated and distributed in a large variety of versions, with different names. At present, these models are collected under the collective name SMx, where x stands for an alphanumeric code indicating the version, with its specific features (the most used recent codes are SM5.42R and SM5.43R), but in the past other names were used such as AMSOL. In one of the most recent papers[167] 19 versions of the method are reported, but other versions are not present in this list.

The first versions known under the name AMSOL were all developed for various semiempirical methods (AMSOL still refers to a semiempirical code[168]), whereas the SMx suite of programs permits ab initio QM calculations at several levels of the theory.[169−172] Some SMx programs are available in the GAMESS-PLUS,[173] which is an add-on module to the GAMESS,[97,98] and in HONDOPLUS[174,175] program. The latest version of the method is called SMx-GAUSS,[176] and it may use Gaussian output files or be connected with Gaussian 03[17] to exploit the many features this last program contains. The objective of making the SMx method more accessible to users is not the only, nor the main, reason for so large a number of versions. The real reasons will be shown later in this subsection.

We have not yet examined how the solvation electrostatic problem is linked to the QM one in continuum methods. This will be done in detail in section 2.4, but it is convenient to anticipate here some aspects to better present the SMx models.

The Fock operator of the solute in vacuo (for simplicity we limit ourselves to the Hartree−Fock case, even if SMx codes can treat higher levels of the quantum molecular theory) is modified by a solute−solvent interaction potential describing the electrostatic interaction according to the GB model, that is, in terms of atomic charges q_i and of the modified Coulomb operator (see eq 53). The q_i charges are derived from the solute electronic wave function via a population analysis performed in different ways in the various versions of the method. First, Mulliken populations were used, then Löwdin charges, and finally charges that according to the Cramer and Truhlar definitions are of classes III and IV. The class IV charges[177] are derived from Mulliken NDDO charges with a mapping to better describe physical observables. Energy minimization cycles in the so-defined Fock equation lead to self-consistent modification of the set of q_i charges and to the introduction of solvent polarization in the solute (see also section 2.4.5 for further comments). The free energy of the electronic polarization, called G_P, can be so computed.

Another term of the free energy difference with respect to the isolated molecule is also computed. This term, called ΔE_{EN}, corresponds to the change in the electronic and nuclear energy of the solute upon relaxation from the gas-phase geometry. These two terms are combined to give the electrostatic

contribution to the solvation free energy:

$$\Delta G_{\text{ENP}} = \Delta E_{\text{EN}} + G_{\text{P}} \qquad (55)$$

We recall that, to compute the complete solvation free energy G_{sol}, other nonelectrostatic contributions have to be included in the model (see section 3). This extension has been done in the SMx set of codes by adding to the free energy of eq 55 further terms (usually indicated with the abbreviation CDS, for cavitation, dispersion, and solvent structural) proportional to the solvent-accessible surface area of the solute.

In all stages of the evolution of the Cramer–Truhlar solvation code a complete parametrization, or reparametrization, has been performed on very large data sets, generally of some thousands of solute–solvent couples, with a coupled fitting for G_{CDS} and ΔG_{ENP}. These parametrizations are quite specific in the sense that for each solvent they are specific for the type of QM calculation (AM1, PM3, HF, DFT, according to the functional, etc.), for the basis set in ab initio methods, for the definition of the q_i model (Mulliken, Löwdin, class III, class IV), for the parameters inside the coulomb operator $1/f_{\text{GB}} = g_{kk'}$ for the Born radius and for the definition of the solvent accessible surface (an alternative definition of SAS has been also given).[178] In addition, reparametrization has been also performed for specific classes of phenomena (solvent partition equilibria, solvatochromic effects, etc.). This remarkable attention to the fitting procedures explains the large number of different versions, each about a specific combination of the above-mentioned parameters of the computation. We note that the accurate documentation available for the users is a fundamental help for selecting the version of the programs best suited for a specific study.

2.3.4. Finite Element (FE) and Finite Difference (FD) Methods

The integral equation we encounter in solvation electrostatics can be solved with the FE method, which makes use of numerical solutions of the integral over the whole space, divided into a number of finite volumes, or domains, here called elements. The philosophy is similar to that of BEM, with the difference being that the reduction to surface integrals is not used here. FEM is older than BEM, and for many years it has been the approach more used in computational engineering and physics. It continues to be amply used, and for FEM (as we remarked for BEM) there is available a large wealth of elaborations that could be profitably exploited in computational chemistry.

Nowadays, FEM is widely used in many fields, such as physics and engineering, but there are also applications in computational chemistry (and in particular in the study of solvation); the best known examples are the method elaborated by Friesner's group[179–181] and implemented in the integrated suite of programs Maestro,[182] with the acronym PBF, and the adaptive Poisson–Boltzmann solver (APBS) by McCammon and co-workers.[183]

In particular, in the PBF method, the discretization of the linearized Poisson–Boltzmann (PB) problem (eq 43) is performed by expanding the electrostatic potential in a linear combination of basis functions and sampling the three-dimensional space over which the calculation is to be carried out with a set of grid points such that there is a one-to-one correspondence between the set of basis functions and the set of grid points. The coefficients of the expansion are the values of the potential at the grid vertices. This method is equivalent to that described in section 2.3.1.6, but this time the grid is over the three-dimensional space and not limited to a surface.

The finite elements are defined using a Lebedev quadrature grid combined with an accurate definition of the cavity including the re-entrant portions of the solvent accessible surface, or SAS (see section 2.2). The finite elements are defined in an adaptive way using a triangulation front-marching algorithm. The use of this three-dimensional mesh leads to a sparse system of equations that are solved iteratively. We note that the density of the corresponding matrix depends on the connectivity of the mesh, and in this three-dimensional triangulation this connectivity is local; that is, a grid vertex is coupled only to its neighbors. As a result, the system of equations to solve is sparse. This contrasts with boundary-element-based approaches in which the reduction in dimensionality achieved results in every surface element interacting with every other surface element. The resulting system of equations is therefore always dense.

The method used for calculating the polarization contribution to the solvation energy starts from the equation

$$G_{\text{pol}} = \frac{1}{2} \int_{\Gamma} \sigma V^0 \, d^3\vec{r} + \frac{1}{2} \int_{R^3_{\text{ion}}} V^0 \, d^3\vec{r} \qquad (56)$$

where Γ is the SAS, R^3_{ion} the ion accessible region, ρ_{ion} is the density of free ions in the solvent, and V^0 is the electrostatic potential produced by the fixed charge distribution of the solute. The polarization charge σ is calculated using the discontinuity of the electric field at the dielectric interface and the polarization vector, namely

$$\sigma(\vec{r}) = \frac{1}{4\pi} (\vec{\nabla} V_{\text{i}}^{\,0} - \vec{\nabla} V_{\text{e}}^{\,0}) \cdot \vec{n} \qquad (57)$$

We note that when the contribution of the free ion term to the polarization energy is extremely small compared to the reaction field term, the method coincides with the DPCM method we have described in section 2.3.1.1. In the more general case, however, the volume term remains, and the finite element discretization provides a simple scheme for evaluating this term by Gaussian quadrature.

In the numerical solution of integral equations both BEM and FEM approaches have advantages and disadvantages, but for the specific case we are now considering there are no doubts: BEM is superior for systems characterized by three-dimensional homogeneous domains (especially if infinite or semi-infinite), and this is exactly the case of dilute

solutions. We give here some reasons supporting this statement.

BEM is capable of giving values of the unknown (in our case the sources of the reaction electrostatic potential) in the interior of the domain in a pointlike form, thus avoiding the interelement continuity problems that disturb FEM applications to solvation. The reduction of the spatial problem from three to two dimensions greatly facilitates mesh refinement studies, and it leads to a system of algebraic equations much smaller than in an equivalent FEM formulation. This advantage is partly compensated by the sparcity of FEM linear equations, which is exploited in the PBF method described above.

Comparison between the two approaches could lead to different conclusions in some specific solvation cases. BEM is less efficient than FEM for systems with one or two spatial dimensions extremely small with respect to the others but dimensionally effective, as is the case of bicontinuous liquid systems. BEM has difficulties in treating problems exhibiting rapid changes in the physical properties of a domain. This last problem has been excellently solved in solvation chemistry for the inhomogeneities and anisotropies of the molecules inside the cavity, but, for example, it remains a problem for the solvent anisotropies due to nonlinear dielectric saturation.

Although BEM and FEM aim at giving a numerical solution of the integral equations, the FD methods aim at solving the differential equations. The differential equation to solve is, once again, the basic electrostatic PB problem (eq 43); we note that, with FD methods, also the nonlinear version of such an equation can be solved.

The FD methods have a long history in continuum solvation, and they are very popular, especially in classical version making no explicit use of QM methods.[184−186]

In these approaches, a discrete approximation to the governing partial PB differential equations is obtained through a volume-filling grid. Ideally, a boundary-conforming grid (i.e., one that does not intersect the molecular surface) is preferred, but such a grid is difficult to generate for a complex molecular shape. Therefore, in most implementations, such as the widely used UHBD[187] (University of Houston Brownian Dynamic)[188−190] and DelPhi[191] code (now included in Insight II package),[192,193] a regular lattice is laid over the molecule and cells are allowed to go over the molecular surface. A regular lattice arrangement is also useful for an efficient multigrid solution technique for solving the algebraic equations resulting from the discretization of the partial differential equations.[194]

A further FDM approach has been developed by Bashford, and it has been implemented in a computational code known as MEAD (macroscopic electrostatics with atomic detail).[195] The MEAD electrostatic model has been coupled with QM techniques: an inner region containing the active-site atoms is treated quantum mechanically, whereas the surrounding region is treated as a classical electrostatic system that generates a reaction field and, possibly, a field due to permanent atomic charges of the protein. This technique has been used to calculate redox properties[196] and pK_a values.[197]

There are many similarities between FE and FD methods. In both cases, a grid of points covering the space is defined. In FE procedures, these points have to be considered as representative points of a finite three-dimensional domain, and in the FD procedures, nodes in which the differential equation has to be solved. In addition, the finite element method differs from the finite difference approach in that variational principles rather than finite difference approximations are used to derive the discrete equations.[198,199] A major reason for adopting a finite element approach is that it accommodates unstructured grids, which offer improved geometric flexibility and variable mesh spacing, albeit at considerably higher per-node storage and CPU costs than a regular lattice arrangement.

2.4. Solution of the Quantum Mechanical Problem

As described in section 1, the Hamiltonian appearing in the Schrödinger equation of the basic model is the effective Hamiltonian of eq 3, namely

$$\hat{H}_{eff}|\Psi\rangle = E|\Psi\rangle \qquad (58)$$

This effective Hamiltonian is composed by two terms, the Hamiltonian of the solute H_M^0 (i.e., the focused part M of the model) and the solute−solvent interaction term $\hat{V}^{int}$ (i.e., the solvent reaction potential);

$$\hat{H}_{eff} = \hat{H}_M^0 + \hat{V}^{int} \qquad (59)$$

The definition of $\hat{V}^{int}$ depends on the method employed to set the electrostatic problem, which has to be solved within the framework of the QM eq 58.

To describe this procedure in more detail let us first consider an intuitive formulation of the problem.

2.4.1. Intuitive Formulation of the Problem

Being interested in a QM problem, let us introduce the currently used Born−Oppenheimer (BO) approximation, which relies on a partition of the solute variables into electronic and nuclear coordinates.

The solute charge distribution is conveniently divided into electronic and nuclear components $\rho_M(r) = \rho_M^e(r) + \rho_M^n(r)$. We recall that the QM procedure does not affect the nuclear component of ρ_M, although it will modify the electronic component with respect to a starting provisional definition. This modification is done in an iterative way under the action of $\hat{V}_{int}$, which is in turn modified in the iterative cycle.

Let us look now at the structure of $\hat{V}_{int}$ in eq 59. This operator can be divided into four terms having a similarity with the two-, one-, and zero-electron terms present in the solute Hamiltonian.

To show it in an intuitive way, we consider the solute−solvent interaction energy U_{int} given as the integral of the reaction potential times the whole charge distribution ρ_M.

The interaction potential has, as sources, the two components of ρ_M, and thus it is composed of two terms, one stemming from the electronic distribution of the solute M and one from its nuclear distribution.

U_{int} can thus be partitioned into four terms

$$U^{\text{int}} = U^{\text{ee}} + U^{\text{en}} + U^{\text{ne}} + U^{\text{nn}} \qquad (60)$$

where U^{xy} corresponds to the interaction energy between the component of the interaction potential having as source $\rho_M^x(r)$, namely, $\hat{V}_{\text{int}}^x$, and the charge distribution $\rho_M^y(r)$.

As in all QM applications to molecular systems, the solution of the Schrödinger eq 58 is based on an expression of the unknown wave function Ψ in terms of molecular orbitals expressed over a finite basis set $\{\chi\}$. Within this framework, it is convenient to consider the ρ_M^e charge distribution expressed as sums of contributions due to the elementary charge distributions $\chi*_\mu\chi_\nu$, whereas $\rho_M^n(r)$ is

$$\rho_M^n = \sum_\alpha^{\text{nucl}} Z_\alpha \delta(r - R_\alpha) \qquad (61)$$

Following this formalism, three different QM operators appear, namely, $\hat{V}^{\text{nn}}$, $\hat{V}^{\text{ne}}$ (it may be shown that U^{ne} and U^{en} are formally identical), and $\hat{V}^{\text{ee}}$. These correspond to zero-, one-, and two-electron operators appearing in H_M^0, respectively. We note that the zero-order term gives rise to an energetic contribution U^{nn}, which is analogous to the nuclei–nuclei repulsion energy V_{nn} and, thus, it is generally added as a constant energy shift term in H_M^0. The conclusion of this analysis is that we have intuitively defined four operators (reduced in practice to two, plus a constant term) which constitute the operator $\hat{V}_{\text{int}}$ of eq 59.

Before proceeding further in this presentation, we note that this analysis has a direct link with the ASC approaches, but it is valid also for the MPE methods, with minor changes, and for the FE and FD methods, as well. Note that the QM versions of the last two approaches describe the interaction potential in terms of cavity apparent surface charges, and thus they exploit the same features of ASC methods. By contrast, for GB methods the formal setting is different. These methods reduce, in fact, the solute density function to atomic charges that are treated in terms of the generalized Coulomb operators we have already introduced (see section 2.2.3).

2.4.2. Electrostatic Operators

The next step consists of solving the QM problem with the determination of the electrostatic interaction operators nested within it. It is convenient now to make explicit use of the apparent surface charges, because they simplify the exposition; as stated above, this does not represent a real restriction as almost all of the QM solvation methods follow the same basic pattern.

The most naive (and transparent) formulation of the process of mutual interaction between real and apparent charges is that used in the first version[48] of DPCM. We recall it here, even though it was already presented in the 1994 review, as helpful in the understanding of the basic aspects of the mutual polarization process.

One starts from a given approximation of ρ_M^e (let us call it ρ_M^0) that could be a guess, or the correct description of ρ_M^e without the solvent, and obtains a provisional description of the apparent surface charge density, or better, of a set of apparent point charges that we denote here $\{q_k^{\text{o,o}}\}$. These charges are not correct, even for a fixed unpolarized description of the solute charge density, because their mutual interaction has not been considered in this zero-order description. To get this contribution, called mutual polarization of the apparent charges, an iterative cycle of the PCM eq 20 (including the self-polarization of each q_k) must be performed at fixed ρ_M^0. The result is a new set of charges $\{q_k^{\text{o,f}}\}$, where f stands for final. The $\{q_k^{\text{o,f}}\}$ charges are used to define the first approximation to V_{int}, and a first QM cycle is performed to solve eq 58. With the new ρ_M^1 the inner loop of mutual ASC polarization is performed, again giving origin to a $\{q_k^{1,\text{f}}\}$ set of charges. The procedure is continued until self-consistency.

We remark that, in this formulation, we have collected into a single set of one-electron operators all of the interaction operators we have defined in the preceding section, and, in parallel, we have put in the $\{q_k\}$ set both the apparent charges related to the electrons and nuclei of M. This is an apparent simplification as all of the operators are indeed present.

It is interesting here to note that this nesting of the electrostatic problem in the QM framework is performed in a similar way in all continuum QM solvation codes, including GB methods, in which there is an iterative updating of the atomic charges during the QM cycle.

We report here the Schrödinger equation of the ASC version of the basic model with the introduction of a new formalism to make the exposition more general:

$$\hat{H}_{\text{eff}}|\Psi\rangle = [\hat{H}_M^0 + \hat{\rho}_r^e \hat{V}_r^R + \hat{\rho}_r^e \hat{V}_{rr'}^R \langle\Psi|\hat{\rho}_{r'}^e|\Psi\rangle]|\Psi\rangle = $$
$$E|\Psi\rangle \qquad (62)$$

With the superscript R we indicate that the corresponding operator is related to the solvent reaction potential and with the subscripts r and rr′ the one- or two-body nature of the operator. The convention of summation over repeated indexes followed by integration has been adopted. The emphasis given in this formula to the density operators is related to a formal problem arising in focused models: the main component of the system, M, interacting with the remainder does not have a wave function satisfying all of the rules of canonical QM. Only the density function has a more definite status (see ref 200 for comments on this point). For this reason we use only density operators and expectation values in expression 62.

The $\hat{\rho}_r^e \hat{V}_r^R$ operator describes the two components of the interaction energy we have previously called U^{en} and U^{ne}. In more advanced formulations of continuum models going beyond the electrostatic description, other components are collected in this

term as we shall show in section 3. $\hat{V}_r^R$ is sometimes called the *solvent permanent potential*, to emphasize the fact that in performing an iterative calculation of $|\Psi\rangle$ in the BO approximation this potential remains unchanged.

The $\hat{\rho}_r^e \hat{V}_{n'}^R \langle \Psi | \hat{\rho}_{r'}^e | \Psi \rangle$ operator corresponds to the energy contribution, which we previously called U^{ee}. This operator changes during the iterative solution of the equation. $\hat{V}_{n'}^R$ is said to be the *response function of the reaction potential*. It is important to note that this term induces a nonlinear character to eq 62. Once again, in passing from the basic electrostatic model to more advanced formulations, other contributions are collected in this term as we shall show in section 3.

The constant energy terms corresponding to U^{nn} and to nuclear repulsion are not reported in eq 62.

Following a historical hierarchy to get molecular wave functions, we introduce here the Hartree−Fock (HF) approach. The generalization to the density functional (DF) approach is straightforward; the only thing to add is the proper exchange correlation term instead−or together, if specific hybrid DFs are used−of the HF one. Extensions to post-HF methods will be described in section 2.4.5.

In this framework we have to define the Fock operator for our model. As before, we adopt here an expansion of this operator over a finite basis set $\{\chi\}$, and thus all of the operators are given in terms of their matrices in such a basis.

The Fock matrix reads

$$\mathbf{F} = \mathbf{h}^0 + \mathbf{G}^\circ(\mathbf{P}) + \mathbf{h}^R + \mathbf{X}^R(\mathbf{P}) \qquad (63)$$

The first two terms correspond to $\hat{H}_M^0$, the third to $\hat{\rho}_r^e \hat{V}_{n'}^R$, and the last to $\hat{\rho}_r^e \hat{V}_{n'}^R \langle \Psi | \hat{\rho}_{r'}^e | \Psi \rangle$.

We take for granted the reader's familiarity with the standard HF procedure and formalism. We recall that all of the square matrices of eq 63 have the dimensions of the expansion basis set and that $\mathbf{P}$ is the matrix formulation of the one-electron density function over the same basis set. According to the standard conventions $\mathbf{P}$ has been placed as a sort of argument to $\mathbf{G}^0$ to recall that each element of $\mathbf{G}^0$ depends on $\mathbf{P}$. For analogy, we have made explicit a similar dependence for the elements of $\mathbf{X}^R$.

We remark that also the standard HF equation is nonlinear in character and that in the elaboration of this method its nonlinearity is properly treated. The new term $\mathbf{X}^R(\mathbf{P})$ adds an additional nonlinearity of different origin but of similar formal nature, which has to be treated in an appropriate way. This fact was not immediately recognized in the old versions of continuum QM methods, giving origin to debates about the correct use of the solute solvent interaction energy. This point will be treated later, in section 2.4.4.

Notice that, as in the previous analysis of the Schrödinger eq 58, in the Fock matrix expression (eq 63) we have used a single term to describe the one-electron solvent term. We remark, however, that in the original formulation two matrices, $\mathbf{j}^R$ and $\mathbf{y}^R$, were

used, namely

$$j_{\mu\nu}^R = \sum_k V_{\mu\nu}(\vec{s}_k) q^n(\vec{s}_k) \qquad (64)$$

$$y_{\mu\nu}^R = \sum_k V^n(\vec{s}_k) q_{\mu\nu}^e(\vec{s}_k) \qquad (65)$$

In both expressions the summation runs over all of the tesserae (each tessera is a single site where apparent charges are located), $V_{\mu\nu}(s_k)$ is the potential of the $\chi_\mu^* \chi_\nu$ elementary charge distribution computed at the tessera's representative point, $V^n(s_k)$ is the potential given by the nuclear charges, computed again at the same point, $q^n(s_k)$ is the apparent charge at position s_k deriving from the solute nuclear charge distribution, and $q_{\mu\nu}^e(s_k)$ is the apparent charge at the same position, deriving from $\chi_\mu^* \chi_\nu$. The two matrices (eqs 64 and 65) are formally identical, as said before, and thus in eq 63 we have replaced them with the single matrix

$$\mathbf{h}^R = \frac{1}{2}(\mathbf{j}^R + \mathbf{y}^R) \qquad (66)$$

We note that in computational practice, the more computationally effective expression (eq 64) is generally used.

The elements of the second solvent term in the Fock matix (eq 63) can be put in the form

$$X_{\mu\nu}^R = \sum_k V_{\mu\nu}(\vec{s}_k) q^e(\vec{s}_k) \qquad (67)$$

with

$$q^e(\vec{s}_k) = \sum_{\mu\nu} P_{\mu\nu} q_{\mu\nu}^e(\vec{s}_k) \qquad (68)$$

In this way, we have rewritten all of the solvent interaction elements of the Fock matrix in terms of the unknown q^e and q^n apparent charges (the last, not being modified in the SCF cycle, can immediately be separately computed).

2.4.3. Outlying Charge

In the previous sections we have introduced a phenomenon always present when we use a QM description of the solute charge density, namely, the phenomenon we have previously designated "escaped" or "outlying" charge. This is due to the fact that a portion of the electronic charge of the solute is always lying outside any cavity of reasonable size.

In all methods that exploit cavities and boundaries to separate solute and solvent domains and QM charge distributions to describe the solute, this effect should be taken into account, but it becomes particularly significant in ASC methods, or better in the older formulations of the ASC methods. Let us try to better understand this statement.

ASC methods based on the standard definition of the apparent surface charge σ in terms of the polarization vector and thus of the normal component of the electric field at the boundary Γ (see eqs 19 and

20) should, in fact, satisfy the Gauss theorem, namely

$$\int_\Gamma \sigma(\vec{s})\,\mathrm{d}\vec{s} = -\frac{\epsilon - 1}{4\pi\epsilon}\int_\Gamma \vec{E}(\vec{s})\cdot\vec{n}(\vec{s})\,\mathrm{d}\vec{s} = -\frac{\epsilon - 1}{\epsilon}Q_M$$

(69)

where Q_M is the total charge of the solute (i.e., zero for neutral solutes). This equation is indeed a very simple and direct numerical test to check the amount of the outlying charge; in fact, if the sum of the apparent point charges, that is, the discretized form of the left-hand integral above, does not fulfill eq 69, then we can assume that the discrepancy is due to the portion of the electronic charge of the solute lying outside the cavity.

Since the very first formulation of PCM (i.e., the D version of this model described in section 2.3.1.1), this possible discrepancy was recognized and strategies were introduced to correct the apparent charges so that eq 69 was satisfied. These strategies were called "renormalization of the apparent charge", and they simply consisted in spreading an additional $\Delta q'$ charge over the tesserae, with a simple recipe trying to respect the correct spatial distribution of the surface charges (in a dipolar molecule, for example, there are positive and negative regions of the apparent charge). The various formulas corresponding to the different strategies can be found in the 1994 review, in which some typographical errors of the original PCM paper[48] were corrected.

For several years this renormalization was considered to be sufficient, taking into account the moderate quality of the ab initio calculations possible at that time. Variants were elaborated by others, but presented no advantages (the interested readers may find a synopsis in the 1994 review). Things changed in the 1990s: the availability of more powerful computers and progress in ab initio methods made it possible to extend the QM solvation codes to more ambitious goals, in particular, geometry optimizations and calculation of molecular response properties (see section 6). To reach these goals, there is the need of accurate codes for the analytic evaluation of derivatives with respect to the nuclear coordinates as well as to external parameters: both types of derivatives are sensitive to the outlying charge. Therefore, the research on this subject acquired a more oriented and practical objective.

To have an appropriate perspective of the outlying charge problem, it is convenient to compare it with that of ionic solutions. In both cases there is a real charge distribution out of the cavity, but the ion charge distribution is distributed in the whole medium, and it has a zone of zero density just around the cavity surface, whereas the solute electronic "tails" rapidly decrease from the cavity surface going to larger distances and they give origin to a volume polarization effect limited to a small region encircling the solute. In general, this density is anisotropic, in the sense that its intensity (and its decaying with the distance) changes in different portions of the cavity surface, being strictly related to the charge distribution of the nearby solute's groups. The problem of the outlying charge, and of the connected

volume polarization, appears to be more delicate to treat than that of ionic solutions.

In addition to this electronic outlying charge, there are other possible sources for the discrepancy of the apparent charges with respect to the Gauss law (eq 69). These are related to the implementation of the computational procedure, in particular, the number and relative positions of the sampling points, and to the expressions used to define the mutual polarization of the apparent charges. For this reason, in 1995 the two components of the solute charge distribution, electrons and nuclei, started to be considered as two different sources of apparent charges, which in turn were separated into two sets, each one checked with the proper Gauss law.[50] Nuclei, in fact, are surely within the cavity, and they do not exhibit outlying charges, so in this case the discrepancy has to be attributed to the numerical aspects. Actually, we found that such discrepancy for the nuclei-induced apparent charges depends on the accuracy in the tessellation (density of points) and on the local geometry of the surface. The main source of these errors could be eliminated by using denser meshes, and in fact in the most recent versions of the ASC methods (such as those implemented in the Gaussian[103] suite of programs) the number of tesserae has significantly increased with respect to the older versions with a parallel increase in the accuracy of the results: now the nuclear contribution to the error on the apparent charges is much smaller than the electronic one. Obviously, the same numerical errors occur also in the electronic apparent charges, and so a new renormalization scheme of the apparent charge was introduced, in which two distinct corrections were used for nuclei-induced and electron charges.[50]

This improvement in renormalization, however, was not sufficient to completely eliminate the unwanted effects due to outlying charge. A direct attack to the problem, without resorting to empirical corrections and based on the integration of the volume potential, was undertaken by the PCM group, by Klamt, and by Chipman.

Within the DPCM approach, an application of the BEM procedures to build up a double-charge model taking into account also the outlying charge was explored by two of the present authors.[86] Applying electrostatic laws, the presence of the outlying charge should give origin to an apparent (or bound) charge distribution ρ_b in the volume of the dielectric

$$\rho_b(\vec{r}) = -\frac{\epsilon - 1}{\epsilon}\rho_M(\vec{r}) \text{ for } r \text{ outside } C$$

(70)

where ρ_M is the real charge distribution out of the cavity. For what was said above about the fast decay of ρ_M, to get a good representation of ρ_b one should use a very refined partition of the volume with an extremely fine grid of points. To overcome this difficulty, we resorted to a mathematical treatment. As here, it is important to describe the effects that the apparent volume charge exerts on the solute, that is, the values of the corresponding reaction potential inside the cavity; then, such reaction potential can be mimicked by that due to an additional apparent surface charge. By using the discretization procedure

used in standard ASC methods, this new procedure leads to a second set of charges, placed at the same points as the original ones. The dimension of the problem is left unchanged, because the two sets of surface charges are put on the same locations, and their sum can be used in defining the reaction potential.

This method has been considered by some as a novel renormalization procedure, but actually it is based on a development of the electrostatic model releasing one of the constraints we set at the beginning of this section and giving for the added feature, the outlying charge, a treatment in line with the BEM.

A parallel approach was proposed by Klamt and Jonas[201] within the COSMO model: after a normal COSMO calculation an additional cavity is constructed around the solute molecule lying at an appropriate distance further from the original one. By calculating the potential arising on the segments of this outer cavity from the solute and the COSMO screening charges on the inner cavity, a further set of charges is obtained and added to the primary ones to get the correct solute−solvent interaction energy.

All of these approaches were subsequently overcome by the elaboration of the IEF method (see section 2.3.1.3), which opened new perspectives for the description of outlying charge effects. This aspect of IEF was clearly expressed only in 2001[202] spurred by the important analysis performed by Chipman starting from 1997.[81−84] In particular, in an article appearing in 2000 in the *Journal of Chemical Physics*, Chipman[203] proposed and examined a new tractable formulation to get an accurate approximation of volume polarization effects arising from the escaped charge without making a calculation in the outer volume. Following a strategy similar to that in the method described above,[86] his proposal was to add to the standard ASC density an additional surface charge density giving rise, inside the cavity, to an electrostatic potential approximately equivalent to that arising from the apparent (or bound) charge $\rho_b(r)$. In this way, as most of the solute electrons are actually confined inside the cavity, the most important effects of the volume polarization are kept, and the computational effort is limited because only surface charges are used. This proposal was translated into a model, namely, the SS(V)PE model we have described in section 2.3.1.4.

As said before, the SS(V)PE and IEF models (when rewritten in terms of the potential only) are formally equivalent; the analysis started by Chipman, and continued by Cances and Mennucci, has clearly shown that both of these models, contrary to DPCM or other ASC methods, take into account the effects arising from the outlying charge. Besides the obvious greater accuracy in the representation of the reaction field, this specificity has also an immediate practical consequence, namely, that IEF and SS(V)PE do not need any renormalization of the surface charge.

2.4.4. Definition of the Basic Energetic Quantity

To use the solution of the QM equations in continuum solvation methods, some important formal aspects have to be reconsidered. To better understand these specificities, it is convenient to start from a brief summary of what is done in QM calculations of an isolated molecule.

The Fock operator

$$\mathbf{F}^0 = \mathbf{h}^0 + \mathbf{G}^0(\mathbf{P}) \tag{71}$$

is used to determine the function $|\Psi_{HF}^0\rangle$ corresponding to the variational approximation to the exact wave function for the system specified by $\hat{H}^0$. This correspondence is determined by minimizing the appropriate energy functional $E[\Psi]$, namely

$$E_{HF}^0 = \langle \Psi_{HF} | \hat{H}^0 | \Psi_{HF} \rangle \tag{72}$$

or, in a matrix form

$$E_{HF}^0 = \mathrm{tr}\, \mathbf{Ph}^0 + \frac{1}{2}\mathrm{tr}\, \mathbf{PG}^0(\mathbf{P}) + V_{nn} \tag{73}$$

where we have used the same formalism used in section 2.4.2 and we have introduced the trace operator ("tr"). Obviously, the nuclear repulsion energy, V_{nn}, in the BO approximation is a constant factor. We remark that in eq 73 there is a factor of $^1/_2$ in front of the two-electron contribution. This factor is justified in textbooks by the need to avoid a double counting of the interactions, but this double counting has its origin in the nonlinearity of the HF equation.

Let us now pass to continuum models. As before, also here the new Fock operator defined in eq 63 determining the new solution $|\Psi_{HF}^S\rangle$ is obtained by minimizing the appropriate functional. However, now, the kernel of this functional is not the Hamiltonian $\hat{H}_{eff}$ given in eq 59 but rather $\hat{H}_{eff} - \hat{V}_{int}/2$, and thus the energy of the system is given by

$$G_{HF}^S = \left\langle \Psi_{HF} \left| \hat{H}_{eff} - \frac{1}{2}\hat{V}_{int} \right| \Psi_{HF} \right\rangle \tag{74}$$

that, expressed in a matrix form similar to that used for E_{HF}^0, reads

$$G_{HF}^S = \mathrm{tr}\, \mathbf{Ph}^0 + \frac{1}{2}\mathrm{tr}\, \mathbf{PG}^0(\mathbf{P}) + \frac{1}{2}\mathrm{tr}\, \mathbf{P}(\mathbf{j} + \mathbf{y}) +$$
$$\frac{1}{2}\mathrm{tr}\, \mathbf{PX}(\mathbf{P}) + V_{nn} + \frac{1}{2}U_{nn} \tag{75}$$

where the solvent matrices, $\mathbf{j}$, $\mathbf{y}$, and $\mathbf{X}$, are those defined in section 2.4.2 (here we have only dropped the "R" superscript).

We have added half of the solute−solvent interaction term related exclusively to nuclei, which in the BO approximation is constant.

Similar expressions hold for other levels of the QM molecular theory: the factor $^1/_2$ is present in all cases of linear dielectric responses; for this reason, in the following, we shall drop the HF index.

The reason for the change of the functional we have introduced lies in the nonlinear nature of the effective Hamiltonian. This Hamiltonian has in fact an explicit dependence on the charge distribution of the solute, expressed in terms of ρ_M^e, which is the one-body

contraction of $|\Psi_{HF}^S\rangle\langle\Psi_{HF}^S|$, and thus it is nonlinear. It must be added that this nonlinearity is of the first order, in the sense that the interaction operator depends only on the first power of ρ_M^e. The model is in fact based on an approximation motivated by physical considerations. The solvent reaction field has, in general, a relatively low strength, and thus a linear response regime is sufficient to describe its effects. For this reason, the expansion of the interaction potential in powers of the reaction field is limited to the first order in almost all of the continuum methods. In other words, it may be said that these methods treat the linear aspect of a nonlinear problem. True nonlinear solvation effects are, however, present. Generally, they are treated in other ways, for example, making reference to phenomenological concepts, such as dielectric saturation or electrostriction, and directly using higher terms in expansion of the interaction potentials (more details on these aspects will be treated in section 4).

Some comments about nonlinearities in the Hamiltonian are here added. This subject is rarely treated in an explicit way in quantum chemistry, despite the large use of the Fock operator, which is nonlinear, and, in the case of ionic solutions, of the use of the Poisson−Boltzmann approach, which also leads to a nonlinear problem. The case we are considering here is called scalar nonlinearity (in the mathematical literature it is also called "nonlocal nonlinearity"):[204] this means that the operators are of the form $P(u) = \langle Au, u\rangle Bu$, where A and B are linear operators and $\langle .,.\rangle$ is the inner product in a Hilbert space. The literature on scalar nonlinearities applied to chemical problems is quite scarce (we cite here a few papers[7,205−210]), but the results justified by this approach are of universal use in solvation methods.

Let us now come back to eq 74. Attentive readers will have noticed that we have changed the symbol for the energy. The symbol G emphasizes the fact that this energy has the status of a *free energy*. The explicit identification of the functional (eq 74) with the free energy was first done by Yomosa,[205] to the best of our knowledge. In the 1994 review alternative justifications for the factor $^1/_2$ in the expression of the energy were given, deduced from the perturbation theory, by statistical thermodynamics and by classical electrostatics, all valid for a linear response of the dielectric. We report here only a consideration based on classical electrostatics. Half of the work spent to insert a charge distribution (i.e., a molecule) into a cavity within a dielectric corresponds to the polarization of the dielectric itself, and it cannot be recovered by taking the molecule away and restoring it in its initial position. This half of the spent work is irreversible, and it has to be subtracted from the energy of the insertion process to get the free energy (or the chemical potential).

2.4.5. QM Descriptions beyond the HF Approximation

In the past few years, a large effort has been devoted to extending solvation models to QM techniques of increasing accuracy. In this way, models originally limited to the Hartree−Fock level can be now used in many post-SCF calculations. This com-putational extension has been accompanied by a reformulation of the various QM theories so as to include the specifics of the solvation model. Such a requirement is particularly pressing for those models in which an effective Hamiltonian is introduced. Electron correlation is more commonly introduced into these techniques using CI or MCSCF and DFT methods.

DFT does not require any specific modification with respect to the formalism presented in the previous section, as far as concerns the solvation terms, and thus there are numerous examples of DFT applications of continuum solvation models. As a matter of fact, continuum solvation methods coupled to DFT are becoming the routine approach for studies of solvated systems.

Applications of continuum solvation approaches to CI or MCSCF wave functions have quite a long history. In 1988 Mikkelsen et al.[134] presented a MCSCF version of their multipole approach (see section 2.3.2) first limited to equilibrium solvation and then extended to nonequilibrium descriptions[137] (see section 5) and to response methods[136] (see section 6). A similar history is presented by the family of PCM approaches, which have been first applied to equilibrium[211] (including gradients[212]) and nonequi-librium[78,213,214] and subsequently to the response method.[215]

Also, configuration interaction (CI) approaches soon attracted the interests of researchers working in the field of solvation methods.[205,216−218] In this case, however, some delicate issues not present for isolated systems appear.

As remarked by Houjou et al.,[219] an important point to analyze is the physical meaning given to the excitation energy of solvated systems when obtained directly from the CI calculation. Karelson and Zern-er[220] have indicated that the solvent effect is incorporated "automatically" into the CI only by adding solute−solvent interaction term(s) to the Fock matrix for the in vacuo state, whereas the resulting excitation energy must be corrected for the electronic relaxation and for the costs required for the polarization of solvent. Similarly, Klamt derived the correction term corresponding to the electronic relaxation, denoted "electronic screening correction" in ref 221, and the diagonal correction in the CI matrix.

In addition, the nonlinear dependence of the solvent reaction field operators on the solute wave function introduces a new element of complexity. In a CI scheme, this nonlinearity is solved through an iteration procedure; at each step of the iteration, the solvent-induced component of the effective Hamilto-nian is computed by exploiting the first-order density matrix of the preceding step. The main consequence of a correct application of this scheme is that each electronic state, ground and excited, requires a separate calculation involving an iteration optimized on the specific state of interest. This procedure has been adopted by Mennucci et al.[78] in their IEFPCM-CI approach as well in the successive extension to multireference CI wave functions (including pertur-bative corrections)[222] within the framework of the CIPSI method.[223−225]

Other examples of correlated ab initio solvent methods have employed Møller−Plesset (MP2) or coupled cluster (CC) theory for the description of the electronic structure of the solute.

Perturbation theory within solvation schemes has been originally considered by Tapia and Goscinski[7-] at the CNDO level. An ab initio version of the Møller−Plesset perturbation theory within the DPCM solvation approach was introduced years ago by Olivares et al.[226−231] following some intuitive considerations based on the fact that the electron correlation which modifies both the HF solute charge distribution and the solvent reaction potential depending on it can be back-modified by the solvent. To decouple these combined effects, the authors introduced three alternative schemes: (1) the non-iterative "energy-only" scheme (PTE), in which the solvated HF orbitals are used to calculate MPn correlation correction; (2) the density-only scheme (PTD), in which the vacuum MPn density matrix is used to evaluate the reaction field; and (3) the iterative (PTED) scheme, in which the correlated electronic density is used to make the reaction field self-consistent. With regard to the last scheme, some further comments are required. The PTED scheme leading to a comprehensive description of the effects separately considered by PTD and PTE is rather cumbersome and not suited for the calculation of analytical derivatives, even at the lowest order of the MP perturbation theory. In addition, it has been shown that a rigorous application of the perturbation theory, in which the nth-order correction to the energy is based on the $(n − 1)$th-order density, the correct MP2 solute−solvent energy has to be calculated with the solvent reaction field due to the Hartree−Fock electron density.[232,233] This means that the PTED scheme at the MPn level is not in analogy with standard vacuum Møller−Plesset perturbation theory as terms of higher than nth order are included.

Other MP2-based solvent methods consist of the MP2-PCM,[234] the Onsager MP2-SCRF,[132] and a multipole MP2-SCRF model,[235] Subsequently, still in the PCM framework, MP2 gradients and Hessians have been developed.[234,236]

In recent years CC methods have proven to be among the most successful electronic structure methods for molecules in a vacuum. Despite this large spreading of CC methods, there has not yet been a parallel effort to extend them to introduce the interactions between a molecule and a surrounding solvent. The only example appearing so far in the literature is the CCSCRF developed by Christiansen and Mikkelsen,[141] using the multipole solvation approach described in section 2.3.2; the same scheme has been also extended to CC response method including both equilibrium and nonequilibrium solvation.[140]

To conclude this brief overview, we cite some recent and less recent extensions of continuum models to the valence bond (VB) method.

One of the first successes in incorporating solvation effects into a VB method was the empirical valence bond (EVB) method formulated by Warshel and Weiss in 1980.[237] However, at the beginning of the 1990s Kim and Hynes[238−240] developed a method for calculating the electronic structure of a solute and its reaction pathways, in a manner that incorporates nonequilibrium and equilibrium solvation effects within a continuum approach. Later, Amovilli et al.[211] presented a method to carry out VB analysis of complete active space-self-consistent field wave functions in aqueous solution by using the DPCM approach.[14] Another method of the same family of solvation methods, namely, IEF of section 2.3.1.3, has recently been used to develop an ab initio VB solvation method.[241] According to this approach, to incorporate the solvent effect into the VB scheme, the state wave function is expressed in the usual terms as a linear combination of VB structures, but, now, these VB structures are optimized and interact with one another in the presence of a polarizing field of the solvent. The Schrödinger equation for the VB structures is solved directly by a self-consistent procedure. This iterative scheme is exactly equivalent to that described above for CI wave functions.

3. Some Steps beyond the Basic Model

The presence of nonelectrostatic terms in the interaction between a solute and the surrounding solvent was well-known to the pioneers of the first QM solvation models (see section 1). In fact, the first model proposed by Claverie in 1972 addressed dispersion terms only,[5] and Rivail in his first attempt in 1973[6] included both electrostatic and dispersion terms.

In our exposition we have privileged the electrostatic term. Historically, continuum models mainly derive from the seminal models of Kirkwood and Onsager, which paid attention mostly to the electrostatic term, and this particular attention to electrostatics has been maintained in the successive elaboration of methods, of both classical and QM types. The practical reason for this is that water surely is the most important liquid medium, and for dipolar solvents the dominant term in the solute−solvent interaction is the electrostatic one. In many codes nonelectrostatic terms are considered as corrections to the dominant term for which a cursory description may be considered to be sufficient. In many published studies, it must be added, nonelectrostatic terms are completely ignored.

Actually, the nonelectrostatic terms cannot be cursorily treated, or ignored, in a good solvation method. There is a delicate balance between electrostatic and nonelectrostatic energy components, of opposite sign, that must be accurately evaluated both in the polar and in the nonpolar solvents in order to have descriptions which could lead to severely biased predictions of properties.

We shall examine now the nature and basic characteristics of these nonelectrostatic interaction terms.

3.1. Different Contributions to the Solvation Potential

The analysis we shall sketch here is not limited to continuum models but also involves discrete solvation

models. Differences between the two approaches will be commented on at the appropriate place.

The basic information on the nature of molecular interactions giving origin to the solvent effect derives from the theoretical analysis and interpretation of the interactions occurring in molecular clusters.

There is an extremely large literature on this subject, covering a span of more that 50 years, that cannot be summarized here. Studies have progressed from simple systems, dimers composed of two very simple molecules, increasing step by step the number of components of the aggregate and the internal complexity of the molecules. Several aspects of these studies are pertinent to our subject, but we shall limit ourselves to the basic information derived from bimolecular associations, complemented by some aspects derived from the analyses of trimers and larger aggregates.

The interaction energy between two molecules A and B can be expressed as the difference between the energy of the supermolecule and that of the two separate partners:

$$\Delta E(AB) = E(AB) - E(A) - E(B) \qquad (76)$$

This energy has been analyzed in a significant number of cases using a variety of techniques based on perturbation theory approaches as well as variational techniques. The details and the variants among the different approaches are not of interest here. What is of interest is to examine a partition of $\Delta E(AB)$ into terms each having a physical interpretation and the possibility of being individually computed. This partition reads

$$\Delta E(AB) = E_{coul} + E_{pol} + E_{exc} + E_{dis} + E_{CT} \qquad (77)$$

The Coulomb term, E_{coul}, is defined as the electrostatic energy among the two unperturbed (i.e., not polarized) partners. This term is very sensitive to the mutual orientation of the two partners and strongly anisotropic at short distances. The interaction may be positive or negative and, for a given A–B system, it may change sign according to the orientation when at least one of the two molecules has a (local) charge distribution with a dipole. The Coulomb energy continues to be numerically important also at large monomer separations; actually, it is the term having the highest long-range character. The typical distance dependency is R^{-1}.

The polarization term, E_{pol}, has its origin in the mutual electrostatic polarization of the two charge distributions, and it is everywhere negative. At short monomer separations, it is moderately anisotropic, being sensitive to the mutual orientation of the two partners. E_{pol} has a relatively long-range character: the typical distance dependency is R^{-4}. $E_{pol}(AB)$ can be easily decomposed into two terms, the polarization of A under the influence of B, $E_{pol}(A \leftarrow B)$, and the polarization of B under the influence of A, $E_{pol}(B \leftarrow A)$.

The exchange term, E_{exc}, is related to the presence in the QM formulation of intermonomer antisymmetrizer operators, which ensure the complete antisymmetry of the electrons in the AB dimer. Complete antisymmetry means to introduce repulsion forces between the electron distribution of the monomers related to the Pauli exclusion principle. E_{exc} is positive for every orientation of the partners, roughly proportional to the mutual overlap of the two charge distributions, and rapidly decaying with the distance. The typical distance dependency is dictated by a R^{-12} term.

The dispersion term, E_{dis}, can be related to dynamical effects, as the formation of an instantaneous dipole moment in a monomer due to the motion of the electrons. This dipole polarizes the charge distribution of the other partner and gives origin to an interaction energy similar in some sense to E_{pol}. It is a distinct phenomenon, however, and must be separately treated. Dispersion energies are negative, relatively weak, and decaying as R^{-6}.

The charge transfer term, E_{CT}, is not present in the standard analyses of ΔE based on perturbation theory, whereas it appears in the decompositions based on the variational approach [i.e., starting from the variational calculation of the $E(AB)$ energy] in a form that seems to be a bit artificial, being present also in symmetric AA dimers under the form of monomer contributions which cancel each other. In chemistry, charge transfer effects are quite important in large classes of chemical reactions; these, when considered under the viewpoint of a theory addressing the general characteristics of solutions, belong to the category of "rare events", and they will not be treated here. However, we also note that small amounts of charge transfer, not related to chemical reactions, can play a role in assessing solvent effects on some molecular properties, and in the elaboration of solvation models we have surely to pay attention to these interactions even if, at present, they have attracted very limited attention (see section 3.2.4).

This very schematic presentation of the decomposition of dimeric interactions is far from being complete, and our presentation of decomposition results should be extended to the more complex analyses performed on trimers and larger aggregates. As a matter of fact, here we shall be even more concise, reporting only the conclusions that seem more interesting for liquids.

(1) There are no new types of interactions to include in the model. Specific interactions, often invoked or described with empirical ad hoc formulas, as, for example, hydrogen bonds, are in this approach described in terms of the contributions we have already presented.

(2) All of the contributions, with the exception of E_{coul}, are nonadditive, and the weights of such nonadditivity ares very different for the different terms. The larger nonadditivity, both in weight and in range, is that due to the polarization energy. Molecules in an assembly are strongly influenced by mutual many-body polarization effects. The nonadditivity of exchange is in se very short-ranged. The nonadditivity of dispersion is moderate and plays an important role in some special cases only, as, for example, in clusters composed of rare gas atoms in which classical electrostatic terms are zero. The nonadditivity of charge transfer has been less stud-

ied. It should be a relatively short-range effect, especially for the energy.

3.2. Use of Interactions in Continuum Solvation Approaches

We have now the elements to give a more detailed appraisal of the use of these interactions in the continuum description of solute−solvent interactions. Among the various solvation methods, reference will be made mostly to the PCM, which is the most complete in this field, and to GB methods (see section 2.3.3) that have paid much attention to the consideration of nonelectrostatic terms.

Continuum methods start from the definition of a liquid, the pure solvent, equilibrated at the given macroscopic conditions (temperature and pressure, for instance). The solute molecule must be inserted within this liquid. This specific aspect of continuum models gives rise to a problem that can be solved by introducing in the definition of the overall intermolecular interaction energy (see eq 77) the concept of the energy of formation of a suitable cavity within the liquid. We shall call it G_{cav}.

The other contributions to the interaction energy can be collected into three terms, named electrostatic, repulsion, and dispersion. There are some changes with respect to the partition given in eq 77. Coulomb and polarization terms are grouped together; the separate calculations of the two contributions can be done (and it has been done in the first DPCM version), but this separation is of no practical help in the QM calculations. In any case, it may be used for more detailed analyses about the origin of the interactions. The repulsion term takes into account the presence of the cavity; the physical origin of the term is unchanged, but all solvent molecules are kept out of the cavity. The dispersion term, too, is left unchanged, and it involves interactions with solvent molecules out of the cavity.

We have now the elements to write the interaction energy decomposed into four terms, the three we have just mentioned and the cavity formation term. Before doing this, we have, however, to consider two additional points.

The first is related to the use of ab initio QM methods. These methods give the molecular energy measured with respect to a quite peculiar reference, that is, noninteracting electrons and nuclei. The second point to consider is related to the existence of free energy contributions due to other degrees of freedom which are present in the focused model but are neglected in the BO approximation we have used so far. These degrees of freedom are related to the thermal motions of nuclei. We shall call G_{tm} the corresponding free energy contribution. More comments will be made below, but we may now give an explicit definition of the energy in continuum ab initio models and of the solvation free energy, two related but not identical concepts.

Definition 1: Free Energy of the Solution in ab Initio Continuum Models. The energy of a system composed by a liquid and a solute is defined making reference to an ideal system composed of the pure liquid at equilibrium under given values of the macroscopic parameters (pressure, temperature) and by the appropriate number of noninteracting electrons and nuclei necessary to describe the solute and at zero kinetic energy. Putting the energy of the reference system equal to zero, the free energy of the solution at the equilibrium is given by the following expression:

$$G = G_{el} + G_{rep} + G_{dis} + G_{cav} + G_{tm} \qquad (78)$$

The definition of the solvation free energy given below can be considered as a supplementary definition drawn from eq 78, but it is the primary definition for computational methods, which do not allow an evaluation of the solute molecular energy. This is the case for computational procedures based on semiempirical QM methods or the use of classical models.

Definition 2. Solvation Free Energy. The solvation free energy, measured with respect to a system composed of the pure unperturbed liquid at equilibrium and by the solute molecule(s) in a separate phase considered as an ideal gas, is given by the following expression:

$$\Delta G_{sol} + \Delta G_{el} + G_{rep} + G_{dis} + G_{cav} + \Delta G_{tm} + P\Delta V \qquad (79)$$

If we define $\Delta G_{el} = G_{el} - G^0$, where $G^0 \equiv E^0$ is the ab initio energy of the isolated molecule in the BO approximation and G_{el} is the analogous quantity computed in solution, we may obtain the first term of eq 79 from ab initio calculations. ΔG_{el} can be computed directly in all non ab initio calculations. The term ΔG_{tm} of eq 79, being a difference between two analogous terms related to the molecule in solution and in the gas phase, may be simpler to compute than the G_{tm} term in eq 78 because any partial contributions cancel each other at a good extent. This fact is often exploited when calculations address solvation energy problems.

In definition 2 we have paid a bit more attention to the thermodynamic definition of the reference state. The reason the $P\Delta V$ term was not inserted in definition 1 will be mentioned later (section 3.2.6).

The second comment involves the internal geometry of the solute. In passing from the gas phase to the solution there is always some change in the internal geometry, which often cannot be neglected when the definition $\Delta G_{el} = G_{el} - G^0$ is used. This problem does not exist for definition 1 because no reference is made to molecules in the gas phase in eq 78. Semiempirical and classical models should consider the energy term due to changes in the equilibrium geometry, but this sometimes is not done.

The first three terms in the right-hand side of eq 78 can be computed all at the same time with a unique QM calculation based on the appropriate Schrödinger equation, or they can be computed separately with semiclassical models. G_{cav} must be computed separately; the same holds for G_{tm}. It is worth remarking that contributions to the free energy due to thermal motions of nuclei are separately treated also in the QM descriptions of isolated molecules; the same standard techniques (largely simplified with respect to a full QM treatment, rarely

used) are employed for molecules both in gas phase and in solution.

The inclusion of nonelectrostatic terms (namely, the cavity formation term, G_{cav}, and the attractive van der Waals solvent−solute interaction terms, G_{vdW}) in GB methods described in section 2.3.3 is generally done in terms of an empirical function based on the surface area of the solute. For this reason, the GB methods are often denoted with the GB/SA abbreviation.[156] In particular, the GB/SA model computes $G_{cav} + G_{vdW}$ together by evaluating solvent accessible surface areas

$$G_{cav} + G_{vdW} = \sum_{k=1}^{N} \sigma_k(SA_k) \qquad (80)$$

where SA_k is the total solvent accessible surface area of all atoms of type k, and σ_k is an empirically determined atomic solvation parameter.

The effort of defining parameters, and of fixing their appropriate numerical values, is an exacting task, amply repaid, however, by the computational efficiency of the method.

In a specific family of GB methods, namely, that of the SMx models developed by Cramer and Truhlar described in section 2.3.3, the nonelectrostatic contributions are described in terms of an empirical expression, which has been differently parametrized in the different versions of the model. We refer here to the universal solvation model, which is "universal" in the sense that a unique code offers options for a large number of solvents of different type, each with its own set of parameters. The SM5.42R and SM5.43R codes we have mentioned in section 2.3.3 are of universal type. In this framework, the nonelectrostatic part of the solvation free energy, usually indicated as G_{CDS}, depends on a fitting over six solvent descriptors: the refractive index (at the wavelength of the Na D line), Abraham's hydrogen bond acidity and bond basicity parameter,[242] the reduced surface tension, the square of the fraction of non-hydrogenic solvent atoms that are aromatic carbon atoms (carbon aromaticity), and the square of the fraction of non-hydrogenic solvent atoms that are F, Cl, or Br (electronegative halogenicity). More details can be found in the already cited paper.[167]

We now examine the separate components first and then give the unified QM definition of the procedure based on a Hamiltonian collecting all of the interaction terms.

3.2.1. Cavity Formation Energy

The idea of formally breaking the process of transfer of a molecule from the gas phase to a liquid into two steps, first the formation of a cavity in the bulk of the liquid and then the insertion of the molecule in the cavity, dates back to 1937.[243] The balance between the reversible work of these two steps gives, according to this model, the excess free energy of the process or, in other words, the solvation free energy. This device to evaluate solvation energy has been used for many decades, without resorting to detailed molecular descriptions of the system.

The different formulations of methods to compute the energy of cavity formation have been amply described in the 1994 review,[1] to which readers are referred. There are reasons, however, to reconsider this subject in the present review.

There is no physical counterpart to this ideal formation of an empty cavity, and as a consequence, there are no experimental values to compare with the results of the models. Actually, no direct checks are possible for any of the contributions into which the solvation energy can be divided, and this fact makes harder the task of getting an accurate modeling of the property in which all of the components have a well-defined meaning. This accuracy in the elaboration of the model is a necessary step to go beyond models limited to the appraisal of solvation energy. There are many other properties to study and many other applications of continuum solvation models, for which accurate descriptions of the separate contributions to the solvation effects are necessary. There are also methods that combine cavity formation energy with other short-range interaction terms: this is a different philosophy to formulate continuum solvent models, reasonable, efficient, and giving good results for properties more directly related to the solvation energy. If extensions of the models belonging to this category to other properties are to be sought, the empirical expressions in use will require modifications.

With regard to the cavity formation energy, the attempts to arrive at reliable values for G_{cav} have a probability of success relatively higher than for the other terms, because the interaction potentials are simpler in this case. The way to get these reliable values is based on the use of computer simulations of liquids, a subject we examine here below.

3.2.1.1. Computer Simulations and G_{cav} Values. A strategy to get G_{cav} values via computer simulations is far simpler than similar strategies for the other components of the solvation energy. G_{cav} in fact depends on the solvent only, and the number of solvents, even if large, is far smaller than the number of possible combinations of solute−solvent systems. For each solvent, the number of degrees of freedom to scan in a systematic way is limited: the macroscopic variables (T and P, for example) and the size and shape of the cavity.

There are several fields in chemistry in which the evaluation of the energy of formation of a microscopic cavity is of interest. Some among them involve cases in which a cavity is spontaneously formed under the action of an external agent; we cite as examples the formation of cavities (or microbubbles) under the action of ultrasound[244] and bubble formation at liquid−solid interfaces,[245] topics of remarkable conceptual and practical interest, but to which our continuum models have not yet been applied. It seems to us appropriate to reserve the expression "cavitation energy" (used in the older literature on solvation models) to phenomena in which real cavities are formed and to use for our cavities, which represent a formal ideal step in solvation, the expression "cavity formation energy".

The cavity formation energy, in the meaning used by Uhlig in 1937,[243] plays an important role in the theory of hydrophobicity. We shall not review hydrophobicity theories here, because they encompass continuum models, and we shall consider hydrophobic solvation only as a specific case of the more general field of solvation phenomena. This remark is not out of line here, because the majority of available calculations of G_{cav} via computer simulations[246−270] have been motivated by hydrophobicity studies, and this introduces a bias to the definition of the simulation, inasmuch as the interests of hydrophobicity are not coincident with those of general solvation.

In fact, from simulations we would have information about a large number of topics, necessary to model methods for the calculation of G_{cav} for the whole domain of solvation problems. The topics of interest range from the chemical nature of the solvent and of its physicochemical properties to the physical macroscopic characteristics of the liquid (temperature, pressure, and also externally applied factors, as electric fields and hydrodynamic flows), to the form of the cavity that must faithfully reproduce the extreme variety of sizes and shapes solutes have.

It would be extremely convenient to have a satisfactory analysis of these factors before we begin to develop G_{cav} computational methods. Parenthetically, we remark that we need analyses and not tables of specific values, because in the chemical applications addressed by continuum models there is often the need of examining the whole solvation free energy, and hence G_{cav}, for a sizable number of solute geometries. It would be impractical and in contradiction with the basic philosophy of continuum models to use computer intensive methods, as simulations are, to compute a single element of the solvation energy at each geometry of the solute. Simulations are to be mainly used as validation tests of simpler expressions describing G_{cav} and are better if they are of analytical type.

Of course, this complete analysis has not been performed, but the available simulations have been of great help in assessing the relative merits of the various methods we shall examine in the remainder of this section.

There are at present a sizable number of G_{cav} values from simulations for small cavities, in general spherical but with a few examples of nonspherical cavities,[258,262] in various solvents. These latter simulations are mostly due to Hofinger and Zerbetto,[269−271] who have recently added to the half score of solvents considered in the past 12 additional solvents, all of chemical relevance. Some of these simulations also give information about temperature and density dependence. These results validate the guesses made years ago (and discussed in the following pages) about the general validity of some simple models, dispelling doubts and criticisms and ending inconclusive discussions.

One may wonder why after more than 30 years of computer simulations only now is there a satisfactory situation (at least for small cavities). One reason is that only in recent years has progress in computational machineries permitted a more efficient evaluation of G_{cav} values. In 1998 Levy and Gallicchio[272] remarked that the intensive computational demand of simulations raised obstacles to the systematic study of solvation in the preceding years. Now the situation is greatly improved, and we are expecting from simulations additional help, especially for larger cavities and for liquids far from the standard thermodynamic state.

We cannot wait, however, and to proceed we have to base our decisions on other criteria such as indirect analyses of the large wealth of G_{cav} values computed with simpler models.

The most extensive analyses performed thus far are, to the best of our knowledge, those performed by the Luque and Orozco group in Barcelona. We refer interested readers to one[273] of their papers as it reflects the evolution of the cavity formation methods over the past 10 years.

In our 1994 review[1] we analyzed a variety of methods; many have been abandoned and, in fact, only two approaches have been considered in successive papers: those based on statistical mechanics and those based on the area of the solute exposed to the solvent. Here we shall consider both approaches.

3.2.1.2. Statistical Mechanics and G_{cav} Values.

The elaboration of PCM has strongly relied on statistical methods to supplement the basic electrostatic code.[274] For the cavity formation two approaches have been presented, one based on the cavity surface and the other, which is the subject of this section, based on a statistical mechanics approach, namely, the scaled particle theory (SPT), introduced and elaborated over the years by Reiss.[275,276] We may anticipate that the analytical expressions of G_{cav} obtained from the SPT version give values in good agreement with numerical simulations.

This is not the appropriate place to fully explore the great merits of the statistical mechanics methods for our understanding of the properties of liquids. A short comment is, however, necessary to put SPT, and the use we are making of this theory, in the appropriate context.

Statistical mechanics methods encountered difficulties in passing from gases to liquids, and to overcome these difficulties very simplified models were adopted. What is of interest here involves the reduction of the fluid particles (atoms or molecules) to hard spheres, neglecting the portion of the interaction called the soft portion (i.e., the electrostatic and dispersion terms which, in this review, we are more interested in). Hard sphere models were extensively used to study the various aspects of the theory for fluid systems. Actually, the detailed and satisfactory description of the properties of the hard sphere fluids was found to be unable to provide numerically acceptable estimates of the properties of real fluids. The connection between the worlds of hard spheres and of real liquids was given by the SP theory, a model based on hard spheres again, but with radii suitably modified with a scaling procedure to satisfy some macroscopic experimental quantity. SPT is a rigorous theory (in the sense that there are no

additional adjustable parameters), trading its efficiency in giving numerical results comparable with experiments with a loss of generality with respect to the formally exact hard sphere model.

Here, we are not interested in studying the general properties of liquids, nor the applications of SPT as a general albeit simplified theory for liquids, but in the specific application of SPT to define the free energy of formation of a cavity. Cavity formation indeed is the starting point of SPT. Work is required to exclude the centers of molecules from any specified region. A cavity is defined as a region in which the centers of the solvent molecules, described as hard spheres of radius RS, are excluded. The radius of the cavity is $R_{MS} = R_S + R_M$, where R_M is the radius of the hard sphere representing in our case the solute. The reversible work necessary to form this cavity is computed with an application of the so-called charging process, in which an integration is performed on the internal energy of the system in terms of a continuous parameter λ ranging from 0 to 1. Here the parameter λ is related to the radius of the inserted particle, put equal to zero at $\lambda = 0$ and arriving at R_M at the upper limit of the integration. Two parameters are necessary to determine the reversible work required to make this cavity, the ratio of the two hard sphere radii R_M/R_S, and the reduced number density of the solvent $\rho = N/V_s$ (where N and V_s are, respectively, Avogadro's number and the molar volume of the liquid) entering in the auxiliary function y:

$$y = \frac{\pi}{6}(2R_S)^3\rho \qquad (81)$$

The analytical form of the free energy of cavity formation was given by Pierotti in terms of an expression in terms of RMS truncated at the third order.[277−279] The complete Pierotti expression can be found in his original papers as well as in our 1994 review.[1] We report here the somewhat simplified form used in PCM:

$$G_{cav} = RT\left\{ -\ln(1-y) + \frac{3y}{1-y}\left(\frac{R_M}{R_S}\right) + \left[\frac{3y}{1-y} + \frac{9}{2}\left(\frac{y}{1-y}\right)^2\right]\left(\frac{R_M}{R_S}\right)^2 \right\} \quad (82)$$

The simplifications we have introduced are due to the negligible values of the contributions related to the pressure P for liquids at ambient pressure (see comments, e.g., in ref 255).

The enthalpy of cavity formation can also be computed within this approach. The simplest way is to use the Helmholtz equation

$$H_{cav} = G_{cav} - T\left(\frac{\partial G_{cav}}{\partial T}\right)_P \qquad (83)$$

with an appropriate evaluation of the derivative.[280] We note, however, that careful attention has to be paid to the enthalpy and entropy values obtained in such a way. There is in fact a sizable literature about limitations and defects in the Pierotti-derived for-

mulas for entropy and enthalpy. Free energy is a more robust quantity, and an indiscriminate use of entropies and enthalpies obtained by stressing the initial conditions set in Pierotti's papers is to be avoided or performed after an accurate scrutiny of these remarks.

Actually, little is left of the original SPT in the current use of Pierotti's formulas for the calculation of G_{cav} made in continuum solvation methods. Alternative formulations, closer to the SPT model, encounter some problems. For example, SPT defines a hard sphere pressure for the liquid, which may be very different from the actual pressure experienced by the real liquid one is simulating. This fact introduces a dilemma in the definition of G_{cav} (see Tang and Bloomfield[281] for a detailed and critical analysis of these problems).

The main reason that the formulas in use are only loosely related to the original SPT derivation lies in the definition of the hard sphere radii. As mentioned above, SPT radii are not exactly the hard sphere radii used in the early statistical treatments of monatomic fluids (which were addressing real atoms deprived of all "soft" interactions) but rather formal sphere radii calibrated on a property of the real fluid. In principle, SPT hard spheres are not limited to spherical (or almost spherical) solvent molecules, and in fact the theory has been applied also to liquids composed of molecules far from sphericity, such as benzene or n-hexane. The essential point is that SPT reduces the interparticle interaction to an isotropic form in which directional properties are mediated (and soft interactions are neglected in the initial step of application of the method).

Hard spheres describing the properties of liquids have been obtained by making reference to a variety of experimental data, such as those measuring vapor pressure,[276] compressibility,[282] heats of vaporization,[279,283] surface tension,[284] and solubility[285] and from the cell theory of liquids.[286] To be rigorous, not all of the cited papers report hard sphere radii obtained with SPT; some are related to other elaborations of experimental data bearing some similarity with the SPT. In particular, use if often made of two different equations of state, the so-called Boublik−Mansoori−Carnahan−Starling−Leland (BMCSL)[287,288] or the simpler Carnahan−Starling (CS)[289] valid for a single-component fluid, which are considered to be superior to the SPT in predicting the free energy of solvation in a hard sphere fluid.[290]

There are available several collections of hard sphere radii. Noteworthy are those given by Ben-Amotz and Willis[291] (supplemented by group volume increments) and the two given by Y. Marcus.[292,293] Also note that different sources give different values for the hard sphere radii. For water, for example, the radii range from 1.25 to 1.58 Å, and Tang and Bloomfield[281] cite eight different papers using different radii.

To these hard sphere radii we may add others derived from models elaborating experimental data with spherical potentials containing also a separate soft interaction component The most famous model is the (6-12) Lennard-Jones (LJ) model. There is a

wealth of LJ values in the literature. This variety of numerical values could raise doubts in a potential user, but the situation is not as bad as it might appear. Two remarks are in order. The first is that it has been argued[285,294−296] that the most consistent radii to use in SPT studies are those obtained with Pierotti's technique, and in fact the radii for water obtained by fitting results of independent computer simulations are in a restricted range around the value given by Pierotti. The second remark is that we are here not interested in a full use of the SP theory nor in other possible applications such as the definition of the solvent accessible surface (see section 2.2) for which the hard solvent radius is used, but solely in the solvent radius to use for the calculation of G_{cav}. We shall come back to this last point after examining the other face of the problem, that is, the definition of the radius for the solute.

The variety of solutes a continuum solvation model should be able to describe is so large that compilations of hard sphere radii, even if supplemented by group increments, will never be sufficient. The solution to this problem has been found by abandoning SPT and making reference to another molecular model, that of van der Waals radii. Chemists are well accustomed to using van der Waals radii, which have a longer history than SPT hard spheres and have been empirically defined in a large variety of ways. There is no unique set of van der Waals radii, but successive refinements confirm the substantial validity of the older compilations (see section 2.2). In addition, there are reliable computational techniques able to give independent descriptions of the molecular van der Waals surfaces and also indirect hints that may be used to compute G_{cav} values.

We have now arrived at defining solute shapes, and the corresponding cavities, in terms of atomic or group interlocking spheres, related to van der Waals values. To do this G_{cav} calculation, a further step is still necessary. The geometrical quantity given by van der Waals-like models of a generic solute does not correspond to the spherical shape considered in Pierotti's formula.

The direct use of a cavity modeled in terms of interlocking spheres for the calculation of G_{cav} according to Pierotti's scheme has been performed by Irisa.[297] Limiting ourselves for the moment to solutes of small size, there are two reasonable ways of reducing an irregular van der Waals envelope to a sphere; they consist of defining the radius R_M of this sphere in terms of the surface S_M of the envelope or in terms of its volume V_M:

$$R_M = \sqrt{\frac{S_M}{4\pi}} \qquad (84)$$

$$R_M = \sqrt[3]{\frac{3V_M}{4\pi}} \qquad (85)$$

In an already cited paper,[273] Colominas et al. examined this problem in a broader context involving the different definitions of G_{cav}. The discussion is based on the statistical analysis of actual values found with different methods in a sizable number of solutes in several solvents. For the specific question we are considering, these authors find no appreciable differences in the performances of the two definitions (called SPT-S and SPT-V, respectively) that are, on the whole, slightly superior to the other examined definitions.

Another point considered in this analysis involves the size consistency of the various procedures. Size consistency is not really relevant when the study is limited to a single molecule, but it becomes important when one considers dissociation or association processes. In both cases, the G_{cav} value should change smoothly along the coordinate describing the process. Both SPT-S and SPT-V lack this property. This point was intensely discussed in Pisa in the early 1980s until Claverie suggested a modification of Pierotti's formula, which he separately published later;[298] this modification was immediately inserted in the Pisa solvation model PCM (see section 2.3.1.1). According to this modification, the cavity formation energy is given by a sum of contributions each related to a single-sphere SPT term weighted by the area of the single sphere exposed to the solvent:

$$G_{cav} = \sum_{k=1}^{N} \frac{A_k}{4\pi R^2_k} G_{cav}(R_k) \qquad (86)$$

This formula has been called the Pierotti−Claverie expression for the cavity free energy and is indicated with the acronym C-SPT in the analysis of G_{cav} reported in the cited paper.[273] In the first implementation of formula 86, the number N of spheres corresponded to the number of atoms in the solute, and their radii were fixed in agreement with the selected definition of van der Waals parameters.[26] We note that, in successive implementations, N is not necessarily equal to the total number of solute atoms, but it can be smaller as now united-atom cavities are generally used (see section 3.2.5). Indeed, the choice of the cavity used to compute G_{cav} in continuum methods has never been uniquely determined and thus different choices have been used. To try to clarify the large number of available options, it is useful to introduce the expressions one cavity and two cavity. The first refers to all calculations in which just a single cavity is used for G_{cav} and ΔG_{el}, whereas the second refers to calculations in which two different cavities are used to compute G_{cav} and ΔG_{el} (see section 3.2.5 for more details). In general, the two-cavity calculations are to be preferred.

To conclude, we may say that statistical analyses[273] and computer simulations, in particular those performed with a molecularly shaped cavity,[258] agree in considering SPT-V and SPT-S to be the best procedures, almost equivalent and marginally better than C-SPT. The size consistency exhibited by this latter seems to us an important factor to keep, even if the price is a minor difference in the value of the cavity formation energy.

We have here sketched the present situation for small solutes for which the algorithms in use work relatively well for solvents with molecules of small size, such as water, irrespective of whether these molecules form hydrogen bonds in the bulk. For other

solvents, in particular those composed of molecules of larger size, rarely considered in theoretical modeling but often used in chemistry, little is known. Recent simulations performed by Hofinger and Zerbetto[270] on organic solvents seem to confirm the validity of the SPT procedure.

For solutes of larger size, no accurate simulations of G_{cav} are available. Studies on hydrophobicity range from very small solutes, such as rare gases and methane, to large, mesoscopic and macroscopic, bodies. The hypothesis of a crossover of two regimes for the cavity formation energy, the first scaling as the volume of the cavity and acting for small cavity radii and the second scaling as the surface and acting for larger cavities, has been strongly advocated.[266,299] The crossover from the first to the second regime should occur at a molecular length scale. Here, we suggest that for small cavities the two regimes should lead to similar cavity formation energies, but for larger cavities the scaling of G_{cav} with the surface of the solute should be more probable.

As a final note about SPT, we recall that it is not limited to spheres. Extensions of the theory to other convex shapes have been known for a long time. The readers are referred to papers by Gibbons[300] for a preliminary examination of a variety of shapes, by Cotter and Martire[301,302] and by Lasher[303] for extension to liquid crystals using spherocylinders, and by Boublik[304,305] for more analyses of the equation of state based on hard dumbbells and spherocylinders. The examples we have reported involve applications of SPT to homogeneous fluids, in which all particles have the same shape. A limited use of these models has been done thus far for continuum calculations, the only exceptions we know being the PCM studies on the determination of the cavity formation energy in nematic liquid crystals.[306]

3.2.1.3. Information Theory Method. The statistical concepts underlying SPT have been used by Pratt and co-workers[307,308] to formulate an interesting approximation to the calculation of G_{cav}.

The key point in this method is the relationship connecting the free energy of formation of a cavity with the probability p_0 of finding in the liquid an empty cavity of given size and shape:

$$G_{cav} = -kT \ln p_0 \qquad (87)$$

In this method p_0 is considered as the first member of a probability distribution where the term p_n is the probability of finding n solvent centers in the volume v corresponding to the selected cavity. To get estimates of the p_n values, use is made of simulation data (performed over a model of the bulk liquid) to get the moments of the fluctuations in the number of solvent centers. The moments of the fluctuation in the particle numbers are given by the following thermal averages:

$$\langle n^k \rangle = \sum_{n=0}^{\infty} p_n n^k \qquad (88)$$

The first three moments, namely, $\langle 1 \rangle$, $\langle n \rangle$, and $\langle n^2 \rangle$, can be obtained from experimental quantities [the

first is a constant, the second derives from the density ρ, and the third derives from the radial distribution function $g_{CC}(r)$ of the molecular centers, upon integration]; the other moments have to be derived from simulations under the normalization constraints given by the three first moments.

An approximation introduced at this point gives the name to the method: ITM, which means information theory method. Following the IT rules, it is possible to define the "best-possible" estimate of the probabilities, in the form of a set $\{p_n\}$, which maximizes the information entropy, under the constraint given by the first three moments.

This definition leads to

$$p_n = p_n^{(0)} \exp(\lambda_0 + \lambda_1 n + \lambda_2 n^2) \qquad (89)$$

where $\{p_n^{(0)}\}$ collects the set of values of an empirically chosen "default" initial model and the λ_i values are Lagrangian multipliers satisfying the moment conditions. Further details can be found in the above-cited references. It is sufficient to add that a flat default distribution (all $p_n^{(0)} = 1$, for $n \leq n_{max}$), giving rise to a Gaussian distribution, has been shown to be sufficient to give good results for the cavity formation energy, expressed in the form

$$G_{cav} = \frac{kT\rho^2 v^2}{2\sigma^2} + ... \qquad (90)$$

where σ is the standard deviation of the data used in the elaboration.

The method is not limited to the calculation of G_{cav} or to water as the liquid system. It may be considered as a new approach to study the physicochemical properties of liquids. Potentialities and limitations of the method are not yet fully explored, despite the sizable work done by Pratt and co-workers in recent years, in particular for the interpretation of the hydrophobic effect.[309] Of remarkable interest is also the formulation recently proposed by Basilevsky and co-workers,[310,311] which introduces a binomial distribution law for a number of solvent particles occupying a given volume (the cavity). The resulting distribution consists of two binomial peaks proportional to the volume and to the surface area of the cavity, respectively. This formulation is, in our opinion, an interesting way to combine cavity formation processes for small and large solutes.

3.2.1.4. Surface Tension and G_{cav} Values. As an alternative to the statistical method described in the previous section, we describe here one based on the surface of the solute exposed to the solvent.

In his seminal paper Uhlig[243] used the surface tension γ of the pure solvent to evaluate G_{cav}:

$$G_{cav} = 4\pi\gamma R^2_M \qquad (91)$$

This expression has been used for years without change, despite the progress in the understanding of curvature and microscopic effects on γ initiated around 1950[312,313] and considerably improved in more recent years in the specular problem of the surface tension for microscopic droplets. A more detailed

version of the Uhlig formula, including microscopic curvature corrections to γ, was elaborated by Sinanoglu in a series of papers spanning the period 1967–1982.[314–317] In 1981–1982 a version of the Sinanoglu models was introduced into PCM, and this code was retained in more recent versions of our program. The use of G_{cav} values obtained with this formula was, however, abandoned because the examination of the trends of this quantity with respect to some parameters (radius of the spherical cavity, temperature, pressure) was not numerically convincing.

Years later, a Monte Carlo simulation[258] showed that the corrections introduced by Sinanoglu for the microscopic curvature were actually worse than the description of G_{cav} given by surface tension without corrections. This study, in addition, indicated that the most appropriate surface to use in combination with γ to get G_{cav} lies between the van der Waals surface and the solvent accessible surface (SAS). This remark, we must stress, is based only on a single set of simulations performed on spheres of relatively small size in water.

Another approach to improve the Uhlig formula was proposed by Tuñon et al.[318] It consists of the introduction of a correction term to eq 91 based on other properties of the solvent, namely, the number density of the solvent, n_s, and the volume of a solvent molecule, V_s:

$$G_{cav} = 4\pi\gamma R^2_M - \ln(1 - V_s n_s) \qquad (92)$$

This formula is still in use and has been applied to a sizable number of studies, performed both with Rivail's MPE method[319–321] and with PCM.[53,273,322]

3.2.2. Repulsion Energy

In our interpretation of the solvation energy, G_{rep} is the portion of the steric contribution to G_{sol} after the ideal process of making the cavity has been performed. We have remarked in passing that each term of the interaction free energy, isolated or in combination with others, can be described in terms of a charging process with respect to an appropriate parameter. The parameter for G_{cav} we have selected corresponds to a length, the radius, or the combination of radii of the hard sphere cavity. This charging process produces a considerable change in the solvent distribution function; a cavity, not existing before, is now present. Ideally, according to the Uhlig model, the presence of this new element should not perturb the distribution function in the other parts of the solvent specimen. Actually, it is not so: hard sphere cavity simulations introduce a perturbation on the whole solvent distribution, because the macroscopic parameters are kept fixed in the simulation. This effect is of little entity on the whole macroscopic liquid system, and we may discard it in our considerations, as we have implicitly discarded another similar effect, that of using, for a very dilute solution, properties of the pure solvent.

The next step in our calculation of the solvation energy consists of using the solvent distribution modified by the cavity to perform the charging processes for the other components of the solvation energy. With PCM it is possible to collect all of the remaining charging processes into a single process, performed at the QM level with the aid of an appropriate Schrödinger equation. This unique feature of PCM, that is, the unification of different processes into a single step (or, in other words, to treat repulsion, dispersion, and electrostatic contributions on the same footing), considerably reduces the problem of couplings. In fact, in a series of different charging processes performed in sequence, one has to use, for the second process, the solvent distribution function modified by the first. There are couplings among charge processes that are neglected in this sequence, and the final result depends to some extent on the chosen sequence. The effect of these couplings has been little studied; an example can be found in ref 323. Almost all continuum solvation models neglect these couplings, with the exception of those, such as Cramer and Truhlar's generalized Born model (see section 2.3.3), which replace explicit calculations with numerical parameters drawn from experiment. In the other methods, an approximation is tacitly assumed: we have called it the "uniform approximation",[323] and it consists of taking the solvent distribution constant equal to that describing the bulk unperturbed solvent in all charging processes.

Having so established a common framework for all of the contributions to G_{sol}, we now examine in more detail how G_{rep} has been described. We start from the QM description, which is not used independently but combined with dispersion and electrostatic terms, as will be shown later, and we move on to nonquantum methods that permit a direct evaluation of this term.

The theory for the repulsion term derives from the theory of the exchange term as expressed in the perturbation theory treatment of noncovalent interactions. The application of perturbation theories to the description of molecular interactions is a quite complex problem, and the main source of this complexity derives from additional elements in the antisymmetry operator for the electronic wave function, which gives rise to the exchange terms. The difficulties found in describing the electron exchange are related to the difficulties quantum mechanics finds in describing a system M interacting with others. An exact expression for exchange contributions to the interaction energy is not available. There are excellent approximations that have given good results for molecular systems of small dimensions, and there is a hierarchy of descriptions introducing more and more simplifications and ending with very simple expressions. An example of this last level of accuracy is the r^{-12} term used in the Lennard-Jones site–site potential.

The expression used in PCM due to Amovilli and Mennucci[324] is based on a dissection of the exchange energy for a dimer into terms depending on the electronic densities of the partners.[325] The elaboration of this expression, derived for the interaction energy of two molecules, to get G_{rep} uses the replacement of the electron density of the second partner (the first is the solute) with a one-electron charge distribution averaged over the whole body of the solvent (the

details can be found in the reference paper). When followed by proper mathematical manipulations, this elaboration reduces the double integral over the whole space to a simple integral of the solute charge distribution lying outside the cavity C multiplied by a constant factor, namely

$$G_{rep} = \alpha \int_{r \notin C} \rho_M(\vec{r}) \, d^3r$$

$$\alpha = k\rho_S \frac{n_{val}^S}{M_S}$$

(93)

where the subscript M refers to the solute (and ρ_M indicates its electronic density), S refers to the solvent, ρ_S is the density of the solvent relative to density of water at 298 K, and n_{val}^S and M_S are the number of valence electrons and the molecular weight of the solvent, respectively.

The integral in eq 93, which represents the portion of solute charge lying outside the cavity, is rewritten as the difference of total solute electronic charge (i.e., the number of electrons) and the electronic charge inside the cavity. By applying the Gauss theorem, we obtain that the internal charge is $1/4\pi \int_\Gamma \vec{E}_M(\vec{s}) \cdot \vec{n}(\vec{s}) \, d^2s$, where $\vec{n}$ is the outward unit vector perpendicular to the cavity surface at point $\vec{s}$ and E_M the solute electric field due to the electrons only. The final step of the procedure is analogous to that used for other contributions to the solvation energy (included the classical expression of G_{rep} we shall examine below): the surface integral is reduced to a summation expressed in terms of contributions of single tesserae, defined in terms of the local value of the component of the solute electric field normal to the cavity surface. To use the same tesserae used in the calculation of the electrostatic solvation energy, which uses a cavity larger than that defined by the van der Waals radii, the single terms are scaled by a proper numerical factor.

This method permits us to introduce the repulsion contribution in the effective Hamiltonian, in the form of a new one-electron operator that we shall call $\hat{h}_{rep}$, which will be inserted in the $\hat{\rho}_r^e \hat{V}_R$ term of the definition (eq 62) of our Schrödinger equation. The presence of this operator acts to modify the solute wave function. Within the same approach used in section 2.4.2, this operator becomes a matrix defined on the chosen basis set $\{\chi\}$, namely

$$(h_{rep})_{ru} = \alpha[\mathbf{S} - \mathbf{S}^{(in)}]_{ru}$$

(94)

where $\mathbf{S}$ is the overlap matrix in the same basis and

$$S_{ru}^{(in)} = 1/4\pi \int_\Gamma \vec{E}_{ru}(\vec{s}) \cdot \vec{n}(\vec{s}) \, d^2s$$

E_{ru} being the electric field integrals on $\{\chi\}$.

Using the operator (eq 94), the repulsion contribution to the solvation free energy defined in eq 93 becomes

$$G_{rep} = \text{tr } \mathbf{P} h_{rep}$$

(95)

where $\mathbf{P}$ is the density matrix obtained by solving

the effective Schrödinger eq 62 in which we have added the repulsion term.

We have thus introduced a formulation in which the repulsion term is treated on the same footing as the electrostatic one, with a completely negligible additional computational cost, because all of the elements necessary for this new term are already present in the electrostatic calculation. This new term does not present a problem for the analytical derivatives (even if the formula has never been implemented), and it noticeably reduces the amount of the outlying solute charge.

PCM codes continue to present an alternative version for the calculation of G_{rep},[326] which we do not present here, because it was thoroughly analyzed in the 1994 review,[1] to which we refer interested readers. Here we recall only that this formulation is completely based on empirical classical potentials for the repulsion interaction and thus, in this case, repulsion effects cannot modify the solute wave function. Once again, the repulsion free energy can be written as a sum of volume integrals, which may be reduced to surface integrals, making use of auxiliary vector functions. The surface integrals are then expressed as discrete sums over the k tesserae of the cavity surface Γ, each with an area a_k:

$$G_{rep} = \rho_s \sum_{k \in \Gamma} \sum_{s \in S} N_s \sum_{m \in M} a_k \vec{A}_{ms}(\vec{r}_{mk}) \cdot \vec{n}_k$$

(96)

$$\vec{A}_{ms}(\vec{r}_{ms}) = -\frac{1}{9} \frac{d_{ms}^{(12)}}{r_{ms}^{12}} \vec{r}_{ms}$$

(97)

with sites m and s corresponding to solvent nuclei and numerical parameters d_{ms} empirically fixed with some criteria.

This classical version of the repulsion energy is faster than the QM version. As a matter of fact, its computational cost is practically zero if the tessellation of the cavity is available; otherwise, it corresponds to the cost of making this tessellation.

The molecular surface is of SAS type, that is, defined as the surface described by a rolling sphere on the molecular surface (see Figure 1). The radius of this rolling sphere should correspond to the minimal distance each site m can reach from the solute, so there is the need to define a surface for each m (for example, with methane as solvent, the sphere to the carbon atom contribution had a radius larger than that for the H contribution by an amount equal to the RCH distance).

We consider it convenient to maintain this classical version in PCM codes, because the method can also be used for semiclassical descriptions of the solute, for which an explicit solution of a Schrödinger equation is not necessary, and it would be senseless to require the use of QM algorithms for a single contribution. We remind the reader, however, that this classical version does not cooperate with the others to define the solvent reaction potential, and it cannot change the effects that this potential has on the electronic charge distribution of the solute.

3.2.3. Dispersion Energy

The dispersion energy term is often collected with the repulsion term into a unique term defining the so-called van der Waals contribution to the interaction energy. Actually, dispersion and repulsion have different physical origins, different ranges of action, different sensitivities to fine details of the electronic charge distribution, and opposite signs. It seems to us better to consider the two terms separately, both for the analysis and for the calculation.

The literature on dispersion is quite large, even larger than the abundant literature on exchange–repulsion interactions. There is no need of repeating here the detailed historical analysis presented in our 1994 review.[1] However, we recall the strong influence that a seminal set of papers by Linder[327] has had in the elaboration of QM continuum solvation models. These papers have subsequently influenced another approach formulated by Hunt[328–331] starting from the revival of a remark about the electrostatic nature of dispersion forces expressed by Feynman years ago[332] and after called "Feynman's conjecture".[333] Hunt's papers have, in our opinion, a strong connection with continuum solvation models, and thus they might be exploited soon to develop new methodologies.

We shall begin the exposition starting from the ab initio codes inserted in PCM, continuing with other QM formulations, and then finishing with simpler semiempirical recipes.

To insert dispersion terms in the Hamiltonian and thus to account for dispersion effects on the solute charge distribution and for possible coupling with other solute–solvent interactions, we need an analytical expression with explicit dependence on the solute charge density. This goal can be reached in different ways, with the introduction of some approximations.

The method implemented in PCM is based on the formulation of the theory given by McWeeny[200] and on the use of dynamic polarizabilities. The steps of the procedure adopted for PCM can be found in the source papers.[324,334] The final formula of the solute–solvent dispersion free energy in the usual framework of a molecular orbital description of the wave function reads

$$G_{dis} = -\frac{\beta}{2} \sum_{rstu} [rs|tu] P_{ru}(S^{-1})_{st} + \frac{\beta}{4} \sum_{rstu} [rs|tu] P_{ru} P_{st} \tag{98}$$

where the subscripts refer to elements of the selected basis set $\{\chi\}$.

The term $[rs|tu]$ has the aspect of a two-electron integral, but simply involves combinations of one-electron integrals in the following way

$$[rs|tu] = \frac{1}{2} \int_\Gamma d\vec{s}\, [V_{rs}(\vec{s})E_{tu}(\vec{s}) + V_{tu}(\vec{s})E_{rs}(\vec{s})] \tag{99}$$

where the integration is done on the cavity surface and V_{ab} and E_{ab} represent the potential and the normal component of the electric field computed at the same point of the surface when expressed on the chosen basis set.

The P_{ru} coefficients in eq 98 are elements of the first-order solute density matrix $\mathbf{P}$ expressed in the same basis set, $\mathbf{S}$ is the overlap matrix in the same basis, and β has the expression

$$\beta = \frac{(n_S^2 - 1)}{4\pi n_S\left(n_S + \dfrac{\omega_M}{I_S}\right)} \tag{100}$$

where n_S is the refractive index of the solvent, I_S its first ionization potential, and ω_M the solute average transition energy.

Expression 98 may be rewritten in a matrix form, making use, once again, of the trace operator and introducing two new matrices with integrals performed over the basis set

$$G_{dis} = \mathrm{tr}\, \mathbf{P}[\mathbf{h}_{dis} + {}^{1}\!/_{2}\mathbf{X}_{dis}(\mathbf{P})] \tag{101}$$

where the elements of the two matrices we have here introduced have the following form:

$$(h_{dis})_{ru} = -\frac{\beta}{2} \sum_{st} [rs|tu](S^{-1})_{st} \tag{102}$$

$$(X_{dis})_{ru}(P) = \frac{\beta}{2} \sum_{st} [rs|tu] P_{st} \tag{103}$$

The integrals defining these matrix elements (see eq 99) can be computed in a discrete form, making use of the tessellation of the cavity surface used to compute the apparent charges in PCM continuum methods.

We have to remark that the nature of β indicates the approximations introduced in this elaboration of the dispersion energy operators: among them one is specific for the solute, the average transition energy. Because the most important transitions in polarization of molecules occur between "frontier" orbitals—the highest occupied and the lowest virtual orbitals—the average transition energy can be approximated by defining a proper window around the energy of the highest occupied orbital.

The computational demand is higher for dispersion than for repulsion as the basic integrals are more complex in the dispersion term, which also includes a second term ($\mathbf{X}_{dis}$) not present in repulsion. In addition, G_{dis} turns out to be quite sensitive to the quality of the basis set; to have good values of this quantity we need to use basis sets decidedly larger that those necessary for geometry optimization and for the calculations of the other components of the solvation energy.

There are other methods, developed at various times, to get dispersion energy contributions with ab initio calculations (see the 1994 review for the complete list).

Perturbation theory, applied first to atoms and then to small molecules, led to the definition of a simple formula for the expansion of the dispersion energy between two atoms in terms of the inverse powers of the interatomic distance, with coefficients

drawn from experiments as well as from calculations:

$$V_{dis}(r_{ms}) = \sum_{n=6,8,10} -\frac{d_{ms}^{(n)}}{r_{ms}^n} \tag{104}$$

The assumption that dispersion energy in more complex systems can be described as a sum of atom–atom terms has been expressed, and accepted as a reasonable approximation, for many years (see ref 335 and references cited therein). Accepting this approximation and indicating by m the atoms of the solute and by s the atoms of the solvent molecules, the dispersion energy can be written as a sum of volume integrals, which in turn may be reduced to surface integrals with the aid of appropriate vector functions $\vec{A}_{dis,ms}^{(n)}(\vec{r}_{ms})$ and reduced to a finite summation of elements defined for each tessera of the cavity surface. The procedure exactly parallels that in use for the repulsion term, and there is no need to repeat what has been summarized in the preceding section and in the 1994 review.[1] Here, it is sufficient to say that the form of the dispersion contribution to the solvation free energy is exactly equivalent to that reported in eq 96 for the repulsion interaction, but this time the vector functions $\vec{A}_{dis,ms}^{(n)}(\vec{r}_{ms})$ become

$$\vec{A}_{dis,ms} = -\frac{d_{ms}^{(6)}}{3r_{ms}^6}\vec{r}_{ms} \tag{105}$$

The serious limits of the use of atom–atom terms for the description of interactions within small clusters composed of polyatomic molecules are well-known. In passing to solutions the constraints imposed by the model (a fixed cavity, a continuous distribution of the solvent molecules) a part of the artifacts specific to the atom–atom model are eliminated. However, the final values of dispersion and repulsion energies depend on the values of the coefficients used in the potential. The availability of QM versions for G_{dis} (as well as for G_{rep}) makes it possible to define a computational strategy to get independent values for these coefficients.[336]

3.2.4. Charge Transfer Term

Among the various components of the intermolecular interaction energy in small clusters we have mentioned in section 3.1, there was a charge transfer term that was not included in the decomposition of the solvation energy we presented in section 3.2. Indeed, charge transfer (CT) is an important term in the decomposition of the variational definition of the interaction energy ΔE, even if it is not included in the standard definition of this quantity performed with the aid of perturbation theory.

We have not put a CT term in the decomposition of ΔG_{sol} because CT effects are quite specific and directional and, thus, not appropriate for description by continuum models that are essentially based on an averaged distribution of solvent molecules. However, ionic and some strongly polar solutes tend to accumulate electronic charge from the media or distribute it to the media, irrespective of the local orientation of the nearby solvent molecules. Envisaging processes of just this type, Gogonea and Merz[337,338] have proposed an addition to QM ASC methods including CT effects. The procedure starts from a standard continuum BEM calculation giving the apparent charge distribution, called by the authors σ_{RF} to signify that it depends on the reaction field (RF). The CT process is mimicked by introducing an additional CT charge, σ_{CT}, spread over the same cavity surface. This charge is related to a new concept introduced in the QM formulation of the theory, the *fractional electron pair* (FEP). The FEP is added to the LUMO, or deleted from the HOMO of the solute, with the continuum medium acting as a generator or a sink of electronic charge, respectively.

The whole calculation consists of an iterative scheme which can be schematized in three steps.

First, the dielectric is charged by distributing σ_{CT} as a charge density onto the BEM grid. Then RF charge densities are obtained from the BEM equations

$$\left(2\pi\mathbf{I} - \frac{\epsilon_i - \epsilon_0}{\epsilon_i + \epsilon_0}\mathbf{K}\right)\sigma_{RF} = \frac{\epsilon_i - \epsilon_0}{\epsilon_i + \epsilon_0}\left[\mathbf{T} - \frac{1}{\epsilon_0}(2\pi\mathbf{I} - \mathbf{K})\sigma_{CT}\right] \tag{106}$$

where σ_{RF} and σ_{CT} are vector quantities containing the set of RF and CT charge densities, respectively, and ϵ_0 and ϵ_i are the solvent and solute dielectric constants. In eq 106 $\mathbf{T}$ is a vector having elements that are normal components of the electric field generated by the solute charge density on the boundary elements, and the K_{ij} terms depend only on the shape of the dielectric interface and have the form

$$K_{ij} = \int_{a_i} \frac{(\vec{r}_i - \vec{r}_j)\cdot\hat{n}}{|\vec{r}_i - \vec{r}_j|^3}\,da_i \tag{107}$$

where i and j are boundary elements and a_i is the corresponding area.

Finally, the RF and CT charge densities are fed into the Hamiltonian, and the solute is (dis)charged by adjusting the density matrix during the SCF procedure (FEP creation) such that the total charge on the solute is less q_{CT}

$$P_{\mu\nu} = 2\sum_i^{occ} c_{\mu i}c_{\nu i} + q_{CT}c_{\mu k}c_{\nu k} \tag{108}$$

where k is either the HOMO or the LUMO orbital, which is determined by the direction of charge flow, and q_{CT} is the pointlike equivalent of the σ_{CT} at each boundary element, with

$$q_{CT} =$$
$$\begin{cases} <0 & \text{charge flow: solute} \rightarrow \text{dielectric } (k=\text{HOMO}) \\ >0 & \text{charge flow: dielectric} \rightarrow \text{solute } (k=\text{LUMO}) \end{cases}$$

The whole procedure has to be iteratively repeated to get convergence on the SCF energy. The final expression of ΔG_{sol} has an additional term, called G_{CT}, whereas the other nonelectrostatic terms are described with the standard procedures we have documented in this section.

We have reported some details of this method, surely not sufficient to provide readers with all of the elements for a full understanding of the procedure but sufficient to show that, in the case of need, extensions of continuum solvation methods to phenomena in which the medium acts as a sink or a source of electronic charge may be implemented. Phenomena that could be studied with models of this type can be easily identified. Gogonea and Merz give some examples. Here we add two other examples.

In the study of molecular anions of relatively complex structure there is a growing interest in examining the relationships between standard valence-type anions and dipole-bound anions.[339,340]

Computational models in which the medium effect is expressed only in terms of a few solvent molecules placed at the positions in which they more strongly stabilize the systems could unduly alter the relative stabilities of the two types of anions. Artifacts of similar type, due to the use of small optimized clusters, are well-known in systems ruled by complex equilibria of hydrogen bonds. The field of molecular anions is far less explored than that of hydrogen-bonded systems, and so artifacts in the description of these relative labile systems are less easy to detect. It is possible that an appropriate continuum−discrete model including CT with the continuum could lead to a more balanced appreciation of the relative stabilities of the various species. To close this remark on molecular anions, we note that the scant experimental evidence indicates that other physical effects, such as electronic polarization and dispersion, could play an important role.[340] Both effects can be described with fair accuracy and with limited computational efforts by using continuum models.

Rydberg states, so common in isolated molecules, are rarely detected for molecules in condensed media. The large size of the Rydberg orbitals would lead to a considerable spread of the corresponding electronic charge on the solvent molecules. This hypothetical phenomenon is surely counterbalanced by repulsion forces related to the exchange, or Pauli, effects, but the possibility of a partial CT to the medium cannot be a priori excluded, and this possibility has not been explored, at the best of our knowledge.

The extensions of the continuum model we have here considered violate the basic assumption of adopting a Hartree partition between solute and solvent. The use of this partition, shared by all continuum and discrete solvation methods (with the exception of solvent molecules included in a QM solvation cluster), means that the solute charge distribution ρ_M may be polarized, or distorted, by the interaction with the medium, but with its integral value left unchanged. This assumption is not a dogma, however, and can be relaxed, opening new perspectives to continuum models. The Gogonea and Merz model is too crude to be directly used to explore such perspectives, but theoretical chemists are accustomed to improving and refining crude models.

3.2.5. Definition of the Cavities in the Calculation of Solvation Energy

In the preceding sections we have encountered different types of cavities and given some remarks

about them. We have now more elements to complete the presentation reported in section 2.2 with a comprehensive display of the cavities in use for the different terms of the solvation energy.

Cavity Formation Energy. The surface is of vdW type when the SPT approach is used, whereas a cavity with a size between vdW and SAS is recommended when a surface tension approach is used (see section 3.2.1.2).

Repulsion Energy. In semiclassical methods the cavity surface is of SA type. Actually some versions of PCM use a hierarchy of SA surfaces, for the reasons explained in section 3.2.2. When the QM repulsion method is used, the cavity is brought to coincide with the cavity used for the electrostatic with the introduction of a simple scaling in the numerical factor α defined in eq 93.

Dispersion Energy. The same remarks reported for the repulsion term hold also for the dispersion term, both for the semiclassical model and for the QM model.

We note that in the parametrized classical models, which calculate G_{dis}, G_{rep}, and G_{cav} as unique contributions (see, for example, section 2.3.3), the SA surface is generally used.

Electrostatic Energy. There are codes using cavities of regular shape. For cavities of molecular shape the semiclassical methods use both SA and SE cavities. In QM calculations use is made of SESs. However, in most cases (e.g., by adopting the GEPOL approach), such surface is not obtained as suggested by Connolly (i.e., considering the surface contact determined by a rolling probe sphere) but as the surface obtained by interlocking spheres of proper dimension and position (see section 2.2). In this case, a scaling factor ($f > 1$) is generally introduced for the vdW radii. The standard value for f is 1.2: this factor was originally introduced in the first PCM paper[48] on the basis of considerations and tests that have been summarized on several occasions (see, e.g., ref 341). Here it is sufficient to recall that these tests, although of different types, were of relatively low numerical accuracy and the value $f = 1.2$ was presented as a provisional value. Tests performed in the following years confirmed that $f = 1.2$ was a good guess, and this value is still in use. There are, however, other suggested values for f. Some among them are based on the measure of some properties of the electron distribution of the solute.[342] These definitions have the defect of asking additional calculations, a strategy in contrast with the basic philosophy of continuum methods, as we have commented in the preceding sections.

Other suggestions are about the modification of the value of f for some specific group.[343] A considerable number of studies have been performed by Luque and Orozco and co-workers for different solvents. According to their analysis the electrostatic term has to be determined by using a solvent-exposed surface created by scaling the atomic radii (taken from the Pauling set) by a solvent-dependent factor, which adopts values of 1.25, 1.50, 1.60, and 1.80 for neutral compounds in water,[344] octanol,[345] chloroform,[346] and carbon tetrachloride, respectively. For small monova-

lent ionic compounds, the same authors[347] suggested that the solute cavity be reduced with respect to neutral species: the optimum cavity for the hydration of ions was defined by scaling the atomic radii by a factor of $1.10-1.15$. This reduction was justified by the fact that due to strong electrostatic interactions solvent molecules are in general closest to the atoms of charged molecules rather than those of the neutral ones. Very recently, a further refinement has been introduced;[348] instead of reducing the whole cavity of the solute, which might be appropriate for small size ions, the scaling down is now limited to the heavy atom (and the hydrogen atoms attached to it) that bears the formal charge.

In 1997 Barone et al.[349] presented a set of rules for determining the atomic radii of spheres used by GEPOL to build the molecular cavities within the DPCM solvation model. The procedure was applied to compute the hydration free energy for molecules containing H, C, N, O, F, P, S, Cl, Br, and I at the Hartree–Fock computational level with a medium size basis set [6-31G(d) with eventual diffuse functions for anionic species]. This new definition of the cavity, which was referred to as the united atom model for Hartree–Fock (UAHF), was based on chemical considerations, basically hybridization, formal charge, and first-neighbor inductive effect. The UAHF parameters were obtained by imposing two initial conditions; the hydrogens do not have individual spheres, but they are included in the spheres of the heavy atoms to which they are bonded (united atom model), and the elements of each periodic table row have the same "basic" radius, modified by the molecular environment. As previously suggested by Orozco and Luque, ions present atomic radii different from (and smaller than) those of the corresponding neutral molecules.

Due to its implementation in the Gaussian code,[17] the UAHF method has been used in many studies; it is, however, important to note here that this method works well when all of the conditions used in the original fitting procedure are maintained, namely, the use of DPCM solvation model and the HF/6-31G(d) level of calculation. Extensions to other more recent versions of PCM (CPCM or IEFPCM) or to other QM levels (for example, DFT), or only to other, larger, basis sets, in fact, cannot reproduce the good results of the original version. It is also important to note here that, due to this limitation, the new version of Gaussian code (G03) no longer considers UAHF cavities as the recommended (or default) cavities for PCM (which, in turn, is no longer DPCM as default but IEFPCM) and, thus, careful attention has to be paid by all users.

We terminate this brief excursion on different proposals to define cavity radii by quoting a paper by Dupuis and co-workers[350] in which they describe a new protocol to define the radii of the spheres to be used for oxoanions, $XO_m{}^{n-}$. These radii are determined by simple empirically based expressions involving effective atomic charges of the solute atoms that fit the solute molecular electrostatic potential and a bond-length-dependent factor to account for atomic size and hybridization.

3.2.6. Contributions to the Solvation Free Energy Due to Thermal Motions of the Solute

We have so far considered the contributions to the solvation energy that may be computed at fixed geometry of the solute (BO approximation). These calculations can be extended to the whole space of the nuclear conformations, a $3N-6$ space, that will be indicated by $\{\mathbf{R}\}$. The energy $G(\mathbf{R})$ (definition 1, see eq 78) defines the PES surface of the focused system in solution. We remark that to act as PES, the $\Delta G_{sol}(\mathbf{R})$ function (definition 2, eq 79) must be supplemented by an $E^0(\mathbf{R})$ function, which has to be independently computed.

The $G(\mathbf{R})$ function replaces the corresponding $E(\mathbf{R})$ function defined for the isolated system. The difference is in the physical nature of the two surfaces (a component of the free energy versus an internal energy) and not in their use. We remark, however, that for the study of some phenomena, it is convenient to expand the $\{\mathbf{R}\}$ space to an $\{\mathbf{R} \oplus \mathbf{S}\}$ space including dynamical solvent coordinates.[351–357] The definition of "solvent coordinates" is indeed a very important subject to which continuum solvation methods have been successfully applied. In this review, we have decided not to consider this topic, not because of less interest but just because the subjects to treat are so many that we had necessarily to make a selection. Therefore, here, we shall not consider dynamical couplings of solute and solvent coordinates and we shall limit ourselves to analyze $G(\mathbf{R})$.

In analogy with what is done for the $E(\mathbf{R})$, each value of $G(\mathbf{R})$ has to be supplemented with additional contributions due to the internal and external motions of the nuclei. We are here only interested in the contributions permitting the calculation of the free energy. For $E(\mathbf{R})$ these contributions depend on the temperature; for $G(\mathbf{R})$ the temperature has been already fixed in the definition of the PES (the dielectric constant ϵ as well other solvent properties used in the calculations depend on T). The calculation of the free energy is often limited to the critical points of the PES corresponding to local minima and to transition states (saddle points of the first type: SP1) for which the calculation of the internal motions contributions (i.e., vibrations) is computationally simpler and similar in vacuo and in solution.

For the contributions due to the external motions (translation and rotation of the whole molecule), the procedure in solution is not so simple as for molecules in the gas phase. It is convenient to make explicit reference to Ben-Naim's definition of the solvation process.[358] According to Ben-Naim, the basic quantity is the free energy change ΔG_{sol}^* for transferring the solute from a fixed position in the ideal gas phase to a fixed position in the liquid phase. The constraint of fixed position in the liquid is released later, with the addition of a further contribution to the energy, called "liberation free energy", related to the momentum partition function Λ_M^3 and to the number density ρ_M. The explicit formula is $\rho_M \Lambda_M^3$. An analogous release of the fixed position is introduced for M in

the gas phase, and the resulting solvation free energy is

$$\Delta G_{sol} = \Delta G_{sol}^* - RT \ln \frac{n_{M,g} \Lambda_{M,g}^3}{n_{M,s} \Lambda_{M,s}^3} \quad (109)$$

where the indices g and s refer to M in gas phase and in solution, respectively.

The freedom one has in defining standard states may be exploited to adopt, for the transfer process, those that give the simplest relationship between ΔG_{sol}^* and ΔG_{sol}. This process is defined by Ben-Naim as the "ρ process", and, in practice, it corresponds to the use of unitary molar concentrations for both states. In this case we have $\Delta G(\rho \text{ process}) = \Delta G_{sol}^*$. Note that this noticeable simplification is only valid for the Gibbs free energy; for other thermodynamic functions the equality between starred and nonstarred quantities does not exist. Within this process, we may write the explicit and complete expression of the solvation energy as

$$\Delta G_{sol} = \Delta G_{el} + G_{cav} + G_{rep} + G_{dis} + RT \ln \frac{q_{rot,g}}{q_{rot,s}} + RT \frac{q_{vib,g}}{q_{vib,s}} \quad (110)$$

The last two terms have been grouped in eq 79 into the ΔG_{tm} term. The contributions related to the molecular motions are expressed in terms of the microscopic rotational and vibrational partition function of M (the last term also includes zero vibrational energy contributions). The usual recipes and simplifications used for gas phase calculations can be used here; the only term requiring some specific modeling for solutions is the rotational contribution.

The last term we have to consider is the $P\Delta V$ contribution we have included in eq 79. With our choice of standard states, the value of this contribution is zero. It assumes other values when other reference states are adopted: the contribution to the energy due to a change of reference is called the *cratic term*.

There is an additional formal point to make concerning the free energy and the thermodynamic ensemble used.

The expressions we have considered refer to the (TPN) ensemble, in which G (Gibbs free energy) is the leading free energy term. In this case, the Helmholtz free energy A is given by the following relationship:

$$\Delta G^*(TPN) = \Delta A^*(TPN) + P\Delta V^*(TPN) \quad (111)$$

Ben-Naim gives[359] some numerical examples to show that in normal cases the last term of this equation is exceedingly small; the ratio $P\Delta V^*/\Delta G^*$ ranges in the interval of $(1-0.1) \times 10^{-3}$.

In the canonical ensemble (TVN) the leading free energy is that of Helmholtz, but when the average volume $\langle V \rangle$ in the (TP) ensemble is taken to be equal to the volume V in the canonical ensemble, the following relationship applies

$$\Delta G^*(TPN) = \Delta A^*(TVN) \quad (112)$$

even if the two quantities are defined with two different processes.

What we have here reported should be sufficient to indicate that people performing calculations on solvent effects with computer simulations may use either ensemble and either definition of the free energy to arrive at practically the same results. Continuum methods, instead, are characterized by the use of dielectric properties measured at given values of T and P. Thus, the thermodynamic ensemble they formally refer to is the TPN, but from the numerical point of view there is an almost complete agreement with the alternative TVN as liquids are practically incompressible. We note that an exception exists, for example, the supercritical fluids, as for them the incompressibility approximation is not valid.

Thermodynamics, however, is a rigorous discipline hiding many subtleties, and also in the apparently simple definition of the basic solvation phenomena there have been fierce debates. We recommend familiarity with Ben-Naim's books;[358,359] his approach has in fact important merits: it is applicable to liquid systems of any type, without limitations in the concentrations; it allows the use of microscopic partition functions; it avoids assumptions about the structure of the liquid and the introduction of artificial concepts such as the free volume available to the solute; it can be applied to heterogeneous systems; and it gives, as we have seen, a transparent connection between the computational continuum procedures and a sound thermodynamic formulation of the solvation process.

4. Nonuniformities in the Continuum Medium

We reconsider the electrostatic aspects but with extensions toward a more detailed description. We shall consider, once again, liquid media at equilibrium, but we shall release the constraint introduced in section 2 of a uniform and homogeneous medium.

The reasons suggesting, or compelling, the release of this constraint are numerous and of very different types. We shall not present a unified description of these reasons, preferring to give first a synopsis of some aspects of the dielectric theory for molecular liquids we have discarded in section 2 and then to analyze three specific problems, namely, nonlocal effects, nonuniformities around ionic and neutral solutes, and systems with phase separation. Before entering into the details of these phenomena, we briefly review the main aspects (and the related literature) of the dielectric theory going beyond the linear approximation.

4.1. Dielectric Theory Including Nonlinear Effects

The electrostatic part of the solvation model we have thus far considered is based on the assumption of a linear relationship between the medium polarization function $\bar{P}$ and the strength of the electric

field $\vec{E}$ acting on the medium and giving rise to this polarization (see eq 4). In other words, the model is based on the linear regime of the dielectric response of the medium. To consider nonlinear response regimes, one has to develop $\vec{P}$ in powers of $\vec{E}$, according to the standard practice of response functions. This analysis has been done by physicists, with measurements on macroscopic dielectrics, since the 19th century. The effects measurable at the macroscopic level can be described with only the first nonlinear term. The experimental determination of the nonlinearity coefficient is usually performed by superimposing a weak alternating field to a strong static field and measuring the slope of the dielectric displacement function $\vec{D}$, which has the same non-linear behavior as $\vec{P}$

$$\vec{D} = \vec{E} + 4\pi\vec{P} = (\epsilon + 4\pi\chi^{(3)}E^2)\vec{E} \qquad (113)$$

where $\chi^{(3)}$ is the third-order susceptibility of the medium. We note that the first nonlinear term is related to the third-order susceptibility as $\vec{P}$ is symmetric with respect to a change of sign of the field $\vec{E}$ and thus only odd powers appear.

The quantity that can be measured is an incremental dielectric constant, which depends on the field, namely

$$\epsilon_E = \nabla_{\vec{E}} \cdot \vec{D} = \epsilon + 12\pi\chi^{(3)}E^2 \qquad (114)$$

From eq 114 it follows that nonlinear effects can be described in terms of the quantity $\Delta\epsilon/E^2 = 12\pi\chi^{(3)}$. Usually this term is negative; that is, the real permittivity is smaller than expected on the basis of a linear response (the "normal saturation" effect), but it may also be positive; several effects may in fact contribute to determine the experimental value of this term.

The main problem in the formulation of electrostatic theories based on nonlinear effects lies in the fact that the Poisson equation found to be valid for linear dielectrics in all regions without charge does not hold in the nonlinear regime. The solution of this electrostatic problem is quite complex, and a full theory has never been completely settled.[360]

Here, we shall limit our attention to the static aspects of this problem for liquids, in particular, for ionic solutions, for which there is an abundant methodological literature covering almost a century.

The formal basis was the elaboration of the dielectric problem with a molecular description in a continuum framework given by Debye,[361,362] who replaced the external field $\vec{E}$ acting on a dipole of the medium with the internal field of Lorentz[363] and introduced an expansion of the Langevin function (conceived for magnetic moments). Similar but not identical versions of the theory, making use of an expansion of the Langevin function, were published by Webb[364] (who also introduced electrostriction effects), Sack,[365,366] and Ingold.[367] The main limitations of these approaches were mostly due to the use of the Lorentz field, which is not adequate for this scope.

Substantial advances were given by the Onsager theory,[131] with the separation of the reaction field from the internal field and the definition of a cavity field, by Kirwood[130] and later by Frölich,[368]who improved the theory of the dielectric constant with statistical mechanics arguments. This collective work paved the way to the elaboration of better theories of liquid dielectrics with saturation effects, done by Booth,[369] which has been amply used but also criticized,[370] and then by Harris and Alder.[371]

This brings us to the beginning of the second half of the past century, immediately before the advent of the era of computers. Computer simulations and advances in the integral equation formulations of statistical mechanics have opened new perspectives to the study of liquid systems. In addition, new aspects have been put in evidence by the impressive advances in the experimental techniques, especially of spectroscopic type. This evolution in research themes and techniques could open another perspective for the use of continuum solvation models toward a more detailed description than in the past, and this is the reason we are here considering fine details of the picture, such as nonlinearities and nonlocal effects.

4.2. Nonlocal Electrostatic Theories

The nonlocal electrostatic theory has been introduced in the studies of solvation by Dogonadze and Kornyshev,[372,373] borrowing it from solid state physics. The basic point in this approach is the introduction of nonlocal structure in the susceptibility connecting the polarization vector $\vec{P}$ to the electric field $\vec{E}$. In this formulation the celebrated relation (eq 4) becomes

$$\vec{P}(\vec{r}) = \int d^3\vec{r}'\chi(|\vec{r} - \vec{r}'|)\vec{E}(\vec{r}') \qquad (115)$$

The susceptibility is no longer a constant factor, namely, $(\epsilon - 1)/4\pi$, as in the standard description of homogeneous isotropic solutions, but the kernel of an integral equation depending on the field felt at all positions of the medium.

The nonlocal electrostatic theory gives an alternative approach to the description of the local anisotropy of the medium traditionally interpreted as nonlinear dielectric saturation effects. The nonlocal theory in use is a linear theory that can be applied by retaining almost all of the elements of the standard continuum solvation energy, such as the molecular cavity and the nonelectrostatic terms.

During the years, the theory has noticeably progressed since its first formulation given in the already cited papers. Kornyshev himself has further developed its original theory,[374-376] but the formal and computational advances most directly related to continuum methods are due to Basilevsky and Parsons,[377-379] who developed a model to account for nonlocal effects within an ASC framework. According to this model, the solute charge density is embedded in a cavity, whereas the external volume is described in terms of the equations of nonlocal electrostatics. The susceptibility kernel is then described as a step function on the boundary surface of the cavity, namely, $\chi(|\vec{r} - \vec{r}'|)$, if $\vec{r}$ and $\vec{r}'$ are outside the boundary and 0 if inside. This model, accounting for matching

conditions on the boundary surface, can be solved analytically for smooth Lorentzian models of the dielectric function $\chi(k)$, which is the Fourier transform of the kernel $\chi(|\vec{r} - \vec{r}'|)$. However, studies of microscopic molecular solvent models have brought into doubt the validity of the Lorentzian solvent model, suggesting that $\chi(k)$ has a pole structure leading to an oscillatory behavior in the corresponding polarizability kernel $\chi(|\vec{r} - \vec{r}'|)$. The most striking result of the pole model, as applied to solvation effects for spherical ions, is an irregular behavior in the solvation energy as a function of ion radius a. Following the analysis made by Basilevsky and Parsons, it appears that the addition of pole terms to a Lorentzian function for $\chi(k)$ violates the positive definiteness of the integral operator governing the basic equation of the theory: this is the fundamental origin of the instability. According to the two authors, oscillations introduced by poles in $\chi(k)$, related to spatial correlations inside a solvent, are incompatible with the frozen solute cavity model, in which the cavity radius is considered as an intrinsic property of a given solute ion. They thus introduce modifications of the cavity model to get more flexibility by allowing for the mutual adjustment of the cavity size and solvent structure in the close vicinity of the ion. Doing this, they almost completely return to a theory with a positive-definite kernel in which no instabilities arise.

4.3. Nonuniformities around Small Ions

The phenomenon most thoroughly studied in connection with the problems we are considering in this section is that of solvation of small ions. The first reason is the importance ionic solutions have in chemistry; the second is the simplicity of the models for isolated ions, an aspect making easier the formulation of theories to extend later to more complex solutes.

4.3.1. $\epsilon(r)$ Models

The systematic calculations of the solvation free energy of ions date back to Born's seminal paper.[148] The use of this model was appealing because of its mathematical elegance, and in fact it was immediately applied to a variety of solvents. However, a few years later, it was realized that the Born equation only qualitatively accounts for much of the available experimental data. The most evident deviation with respect to such data was a deviation toward too negative free energy values. Attempts aiming at eliminating the "errors" of the model by increasing the ionic radius beyond its crystallographic value have been performed.[380–384] This correction considerably reduced the errors, but the increase of the radius for highly charged ions was excessively large, and the lack of a serious justification of the procedure (despite several attempts) led the scientists to consider this approach purely empirical and of no help for an explanation of the phenomenon.

In addition to the ionic radius, the Born model involves a second parameter, namely, the dielectric constant. An interpretation of the "failures" of the Born prediction in terms of nonlinear effects in the dielectric response was immediately advanced (actually the ions were considered to be the only source of nonlinearities in liquids not subjected to external fields).[385] We have already presented the evolution in the elaboration of a dielectric theory for dipolar liquids. Following this evolution, a permittivity function $\epsilon(r)$, replacing the dielectric constant (or permittivity) ϵ with a function of the distance from the ion, was introduced. We note that the spherical symmetry of the ionic systems permits the reduction of the position argument of the function, $\vec{r}$, to a single parameter only, the distance r.

The $\epsilon(r)$ function is an empirical function; the theory of dielectrics is not able to give the details necessary for an accurate definition of this function. It is in fact an approximate and not fully developed theory, as we have seen in section 4.1, collecting into a single term ($\Delta\epsilon/E^2 = 12\pi\chi^{(3)}$) contributions of different physical origins. On the other hand, empirical determinations suffered from the scarcity of experimental data, which in practice are limited to the integral values of the thermodynamic solvation functions and thus subject to uncertainties and also including nonelectrostatic contributions. As a consequence, the attempt to define appropriate analytical forms of $\epsilon(r)$ was a delicate task requiring an accurate evaluation of the available data and some ingenuity. The papers we cite here[383,386–398] have been selected from a longer list because they present analyses and remarks that might be exploited in further elaborations of the model. Having in view these possible developments, it is worth citing some papers by Ehrenson, who has given illuminating analyses on this subject.[399–401]

4.3.2. Layered Models

Another approach to describe the nonuniformities (or local anisotropy) of the medium around ions is based on the introduction of a layering of the solvent, with each layer characterized by a different dielectric constant.

Layers in continuum models were first introduced by Kirkwood[130] and by Oster[402] to treat ionic solutions and mixed solvent around a dipolar solute, respectively. Here we consider layers with progressively increasing permittivities to mimic the dielectric saturation effects.

Analytical formulations of the layered continuum electrostatic solvation model were first given by Beveridge and Schnuelle[403] and then by Abraham et al.[404] in the framework of the MPE formulation (see section 2.3.2). The one-layer version of these models has been employed by Abraham in a set of papers[405–410] on monatomic ions in a set of solvents to get appreciably accurate values of the thermodynamic solvation functions and a good deal of information about the properties of the solutions. The layered model, called "dual solvent region" method, has been described by Ehrenson in the above-cited critical examination of dielectric saturation models as simpler and more transparent and giving results comparable to the those of the best $\epsilon(r)$ models. The "transparency" noted by Ehrenson is due to the values of the two additional parameters present in

this model, the value of the dielectric constant in the layer, and the thickness of the layer, which have been numerically optimized in the context of the cited studies.[399–401] In the dual solvent region model, the dielectric constant of the layer corresponds, in a good approximation, to the optical dielectric constant of the solvent and its thickness to the solvent molecular diameter. The numerical optimization leads to a description of the phenomenon acceptable on intuitive grounds; the first solvent layer is immobilized and dipole-oriented, contributing to the polarization with its electronic term only. Of course, there is compensation of effects, but these findings reinforced the opinion, already expressed in the literature, that pure continuum models could exploit the difference between the electronic and total permittivity to introduce effects due to electric saturation.

Considerations of this type have led Basilevsky and co-workers to formulate a layered model without constraints on the symmetry of the two surfaces (it is based on an ASC approach).[411–413] The approach, called the frequency-resolved cavity model (FRCM), is based on the use of the electronic permittivity in the first zone and on the static value in the outer space; more details on this method will be given in section 5.3.

4.3.3. Molecular Cluster Models

A third way to describe dielectric saturation effects around ions consists of replacing the continuous dielectric in the vicinity of the ion with solvent molecules. We are here at the border between two approaches, the continuum approach, which adds some discrete molecules in critical positions, and the discrete model, which replaces distant molecules with a continuous distribution. We shall return to this subject, with a discussion of where to put the border between the two approaches (see section 7). Here we are in the continuum domain with the addition of discrete elements.

Attempts at inserting some discrete solvent molecules in the Born-like description initiated very early to try to eliminate the "failures" of this model; we report here a selection of some old references.[390,414–419] By comparing these references with those reported in section 4.3.1 (more recent), it appears that the main attention has shifted from solvation energies to the structure of the liquid around the ion. These references are also testimony to the beginning of the use of QM calculations in the study of condensed systems. Actually, the discrete solvent molecules used in these, and in other successive papers, were modeled at a level that was practically unable to describe the electronic solute polarization considered to be essential in the models of the preceding subsections.

We have already described several shortcomings of the use of semiclassical discrete solvent models for simulations. In the present case, the need for using simplified models is less justified, because the number of molecules is small.

The models to be used here should combine the features necessary to describe molecules in a liquid, which are different from those of molecules interacting in the gas phase, and the features specific for molecules feeling the strong field of the ion. An attempt to formulate a procedure able to introduce both features in semiclassical models was elaborated by Floris et al.[420–424] According to this procedure, ab initio effective pair potentials can be obtained using a continuum solvation model (the PCM in the cited papers). In this way, many-body effects are included in the ion–solvent potential at the same time keeping the computational convenience and simplicity of two-body functions in the development process. These potentials are then used in fully discrete computer simulations. Molecular dynamics in particular is appropriate for the study of the dynamical features of the system, such as the persistence time of a solvent molecule in the first or second solvation shell, the determination of the diffusion coefficients, the spectra of the solvation shell, and the dynamics of exchange of solvent molecules of different nature in mixing solvents. All of the aspects we have here mentioned have been studied for a variety of cations in the above-cited papers, to which we add here a more recent one on Cd(II) in aqueous solution.[425]

Other semiclassical potentials including polarization have been employed. We cite among them the effective fragment potential (EFP) developed by Gordon and collaborators,[426] which has given good results in modeling solvent molecules, especially for neutral solute (see also section 7.3.2). The EFP description presents shortcomings when there is remarkable charge transfer such as in anions and in some cations.[427,428]

The use of a full QM description of the cluster, however, is advisable when the property under examination is suspected to be sensitive to layering effects. It is not yet fully ascertained when an accurate and well-balanced description of the solvation cluster is compulsory, but surely it is convenient to have available descriptions of this type. An appreciable number of studies have been performed on isolated metal–solvent clusters of the type $[MS_n]^{k+}$,[429–433] but often, when the number n of solvent molecules reaches or exceeds the number necessary for the first solvation shell, the geometry does not correspond to that found in solution. The concept of a "hydrated ion" as a new species formed in solution by the ion and a limited number of water molecules is now widely accepted.[434] A simplified strategy is often employed to study these systems. It consists of performing a geometry optimization of the hydrated ion in the gas phase followed by a refinement of the geometry with the hydrated ion within the continuum solvent.[435,436] It is noteworthy that these geometry optimizations of the clusters are sensitive to details in the continuum solvation model. This fact was pointed out by Sanchez Marcos and co-workers,[436] who noticed that there was ambiguity in the results according to the procedure used. In particular, it was shown that the incorrect lengthening of the metal–oxygen distance found in some optimizations with continuum models was due to the spherical shape of the cavity used in those models; with a molecular shaped cavity the correct shortening is in fact recovered.

4.4. Nonuniformities around Neutral Molecules

Some of the early attempts to model dielectric saturation for ions in solution were also extended to small neutral molecules, reduced to a point dipole. However, the electric field produced by a dipole is decidedly smaller than that produced by a localized charge, and thus the saturation effect on the solvation energy is far smaller; this induced the consideration of ions only. More recently, the progress in computational methods and the availability of data on time-dependent phenomena have renewed the interest in larger and more complex molecular systems. For example, the method of Basilevsky and co-workers[411−413] considered in section 4.3.2 is not limited to atomic ions, but it can be extended to molecular systems, charged or uncharged.

A method addressing equilibrium solvation energies of polyatomic molecules has been recently proposed by Edholm et al.[437] The description of the dielectric nonlinearity is based on a modification of the Langevin−Debye model,[438] with a finite difference method applied to calculate the spatial dependence of the electrostatic potential using a quite fine grid borrowed from DFT methods and limited to a layer of 1.2 nm (the solvent outside this layer is described with a linear continuum). The method also contains the calculation of the nonelectrostatic terms, van der Waals and cavity formation, according to the schemes discussed in section 3. The solute is described at fixed geometry, not influenced by the solvent, and with atomic charges drawn from the OPLS-AA force field.[439,440] In addition, solvent polarization effects are neglected. The hydration free energy values for around 200 neutral organic compounds with their decomposition into electrostatic, van der Waals, cavity formation, and nonlinear electrostatic terms are reported. The nonlinear contribution is decidedly smaller that the cavity formation and van der Waals terms, but comparable to or even larger than the sum of these two terms, which, in water, compensate each other to a good extent. The authors remark that the extensive parametrization used in the Cramer and Truhlar SMx models (see section 2.3.3) should implicitly include nonlinear effects and that PCM (see section 2.3.1) uses adjusted cavity radii, which will quench the saturation effects. In our 1994 review, we explained the origin of the scaling factor, applied both to polar and nonpolar molecules, and we confirm here that neither dielectric saturation nor electrostriction (the opposite term related to nonlinearity) have been considered in fixing this scale factor, but we accept the remark about the quenching.

Sandberg and Edholm have expressed two other formulations of the nonlinear response solvation. One already cited paper[398] involves spherical ions and gives an analytical formulation exploiting the simplifications made possible by the symmetry of the problem. The other[441] uses for the charge distribution a dipole, derived from the GROMACS force field[442] and specialized for amino acids. These methods seem to be still in evolution, and it is convenient to await future developments to assess their validity to compute solvation energies.

4.5. Nonuniformities around Systems of Larger Size

In extending our survey to larger molecules we enter into a field dominated by computations on biomolecules. The solvation methods we have described also apply to biomolecules, and we do not intend to open here a chapter dedicated to this very important domain of computational chemistry, for which there is a wealth of specialized reports. Our attention will be limited to the very specific aspect of the description of nonuniformities arising from the large size of biomolecules.

There is a long tradition of using molecular mechanics (MM) methods to describe large molecules. Molecular mechanics, we remind, is based on empirical force fields in which classical terms related to intermolecular energy deformations are accompanied by site−site non-covalent interactions of van der Waals and electrostatic type. These last are expressed in terms of point charge interactions, which are not screened because electronic polarization is missing in standard MM models. This defect of the model has been empirically corrected by introducing in the calculation of Coulombic interactions a dielectric constant, with values ranging from 2 to 20 (the definition of a proper value of ϵ to be used with biomolecules has given rise to considerable controversy).[443−446] The fact that a "constant" value of ϵ was not sufficient, at least for groups bearing a net charge, was soon noticed. In 1923 Bjerrum[447] proposed the use of a distance-dependent dielectric function to describe the ionization constants of bifunctional organic acids. Bjerrum's proposal was later elaborated by Kirkwood and Westheimer[448] and thereafter amply used, especially for the calculation of pK_a of titrable groups in proteins. Numerous checks have been done, and several modifications have been proposed. There is in the literature a sizable number of variants of a linear form of the distance-dependent dielectric function: $\epsilon(r) = kr$, with k determined in different ways.

However, a linear relationship of this kind is not appropriate to describe the saturation effects determining the nonlinearity (see section 4.1). Many proposals have been suggested[449−462] to take into account the physical origin of the problem using one among the various models we have reviewed, or defining, through other ways, $\epsilon(r)$ functions with a sigmoidal shape.

Here we cannot discuss all of these proposals, but we can point out some authors whose work has had a larger impact on the literature. Warshel et al.[463] used experimental pK_a values and redox potentials to derive a distance-dependent dielectric function, and Mehler and Eichele[464,465] introduced a sigmoidal distance-dependent dielectric permittivity function to calculate the electrostatic effects in water accessible regions of proteins. For metal ion−nucleic acid interactions, Hingerty et al.[466] proposed a modification of Debye's distance-dependent dielectric function, which is sigmoidal and rises rapidly with distance. An alternative mathematical expression for this function was proposed by Ramstein and Lavery.[467] Guarnieri et al.[468] proposed an extension of Mehler

and Eichele's work, in which the position dependence of the screening is partly accounted for by using different values of a parameter for buried and for exposed atoms. More recently, in an attempt at a more generally applicable function, Sandberg and Edholm[469] proposed a modification of the function of Warshel et al., with parameters depending on the mean distance of the atoms from the protein surface. Hassan et al.,[470] following a formulation originally developed by Bucher and Porter[471] and subsequently by Ehrenson,[472] obtained a reaction-field-corrected form of the radial-dependent permittivity profile.

In our rapid exposition we have simplified several aspects of the methodological exposition of the use of "screened" Coulomb potentials (for example, no mention has been made of the use of models without and with solvent cavity). Interested readers are referred to the above-cited papers to which we add here an older but rich review by Mehler,[473] but further comments as well as additional references will be reported in section 7.1.

4.6. Systems with Phase Separation

We consider another class of systems to which the concepts related to nonuniformities in the local properties of the liquid can be applied, namely, systems with phase separation boundaries. This is a very large class of systems, collecting elements of quite disparate nature. We anticipate that in some cases the explicit consideration of local deviations of the liquid properties with respect to the bulk is compelling, whereas in others the description of these changes is optional, in the sense that they need to be considered only when one aims at a more accurate description of fine details not given by simpler descriptions of the medium.

Local changes involve several aspects of the liquid, the density, the local concentration of dissolved species (an aspect of particular relevance in ionic solutions), the viscosity, and other parameters related to the motion of solvent molecules, and, of course, the dielectric function to which our attention will be here limited. Before entering into details, we need to introduce additional characterizing elements in our set of systems, thus far defined only in terms of the presence of phase boundaries. In this way, in fact, we can obtain subclasses that are more homogeneous with respect to the methodological tools to use. We shall limit ourselves to a rough level of classification, finer classification being necessary only for more specific reviews.

An important feature, useful for our attempt of classification, is the length scale for the boundaries. This feature has been proposed to define "complex liquids" in which the appropriate scale length is in the mesoscopic range.[474] This definition of complex liquids collects, for example, colloidal suspensions, micellar solutions, microemulsions, closed bilayers, foams, gels, and other variants of the basic types we have here mentioned as bicontinuous liquids. We shall consider the complex liquids no further in this review, but we note that a description of complex liquids coherent with continuum models can be given, even if not in a straightforward way.

The local effects due to the surface play a far more important role in systems with multiple mesoscopic phase boundaries than in systems with a single phase boundary, and in general there will be the need of extending the model to include mutual interactions among the mesoscopic domains, an extension that was not yet considered in the QM continuum models. We have here mentioned multiple mesoscopic systems because in our opinion they represent one of the most important perspectives of development of continuum models

Other subclasses with macro- or mesoscopic length scale for the boundary may be characterized by the number of phases, by their geometry, and by the physical and chemical nature of the components. Some among them (liquid surfaces, pores, thin films, etc.) are the subject of intensive studies, deserving separate reviews.

Let us here consider some examples of two-phase systems, namely, systems with a liquid/gas, liquid/liquid, or liquid/solid surface. The continuum model we have examined in the preceding sections can be applied to these systems with minor changes. We thus return to models in which the focused component continues to be a single molecule or a small cluster, whereas the remainder has a more complex definition, possibly including local modifications near the boundary (for the definition of focused models see section 1).

The scientific and practical interest of two-phase systems has led to a detailed experimental characterization of at least some among them, and it has spurred a considerable number of attempts of theoretical modeling also including continuum models. These models exhibit specific features as the characteristics of two-layer models may be quite different. For example, the characteristics to model in processes occurring at the electrode surface are remarkably different from those necessary in the study of the effects of a metal on the spectroscopic properties of a chromophore, and both have little to do with those required to model processes and equilibria in aerosols of environmental interest. For this reason we limit ourselves to a few selected examples, covering the three types of two-phase systems mentioned above and bearing a strict connection with the methods presented in sections 2 and 3.

As remarked above, in some cases the explicit use of local corrections to the bulk properties is not compulsory, and we start to examine some methods of this simpler type.

An ASC method, based on PCM and aiming at studying systems of this type, has been elaborated years ago by Sakurai and co-workers in Japan.[475−477] The description of the medium is given in terms of nonoverlapping portions of a homogeneous continuum with different values of the dielectric constant within each portion. The code was later improved[219,478] and used for a number of studies, mostly of organic−biologic interest, from which the versatility of the approach may be appreciated.[479−483]

Among the successive variants of Sakurai's procedures, one deserves explicit mention in this review.[484,485] It involves a QM/MM method in which the

feature of separate dielectric domains is exploited to allow instantaneous differential polarization in the protein fragments. In this model, called the polarizable mosaic model (PMM), every covalent bond in the MM region is replaced by a cylindrical stick made of dielectric, the permittivity of which depends on the nature of the original bond. As a consequence, a protein molecule is represented by a *mosaic* consisting of cylinders with various polarizabilities. This model offers a perspective of solution to two kinds of problems. First, other bodies can be described in a first approximation as a whole region, introducing then local anisotropies with a similar procedure—as, for example, a relatively homogeneous membrane with local elements involved in some local processes. Second, the introduction of mutual polarization of the classical elements in QM/MM simulations is a computational challenge, and this approach is a possible way of solving this problem.

The first version of PCM, namely DPCM, was also used to study problems characterized by the presence of a boundary. The first paper, published in 1986,[486] presented a model addressing energy changes in long DNA fragments subjected to large-scale deformations and to local opening of the double helix. The problems posed by this model are representative of those occurring in "complex liquids" and in related systems. Around the double helix (a polyion) there is a portion of solvent showing large nonlinear dielectric effects, combined with partial counterion condensation, and both effects change when the double helix is bent or open. In this model, the local nonlinear dielectric effects were described in terms of the layered model described in section 4.3.2. Another application was on the effects of partial solvation in modifying the molecular electrostatic potential of a substrate placed in the cleft of the active site of a model enzyme.[487] Other studies involved polar solutes (with hydrophobic tail) placed near the flat separation surface of two immiscible liquids (or at a liquid/vacuum separation).[488−491]

In all of these DPCM studies, use was made of a tessellation of the boundary (of planar infinite, spherical, or irregular shape, according to the case). More recently, the same systems were reformulated within the IEF version of PCM.[80] Within this formalism, by introducing novel Green-type operators of analytical form, tessellations of the infinite plane (or the spherical boundary) separating the two phases are no longer required, and thus the dimension of the problem is identical to that of a homogeneous and isotropic solution. We note that full analytical Green operators are relatively easy to obtain for surfaces with a regular shape but not for more complex shapes. In these cases it is thus useful to introduce Green operators of semianalytical form (requiring a partial numerical integration) or to combine the IEF formalism with the original BEM formulation based on a tessellation of the boundary surface.

The use of the IEFPCM formalism also allows us to introduce an $\epsilon(r)$ function for the liquid portion. The present version of the computational code can deal with $\epsilon(r)$ functions limited to a single spatial variable (in practice, all of the models considered in

section 4.3.1); these kinds of functions, for example, are well suited for planar surfaces and spheres. The extension to some other cases, such as cylindrical surfaces or liquid with a simple surface combined with a tensorial permittivity, is immediate, but not tested yet. The extension to more anisotropic permittivities exhibiting a dependence on all three spatial coordinates would require a more intensive computational elaboration, but it is surely feasible. This model, which eliminates all of the divergences occurring in simpler image charge models with a sharp surface, has thus far been applied to the crossing of liquid/vapor and liquid/liquid surfaces by neutral and charged molecules, namely, a two-surface model mimicking a membrane has been studied,[80] as well as the changes of the polarizability of the halide anions passing from water to air.[492] In both cases the function, $\epsilon(r)$, has been modeled on the corresponding density profile, $\rho(r)$, derived from simulations, assuming proportionality between the two functions.

Another continuum electrostatic model to treat solute at interfaces has been elaborated by Benjamin, especially to compute the spectral line shape at liquid interfaces and surfaces.[493] In this model based on the image charge approach, the interface is described as a sharp boundary separating two bulk media, each characterized by different optical and static dielectric constants, and the chromophore is modeled as a pair of spherical cavities in which two equal and opposite point charges are embedded.

As a matter of fact, Benjamin's contribution to the knowledge of interfaces and their modelization goes well beyond this model.[493−499] His main activity has in fact involved molecular dynamics (MD) simulations and has been focused on the study of electronic properties of chromophores as a function of their location at the interface.

Let us now pass to another kind of system with boundaries, namely, that represented by lipid bilayer membranes. These systems have been treated within the framework of continuum electrostatics by considering a slab of low dielectric material intended to represent the hydrocarbon tails of the lipid molecules, surrounded by high dielectric material intended to represent the headgroups and aqueous solution. As a matter of fact, a solvated lipid bilayer considered at the nanometer length scale is an example of a system nonuniform in one dimension, that is, along the axis normal to the bilayer. In general, the dielectric permittivity for such a system will be a function of the position along one axis. Furthermore, it will not be a scalar, as has been assumed in virtually all applications of continuum electrostatics to molecular systems, but will be a second-rank tensor.

Several authors have presented methods for calculating the local dielectric constant for a nonuniform system. King, Lee, and Warshel[500] and Simonson and co-workers[450,501] have presented methods for determining the dielectric constant of a spherically symmetric but nonuniform system and applied them to proteins solvated in water. These methods are based on a partition of the system into two or more concentric spherical shells. Once an estimate of the

dielectric constant in the outer shells is made, the dielectric constant in the inner shell can be calculated either from fluctuations of the total dipole moment for that region or by direct observation of the polarization response to a uniform field. A dielectric profile for a lipid bilayer in solution was presented earlier by Zhou and Schulten.[502] Their approach was to divide the membrane into slices and compute the permittivity for each slice with the usual expression for a uniform, isotropic system. The implicit assumption is that the slices do not interact, which seems hard to justify. More recently, Stern and Feller[503] presented a method for calculating the static dielectric permittivity profile for a system nonlinear in one dimension under the periodic boundary conditions used in computer simulations.

As a last example of systems with phase separation, we consider liquid/metal systems with particular attention to the surface enhancing (SE) effects of a metal on the photophysical properties of a molecular chromophore placed in the vicinity of the surface. Some of these studies will be examined in more detail in sections 5 and 6, and here we limit ourselves to presenting some methodological aspects related to the theme of this section.

The two models we consider describe the metal on the same footing as the solvent in homogeneous solutions, in the sense that the metal contributions to the proprieties of the focused part (the chromophore) are treated in terms of a continuous response function without explicit consideration of the atomistic structure of the metal itself. The definition of the dielectric function for a metal specimen is more complex than for a liquid, and thus specific modifications have to be introduced.

In the first model[79,504−509] we cite (which belongs to the family of PCM methods), the metal is considered to be a perfect conductor for time-independent external electric fields. To study photophysical properties, however, one needs to introduce a frequency-dependent electrical perturbation and thus, in this case, the metal is considered as a dielectric with a frequency-dependent dielectric function. The starting point to model this basic quantity may be given by the Drude theory presented in all textbooks of solid state physics,[510] which gives an expression of the dielectric function suitable for the bulk of the metal. The metal specimens used in SE measurements, however, often have a finite size, and are all subjected to other sources of electric potential, static as well as frequency dependent, related to the presence of a chromophore of molecular size. The finite size of metal specimens first affects the relaxation time, which surely has not the value of the bulk used in the Drude theory. To account for these effects, a correction based on the Fermi velocity of the electrons has been introduced in the model. In addition, the dielectric response of the electrons in the metal has a nonlocal character, in the sense that the polarization vector at a given point depends on the value of the electric field over all other points. This nonlocality, completely neglected in the original Drude formula, has been partially described in the model[506] making use of a hydrodynamic model[511] to introduce

a correction in the Drude expression, or, more accurately,[508] using the Lindhard theory[512] with Mermin corrections for the finite relaxation time.[513] Another correction introduced in the model involves the effect of surface roughness, found to be important to realistically describe the numerical output of some experiments. To this end a modified version of the Green function proposed by Rahman and Maradudin[514] has been employed.[508]

The second model[515−517] we cite assumes that the molecular system is enclosed in a half-spherical cavity embedded in a linear, homogeneous, isotropic dielectric medium and adsorbed on the surface of a perfect conductor. The effects of the media on the properties of the molecular system are described using the method of image charges. According to this method, a charge located in the cavity induces three charges in the surrounding dielectric environment: one charge in the metal surface, due to the perfect conductor/vacuum interface, a second charge due to the half-spherical environment between the vacuum and the dielectric medium, and a third charge that is the image in the metal due to the interactions between the perfect conductor and the induced charges in the solvent.

5. Nonequilibrium in Time-Dependent Solvation

In the sections 3 and 4 we have presented extensions of the basic model but with the common feature of retaining the condition of equilibrium between solute and solvent. In this section we instead review the physics we have to change and/or add to this basic model to properly describe time-dependent (TD), or nonequilibrium, processes.

TD processes embrace a large variety of phenomena, which span an impressive range of time scales (from 10^{-15} s for linear and nonlinear spectroscopy to 10^{-2} s for diffusion-controlled reactions in dilute aqueous solution). Obviously this broad range involves many physical aspects of solvation. Here, we limit ourselves to consider only those related to the most recent progress in the description of the dynamic effects in QM solvation models.

Rigorously, the dynamic evolution of the molecular solute should require that we postulate the proper TD QM equations, which generalize the time-independent effective Schrödinger equation introduced in section 2.4 for the "static" basic model.

As a matter of fact, not all dynamic processes require an explicit TD description. For example, if the time dependence of the solute−solvent interactions is sufficiently slow (as in the case of diffusive relaxation processes of the slow degrees of freedom of the solvent), it is possible to apply the adiabatic approximation and the state of the solute at time t can be obtained as the eigenstate of $H(t)$ using time-independent formalism. In contrast, the dynamic QM equation for the solute must be explicitly introduced in describing its response properties to TD electromagnetic perturbations. This aspect will be considered in section 6 devoted to solvent effects on solute response properties.

In the presence of a time evolution of the solute we have also to extend the description of the solvent

response properties to the time (i.e., frequency) domain. In principle, we should consider all of the solute−solvent interactions described in section 3, but here we shall limit ourselves to the electrostatic component only. This is in fact the most important when a dynamic evolution has to be studied.

5.1. Dynamic Polarization Response

The responses of the microscopic particles (molecules, atoms, electrons) of the solvent required to reach a certain equilibrium value of the polarization have specific characteristic times (CT). When the solute charge distribution varies appreciably within a period of the same order as these CTs, the response of the microscopic particles will not be sufficiently rapid to build up a new equilibrium polarization, and the actual value of the polarization will lag behind the changing charge distribution.

The actual polarization $P(t)$ is determined by the Maxwell field in the medium not only at time t but also at a previous time t', in a form expressed by the integral[518,519]

$$\vec{P}(t) = \int_{-\infty}^{t} dt' G(t - t')\vec{E}(t') \qquad (116)$$

where the kernel $G(t - t')$ is the solvent response function and $E(t')$ the Maxwell field. Transforming the convolution integral (eq 116) to the Fourier frequency space we obtain[520]

$$\vec{P}(\omega) = \frac{\hat{\epsilon}(\omega) - 1}{4\pi}\vec{E}(\omega) \qquad (117)$$

where $\hat{\epsilon}(\omega)$ is the complex dielectric constant

$$\hat{\epsilon}(\omega) = \epsilon'(\omega) + i\epsilon''(\omega) \qquad (118)$$

The real part $\epsilon'(\omega)$ is the frequency-dependent dielectric constant, describing the component of the polarization density in phase with the oscillating field while the complex part, or loss factor, $\epsilon''(\omega)$, determines the component of the polarization with a phase difference of $\pi/2$ with respect to the Maxwell field, giving rise to the loss of energy of the electric field in the medium.

The frequency-dependent dielectric constant $\epsilon'(\omega)$ and the loss factor $\epsilon''(\omega)$ can be determined by experimental or theoretical methods.[518] For most polar solvents, at low frequency, $\epsilon'(\omega)$ is equal to the static dielectric constant ϵ, and $\epsilon''(\omega)$ is zero. As the frequency increases, $\epsilon'(\omega)$ initially decreases rather slowly, then, in the IR, vis, and UV range of frequencies, there are sharp increases followed by a decrease. The loss factor $\epsilon''(\omega)$ has peaks in the neighborhood of the frequencies where $\epsilon'(\omega)$ changes.

The explanation of the correspondence in the behavior of all polar compounds in an electromagnetic field is found in the fact that the electric polarization is built up of three parts, the orientational, the atomic, and the electronic polarization, each part corresponding to motions of a different kind of particle (molecules, atoms, electrons, respectively) with different CTs. As the frequency increases, the so-called nonequilibrium effects appear subsequently

in the different contributions of the polarization. Orientational contribution (CT below 10^{-12} s) will first start to lag behind the variations of the electromagnetic field; next, atoms (CT around 10^{-14} s) will not be able to follow the field, and finally, at very high frequencies, electrons (CT around 10^{-16} s) also will lag behind the electromagnetic field.

Orientational polarization arises from different relaxation processes but, if we assume that it can be described in terms of only one of these processes, characterized by a relaxation time τ, then the frequency dependence of the dielectric constant may be adequately described by the Debye equation

$$\epsilon'(\omega) = \epsilon_\infty + \frac{\epsilon - \epsilon_\infty}{1 + \omega^2\tau^2} \qquad (119)$$

$$\epsilon''(\omega) = \frac{(\epsilon - \epsilon_\infty)\omega\tau}{1 + \omega^2\tau^2} \qquad (120)$$

where ϵ_∞ is the dielectric constant at a frequency at which the orientational polarization can no longer follow the changes in the field; in other words, it is the dielectric constant characteristic of the induced polarization.

Also, the behavior of the induced polarization, connected with atoms and electrons motions, in time-dependent fields can be described phenomenologically in terms of a number of resonance processes. At frequencies corresponding to the characteristic times of the intramolecular motions by which the induced polarization occurs, there are sharp absorption lines, due to the discrete energy levels for these motions. By approximating these absorptions with delta functions, we obtain for the frequency dependence of the imaginary part

$$\epsilon''(\omega) = \sum_k A_k \delta(\omega - \omega_k) \qquad (121)$$

whereas the corresponding frequency dependence of the real part is obtained from one of the Kronig−Kramers relationships:

$$\epsilon'(\omega) = 1 + \frac{2}{\pi}\sum_k \frac{A_k\omega_k}{\omega^2_k - \omega^2} \qquad (122)$$

In the following sections we shall present two classes of phenomena for which the concepts here introduced about orientational and induced polarization and nonequilibrium become of fundamental importance. These two classes can be seen as two faces of the same, more general, problem of solvation dynamics, but at the same time they present very different aspects. The first is in fact limited to a very short time scale, namely, that involved in a vertical electronic transition, and thus only the induced polarization will be involved, whereas the second covers much longer times, thus allowing a complete analysis of the solvent dynamic response due to both resonance and relaxation processes.

5.2. Vertical Electronic Transitions

All of the phenomena in which the solute undergoes a sudden change in its charge distribution require a

Table 2. Basic Equations within Partitions I and II[a,b]

partition I	partition II
$\vec{P}^A = \vec{P}^E_{or} + \vec{P}^A_{el}$	$\vec{P}^A = \vec{P}^E_{in} + \vec{P}^A_{dyn}$
$\vec{P}^E_{or} = \dfrac{\chi_{or}}{\chi}\vec{P}^E(\epsilon_0)$	$\vec{P}^E_{in} = \vec{P}^E(\chi) - \vec{P}^E_{dyn}(\chi_{el})$
$\vec{P}^A_{el} = \chi_{el}\vec{E}[\rho^A,\vec{P}^E_{or},\vec{P}^A_{el}]$	$\vec{P}^X_{dyn}(\chi_{el}) = \chi_{el}\vec{E}[\rho^X,\vec{P}^X_{dyn}]$ with $X = A, E$
$-\nabla^2 V = 4\pi\rho^A$	$-\nabla^2 V = 4\pi\rho^A$
$-\epsilon_\infty\nabla^2 V = 0$	$-\epsilon_\infty\nabla^2 V = 0$
$V_{in} - V_{out} = 0$	$V_{in} - V_{out} = 0$
$\left(\dfrac{\partial V}{\partial n}\right)_{in} - \epsilon_\infty\left(\dfrac{\partial V}{\partial n}\right)_{out} = 4\pi\sigma^E_{or}$	$\left(\dfrac{\partial V}{\partial n}\right)_{in} - \epsilon_\infty\left(\dfrac{\partial V}{\partial n}\right)_{out} = 0$
$G^{neq} = G^{or-el}_\infty + \int\rho^A V^E_{or}\,dr^3 - \dfrac{1}{2}\int\rho^E V^E_{or}\,dr^3 -$ $\dfrac{1}{2}\int V^E_{or}(\sigma^E_{el} - \sigma^A_{el})\,dr^2$	$G^{neq} = G^{in-dyn}_\infty + \int\rho^A V^E_{in}\,dr^3 - \dfrac{1}{2}\int\rho^E V^E_{in}\,dr^3$
$G^{or-el}_\infty = E^A_0 + \dfrac{1}{2}\int\rho^A V^A_{el}\,dr^3$	$G^{in-dyn}_\infty = E^A_0 + \dfrac{1}{2}\int\rho^A V^A_{dyn}\,dr^3$

[a] $\chi = (\epsilon_0 - 1)/4\pi$, $\chi_{el} = (\epsilon_\infty - 1)/4\pi$ and $\chi_{or} = \chi - \chi_{el}$. [b] Even if not indicated, the potential V has the same sources of the corresponding electric field $\vec{E}$.

specific analysis when in the presence of a polarizable solvent. In this case, in fact, it becomes fundamental to properly account for the dynamic response of the solvent.

This class of phenomenon is of very general occurrence; here, in particular, we shall focus on the vertical electronic transitions, but electron and energy transfers, or nuclear vibrations, are also examples of the same class.

Historically, in continuum models large use has been made of the approximation according to which it is sufficient to decompose the response function into two terms. Within this approximation, also known as the Pekar or Marcus partition, the polarization vector $\vec{P}$ described in the previous section becomes

$$\vec{P} \approx \vec{P}^{fast} + \vec{P}^{slow} \tag{123}$$

where fast indicates the part of the solvent response that always follows the dynamics of the process and slow refers to the remaining inertial term. Such splitting in the medium response gives rise to the so-called "nonequilibrium" regime. Obviously, what is fast and what is slow depends on the specific dynamic phenomenon under study.

In a very fast process such as the vertical transition leading to a change of the solute electronic state via photon absorption or emission, P^{fast} can be reduced to the term related to the response of the solvent electrons, whereas P^{slow} collects all of the other terms related to the various nuclear degrees of freedom of the solvent.

The operative partition of the total polarization can be performed using two alternative, but equivalent, schemes, which we prefer to indicate without using Marcus and Pekar names because in the literature there is an annoying confusion about these names.

One scheme, which we shall call partition I, was proposed by Marcus in 1956 in his landmark paper[521] on the nonequilibrium polarization in a classical continuum solvation framework. The Marcus partition has been extended to QM continuum models by several authors[78,137,213,221,238,239,522,523] to properly describe excited/de-excited electronic states after a vertical (Franck−Condon) transition. In this scheme, eq 123 is rewritten as

$$\vec{P}^A = \vec{P}^E_{or} + \vec{P}^A_{el} \tag{124}$$

where superscripts E and A refer to the "early" (or initial) and the "actual" time in relation to the chronological order of the transition process. In this partition, the previous slow and fast indices are replaced by the subscripts or and el referring to "orientational" and "electronic" polarization response of the solvent, respectively.

In the second scheme, which we shall indicate as partition II, eq 123 has to be rewritten as

$$\vec{P}^A = \vec{P}^E_{in} + \vec{P}^A_{dyn} \tag{125}$$

where the subscripts in and dyn refer now to an "inertial" and a "dynamic" polarization response of the solvent, respectively. The use of eq 125 within the continuum solvation methods has been applied both to classical and to QM approaches.[56,214,216,219,524]

The differences between the two schemes are related to the fact that, in partition I, the division into slow and fast contributions is done in terms of physical degrees of freedom (namely, those of the solvent nuclei and those of the solvent electrons), whereas in partition II, the concept of dynamic and inertial response is exploited. This formal difference is reflected in the operative equations determining the two contributions to $\vec{P}$ as, in II, the slow term (P_{in}) includes not only the contributions due to the slow degrees of freedom but also the part of the fast component that is in equilibrium with the slow polarization, whereas, in I, the latter component is contained in the fast term P_{el} (see Table 2 in which we compare the electrostatic equations identifying the two schemes).

To better illustrate this aspect, let us consider two polarizable dipoles having centers fixed at r and r', both placed in a homogeneous external field. This electric field determines the mean orientation of the dipole at r'. The induced dipole in r has two contributions, the first resulting from the external field and the second originating from the interaction with the mean orientation of the dipole in r'. If the external field suddenly changes so that the mean orientation of the dipole in r' has not enough time to relax, the induced dipole in r will change only as far as concerns the component related to the interaction with the external field, whereas the second component will maintain the value corresponding to the initial field. As a consequence only the first component presents a dynamic character in response to the changes of the external field.

It is important to stress that the two schemes I and II differ in the form of the slow and fast components of the polarization, but they are practically and physically equivalent (in the limit of a linear response regime) in the sense that they give the same value of the total reaction potential and, thus, the same effects on the solute as well as the same interaction energies. This equivalence has not been always recognized in the literature,[221,525] and thus some confusion exists on the use of these two partitions. However, as shown by Cammi and Tomasi[522] and, more explicitly, by Aguilar,[526] such confusion disappears when the proper expression for the nonequilibrium free energy functional is used in each approach.

The use of one partition instead of the other is dictated only by the requirements of the specific computational code in which the model is implemented; for example, in Gaussian,[17] the nonequilibrium version of PCM has been implemented in the framework of partition I, exactly as the nonequilibrium version of the MPE implemented in Dalton.[135]

In addition to the proper description of the solvent response, another aspect must be considered when we simulate electronic excitations of solvated molecules. This additional aspect, however, appears only when a QM description is used.

Within the continuum solvation framework, as in the case of isolated molecules, it is practice to compute the excitation energies (or better excitation free energies) with two different QM approaches: the state-specific (SS) method and the linear-response (LR) method. The former has a long tradition and is related to the classical theory of the solvatochromic effects (see references in our 1994 review[1]). The latter was introduced later in connection with the development of the linear response theory for continuum solvation models,[136,138,140,215,527−529] which will be described in section 5.6. Here, however, we anticipate a relevant aspect of the theory when compared to the SS method for the calculation of transition energies of solvated molecules.

The state-specific method solves the nonlinear Schrödinger equation for the state of interest (ground and excited state) usually within CI or MCSCF descriptions, and it postulates that the transition energies are differences between the corresponding values of the free energy functional, the basic energetic quantity of the QM continuum models. As discussed in section 2.4.6, the nonlinear character of the reaction potential requires the introduction in the SS approaches of an iteration procedure not present in parallel calculations on isolated systems. At each step of this iteration, the additional solvent-induced component of the effective Hamiltonian is computed by exploiting the first-order density matrix of the preceding step, and the resulting energy, $E = \langle \Psi | H_{\text{eff}} | \Psi \rangle$, is corrected for the work required to polarize the dielectric $G = E - (1/2)\langle \Psi | V_R | \Psi \rangle$ (we note that the inclusion of the nonequilibrium needs some further refinements, as indicated by all of the most detailed papers on this subject mentioned above). An important consequence (and disadvantage) of this iterative approach is that one has to solve a different problem for each different state instead of obtaining the energies of all states in a single run as for isolated systems.

A different analysis applies to the LR approach (in either Tamm−Dancoff, RPA, or TDDFT version) in which the excitation energies, defined as singularities of the frequency-dependent linear response functions of the solvated molecule in the ground state, are directly determined by avoiding explicit calculation of the excited state wave function (see section 5.6). In this case, the iterative scheme of the SS approaches is no longer necessary, and the whole spectrum of excitation energies can be obtained in a single run as for isolated systems.

Although it has been demonstrated that for an isolated molecule the SS and LR methods are equivalent (in the limit of the exact solution of the corresponding equations), a formal comparison for molecules described by QM continuum models shows that this equivalence is no longer valid. By using a nonequilibrium approach in both frameworks, it can be established that these intrinsic differences are related only to the interaction of the solute with the fast response of the solvent medium, and they are connected with the basic assumption of a Hartree partition between solute and solvent.[530] The analysis of this aspect is quite new, and thus further investigations will surely appear in the future.

5.3. Solvation Dynamics

Solvation dynamics is the time-dependent, nonequilibrium, relaxation of the solvent due to an instantaneous change in the interactions between the solvent molecules and a different, newly created electronic state on the solute. Upon excitation of the solute, the surrounding solvent molecules, which were initially equilibrated with the ground electronic state of the solute, are in a nonequilibrium state and will adjust their positions and momenta in order to relax to equilibrium with the new interactions associated from the new electronic state. This relaxation is driven by a decrease in the solvent system interaction energy, and as a result, any measurement that probes this energy will mirror the underlying solvation dynamics of the system.

Among the techniques used to investigate solvation dynamics, the time-resolved fluorescence Stokes shift

(TRFSS) measurement is the most widely used. The TRFSS technique measures the time-dependent red shifting (Stokes shift) of the emission spectrum of the solute as the system relaxes. A time-dependent Stokes shift (TDSS) function, $S(t)$, can then be constructed that describes the spectral diffusion of the excited molecules and contemporaneously monitors the response of the solvation to the new solute excited state

$$S(t) = \frac{\nu(t) - \nu(\infty)}{\nu(0) - \nu(\infty)} \qquad (126)$$

where $\nu(t)$ is the peak of the fluorescence spectrum at time t and $\nu(0)$ and $\nu(\infty)$ are the values immediately after the excitation and at sufficiently long times for the solvent to re-equilibrate to the solute excited state.

To apply theoretical models to the study of solvation dynamics, it is fundamental to connect the nonequilibrium function $S(t)$ to quantities related to the solute−solvent interaction energy: this quantity is represented by the time correlation function $\langle \delta E(0) \delta E(t) \rangle$ that represents the ensemble-averaged ("⟨ ⟩") behavior of the solvent fluctuations. In fact, if one observes the interaction energy between a solute molecule and its solvent surroundings as a function of time, $E(t)$, one finds that it fluctuates rapidly about some average value $\langle E \rangle$. The time dependence of these fluctuations, $\delta E(t) = E(t) - \langle E \rangle$, is intimately connected to the frictional forces that mediate a variety of dynamical processes that take place in a solvent environment.

Assuming that the perturbation caused by the electronic transition is not too large, a simple linear response calculation provides the relationship

$$S(t) \equiv C_{\Delta E}(t) \equiv \frac{\langle \delta \Delta E(0) \delta \Delta E(t) \rangle}{\langle \delta \Delta E^2 \rangle} \equiv \frac{\Delta E(t) - \Delta E(\infty)}{\Delta E(0) - \Delta E(\infty)}$$
$$(127)$$

The physical content of this "fluctuation−dissipation" connection is that, if the perturbation is not too large (or if the interactions are harmonic), relaxation of the "forced" departure from equilibrium produced by the electronic transition is not different from the relaxation of a naturally occurring fluctuation in the unperturbed system.

The relationship (eq 127) between $S(t)$ and the function $C_{\Delta E}(t)$ (generally known as the solvation time correlation function, STCF) is the basis of many theoretical models that have provided important physical insights into the solvation dynamics.

The dynamical mean spherical approximation (MSA)[531,532] as applied by Wolynes and others[533−535] was the first and most influential of theories to address solvation dynamics. Other approaches have been devised.[536−540] These treatments involve merging liquid structure theory with linear models of relaxation, often incorporating empirical information such as the frequency-dependent dielectric constant of the bulk solvent, $\epsilon(\omega)$. In particular, much atten-

tion has been devoted to treating the spatial dependence of the dielectric response function, $\epsilon(\mathbf{k}, \omega)$, which includes the molecular nature of the solvent.

A different approach, employing the perspective of a continuum model, was originally developed in 1997 by Marcus and co-workers[541] to calculate the STCF of eq 127.

The continuum model used by Marcus and co-workers is that of a dipole in a spherical cavity or an ellipsoid filled with dipole density. In both cases the entire dielectric spectral response function $\epsilon(\omega)$, without explicitly considering the spatial dependence of dielectric relaxation, is exploited. The starting assumption is that the optical excitation of the solute molecule occurs instantaneously and the dipole moment of the molecule is changed from μ_g to μ_e at time $t = 0$. Thus, the dipole moment of the solute at time t, $\mu(t)$, can be written as $\mu(t) = \mu_g + \theta(t)(\mu_e - \mu_g)$, where $\theta(t)$ is the unit step function. Following the Onsager model, the energy of interaction of such a dipole with the solvent is

$$E^{\text{solv}}(t) = - m(t) R(t) \qquad (128)$$

where $R(t)$ is the reaction field at time t due to the surrounding solvent acting on the solute dipole. The reaction field $R(t)$ can be obtained from linear response theory as

$$R(t) = \int_{-\infty}^{'} dt' r(t - t') \mu(t') \qquad (129)$$

where $r(t - t')$ is the Onsager reaction field expression for a point dipole in a sphere.

The resulting solvation energy difference between the excited state and the ground state molecule, at time t, can be thus rewritten as

$$\Delta E(t) = -[\int_{-\infty}^{'} dt' r(t - t') \theta(t')] \Delta \mu^2 =$$
$$- \frac{4(\Delta \mu)^2}{a^3 \pi} \int_0^{\infty} d\omega \frac{\cos \omega t}{\omega} \text{Im}\left[\frac{\epsilon(\omega) - 1}{2\epsilon(\omega) + 1} \right] \quad (130)$$

where all of the constant terms have been eliminated and Im indicates the imaginary part. To obtain eq 130, one has to introduce first the Fourier transform of $\Delta E(t)$ by using the complex Fourier transform of $\theta(t)$ and then the inverse Fourier transform of the resulting equation.

Basically, eq 130 is resolved by numerically integrating on different frequencies and by knowing the dielectric permittivity in the whole frequency range. In the low-frequency region Debye's formula is used, whereas for the rest, a spline fit to experimental data is used for both the real and imaginary parts of $\epsilon(\omega)$.

In 1998 Song and Chandler[542] reformulated this model so as to treat molecules of arbitrary shapes and more realistic charge distributions. The algorithm they developed is based on the Gaussian field formulation of dielectric continuum theory formulated by Song et al. in 1996.[543] In such a formulation, the solvent is described in terms of a linear responding field, that is, a Gaussian field, that is expelled from the region of space occupied by the solute. In the 1998 extension, a new reformulation of the time-

dependent solvation energy of a generic distribution of point charges (representing the chromophore) due to the dielectric is reduced to an integral over the chromophore molecular surface by introducing a time-dependent generalization of the BEM. As an application, a comparison with experimental measurements of solvation relaxation functions for coumarin 343^- (C343$^-$) in water and C153 in methanol and acetonitrile was reported. The required data for the calculations are the atomic charge distribution change of the chromophore from the electronic ground state to its first electronically excited state, the chromophore's molecular surface, and the frequency-dependent dielectric constant of the solvent.

More recently, the approach developed by Marcus and co-workers has been reformulated by Ingrosso et al.[544] within the IEFPCM continuum model and, for the first time, coupled to a QM description of the solute electronic states. In this case the time-dependent solvation energy, $E^{solv}(t)$, is the electronic component of the solute−solvent electrostatic interaction (the nuclear part is a constant independent of time if we assume a negligible role of solute nuclear relaxation)

$$E^{solv}(t) = -\mathbf{V}_{el}^{\dagger}\mathbf{q}_{el}(t) \qquad (131)$$

where $\mathbf{V}_{el}$ and $\mathbf{q}_{el}$ are the vectors collecting the solute potential at the surface and the solvent apparent charges. By comparing eq 131 with the corresponding one (eq 128) in the Onsager-like model, it is evident that the solute property of interest is no longer the dipole moment but the electrostatic potential, and the solvent response is here represented in terms of the time-dependent apparent charges. Thus, assuming for $\mathbf{V}$ the same evolution used in the Marcus model to define $\mu(t)$ in terms of the step function $\theta(t)$ and applying the same mathematical framework of Fourier and anti-Fourier transformations, one obtains the IEFPCM equivalent of the right-hand side of eq 130. The model has been applied to the calculation of the STCF for coumarin 153 in various polar solvents (water, acetonitrile, dimethyl sulfoxide, and methanol) described in terms of a generalized dispersion relation (in the form of a Cole−Davidson or Cole−Cole equation) for $\epsilon(\omega)$ in the low-frequency limit and a fit of experimental data at high frequencies. Using a configuration interaction approach including all singly substituted determinants (CIS) for the calculation of the coumarin excited states, all of the major features observed in experimental results of $S(t)$, the initial inertial decay and the multiple exponential long time relaxation, are reproduced almost quantitatively by the calculations.

Subsequently, the same model has been extended to describe a general time-dependent relaxation of the solvent. This extension has been initially proposed within the DPCM scheme by Caricato et al.[545] and then applied to the IEFPCM.[546] Once again the starting assumption is that the change in the solute molecule occurs instantaneously (at time $t = 0$) and the corresponding variation of the electrostatic potential $\mathbf{V}$ between the initial (0) and the final (fin) state is a step change. The time-dependent solvent

polarization charges at a generic time t can thus be written as

$$\mathbf{q}(t) = \mathbf{q}^0 + \delta\mathbf{q}(\Delta V, t) \qquad (132)$$

where the vector $\mathbf{q}^0$ collects the polarization charges in the initial solute−solvent equilibrium.

Under the assumption of linear response of the solvent the variation of the polarization charges $\delta\mathbf{q}$ at time t due to a change in the electrostatic potential at time $t = 0$, one obtains

$$\delta\mathbf{q}(\Delta \mathbf{V}, t) = \int_{-\infty}^{t} dt' \mathbf{R}(t - t')\theta(t')\Delta \mathbf{V} \qquad (133)$$

where $\mathbf{R}$ now indicates the PCM solvent response function. As done before in eq 130, this expression is transformed in a numerical procedure by passing from the time domain to the frequency domain by using Laplace transformations. This change is required as the dielectric response of the solvent is described in terms of its complex dielectric permittivity as a function of a frequency $\epsilon(\omega)$. The use of Laplace-transformed equations to pass from the time to the frequency domain has the effect of simplifying the formalism and of allowing the straightforward use of the function $\epsilon(\omega)$. Starting from eq 133, in fact, the variation of the charges becomes

$$\delta\mathbf{q}(\Delta \mathbf{V}, t) \cong \delta\mathbf{q}'(\Delta \mathbf{V}, t) + \mathbf{K}\Delta \mathbf{V}$$

$$\delta\mathbf{q}'(\Delta \mathbf{V}, t) = \frac{2}{\pi}\int_0^\infty \frac{d\omega}{\omega}\text{Im}[\mathbf{R}(\omega)]\cos(\omega t)\Delta \mathbf{V} \qquad (134)$$

where the definition of the matrix $\mathbf{K}$ for the different PCM schemes can be found in Table 1.

To find the proper form for the frequency-dependent response function $\mathbf{R}(\omega)$, it is useful to resort to the iterative form of the PCM equations (see section 2.3.1.5), obtaining

$$\delta q_i'^{(n)} = \frac{2\pi}{S_{ii}}g_i(t)\Big[b_i + \frac{1}{2\pi}z_i[a_j(S_{jj}\delta q_j'^{(n-1)} +$$

$$y_j[\delta q_k'^{(n-1)}])] - \frac{1}{2\pi}z_i[a_j](S_{ii}\delta q_i'^{(n-1)} + y_i[\delta q_i'^{(n-1)}])\Big] -$$

$$S_{ii}^{-1}y_i[\delta q_j'^{(n-1)}] \quad (135)$$

where

$$g_i(t) \cong \frac{2}{\pi}\int_0^\infty \frac{d\omega}{\omega}\,\text{Im}\Big[\Big(\frac{4\pi\hat{\epsilon}(\omega)}{\hat{\epsilon}(\omega) - 1}\Big)^{-1}\Big]\cos(\omega t) \qquad (136)$$

The integral in eq 136 can be solved analytically if we use the Debye expression for $\epsilon(\omega)$; however, the approach can be applied to any other functional form for the complex dielectric permittivity (like, for example, a multiple Debye, a Davidson−Cole, or a Cole−Cole form) as well as to a combined scheme including a fit of experimental data for the high-frequency portion of $\epsilon(\omega)$. The only practical difference is that in the latter case, the integral in eq 136 is solved.

Another continuum model used to describe solvation dynamics is the frequency-resolved cavity model (FRCM) formulated by Basilevsky and co-workers.[547]

The FRCM model coincides with the DPCM scheme for the electrostatic equations of the apparent charges (it is known by the acronym BKO as described in section 2.3.1.1), but differs from it in the use of two surfaces instead of a single one. The two surfaces are here introduced to separate the inertialess (high-frequency) response of the medium from the inertial (low-frequency) one. Between the two surfaces the medium is modeled by the inertialess high-frequency dielectric constant ϵ_∞; outside the outer cavity the medium is modeled by the static dielectric constant ϵ_0. The layer between the two surfaces corresponds to the first solvation shell.

Calculations in this scheme amount to simultaneously solving two equations describing the surface charge densities on the two cavities, namely, σ_∞ (on the inner surface) and σ (on the outer). In general, a simplification is applied to the FRCM model, namely, the charge density on the outer surface is assumed to be sufficiently small for its influence on the inner charge density to be neglected. Using this approximation, the equation describing σ_∞ may be separated from that determining σ, and thus it is identical to the ordinary BKO equation but with a dielectric constant now given by ϵ_∞. σ_∞ then enters as a parameter into the equation describing σ, which effectively becomes a BKO equation with scaled parameters.

Dynamics calculations are performed by replacing ϵ_0 with the complex number $\epsilon(\omega)$, thereby splitting the equation in σ into two equations describing its real and imaginary parts. Solving these equations proceeds in a similar way as for the standard BKO case. Once again, the STCF $C_{\Delta E}(t)$ is expressed in terms of $\Delta E(t)$, the inverse Fourier transform of the reorganization energy $E(\omega)$, which can be considered as a solvation energy for the charge distribution difference between ground and excited state.

The one-cavity BKO and the two-cavity FRCM approaches have been also extended to dynamical nonlocal models for the dielectric function by using the equation

$$\epsilon(k,\omega) = \epsilon_\infty + (\epsilon(\omega) - \epsilon_\infty)\Delta_k(k) \qquad (137)$$

where the spatial dispersion is determined in terms of a Lorentzian model [$\Delta(k) = 1/(1 + \lambda^2 k^2)$]. This nonlocal model when applied to the calculation of the solvation time correlation function $C_{\Delta E}(t)$ gives a long-time asymptote which differs markedly from that of the local theories and of the experiments. In this region, corresponding to the low-frequency limit $\omega \to 0$ in the frequency domain, the STCF behavior is completely determined by the size difference between the solvent and solute particles. A detailed analysis of these findings led the authors to observe that the dynamics for the nonlocal spherical model reduces to the single-exponential dynamics of the simplest dynamical continuum theory, and thus more realistic models of the nonlocal dielectric functions should be introduced.

The examples we have described above demonstrate that reasonable modifications of the conventional continuum solvent model enable one to overcome the common belief that continuum medium models are incapable of adequately treating solvation dynamics. The improved versions of the continuum theories are in fact able to qualitatively monitor the same picture of polar solvent dynamics as do molecular theories. Then, by properly adjusting the model parameters (a feature that is common for both molecular and continuum models), experimental dependencies can be well reproduced. The key step in all continuum treatments is to use the complex-valued solvent frequency-dependent dielectric function $\epsilon(\omega)$ as a phenomenological characteristic of solvent dynamics.

Indeed, continuum treatments present an important advantage with respect to standard molecular simulations, and this could become decisive soon: when combined with modern quantum chemical calculations, they allow a precise description of electronic structure and charge distributions in chemically nontrivial solute species, whereas current molecular treatments still invoke crude solute models and concentrate on a description of the details of solvent structure.

We finish this section by noting that almost all of these detailed studies on time scales and mechanisms of solvation dynamics have been limited to polar solvents. For nonpolar solvation, with the notable exceptions of the works from Berg and co-workers[548−550] and from the Maroncelli group,[551,552] few experimental studies exist. In addition, the feedback between theory and experiment that has been so productive for polar solvation has not yet been achieved for nonpolar or, more generally, non-dipolar systems, where nonpolar systems refer to systems that interact via weak nonelectrostatic forces, such as dispersive and repulsive interactions, whereas non-dipolar systems include higher electrostatic multipole (e.g., quadrupole or octupole) moments in addition to the nonpolar interactions. There are a number of reasons why non-(di)polar solvation has been less deeply analyzed. First, there is no obvious method to extract the dynamical time scales in non-dipolar liquids from existing frequency domain data such as dielectric relaxation measurements, because non-dipolar systems do not exhibit significant dielectric signals. Second, the assumptions that greatly simplify the understanding of dipolar solvation, linear response and the relative insensitivity of the time scales to the specific nature of the probe molecule, may not hold for nonpolar or non-dipolar solvation.[539] In other words, the short-range nature of the interactions implies that the molecular properties of the solvent−solute combination play a more important role in the solvation dynamics of non-dipolar systems than in the dipolar case.

Despite this increased difficulty, there are some models that can successfully predict the long time dynamics observed in nonpolar systems.

For instance, Berg[553,554] formulated a novel theory to describe nonpolar solvation in which the response of the nonpolar solvent is not based on dipolar interactions, but instead treats the solvation dynamics as a re-equilibration of the solvent to a changing volume of a solute. This model is an analogue of continuum models of polar solvation, which predict

solvation dynamics from the frequency-dependent dielectric constant, but here the solvation reponse function is calculated from the time- or frequency-dependent mechanical moduli of the solvent. The hypothesis is the assumption that a change in the solute's effective size or shape upon electronic excitation is the primary interaction driving nonpolar solvation. Following excitation, the solvent must move to allow the solute cavity to expand. This movement is modeled by treating the solvent as a viscoelastic (VE) continuum. This VE model predicts two distinct time scales that can be associated with the inertial and diffusive mechanisms and time scales. Comparisons with experimental data show this model fits long time solvation dynamics well.

5.4. Spectral Line Broadening and Solvent Fluctuations

The progress in solvation dynamics we have summarized in the previous section has also stimulated the application of continuum models to the study of the line shape of bands corresponding to absorption/emission processes and of the solvent fluctuations.

Such fluctuations in the structure of the solvation shell surrounding the chromophore[555] and the consequent variation in the local electric field lead to a statistical distribution of the energies of the electronic transitions. This phenomenon is called inhomogeneous broadening and, in most cases, its extent is much greater than that of homogeneous broadening due to the existence of a continuous set of vibrational sublevels in each electronic state. For obvious reasons we focus here only on the inhomogeneous broadening by giving a short review on the main issues related to its modelization.

A widely used approach to the analysis of solvent spectral broadening is based on the model formulated by Mukamel and co-workers[556,557] in which the solvent is represented as a bath of Brownian oscillators. This model provides convenient analytical expressions for the line broadening function $g(t)$. Implementation of the Brownian oscillator model requires only two adjustable parameters: the frequency and the variance of solvent-induced frequency fluctuations, which in turn is related to the solvent reorganization energy.[558,559] The application of the Brownian oscillator model to solvent-induced line broadening typically assumes that the solvent modes coupled to the electronic transition are overdamped, and thus the time correlation function for solvent-induced frequency fluctuations follows an exponential relaxation. However, as we have described in the previous section, theory and experiments on solvent relaxation suggest that at sub-picosecond times this relaxation is a Gaussian function of time, resulting from inertial solvent motion, followed by exponential decay characteristic of diffusional motion on the picosecond time scale.

To account for this inertial part of solvent relaxation, one can start from a phenomenological correlation function, which is a Gaussian function of time. In the limit of linear solvent response, in which the solvent dynamics are assumed to be independent of the electronic state of the chromophore, the frequency−frequency correlation function (FFCF) is defined by

$$C(t) = \langle \delta\omega_{eg}(t)\omega_{eg}(0) \rangle \qquad (138)$$

where $\delta\omega_{eg}(t)$ is the solvent-induced fluctuation in the frequency ω_{eg} of the electronic transition of the chromophore and the angle brackets indicate an equilibrium average over the solvent coordinates. We note that in this linear solvent response limit the FFCF of eq 138 is related to the function $S(t)$ determined from time-resolved Stokes shift measurements as shown in eq 127 (namely, the previously defined STCF is the FFCF normalized to unity at $t = 0$).

Several very general relationships between optical observables can be obtained for such linearly responding (Gaussian) solvents interacting with a fixed charge distribution of the solute. More precisely, these spectroscopic observables can be related to the solvent reorganization energy, λ_s.[560] This is in fact the only parameter needed to characterize the energetic intensity of the solvent nuclear fluctuations coupled to the solute.

The relationship between λ_s and the solvent-induced absorption, and emission, spectral width ($\sigma_{abs/em}$), can be written as[561,562]

$$\lambda_{abs}^{w} = \beta\sigma_{abs}^{2}/2 \quad \text{and} \quad \lambda_{em}^{w} = \beta\sigma_{em}^{2}/2 \qquad (139)$$

where $\beta = 1/k\mathrm{T}$. This relationship is exact for any fixed charge distribution of the solute in a linearly responding solvent.

Here, we do not want to enter in the large field of theoretical models to determine the solvent reorganization energy, which followed the original Marcus formulation of electron transfer[521] (some reviews can be found in refs 563 and 564). Here, it is important to recall that this concept is strictly connected to the difference in solvation free energy between the initial nonequilibrium and the final equilibrium relaxed solvent configurations originated by any fast process of solute charge redistribution such as the vertical electronic transition described in section 5.2.[240,412,545,565]

The effect of relaxing the assumption of a fixed charge distribution of the solute allowing the electronic density to flow between the initial and final states (electronic delocalization) is to alter the solute electric field, thus modifying the solute−solvent coupling and the line shift, and, even more, the inhomogeneous broadening and the observed optical width. This is because, in an electronically delocalized solute, the charge distribution changes instantaneously with solvent configuration, so that each configuration "sees" a different charge distribution.[566−568] This self-consistent action results in essentially nonlinear features of the solvent effect.[569−571]

We conclude this section by mentioning a different class of approaches to the study of the line shape in solvated systems, which explicitly account for the positional fluctuations of solvent molecules around the solute. For example, this is the approach developed by Kato and co-workers[572] within the RISM-SCF model (see section 7.4.2). In this framework the spectral bandwidths are estimated by calculating the

derivatives of the solute−solvent radial distribution function analytically.

Within the framework of continuum models, where the solvent loses its molecular nature, things are more complex. An interesting proposal to account for solvent fluctuations still maintaining a continuum description has been made by Kim.[567,573] Starting from the quantum dielectric continuum solvent formulation of Kim and Hynes,[240] Kim develops a method to include cavity size variation with the solute electronic charge distribution and its thermal fluctuations. By employing a coherent state description for the solvent electronic polarization, he obtains electronically adiabatic free energies as a function of the cavity radius variable that measures the fluctuating cavity size and the solvent coordinates that gauge the nonequilibrium solvent orientational polarization. These define multidimensional electronic free energy surfaces, upon which nuclear dynamics occur. The effects of the cavity size variation on the electronic spectra are illustrated by using a simple two-state model description for the solute. It is found that even in a nonpolar solvent, there can be a significant Stokes shift arising from the cavity size relaxation after the Franck−Condon transition. The cavity size fluctuations can also make a non-negligible contribution to the spectral line broadening.

5.5. Excitation Energy Transfers

It is well-known that de-excitation of the electronically excited states of molecules depends on many different processes (the sum of the rate constants for these processes is equal to the reciprocal of the excited state lifetime). Most of these processes involve interaction (collisions, excimer/exciplex formations, proton and electron transfers, and energy transfers) of an excited molecule M with another molecule. The fluorescence characteristics (decay time and/or fluorescence quantum yield) of the excited molecule are affected by the presence of the other molecule as a result of competition between the intrinsic de-excitation and these intermolecular processes.

Of course, intramolecular excited state processes can also affect the fluorescence characteristics of a given molecule: intramolecular charge transfer, internal rotation (e.g., formation of twisted charge transfer states), intramolecular proton transfer, etc., as well as photochemical de-excitation can apply.

All of these possible mechanisms determining the excited state lifetime can be strongly affected by the medium in which the molecules are embedded. Due to this importance, many theoretical models have been formulated to account for medium effects on excited state lifetimes. We cannot give an exhaustive review as this would require a specific volume by itself, but we restrict the analysis to intermolecular photophysical processes only and, in particulr, to those involving energy transfers.

Nonradiative transfer of excitation energy requires some interaction between a donor molecule (D) and an acceptor molecule (A), and it can occur if the emission spectrum of the donor overlaps the absorption spectrum of the acceptor, so that several vibronic transitions in the donor have practically the same energy as the corresponding transitions in the acceptor. Such transitions are coupled, that is, in resonance. The term resonance energy transfer (RET) is often used. In some papers, the acronym FRET is also used, denoting fluorescence resonance energy transfer.

Energy transfer can result from different interaction mechanisms.[574] The interactions may be Coulombic and/or due to intermolecular orbital overlap. The Coulombic interactions consist of long-range dipole−dipole interactions (Förster's mechanism[575]) and short-range multipolar interactions. The interactions due to intermolecular orbital overlap, which include electron exchange (Dexter's mechanism[576]) and charge resonance interactions, are of course only short range. For allowed transitions of D and A, the Coulombic interaction is predominant, even at short distances. For forbidden transitions of D and A (e.g., in the case of transfer to triplet states), the Coulombic interaction is negligible and the exchange mechanism prevails, but it is operative only at short distances (<10 Å) because it requires overlap of the molecular orbitals. In contrast, the Coulombic mechanism can still be effective at large distances (up to 80−100 Å).

It is evident that both Coulombic and overlap interactions will be heavily affected by the presence of a solvent around and possibly between the two interacting molecules.

In his unified formulation of EET,[575] Förster introduced the effects of a dielectric medium, that is, a solvent. His idea was in fact that the Coulomb interaction between donor and acceptor, approximated as a dipole−dipole interaction between transition dipole moments of the donor and acceptor molecules, is screened by the presence of the dielectric, namely

$$V^{\mathrm{Coul}} \approx \frac{1}{n^2}\left[\frac{\vec{\mu}_{\mathrm{D}}\cdot\vec{\mu}_{\mathrm{A}}}{R^3} - 3\frac{(\vec{\mu}_{\mathrm{D}}\cdot\vec{R})(\vec{\mu}_{\mathrm{A}}\cdot\vec{R})}{R^5}\right] \quad (140)$$

where R is the distance between the donor and acceptor and n is the solvent refractive index.

The screening factor $(1/n^2)$ in eq 140, however, is just an approximation of a part of the global effects induced by a polarizable environment on the EET process. The presence of a solvent, in fact, not only screens the Coulomb interactions as formulated by Förster but also affects all of the electronic properties of the interacting donor and acceptor.[577]

An example of a more detailed description of the solvent effects on EET was given by Juzeliunas and Andrews,[578] who reported a many-body description of EET based on quantum electrodynamics (QED). By considering the energy transfer to be mediated by bath polaritons (medium-dressed photons), this theory accounts for the modification of the bare coupling tensor both by screening effects of the medium, as in the Förster theory, and by local field effects. Also in this theory, however, a dipole approximation is used to introduce medium effects, and in fact the expression they derive is essentially Förster's dipole−dipole coupling scaled by a prefactor,

$[(\epsilon + 2)/3]^2$, where ϵ is the optical dielectric constant of the medium. Agranovich and Galanin obtained the same prefactor in 1982 from basically the same considerations in a classical theory.[579] More recently, two QM models for EET including solvent effects have appeared in the literature. Both models are based on a time-dependent variational approach even though they follow two completely different paths. In the first model by Tretiak et al.[580,581] a Hartree–Fock approximation is combined with semiempirical Hamiltonians, whereas in the second, by Hsu et al.,[582] a DFT description is used. To account for solvent effects, both methods introduce a simplified continuum description based on two important approximations, one on the form of the molecular cavity, which is always limited to a sphere, and the other on the solute electronic densities, which are represented in terms of a dipolar (or a multipolar) expansion.

More recently, a new model has been presented by Iozzi et al.[583] This is still based on a continuum description of the solvent, exactly as in the models described above, but it differs from them in two fundamental aspects. On the one hand, it introduces the solvent effects in all of the steps of the QM calculation of the EET process without requiring any simplification in the representation of the molecular charge distributions or the introduction of fixed prefactors, but defining proper operators to be added to the Hamiltonian and to the resulting response equations. On the other hand, it describes the molecular cavity on the real three-dimensional structure of the interacting solutes without imposing an artificial spherical boundary. In this framework, the EET process is described through the time-dependent density response theory (or TDDFT, see section 5.6) originally proposed in the paper by Hsu et al.,[582] whereas the introduction of the solvent effects is realized in terms of the IEFPCM described in section 2.3.1.3.

The model considers two solvated chromophores, A and D, with a common resonance frequency, ω_0, when not interacting (this condition is trivially fulfilled when A $\equiv$ D, but it is still realistic in the case of either large or condensed systems, i.e., whenever high density of nuclear states can be found). When their interaction is turned on, their respective transitions are no longer degenerate. In contrast, two distinct transition frequencies ω_+ and ω_-, appear. The splitting between these defines the energy transfer coupling, $J_{DA} = [\omega_+ - \omega_-]/2$, which can be evaluated by computing the excitation energies of the D $\oplus$ A system, as, for example, through a proper TDDFT scheme (see eq 152 in the following section).[584−589] The alternative strategy used in the model is based on a TDDFT-perturbative approach,[582] which considers the D/A interaction as a perturbation and includes solvent effects defining an effective *coupling matrix*, which couples transitions of D with those of A in the presence of a third body represented by the IEF dielectric medium. Within this framework, the first-order coupling J becomes a sum of two terms, one of which is always present (i.e., also in isolated systems) and another that has an explicit

dependence on the medium, namely

$$\mathcal{J}^0 = \int d\mathbf{r} \int d\mathbf{r}' \, \rho_D^{T*}(\mathbf{r}') \left(\frac{1}{|\mathbf{r} - \mathbf{r}'|} + g_{xc}(\mathbf{r}',\mathbf{r},\omega_0) \right) \rho_A^T(\mathbf{r}) - \omega_0 \int d\mathbf{r} \, \rho_D^{T*}(\mathbf{r}) \rho_A^T(\mathbf{r}) \quad (141)$$

and

$$\mathcal{J}^{IEF} = \sum_k \left(\int d\mathbf{r} \, \rho_D^{T*}(\mathbf{r}) \frac{1}{|\mathbf{r} - \mathbf{s}_k|} \right) q(\mathbf{s}_k; \epsilon_\omega, \rho_A^T) \quad (142)$$

where $\rho^T(\mathbf{r})$ indicates transition densities of the solvated systems D and A in the absence of their interaction. In particular, $\mathcal{J}^0$ describes a solute–solute Coulomb and exchange correlation interaction (through the exchange correlation functional of the proper DFT scheme), corrected by an overlap contribution. The effects of the solvent on $\mathcal{J}^0$ are implicitly included in the values of the transition properties of the two chromophores before the interaction between the two is switched on. These properties can in fact be significantly modified by the "reaction field" produced by the polarized solvent. In addition, the solvent explicitly enters into the definition of the coupling through the term $\mathcal{J}^{IEF}$ of eq 142, which describes a chromophore–solvent–chromophore three-body interaction (we note that this term is originated from the explicit solvent term defined in the TDDFT/IEFPCM eq 155 of the following section).

The $\mathcal{J}^{IEF}$ term can account for effects due to dynamic solvation by introducing the dynamic (ϵ_ω) instead of the static permittivity in the definition of the transition apparent surface charges $q(s_k; \epsilon_\omega, \rho^T)$. These latter generalize the concept of ASC described in section 2.3.1 to transition densities as the source of polarization, but their definition is exactly equivalent to that given when the source is represented by a standard state density.

There are two the fundamental advantages of the perturbative TDDFT/IEFPCM description of the coupling: one of a physical nature and the other numerical. The conceptual aspect, unique to this approach, is that the coupling is computed within a scheme coherently accounting for different kinds of interactions (namely, direct and indirect—i.e., solvent-mediated Coulomb, exchange, possibly including correlation effects and overlap interactions). In this way, both the reaction and the screening effects due to the solvent are introduced in a unified model, which merges Förster- and Dexter-type approaches. The numerical advantage of the perturbative approach with respect to the standard one in which the TD scheme for the supermolecule (D $\oplus$ A) is solved is that only the properties of the solvated chromophores (D and A) are required to get the coupling.

This feature of the TDDFT-PCM perturbative approach becomes particularly important when one applies the model to the calculation of excitonic splittings[590] in conjugated organic materials formed by equivalent polymeric chains in a three-dimensional array.[591] In this case, in fact, one can introduce both short-range and long-range interchain effects simply by computing the properties of a single chain embedded in a continuum medium characterized by

an anisotropic dielectric tensor (the two different components of the tensor correspond to the dielectric permittivity along and perpendicular to the main axis of the polymer chain). This extension to anisotropic dielectrics is made possible by the use of the IEFPCM formalism presented in section 2.3.1.3.

Processes of energy transfer are also responsible for another interesting phenomenon strongly dependent on the environment. It is well-known that the presence of a metal body can strongly affect the response properties of a molecule placed in its close proximity. In section 6.1.3, we shall examine the well-known surface-enhanced Raman scattering (SERS) for which enhancement factors of >10 orders in the magnitude of the Raman scattering of molecules close to metal particles have been reported. As far as concerns the excited state properties, the presence of the metal can have also the opposite effect and is responsible, in many cases, for a decrease of the molecular responses. This result is due to the fact that the excitation energy of the molecule can be efficiently transferred to the metal body (for example, via the resonant energy transfer we have just described) and can undergo, inside this medium, several dissipation processes.

The great technological interest in these phenomenona has led to the formulation of many theoretical models. Most of them consider the molecule as a polarizable pointlike dipole.[592–595] For metal−molecule distances of less than a few nanometers (a situation that occurs in many experimental situations) this approximation can be too rough and a QM description of the whole molecule would instead be necessary. On the other hand, for many of the physical systems of interest, the metal shape is one of the most important factors, and a proper description of this aspect is compulsory.

To account for both of these demands, Corni and Tomasi[79,504,506] have formulated a QM method for the calculation of dynamic response properties of a molecule in close proximity to metal bodies and possibly in the presence of a solvent. Such a model (see also sections 4.6 and 6.1.3) treats the molecule at a QM level and can explicitly consider metal particles of complex shape. The metal (and the solvent, if present) is described as a continuous body characterized by its (dielectric) response properties to electric fields, both those imposed on the system from outside and those arising from the molecular charge distribution. The metal−molecule and solvent−molecule interactions are treated within the PCM approach in its D and IEF versions. Recently, this procedure has been generalized for the calculation of the contribution to the molecular deexcitation rate due to the metal;[508,509] this generalization is based on the response theory (applied at a TDHF or TDDFT method, see the following section), in which excitation energies and lifetimes can be obtained from the real and imaginary parts of the poles of the linear response function. Strictly speaking, the lifetimes obtained in this way are related to the width of the absorption peaks of the molecule.

5.6. Time-Dependent QM Problem for Continuum Solvation Models

We conclude section 5 devoted to time-dependent (TD) solvation by considering in a more detailed way all of the QM issues implicitly or explicitly cited in the previous subsections more focused on the physical and modelistic aspects of the phenomenon.

Once again, the key point is the nonlinear character of the effective Hamiltonian defining the molecular system in the presence of the solvent (see section 2.4.5).

Here, in particular, such an effective Hamiltonian becomes time dependent. There are a large variety of processes in solution that can give rise to this time dependency. Here we limit ourselves to two cases: (a) the solvent dynamics relaxation and (b) the presence of an external time-dependent perturbing field. In general, we can write

$$H_{eff}(t) = H_M^0 + V_{int}(t) + W(t) \qquad (143)$$

where $\hat{H}_M^0$ is the Hamiltonian of the unperturbed solute, V_{int} the solute−solvent interaction term, and $W(t)$ a general time-dependent perturbation term that drives the system.

In case a discussed in section 5.3 we have that $W(t) = 0$ and the time dependence of the solute−solvent interaction $V_{int}(t)$ originates from dynamical processes involving inertial degrees of freedom of the solvent. The time scale of these processes is orders of magnitude higher than the time scale of the electron dynamics of the solute, and an adiabatic approximation can be used to follow the electronic state of the solute, which can be obtained as eigenstate of the time-dependent effective Hamiltonian (eq 143).

This approach is a direct extension of the QM problem for the basic model (see eq 58) to the effective Hamiltonian $H_{eff}(t)$ and, as shown in section 5.3, has been used by various authors[377,544,545,596] to study the time correlation function for the time-dependent Stoke's shift following a vertical excitation and to study electron-transfer processes of molecular solutes.

For case b, which will be considered in more detail in section 6, the external perturbing fields of interest are usually optical field, and the study of response properties of a molecular solute to the field requires an extension of the basic model to describe the time-dependent nonlinear Schrödinger equation for the solute, namely

$$i \frac{\partial \Psi(t)}{\partial t} = [H_M^0 + V_{int}(t) + W(t)]\Psi(t) \qquad (144)$$

This extension has been formulated by Mikkelsen et al.[136] for the MPE solvation model (see section 2.3.2) and by Cammi and Tomasi[597] within the framework of the PCM model (see section 2.3.1).

Mikkelsen and co-workers have considered the response of a reference variational (HF/MCSFC)[136–138,598] state by using the Frenkel variation principle for the TD-QM problem in the form of the Ehrenfest equation, which describes the time evolu-

tion of the expectation values for any operator B. The E-equation has the form

$$\frac{d}{dt}\langle B \rangle = \left\langle \frac{\partial B}{\partial t} \right\rangle - i\langle [B, H_{\text{eff}}] \rangle \qquad (145)$$

where the expectation values $\langle .. \rangle$ are determined from the time-dependent wave function $\Psi(t)$ at time t. The time evolution of $\Psi(t)$ may be determined by requiring that the E-equation (i.e. "the equation of motion") be satisfied by the excitation/de-excitation operators through each order in the interaction operator. By inserting such an expansion into the evolution of the expectation value of an operator A, assuming A to be time-independent in the Schrödinger picture, we obtain the linear and nonlinear response functions $\ll A; W^{\omega_1} \gg_{\omega_1 + i\epsilon}$, $\ll A; W^{\omega_1}, W^{\omega_2} \gg_{\omega_1 \pm \omega_2 + 2i\epsilon}$ of the solute.

Cammi and Tomasi using the PCM model give a slightly more general approach to the problem by using the Frenkel variation principle in the form of the stationarity equation

$$\delta\left\langle \Psi(t) \middle| G - i\frac{\partial}{\partial t} \middle\| \Psi(t) \right\rangle + i\frac{\partial}{\partial t}\langle \delta\Psi(t) | \Psi(t) \rangle = 0 \qquad (146)$$

where G is the time-dependent generalization of the free energy functional G introduced in section 2.4.4 (eq 74). From this stationary condition a variety of specific time-dependent equations at HF, MCSCF, and DFT levels have been developed,[215,527,597,599,600] from which linear and nonlinear response functions for the solute can be obtained. Further details will be given in the next section. In the time-independent limit eq 146 reduces to the variational equation for the basic model (section 2.4).

The generalized Frenkel stationary condition, eq 146, has been subsequently reformulated by Christiansen and Mikkelsen[140,141] to derive the response functions for solutes described at the coupled cluster (CC) level within the framework of spherical MPE solvation model.

Some comments on the Frenkel variation principle are here of interest. The time-dependent variational principle for the linear Hamiltonian has been the subject of several formulations,[601-603] which generated some confusion and ambiguity in the literature. A careful analysis by van Leuven[604-606] and by other authors[200,602,603,607-613] has shown that the equivalence of the various formulations is satisfied in a number of important cases for electronic structure calculations including also the nonlinear Hamiltonian case and thus continuum solvation models.

We conclude the analysis of TD-QM approaches for solvated systems by reporting a brief description of the linear response (LR) theory cited many times in this and in the previous subsections. We make here this short digression, at the end of the section devoted to TD solvation and immediately before the section focused on molecular properties, as LR is becoming one of the most important methodologies both in the study of time-dependent phenomena and in the determination of the response to applied fields.

The starting point is again the Frenkel stationary condition (eq 146); if we express the TD variational wave function $\Psi(t)$ in terms of the time-independent

unperturbed variational wave function

$$\Psi(t) = \Psi_0 + \nabla\Psi_0 \mathbf{d} + ... \qquad (147)$$

and we limit the time-dependent parameter $\mathbf{d}$ to its linear term, we get[200]

$$\nabla W + \nabla\nabla G \mathbf{d}^* + \nabla G \nabla \mathbf{d} = i\nabla Q \nabla \dot{\mathbf{d}} \qquad (148)$$

where Q is the project operator and $\nabla\nabla G$ and $\nabla G\nabla$ collect the Hessian components of the free energy functional with respect to the wave function variational parameters.

Instead of working in terms of time, we may consider an oscillatory perturbation and express $W(t)$ by its single Fourier component $A \exp(-i\omega t)$. In this framework, the linear term in the parameter assumes the form $d = [\mathbf{X}\exp(-i\omega t) + \mathbf{Y}\exp(i\omega t)]/2$ and eq 148 becomes

$$\begin{pmatrix} \nabla A \\ A\nabla \end{pmatrix} + [\Omega - \omega\Delta]\begin{pmatrix} X \\ Y \end{pmatrix} = 0 \qquad (149)$$

where

$$[\Omega - \omega\Delta] = \begin{pmatrix} \nabla G\nabla & \nabla\nabla G \\ G\nabla\nabla & \nabla G\nabla^* \end{pmatrix} - \omega\begin{pmatrix} \nabla Q\nabla & 0 \\ 0 & -\nabla Q\nabla \end{pmatrix} \qquad (150)$$

is the inverse of the linear response matrix for the molecular solute. This response matrix depends only on intrinsic characteristics of the solute–solvent system, and it permits one to obtain linear response properties of a solute with respect to any applied perturbation in a unifying and general way. For example, the time-dependent change in the expectation value of any quantity B (with associated operator) as the result of the perturbation containing the operator A can be expressed in terms of the corresponding linear response function as

$$\langle\langle B; A \rangle\rangle_\omega = \begin{pmatrix} \nabla B \\ B\nabla \end{pmatrix} [\Omega - \omega\Delta]^{-1} \begin{pmatrix} \nabla A \\ A\nabla \end{pmatrix} \qquad (151)$$

In addition, the poles $(\pm\omega_n)$ of the response function $[\Omega - \omega\Delta]^{-1}$ give an approximation of the transition energies of the molecules in solution (see section 5.2 for more comments); these are obtained as eigenvalues of the system

$$[\Omega - \omega_n\Delta]\begin{pmatrix} X_n \\ Y_n \end{pmatrix} = 0 \qquad (152)$$

where $(X_n \, Y_n)$ are the corresponding transition eigenvectors.

This general theory can be made more specific by introducing the explicit form of the wave function; in such a way, by using an HF description, we obtain the random phase approximation (RPA) (or TD-HF). In this case the expansion (eq 147) becomes[527,614]

$$\Psi(t) = \Psi_0 + \sum_{i,m} p_{mi}\Psi(i \rightarrow m) + \sum_{i \neq j, m \neq n} p_{mi}p_{nj}\Psi(i \rightarrow m, j \rightarrow n) + ...$$

where we have used the standard convention in the

labeling of molecular orbitals, that is, $(i, j, ...)$ for occupied and $(m, n, ...)$ for virtual orbitals, and indicated with $\Psi(i{\rightarrow}m)$ and $\Psi(i{\rightarrow}m,j{\rightarrow}n)$ the functions obtained from the unperturbed Ψ_0 by substituting one or two occupied orbital(s), respectively.

In parallel, the free energy Hessian terms yield

$$(\nabla\nabla G)_{mi,nj} = \langle mn||ij\rangle + B_{mi,nj}$$

$$(\nabla G\nabla)_{mi,nj} = \delta_{mn}\delta_{ij}(\epsilon_m - \epsilon_i) + \langle mj||in\rangle + B_{mi,nj} \quad (153)$$

where $\langle mn||ij\rangle$ indicates two-electron repulsion integrals and ϵ_r orbital energies.

In the definitions (eqs 153) the effect of the solvent acts into ways, indirectly by modifying the molecular orbitals and the corresponding orbital energies (they are in fact solutions of the Fock equations including solvent reaction terms, see section 2.4.2) and explicitly through the perturbation term $B_{mi,nj}$. This term can be described as the electrostatic interaction between the charge distribution $\psi_m^*\psi_i$ and the *dynamic* contribution to the solvent reaction potential induced by the charge distribution $\psi_n^*\psi_j$ (see section 5.2).

A parallel theory can be presented also for a DFT description; in this case the term TDDFT[584−589,615−617] is generally used as we have already noted in section 5.5.

In the TDDFT approach, the starting expansion is on the electronic density the first-order variation of which, $\delta\rho$, is conveniently written in the hole-particle, particle-hole formalism (within the frequency domain) as

$$\delta\rho(\omega) = \sum_{mi}\delta P_{mi}(\omega)\psi_m\psi_i^* + \sum_{mi}\delta P_{im}(\omega)\psi_i\psi_m^* \quad (154)$$

where $\delta P_{mi}(\omega)$ is the linear response matrix in the reference of unperturbed molecular orbitals ψ.

Within this formalism an analogue of eq 149 is found by using

$$(\nabla\nabla G)_{mi,nj} = K_{mi,jn} + B_{mi,nj}$$

$$(\nabla G\nabla)_{mi,nj} = \delta_{mn}\delta_{ij}(\epsilon_m - \epsilon_i) + K_{mi,nj} + B_{mi,nj} \quad (155)$$

where now the indices (i,j) and (m,n) refer to occupied and virtual Kohn−Sham orbitals and the two-electron repulsion integrals have been substituted by the coupling matrix $K_{mi,nj}$ containing the Coulomb integrals and the proper "exchange repulsion" integrals determined by the functional used.

We note that the explicit solvent term $B_{mi,nj}$ has exactly the same meaning (and the same form) of the equivalent one defined in the HF method.[583]

6. Molecular Properties of Solvated Systems

The characterization and interpretation of molecular properties have always been important subjects

in quantum chemistry since the beginning of the discipline. The extremely rapid evolution of these studies in recent years witnesses the combination of two factors, the advances in experimental techniques, leading to more accurate determinations and also to the discovery of new properties, and the progress in the formulation of new, or renewed, methodological methods for the theoretical and computational analysis.

QM solvation models have followed this evolution, examining in recent years more properties at a more accurate level and reformulating for the specific case of molecules in a medium a good number of the most recent advances in the methodology. To summarize these developments we have to consider that the subject is so large and the related physical phenomena so numerous that we shall necessarily limit our exposition to some specific aspects according to the following classification:

> I. energy properties
>   (a) geometrical derivatives
>   (b) IR/Raman intensities
>   (c) surface-enhanced IR and Raman
> II. external or response properties
>   (a) to electric fields
>   (b) to magnetic fields
>   (c) of chiral molecules

For both sets of properties we shall give first an introduction that summarizes some aspects of the general methodologies developed so far for solvated systems and then the description of the application of these methodologies to the study of specific properties. In particular, for the first set, here called energy properties, we shall consider properties that can be obtained from the potential free energy surface $G(\mathbf{R})$, that is, the free energy functional as a function of the nuclear coordinates (see section 3.2.6), whereas for the second set we shall consider response properties that describe the effects of any externally applied field on a molecular system such as dipole (hyper)-polarizabilities, both static and frequency dependent, and magnetic and chiro-optic properties.

In the following analysis of both energy and response properties we shall limit our exposition to molecules in their electronic ground state. We must, however, not neglect to say that in recent years, thanks to the evolution of both QM and solvation models, increasing attention has been paid to the study of the same properties for solvated systems in electronic excited states. The first examples[618−621] of these studies often used incomplete descriptions of the solvent effects (for example, neglecting the explicit effects on the excited state geometries), whereas in the past few years more complete studies have started to appear. Many of these more recent applications of QM continuum models[622−627] are based on the extension of the PCM model to the CI single (or CIS) approximation for the calculation of solvent effects on excited state geometries.[614]

More accurate QM methods such as CASPT2 and MRCI (see also section 5.2) have also been applied to the study of the photophysics of solvated sys-

tems;[624,625,628] in these cases, as no analytical derivatives are available, studies of geometry effects have been limited to a few important motions such as twisting and wagging modes in push−pull aromatic molecular systems.[629] In parallel, linear and nonlinear response methods (see section 5.6) have been used to calculate solvent effects on excited state properties such as dipole moments and (hyper)polarizabilities.[215,630−632]

6.1. Energy Properties

Modern quantum chemistry has been revolutionized by the ability to calculate analytical derivatives of the wave function and of the energy with respect to various parameters. A reference book by Yamaguchi et al., published in 1994,[633] is rightly titled *A New Dimension to Quantum Chemistry. Analytical Derivative Methods in ab Initio Molecular Electronic Structure Theory*. The appreciation of the role of analytical derivatives expressed in this title was speculative when formulated in 1993, but now may be considered a reality. Nowadays, practically all ab initio methods are provided with analytical derivatives, and this availability has had a remarkable impact on computational strategies.

In the past decade there has been a similar evolution in QM solvation models, and in this section we describe how the methodologies originally formulated for isolated systems have been generalized to evaluate energy properties such as IR and Raman spectra.

6.1.1. Geometrical Derivatives

The characterization of the free energy hypersurface of solvated molecules, $G(\mathbf{R})$, is based on free energy gradients, refined by second-order derivatives with respect to the nuclear coordinates. The definition of the equilibrium geometry is based on the search of critical points corresponding to local minima on $G(\mathbf{R})$, the definition of molecular motions leading, for example, to chemical reactions are again based on the examination of the gradient, supplemented by the examination of the sign of the local Hessian matrix to characterize transition states and minima. The diagonalization of the Hessian is also necessary to have the elements to characterize the molecular vibrations, and thus to study all of the properties that depend in some way on nuclear motions.

These geometrical derivatives can be computed as finite differences as currently done in classical and semiempirical continuum models, in which repeated calculations of the energy are not excessively costly. For ab initio methods the use of numerical derivatives strongly reduces the size of the systems subjected to scrutiny and the quality of the QM formulation.

The elaboration of analytic QM methods to compute derivatives of the free energy with respect to nuclear coordinates in continuum solvation models started at the beginning of the 1990s. The evolution of this elaboration, which started from methodologies

developed in the 1970s for ab initio methods in vacuo, has encountered additional specific problems. Most of these problems have been solved, but the development in the algorithms is still in progress.

Some among the first codes for gradients in continuum methods adopted the approximation of keeping the cavity rigid (see, for example, ref 634). This is a minor approximation for crude cavities, but it represents a strong approximation when the cavity is accurately modeled in terms of spheres centered on nuclei as done in the most recent versions of the continuum methods. The infinitesimal displacement of a nucleus, considered in a given partial derivative, entails an analogous infinitesimal motion in the corresponding atomic sphere, which in turn produces an infinitesimal change in the intersection of this sphere with the others. The neglect of this infinitesimal motion of the cavity gives origin to apparent forces acting on the surface, which can have an important effect, as it results from the comparison of the derivatives computed with or without this approximation.

These considerations hold for all methods using a cavity modeled on the molecular volume. Methods belonging to the ASC family, or making otherwise use of a discretization of the cavity (see section 2.3.1.5), have other specific problems. For example, using a cavity formed by interlocking spheres, surface elements at the intersection of two spheres in general have an irregular form, depending of the position of the intersection circle with respect to the mesh. A correct procedure for analytical derivatives must be able to give a satisfactory solution to this problem. In addition, in some of the algorithms used to build the cavity (for example, the GEPOL approach[43−45,92] used in the PCM class of models) an additional problem appears. To avoid crevices in which solvent cannot enter, additional spheres not centered on the nuclei can be automatically introduced by the algorithm; the positions of these added spheres depend on the infinitesimal displacements of nuclei, and thus their contribution to the analytical derivatives must be correctly taken into account. Analogous considerations hold for cavities making use of re-entrant portions of the surface (the Connolly surface, for example).

Another point deserving mention is the use of derivatives for solutes of large size. Methods for analytical derivatives in molecules now scale linearly with the size of the system. Linear scaling in continuum methods is being actively pursued, and the solutions to this problem require notable changes in the formulation of analytical derivatives. Some examples in the direction of more efficient computational strategies to compute geometrical derivatives of large solvated systems have recently been presented within the framework of PCM.[62,635]

Following the formalism used in section 2.4.2, analytical derivatives for solvated systems can be obtained by directly differentiating the expression of the free energy G given in eq 75, taking into account the SCF stationarity constraints. In this way we

obtain for the first and second energy derivatives[636,637]

$$G^\alpha = \text{tr } \mathbf{P}h^\alpha + \frac{1}{2} \text{ tr } \mathbf{P}G^\alpha(\mathbf{P}) + \text{tr } \mathbf{P}h_R^\alpha +$$
$$\frac{1}{2} \text{ tr } \mathbf{P}X_R^\alpha(\mathbf{P}) - \text{tr } \mathbf{S}^\alpha \mathbf{W} + V_{nn}^\alpha + \frac{1}{2} U_{nn}^\alpha \quad (156)$$

$$G^{\alpha\beta} = \text{tr } \mathbf{P}h^{\alpha\beta} + \frac{1}{2} \text{ tr } \mathbf{P}G^{\alpha\beta}(\mathbf{P}) + \text{tr } \mathbf{P}h_R^{\alpha\beta} +$$
$$\frac{1}{2} \text{ tr } \mathbf{P}X^{\alpha\beta}(\mathbf{P}) - \text{tr } \mathbf{S}^{\alpha\beta}\mathbf{W} + \frac{1}{2} U_{nn}^{\alpha\beta} + V_{nn}^{\alpha\beta} +$$
$$\text{tr } \mathbf{P}^\beta h^\alpha + \text{tr } \mathbf{P}^\beta G^\alpha(\mathbf{P}) + \text{tr } \mathbf{P}^\beta h_R^\alpha + \text{tr } \mathbf{P}^\beta X^\alpha(\mathbf{P}) -$$
$$\text{tr } \mathbf{S}^\alpha \mathbf{W}^\beta \quad (157)$$

where α and β are nuclear coordinates.

In eqs 156 and 157 we have introduced the shortened notation $G^\alpha = \partial G/\partial\alpha$ and $G^{\alpha\beta} \ \partial^2 G/\partial\alpha\partial\beta$, omitted the superscript 0 for the matrices h^0 and G^0, and added superscripts on the matrices to denote derivatives of the corresponding integrals over the basis set.

The solvent-induced terms, $h_R^\alpha, X^\alpha(\mathbf{P})$ and $X^{\alpha\beta}(\mathbf{P})$, are obtained by differentiating once or twice the matrices of eqs 64–67, for example

$$X_{\mu\nu}^\alpha(\mathbf{P}) = \sum_k \left[\frac{\partial V_{\mu\nu}(s_k)}{\partial\alpha} q^e(s_k) + V_{\mu\nu}(s_k) \frac{\partial q^e(s_k)}{\partial\alpha} \right] \quad (158)$$

where the second term in brackets involves derivatives of the apparent charges.

In eqs 156 and 157 we have introduced the additional matrix, $\mathbf{W} = \mathbf{PFP}$, and its derivatives, for instance

$$\mathbf{W}^\beta = \mathbf{P}^\beta \mathbf{FP} + \mathbf{PF}^{(\beta)}\mathbf{P} + \mathbf{P}[G(\mathbf{P}^\beta) + X_R(\mathbf{P}^\beta)]\mathbf{P} + \mathbf{PFP}^\beta \quad (159)$$

where $\mathbf{F}$ is the Fock matrix including solvent terms (see eq 63) and $\mathbf{F}^{(\beta)}$ its derivative, namely

$$\mathbf{F}^\beta = h^\beta + h_R^\beta \mathbf{P} + G^\beta(\mathbf{P}) + X_R^\beta(\mathbf{P}) \quad (160)$$

We note that the derivative of the density matrix $\mathbf{P}$ is not necessary for the first derivative G^α because the SCF stationary condition leads to the equivalence $\text{tr } \mathbf{P}^\alpha \mathbf{F} = \text{tr } \mathbf{S}^\alpha \mathbf{PFP}$ as for the isolated molecule. In contrast, density matrix derivatives are necessary for the second- and higher order derivatives. In particular, the second derivatives require the first derivatives of $\mathbf{P}$ (one for each parameter), which can be obtained by solving the appropriate coupled perturbed equations. These equations can be put in the general form

$$\mathbf{FP}^\alpha + \mathbf{F}^\alpha \mathbf{P} - \mathbf{P}^\alpha \mathbf{F} - \mathbf{PF}^\alpha + \mathbf{FPS}^\alpha - \mathbf{S}^\alpha \mathbf{PF} = 0 \quad (161)$$

with the usual orthonormality condition:

$$\mathbf{PP}^\alpha + \mathbf{P}^\alpha \mathbf{P} + \mathbf{PS}^\alpha \mathbf{P} = \mathbf{P}^\alpha \quad (162)$$

The elements of the matrices $h_R^\alpha, X^\alpha(\mathbf{P})$ and $h_R^{\alpha\beta}, X^{\alpha\beta}(\mathbf{P})$ contain the derivatives of the surface apparent charges with respect to nuclear displacements. These derivatives depend on the specific equation used to compute $\mathbf{q}$ (see eq 34), but in any case they require that we differentiate all of the geometrical factors which define the ASC matrix $\mathbf{K}$.[93]

Cancès and Mennucci[638,639] proposed an alternative way to proceed within the IEFPCM framework; such a procedure avoids computing any geometrical derivative of the surface charges. Their approach consists of differentiating first the basic electrostatic equation

$$-\text{div}[\epsilon(\lambda)\nabla V(\lambda)] = 4\pi\rho(\lambda) \quad (163)$$

where λ indicates a solute nuclear coordinate and $\epsilon(\lambda) = 1$ inside the cavity and $\epsilon(\lambda) = \epsilon$ outside, and obtaining $\partial V/\partial\lambda$ as a solution of the differentiated equation. This quantity is then inserted in the formula of the derivatives of the solute–solvent interaction energy. Within this approach, the only term coming from the dependence of the cavity on the motions of the nuclear coordinates is reduced to a simple sum of the apparent charges $q(s_k)$ lying on the moving part Γ of the cavity itself, namely

$$\tau = \frac{4\pi\epsilon}{\epsilon - 1} \sum_k \frac{q^2(s_k)}{a_k} [U_\Gamma(s_k) \cdot n(s_k)] \quad (164)$$

The function U_Γ assumes a very simple form for standard cavities given as unions of spheres, each of them centered on a solute nucleus. In this case we can write

$$U_\Gamma(s_k) = \begin{cases} 0 & \text{if } s_k \notin \Gamma_l \\ e_\alpha & \text{if } s_k \in \Gamma_l \end{cases} \quad (165)$$

when λ is the αth coordinate of the lth nucleus. In the aforementioned expression, (e_1, e_2, e_3) is the orthonormal basis of the real space and Γ_l is the part of the cavity belonging to the sphere centered on the lth nucleus.

Going back to the QM expressions, the free energy derivative (eq 156) reduces now to

$$G^\alpha = \text{tr } \mathbf{P}h^\alpha + \frac{1}{2} \mathbf{P}G^\alpha(\mathbf{P}) - \text{tr } \mathbf{S}^\alpha \mathbf{W} + V_{nn}^\alpha + D(\partial\rho/\partial\lambda, q) + \frac{1}{2}\tau \quad (166)$$

where the fifth and sixth terms are those collecting the explicit solvent terms. The cavity-dependent term τ is shown in eq 164, whereas D, which denotes the interaction energy between the variation of the solute charge distribution $\partial\rho/\partial\lambda$ and the apparent charges, is expressed as

$$D(\partial\rho/\partial\alpha, q) = \sum_k \frac{\partial V}{\partial\alpha}\bigg|_{s_k} q(s_k) \quad (167)$$

From eqs 164–167 it appears evident that no derivatives of the apparent charges q are required. The same method has been extended to second derivatives;[640] also in this case no derivatives of the charges are required.

Equations 166 and 167 represent an important computational gain with respect to the standard method described above in which the solvent matrices $\mathbf{h}_R$ and $\mathbf{X}_R$ are explicitly differentiated. This approach, however, is much more sensitive to the quality of the cavity surface as the cavity term τ of eq 164 can be strongly affected by the singular nature of the surface in the regions where two or more spheres intersect. As a matter of fact, numerical tests have shown that, with GEPOL-like cavities, this approach gives larger numerical instabilities than the standard one. At the moment, these numerical difficulties prevent the method from being competitive, but it is surely worth continuing to check other forms of cavities with sufficient smoothness as this approach could represent a computationally powerful approach, especially for large solutes.

We finish this section by noting that the equations have been presented in the PCM framework; a similar formalism, however, has been also developed for other ASC methods such as COSMO,[641,642] whereas a different approach is required for continuum models not belonging to the ASC class. For MPE methods, Wiberg and co-workers[634] presented the formulation within the Onsager formalism for spherical fixed cavities. Mikkelsen et al.[136] presented multipolar one-center formulations still for spherical fixed cavities, and Rivail and co-workers presented a theory for both spherical and ellipsoid cavities with one-center multipolar expansion and molecular cavities with multicenter multipolar expansions.[145,643] Within the GB approach, analytical energy gradients have been formulated by Cramer and Truhlar and co-workers using a SMx solvation model based on CM2 atomic charges.[171]

For some of these models derivatives for post-HF methods have also been presented both for variational (see refs 96, 212, and 644 for MCSCF) and for nonvariational (MP2[234,236] and CC[140]) methods. The formal apparatus looks more complex, but actually it is not much different from that used for analogous derivatives in vacuo: for variational methods the formalism resembles that of Hartree–Fock, whereas nonvariational methods have required the extension of the relaxed density matrix approaches to the continuum solvation methods.

6.1.2. IR and Raman Intensities

Theoretical modeling of solvent effects on IR and Raman intensities has been a matter of study for many years within semiclassical continuum models.[645–651] The various formulations were based on the consideration that when the light interacts with a molecule in condensed phase, the "local field" that is experienced by the molecule is different from the Maxwell field in the medium.

Local field effects, which are also important in the study of other properties, such as linear and nonlinear optical properties (see section 6.2.2) and optical and vibrational properties of chiral molecules (see section 6.4), can be separated into two terms. The first one, the "reaction field", is connected with the response (polarization) of the medium to the molecule charge distribution. The second term (the "cavity field", E^c) depends on the polarization of the medium induced by the externally applied electric field once the cavity, which hosts the molecule, has been created.

A further aspect introduced by some of these models concerns nonequilibrium solvation effects associated with nuclear vibrational motions.

Only recently, both local field and nonequilibrium effects have been reconsidered within the framework of QM solvation models to study vibrational properties. We present some details about these solvent effects on the IR intensities, but similar considerations can be applied to Raman intensities.

We shall start from the analysis of "local field" effects and follow the approach used in refs 652–654 within the framework of the PCM solvation model.

6.1.2.1. Cavity Field Effects. The starting point is the expression for the transition probability of an isolated system in the dipolar approximation between two vibrational states 0 and 1 induced by radiation of frequency ω

$$W_{1\leftarrow 0}^{\text{gas}} = \frac{2\pi}{\hbar}\,\delta(E_1 - E_0 - \hbar\omega)|\langle 1|\vec{\mu}\cdot\vec{E}^{\text{gas}}|0\rangle|^2 \qquad (168)$$

In eq 168 E_1 and E_0 are the energies of the vibrational states 1 and 0, respectively, $\vec{\mu}$ is the dipole moment, and $\vec{E}^{\text{gas}}$ is the electric field acting on the molecule.

Passing to molecules in solution, the transition probability can be expressed in two alternative but equivalent ways. We introduce the cavity field E^c, which interacts with the dipole moment $\vec{\mu}$ of the solvated molecule, or we use the (Maxwell) electric field of the radiation in the medium, $\vec{E}$, which interacts with the so-called external dipole moment. Following Onsager, this quantity is defined as the sum of the molecular dipole moment and the dipole moment $\tilde{\mu}$ arising from the polarization induced by the molecule on the dielectric. The resulting expression for the transition probability in solution yields

$$W_{1\leftarrow 0}^{\text{sol}} = \frac{2\pi}{\hbar}\,\delta(E_1 - E_0 - \hbar\omega)|\langle 1|(\vec{\mu} + \tilde{\mu})\cdot\vec{E}|0\rangle|^2 \qquad (169)$$

and the corresponding integrated absorption becomes

$$A^{\text{sol}} = \frac{\pi N_A}{3 n_s c^2}\left(\frac{\partial(\vec{\mu} + \tilde{\mu})}{\partial Q}\right)^2 \qquad (170)$$

where N_A is Avogadro's number, c the velocity of light in vacuo, and n_s the refractive index of the solvent under study. In eq 170 Q collects the solute mass weighted normal coordinates associated with the vibrational mode.

The computational expression for $\tilde{\mu}$, within the PCM framework,[652] is given in terms of apparent surface charges, q^{ex}, analogous to those defined in section 2.3.1.5, but having the external Maxwell field as a source of polarization.[655,656] The final expression is

$$\tilde{\mu} = -(\sum_k V(s_k)\vec{\nabla}_{\bar{E}}[q^{\text{ex}}(s_k)]) \qquad (171)$$

where the sum runs over the number of tesserae, V

is the potential generated by the solute on the same tesserae, and the symbol $\nabla_{\bar{E}}$ indicates the differentiation of the apparent charges with respect to the components of the external Maxwell field.

6.1.2.2 Nonequilibrium Effects. Looking at typical vibration times, namely, $10^{-14}-10^{-12}$ s, it is evident that the orientational component of the solvent polarization is not able to follow the oscillating charge distribution of the solute and a nonequilibrium polarization (comparable to that presented in section 5.2 for electronic motions) must be considered.

In common practice, the polarization is partitioned into two terms: one term accounts for all motions that are slower than those involved in the molecular vibrations and the other includes the faster contributions. The next assumption usually made is that only the latter are instantaneously equilibrated to the momentary molecule charge distribution, whereas the former cannot readjust.

In the case of vibrations of solvated molecules the slow term contains contributions arising from the motions of the solvent molecules as a whole (translation and rotations), whereas the fast term takes into account the internal molecular motions (electronic and vibrational). Such a division is reasonable when the solute vibration under study is sufficiently far in the frequency from those of the solvent; when necessary, this distinction may be modified.

The first attempt to introduce nonequilibrium effects into the QM vibrational studies with continuum models is due to Olivares del Valle et al. using the DPCM formulation.[657,658] They introduced a set of models spanning from a complete decoupling of the vibrational charge distribution and the solvent polarization to a complete equilibrium coupling, passing through a nonequilibrium model (see ref 1 for more details) to compute both vibrational frequencies and intensities.

Also, Rivail and co-workers[659] elaborated a nonequilibrium scheme (in the framework of the MPE method using an ellipsoidal cavity) but limited to the study of the frequencies. Their formulation is the first to exploit analytical first and second derivatives of $G(\mathbf{R})$. The numerical applications they presented showed that nonequilibrium solvation has little effect on the vibrational frequencies. We remark that Rivail used a nonequilibrium polarization scheme based on the partition approach described in section 5.2.

More recently, Cappelli et al.[653] elaborated a more sophisticated nonequilibrium formulation for the PCM scheme. Their method allows for analytical derivatives of the nonequilibrium free energy G_{neq}-$(\mathbf{R})$ to compute IR frequencies and intensities. In this model a rigid cavity is exploited consistently with a nonequilibrium scheme in which the orientational and translational motions of the solvent molecules are not able to follow the vibrating charge distribution of the solute. The computational scheme is based on the partition of the polarization into inertial and dynamic terms and on the use of the corresponding expression for the free energy functional (see section 5.2). In this model, the nonequilibrium is due to the oscillating motion of both electrons and nuclei. The

analytical derivatives of $G_{neq}(\mathbf{R})$ were computed by exploiting the same techniques used for the corresponding derivatives of the equilibrium free energy functional (see eq 157). However, this time the cavity is kept fixed, and thus the evaluation of the geometrical derivatives is less computationally demanding. Numerical applications to carbonyl frequencies in ketones confirm the previous finding of Rivail that nonequilibrium solvation has little effect on the frequencies, whereas they found that nonequilibrium polarization has large effects on the IR intensities.

Cappelli et al. have subsequently extended their nonequilibrium formulation to the study of Raman scattering factors for solvated molecules.[505,654,660] The starting point of this formulation was the consideration of the Raman scattering as the result of the modulation in the electric-field-induced oscillating dipole moment due to vibrational motions. The dynamic aspects of Raman scattering are to be described in terms of two time scales, one connected to the vibrational motions of the nuclei and the other to the oscillation of the incoming electric field; both give origin to oscillations in the solute electronic density). In the presence of a solvent, both time scales originate nonequilibrium effects in the solvent response to the fast oscillations in the solute electronic density. The proposed model, which includes such a nonequilibrium effect, has been applied to the study of Raman intensities of simple molecules in various solvents.

6.1.3. Surface-Enhanced IR and Raman

Molecules adsorbed on metal surfaces exhibit an infrared light absorption (due to vibrational transitions), which is amplified by a factor of 10^2-10^3 compared to the molecule without the metal [this phenomenon is called surface-enhanced infrared absorption (SEIRA)].[661,662] In parallel, molecules adsorbed on specially prepared metal surfaces or on metal colloids exhibit Raman spectra with some bands enhanced by a factor of up to $10^{10}-10^{14}$ in comparison with the spectra of nonadsorbed molecules, enabling the detection of a single molecule. This phenomenon is generally known as surface-enhanced Raman scattering (SERS).[663-667] The metals that promote SERS more readily are Ag, Au, and Cu (coinage metals), although SERS has been reported for a large variety of metals.

When an electromagnetic field is applied to a metal specimen having a curved surface (such as a rough surface, a metal nanoparticle deposited on a surface, or a metallic colloids), it can excite collective resonances of the electron gas in the metal (surface plasmons). Such resonances can create an evanescent electromagnetic field of high intensity, localized in proximity of the metal surface. A molecule close to such a metallic specimen feels a local field much more intensely than the incident one, so its effective response properties will be greatly amplified. In particular, local enhancements of the field give origin to so-called "hot spots", that is, points at which the chromophore, interacting with the resulting total field, shows an enhanced IR/Raman signal. The enhancement factors tentatively considered are that

of the incident electric field due to the whole metal aggregate, that due to the interaction of the molecule with the local hot spot combined with the effect of interaction of the molecule with the liquid phase (if present), that due to the interaction of the light emitted by the molecule plus hot spot system with the rest of the metal cluster, and that due to chemical interaction of the molecule with the metal.

The effects on electromagnetic fields due to the presence of metal bodies represent a unifying element in the origin of the SEIRA and SERS phenomena even if each phenomenon has its own features. Because SERS has been the most studied, here we shall focus on that only.

A considerable amount of theoretical work on this subject has been done since the discovery of SERS, but most of these, although quite refined in the description of the metal,[668] represent the molecule just as a polarizable point dipole. Another approach used on some occasions[669,670] consists of a whole ab initio description of the molecule interacting with a metal cluster of a few atoms. This model accounts also for chemisorption effects, but the small metal cluster clearly cannot reproduce the behavior of, for instance, a nanosized metal particle, which is composed of thousands of atoms.

If we limit ourselves to the study of molecules physisorbed on a metal, that is, molecules which are not chemically bound to the metal surface, the problem of a proper description of such systems strongly resembles that for solvated molecules. In fact, a molecule in solution weakly interacts with a great number of other electrons and nuclei, feeling all of the fields of external as well as internal origin, as a molecule physisorbed on a metal surface does. Following the theoretical lines of the PCM approach, an extension of such a model to treat molecules close to metal particles (which, in turn, can be immersed in a dielectric medium) has been presented[79,504,507] (see also section 5.5). In such an extension, the metal is described as a continuous body characterized by electric response properties only, which behaves as a perfect conductor for static fields and as a dielectric for time-dependent fields. Infinite planar metal surfaces, complex shaped nanoparticles, and aggregates of nanoparticles have been considered, but in any case the only interactions considered among the various portions of the complex system (the molecule, the metal, and, possibly, the solvent) are electrostatic in origin.

The basic idea underlying this model is that it is not necessary to treat the whole system (metal particle plus molecule) to the same degree of accuracy, but it is better to focus the attention on the portion of the system of which we want to study the properties.

Subsequently, the model has been improved[507] by partitioning the system into three "layers," described at different levels of accuracy. The whole metal cluster (the first layer) is treated as a collection of spherical metallic particles described as polarizable dipoles to be able to recognize where the hot spots are at a given excitation wavelength and how strong the electric field locally acting on them is. The metal

particles in a given hot spot (the second layer) can be considered as a unique complex shaped particle and treated by using the original model, which neglects the detailed atomic and electronic structure of the metal but which takes into account effects on the electric field due to the complex shape (union of interlocking spheres). Finally, the molecule (the third layer) is described at the ab initio level, taking into account electrostatic interaction with the metal particle and properly treating the electric field acting on it. By exploiting this model, huge enhancement factors have been found for Raman spectra of molecules close to different metal particle aggregates, which compare well with experiments.

6.2. Response Properties to Electric Fields

The investigation of linear and nonlinear optical (NLO) properties of solvated molecules and liquids has been one of the most important developments of the QM continuum solvation models in recent years. Such progress has been prompted by the success of modern quantum chemical tools in predicting response properties for molecules in the gas phase.

The experience gained for isolated molecules has in fact represented a fundamental background as concerns theoretical issues as well as more physical aspects. Following these studies, for example, continuum solvation models have been extended to treat not only the leading electronic term of the optical properties but also (even if in a less widespread way) the vibrational contributions. Due to the far larger number of studies present in the literature, in the following sections we shall focus on the electronic contribution only. However, it is interesting to add some notes on the vibrational part also because studies appeared so far seem to show that vibrational effects can become very important (if not dominant) for NLO properties of solvated molecules.[671,672]

Vibrational contributions are generally divided into two components,[673−676] the "curvature" related to the field dependency of the vibrational frequencies (i.e., the changes in the potential energy surface in the presence of the external field) and including the zero-point vibrational correction and the "nuclear relaxation" arising from the field-induced nuclear relaxation (i.e., the modification of the equilibrium geometry in the presence of the external field).

The nuclear relaxation is generally the dominant contribution, especially when in the presence of applied static fields. The most largely used method to account for these effects is based on series expansion of the energy and of the electric dipole with respect to both the nuclear coordinates and the external field components. As shown in refs 671, 672, and 677, the same procedure can be applied to solvated systems when described through continuum solvation models; this equivalence is made possible if expansions of the free energy functional are used and the related dipole and polarizability derivatives with respect to normal coordinates are computed in the presence of the solvent.

The equivalence between condensed phase and gas phase systems concerning the calculation of optical properties, however, is not complete as the presence

of the environment introduces more critical issues than for isolated systems, but it also offers the possibility to compare the computed microscopic properties with experimental macroscopic quantities. Formal correspondences and physical differences will be analyzed in the following two subsections, respectively.

6.2.1. QM Calculation of Polarizabilities of Solvated Molecules

In section 5.6 we have presented the general time-dependent QM theory for solvated systems; here, we come back to such a theory but specialize it to the case of a perturbation represented by the combination of a static (E^0) and an oscillating electric field (E^ω). In this case, the operator $W(t)$ in eq 143 becomes

$$\hat{W}(t) = \hat{\mu} \cdot [\vec{E}^\omega(e^{i\omega t} + e^{-i\omega t}) + \vec{E}^0] \quad (172)$$

where μ is the electronic dipole moment operator of the solute.

By using the Frenkel variational principle (eq 146) within the restriction of a one-determinant wave function with orbital expansion over a finite atomic basis set, we obtain the following time-dependent Hartree−Fock (or Kohn−Sham) equation

$$\mathbf{F}'\mathbf{C} - i\frac{\partial}{\partial t}\mathbf{SC} = \mathbf{SC}\epsilon \quad (173)$$

with the proper orthonormality condition; $\mathbf{S}$, $\mathbf{C}$, and ϵ represent the overlap, the MO coefficients, and the orbital energy matrices, respectively.

In eq 173 the prime on the Fock matrix indicates that terms accounting for the solvent effects are included, that is

$$\mathbf{F}' = \mathbf{h} + \mathbf{G}(\mathbf{P}) + \mathbf{j} + \mathbf{X}(\mathbf{P}) + \\ \mathbf{m} \cdot [\mathbf{E}^\omega(e^{i\omega t} + e^{-i\omega t}) + \mathbf{E}^0] \quad (174)$$

where the first four terms on the right-hand side of the equation represent the Fock operator for the solvated molecule (see section 2.4.2 for more details) and $\mathbf{m}$ represents the matrix containing the dipole integrals; we note that in eq 174 we have discarded the superscript "0" used in the previous sections to indicate the Hamiltonian terms of the isolated molecule (here the same superscript is used to indicate static fields) and the superscript R for the solvent-induced terms, $\mathbf{j}$ and $\mathbf{X}(\mathbf{P})$.

The solution of the time-dependent HF or KS eq 173 can be obtained within a time-dependent coupled HF (or KS approach). We first expand eq 174 to its Fourier components, and subsequently, each component is expanded in terms of the components of the external field. The separation by orders leads to a set of CPHF equations for which the Fock matrices can be written in the form

$$\mathbf{F}'^a(\omega) = \mathbf{m}_a + \tilde{m}^\omega + \mathbf{G}(\mathbf{P}^a(\omega)) + \mathbf{X}_\omega(\mathbf{P}^a(\omega))$$

$$\mathbf{F}'^{ab\ldots}(-\omega_T;\omega_1,\omega_2,\ldots) = \mathbf{G}(\mathbf{P}^{ab}(-\omega_T;\omega_1,\omega_2,\ldots)) + \\ \mathbf{X}_{\omega_T}(\mathbf{P}^{ab}(-\omega_T;\omega_1,\omega_2,\ldots)) \quad (175)$$

where a,b, ... indicate the Cartesian components of the field and ω_x are the frequencies related to the external fields (eventually static and thus $\omega_x = 0$). We note that the elements of the solvent-reaction matrices $\mathbf{X}_{\omega T}$ (see eqs 67 and 68) depend twice on the frequency-dependent nature of the field, in the perturbed density matrices $\mathbf{P}^{ab\ldots}(\omega_1,\omega_2,\ldots)$, and in the value of the solvent dielectric permittivity $\epsilon(\omega_T)$ at the resulting frequency $\omega_T = \Sigma\omega_x$ (see section 5.2).

Once solved, the proper CPHF equations, the dynamic polarizabilities of interest, can be expressed in the following forms:

$$\alpha_{ab}(-\omega;\omega) = -\text{tr}[\mathbf{m}_a\mathbf{P}^b(\omega)]$$

$$\beta_{abc}(-\omega_T;\omega_1,\omega_2) = -\text{tr}[\mathbf{m}_a\mathbf{P}^{bc}(-\omega_T;\omega_1,\omega_2)] \quad (176)$$

$$\gamma_{abcd}(-\omega_T;\omega_1,\omega_2,\omega_3) = -\text{tr}[\mathbf{m}_a\mathbf{P}^{bcd}(-\omega_T;\omega_1,\omega_2,\omega_3)]$$

We note that an alternative (but equivalent) method can be used to get $\alpha_{ab}(\omega)$; namely, we can resort to the linear response theory presented at the end of section 5.6 and use eq 151 with B and A being the dipole moment operators, that is, $\langle\langle\hat{\mu}_a;\hat{\mu}_b\rangle\rangle_\omega$ (to get the analogue equation for β and γ a quadratic and a cubic response theory have to be invoked).

Applications of the QM theory for the calculation of linear and nonlinear optical properties of solvated molecules have been carried out by Willets and Rice,[678] Yu and Zerner,[679] Mikkelsen and co-workers,[139,516,680−684] and the PCM group,[599,655,656,671,685−689] all applying different solvent models as well as different levels of the quantum theory.

6.2.2. Definition of Effective Properties

A key factor in the study of response properties is the relationship between the molecular and the material properties, that is, the distinction between the microscopic field at a molecule and the macroscopic field applied to the material.[690] The macroscopic field is determined directly from the experimental conditions, but the microscopic field has to be calculated using a suitable theory.

The classical approach is to use the Onsager−Lorentz model and write the measured susceptibilities (the macroscopic equivalent of the linear and nonlinear optical, NLO, molecular properties) in terms of the gas phase molecular values multiplied by so-called *local field factors* (see also section 6.1.2). In recent years different models have been proposed to improve such a description. Most of them are based on the concept of a solute in a cavity in a dielectric continuum provided by the rest of the material. Within the framework of semiclassical descriptions, important generalizations of the Onsager−Lorentz model for NLO properties have been made by Wortmann and Bishop[691] and by Ågren and co-workers,[677,692−695] whereas a QM approach has been formulated within the PCM approach described in section 2.3.[655,656,689]

The PCM extension to get macroscopic susceptibilities that can be directly compared with experiments has been achieved by introducing so-called effective

properties: the properties describing the change of molecular polarization with respect to the external applied fields. Here we briefly describe the main aspects of this extension emphasizing when useful the connection with semiclassical approaches.

The response of the medium to a macroscopic field $\vec{E}(t)$ generated by the superposition of a static and an optical component is represented by the dielectric polarization vector (dipole moment per volume) $\vec{P}(t)$, which in terms of Fourier components yields

$$\vec{P}(t) = \vec{P}^0 + \vec{P}^\omega \cos(\omega t) + \vec{P}^{2\omega} \cos(2\omega t) + \dots \quad (177)$$

Exactly as for the molecular dipole expansion usually introduced for isolated molecules, each Fourier amplitude can be rewritten as a power series with respect to the applied macroscopic (or Maxwell) field in the medium, for example

$$\vec{P}^\omega = \chi^{(1)}(-\omega;\omega)\cdot\vec{E}^\omega + 2\chi^{(2)}(-\omega;\omega,0)\cdot\vec{E}^\omega\vec{E}^0 + \dots \quad (178)$$

where the tensorial coefficients are the nth-order macroscopic susceptibilities $\chi^{(n)}$. They are tensor of rank $n + 1$ with $3^{(n+1)}$ components. The argument in parentheses describes the kind of interacting waves; in all cases the frequency of the resulting wave is stated first, then the frequency of the incident interacting wave(s) (two in a first-order process, three in the second-order analogue, and four in the third-order case). The different susceptibilities involved in the various Fourier amplitudes correspond to experiments in linear and nonlinear optics; in eq 178, for example, $\chi^{(1)}(-\omega;\omega)$ is the linear optical susceptibility related to the refractive index n at frequency ω and the Pockels susceptibility $\chi^{(2)}(-\omega;\omega,0)$ describes the change of the refractive index induced by an externally applied static field.

If we consider as macroscopic sample a liquid solution of different molecular components, each at a concentration c_J (moles per volume), the global measured response becomes[696−699]

$$\chi^{(n)} = \sum_J \zeta_J^{(n)} c_J \quad (179)$$

where the effects of the individual components have been assumed to be additive and $\zeta_J^{(n)}$ are the nth-order molar polarizabilities of the constituent J. The values of each $\zeta_J^{(n)}$ can be extracted from measurements of $\chi^{(n)}$ at different concentrations. The calculation of the molar polarizabilities $\zeta_J^{(n)}$ involves statistical mechanical averaging over orientational distributions of the molecules. In particular, by introducing the Z space-fixed axes of the laboratory, we obtain for a general nth-order molar polarizability

$$\zeta_{ZZ\dots}^{(n)}(n\omega) = N_A \left(\frac{\partial^n \langle \bar{u}_Z(n\omega) \rangle}{\partial E_Z \partial E_{Z}\dots} \right)_{E\to 0} \quad (180)$$

where N_A is Avogadro's number and m is the effective dipole.[656]

We note that in the case of a pure liquid, the definition (eq 179) becomes[700]

$$\chi^{(n)} = c\zeta_{ZZ\dots}^{(n)}(n\omega) = \rho \left(\frac{\partial^n \langle \bar{u}_Z(n\omega) \rangle}{\partial E_Z \partial E_{Z}\dots} \right)_{E\to 0} \quad (181)$$

where ρ is the number density of the liquid.

The derivation of the expressions for the molar polarizabilities in terms of the proper effective properties can be found in ref 656. We only stress that as the molar polarizabilities represent an easily available "experimental" set of data, these expressions become important for the theoretical evaluation of molecular response properties. In fact, they represent the most direct quantities to compare with the computed molecular effective properties.

The theory for the calculation of the effective polarizabilities has been presented both at semiclassical[691] and quantum mechanical level.[656] The QM theory is parallel to that presented in section 6.2.1; now, however, we have to introduce a further perturbing term for a correct comparison with experimental results. As a result, the operator $W(t)$ in eq 172 becomes

$$\hat{W}(t) = \hat{\mu}\cdot[\vec{E}^\omega(e^{i\omega t} + e^{-i\omega t}) + \vec{E}^0] +$$
$$\sum_k \hat{V}_k(\vec{\nabla}_{\bar{E}^x}[q_\omega^{ex}(k)]\cdot\vec{E}^\omega(e^{i\omega t} + e^{-i\omega t}) +$$
$$\vec{\nabla}_{\bar{E}^0}[q_0^{ex}(k)]\cdot\vec{E}^0) \quad (182)$$

In eq 182 "external" ASCs, q^{ex}, have been introduced exactly as in eq 171; these charges can be described as the response of the solvent to the external field (static or oscillating) when the volume representing the molecular cavity has been created in the bulk of the solvent. This effect must be summed to the standard reaction field in order to fully consider the effective response of the solvent to the combined action of the internal (due to the solute) and the external fields.[655,656] We note that the effects of q^{ex} in the limit of a spherical cavity coincide with that of the cavity field factors historically introduced to take into account the changes induced by the solvent molecules on the average macroscopic field at each local position inside the medium.

Due to the presence of the additional term also, the Fock matrix defined in eq 174 changes to

$$\mathbf{F}' = \mathbf{h} + \mathbf{G}(\mathbf{P}) + \mathbf{m}\cdot[\mathbf{E}^\omega(e^{i\omega t} + e^{-i\omega t}) + \mathbf{E}^0] +$$
$$\mathbf{j} + \mathbf{X}(\mathbf{P}) + \tilde{\mathbf{m}}^\omega\cdot\mathbf{E}^\omega(e^{i\omega t} + e^{-i\omega t}) + \tilde{\mathbf{m}}^0\cdot\mathbf{E}^0 \quad (183)$$

where the last two terms, $\mathbf{m}^\omega$ and $\mathbf{m}^0$, are the matrices related to the apparent charge q^{ex} induced by the external oscillating and static field, respectively, namely (see eq 171)

$$\tilde{\mathbf{m}}^x = -\left(\sum_k V(s_k)\nabla_{\bar{e}^x}[q^{ex}(s_k)]\right) \quad \text{with } x = 0,\omega \quad (184)$$

where $\mathbf{V}(s_k)$ is the matrix containing the solute potential atomic integrals computed on the surface cavity.

By solving the new time-dependent coupled HF (or KS) equation, the dynamic effective polarizabilities of interest can be expressed exactly as in eq 176; the

only difference is that now perturbed electron density $\mathbf{P}^a(\omega)$ [or $\mathbf{P}^{ab}(\omega)$] is different due to the presence of the new perturbing term (eq 184) in the related Fock matrices.

We conclude by noting that to extend the QM calculations of effective polarizabilities to pure liquids, a further element has to be introduced. In that case, the optical radiation at the fundamental frequency ω produces in the liquid a macroscopic polarization density at the output frequency, which acts as source of an additional perturbing term.[700]

6.3. Response Properties to Magnetic Fields

In this section, we present a research field relatively new for QM continuum solvation models, namely, that of the study of solvent effects on magnetic molecular properties, which determine nuclear magnetic resonance (NMR) and electronic paramagnetic resonance (EPR) phenomena. Due to this "young existence", many aspects of both formal and physical nature have yet to be deeply understood, but the research is very active in many laboratories. To date, almost all of the studies in this field have involved two classes of continuum models, that based on a multipolar expansion (MPE) of the reaction field and that introducing an apparent surface charge (ASC). In particular, we note that greatest progress has been achieved within the ASC approach [in its different formulations, CPCM, IEFPCM, and SS(V)-PE]. On the one hand, generalizations to include more detailed aspects of solvation, such as specific solute–solvent interactions, through couplings with discrete pictures have been presented using solute–solvent clusters obtained through QM minimization methods or taken from MD simulations. On the other hand, extensions to more complex environments have been also realized; we recall here, as an example, the recent extension of the IEFPCM for anisotropic dielectrics to the study of NMR properties of solutes immersed in liquid crystalline solvents.[102,701] Both of these extensions indicate new perspectives of applications of continuum models toward systems of increasing complexity, heretofore considered as completely prohibitive for a continuum description.

To better quantify the importance that QM studies of solvent effects on magnetic properties are rapidly achieving, in Table 3 we try to summarize recent papers in which continuum solvation models have been used.

6.3.1. Nuclear Shielding

The effects of solvent on nuclear magnetic shielding parameters derived from NMR spectroscopy have been of great interest for a long time. In 1960 Buckingham et al.[743] suggested a possible classification in terms of various additive corrections to the shielding arising from (i) the bulk magnetic susceptibility of the solvent, (ii) the magnetic anisotropy of the solvent molecules, (iii) van der Waals interactions, and (iv) long-range electrostatic interactions. In the original scheme, strong specific interactions, such as those acting in intermolecular hydrogen bonds, were not specifically dealt with but just mentioned as a possible extreme form of the electro-

Table 3. NMR and EPR Properties (Nuclear Shielding, Magnetizability, Spin–Spin Coupling, EPR) Calculated with Continuum Solvation Models (or Their Hybrid Discrete/Continuum Generalizations)

solvation model	author[a]	refs
MPE	Mikkelsen	702–708
	Pecul	709, 710
	Pennanen	711
ASC	Cammi/Mennucci	102, 701, 712–722
(CPCM,	Barone/Cossi	723–734
IEFPCM, SS(V)PE)	Manalo	735, 736
	Chipman	104
	Cremer	737, 738
	Zaccari	739, 740
	Ciofini	741
	Rinkevicius	742

[a] Reference name, not necessarily the first author.

static, or, more generally "polar", effect; in the numerous applications that followed Buckingham's classification, however, this further effect has been always included as a separate contribution.

On the basis of such a classification an empirical approach based on the so-called solvent empirical parameters was formulated to evaluate solvent effects on nuclear shieldings. In brief, this approach, originally proposed by Kamlet, Taft, and co-workers,[744] does not involve QM or other types of calculations but introduces a numerical treatment of experimental data obtained for a given reference system to obtain an estimate of solvent effects on various properties. Its generalization to the study of the solvent effect on nitrogen nuclear shielding in various compounds has been proposed by Witanowski et al.[745–749]

In parallel to these semiclassical analyses, recently we have observed growing attention to an explicit description of the electronic aspects of the solvent effects on NMR properties and in particular on the nuclear shielding. This change of perspective has been made possible by the large development of QM solvation models we have described in section 2, which have been coupled to QM methodologies initially formulated for isolated systems.

The theory of chemical shielding was originally developed many years ago,[750,751] but only later have ab initio methods[752–756] and density functional theories (DFT)[757,758] been reliably used for the prediction of chemical shielding for molecular systems.

Because these recent developments greatly improved the accuracy of the calculation of the nuclear shieldings, the following step has been the inclusion of solvent-induced shifts. This has been achieved by extending the cited theoretical methods to continuum solvation models. Such extension began by redefining the components of the shielding tensor σ, as second derivatives of the free energy functional defined in section 2.4[712]

$$\sigma_{ab}^{\mathrm{X}} = \frac{\partial^2 G}{\partial B_a \partial M_b^{\mathrm{X}}} \tag{185}$$

where B_a and M_b ($a,b = x, y, z$) are the Cartesian components of the external magnetic field B and of

the nuclear magnetic moment of nucleus X, respectively. In this way, the general description of the nuclear magnetic shielding for an isolated molecule in terms of the influence on the total energy of the molecule of the nuclear magnetic moment and of the applied uniform magnetic field has been translated to molecular solutes in the presence of solvent interactions.[705,712]

We recall here that in order to reliably calculate the nuclear shielding in ab initio calculations, the gauge invariance problem has to be faced. Gauge factors are generally introduced into the atomic orbitals of the basis set by using gauge invariant atomic orbitals (GIAO).[752,753] The GIAO method is used in conjunction with analytical derivative theory (see section 6.1.1). In this approach the magnetic field perturbation is treated in an analogous way to the perturbation produced by changes in the nuclear coordinates (see eq 157), and the components of the nuclear magnetic shielding tensor are obtained as

$$\sigma_{ab} = \text{tr}[\mathbf{P}\mathbf{h}^{B_a M_b^X} + \mathbf{P}^{B_a}\mathbf{h}^{M_b^X}] \qquad (186)$$

where $\mathbf{P}^B$ is the derivative of the density matrix with respect to the magnetic field. Matrices $\mathbf{h}^M$ and $\mathbf{h}^{B,M}$ contain the first derivative of the one-electron term of the Hamiltonian with respect to the nuclear magnetic moment and the second derivative with respect to the magnetic field and the nuclear magnetic moment, respectively. Neither matrix contains explicit solvent-induced contributions as the latter do not depend on the nuclear magnetic moment of the solute, and thus the corresponding derivatives are zero. On the contrary, solvent effects act on the first derivative of the density matrix $\mathbf{P}^B$, which can be obtained as solution of the corresponding coupled perturbed first-order HF or KS equations (see eqs 161 and 162).

As shown by the literature reported in Table 3, the applications of continuum models to the QM study of nuclear shieldings are numerous and they involve many different aspects; here, we comment on two of them.

The first aspect concerns the analysis of the solvent effects on the chemical shielding in terms of two distinct contributions:[713] a direct one due to the perturbation of the solvent on the electronic wave function of the solute held at the geometry optimized in vacuo, and an indirect one due to the relaxation of this geometry under the influence of the solvent. The studies reported in Table 3 have shown the importance of a proper description of the solvent-induced changes on the geometry of solvated systems, in particular for polar and flexible molecules.

The second aspect, already introduced above in terms of the Buckingham and Kamlet−Taft analyses, concerns the importance that both short-range and long-range solute−solvent interactions have in determining the solvent effect on the nuclear shieldings. As will be further discussed in the following sections, the currently held idea is that short-range interactions can be effectively handled by supermolecule calculations involving a solute surrounded by a number of explicitly treated solvent mole-

cules,[713,719,759−762] whereas reaction field (or continuum) methods generally provide an effective alternative to describe long-range electrostatic interactions. As a result, the combination of the two approaches when coupled to accurate QM methods gives an effective computational tool to include solvent effects into nuclear shielding calculations.[716,717,720−722,729,732,733] It must also be noted that, with respect to other properties of optical origin, the nuclear shielding presents a further specificity to be accounted for when the comparison with experimental data is sought. The NMR spectroscopy is in fact characterized by medium-long times of measure; as a consequence, anytime explicit solvent molecules are used, it becomes compulsory to correctly account for the statistical picture inherent in the nature of the solvation shells for either weakly or strongly interacting solute−solvent systems.[721,722]

6.3.2. Indirect Spin–Spin Coupling

Solvent effects on indirect nuclear spin−spin coupling constants J have their origins in intermolecular interactions, repulsion, dispersion, electrostatic, and induction forces, as well as hydrogen bonding effects. As for nuclear shieldings, also for J two main approaches are used in the recent literature to account for these effects: the continuum approach and the supermolecule method.

Many applications on J mediated through hydrogen bonds[763−768] can be considered to fall into the supermolecule category, although the goal there is in calculating actual intermolecular couplings.

Until 2003 only one implementation of a dielectric continuum model for studying solvent effects on spin−spin coupling constants was present in the literature.[706] It was initially used to study solvent effects on the spin−spin couplings of H_2Se, H_2S, and HCN,[706,707] but has in recent years been used for studies on larger molecules, often together with supermolecular models to account for the effects of specific solute−solvent interactions.[710] The dielectric continuum model presented in this first application was the MPE approach described in section 2.3.2.

In 2003 a new approach for calculating solvent effects on indirect spin coupling constants based on the IEFPCM model described in section 2.3.1.3 was presented.[718] The implementation is based on the extensions of the PCM model to the singlet linear response functions we have described in section 5.6,[215,527] but it can include triplet linear response functions as well. In this approach, based on DFT reference states, the indirect spin−spin coupling parameters are determined as second derivatives of the electronic free energy functional G defined in section 2.4.4 with respect to the nuclear magnetic moments $\bar{M}^K$

$$J_{ab}^{KL} = h\frac{\gamma_K\gamma_L}{2\pi 2\pi}\frac{d^2G}{dM_a^K\,dM_b^L} \qquad (187)$$

where γ_K are the nuclear magnetogyric ratios, that is, the ratio between the nuclear magnetic moments and the nuclear spins. The evaluation of the spin−spin coupling constants as second derivatives of the

free-energy functional G requires a procedure based on the linear response theory for molecular solutes, that is, a variational-perturbative scheme which ensures the stationary condition of the free energy functional at first order with respect to any value of the nuclear magnetic moments. Ignoring the details of the parametrization, we denote the free energy as $G(\mathbf{M}_K, \lambda_S, \lambda_T)$, where λ_S and λ_T are two sets of variational parameters associated with singlet and triplet variations of the electronic state, respectively.[769] For the optimized free energy state, the second derivatives of eq 187 may then be calculated as

$$\frac{\mathrm{d}^2G}{\mathrm{d}M_a^K \, \mathrm{d}M_b^L} = \frac{\partial^2G}{\partial M_a^K \partial M_b^L} + \frac{\partial^2G}{\partial M_a^K \partial \lambda_S}\frac{\partial\lambda_S}{\partial M_b^L} + \frac{\partial^2G}{\partial M_a^K \partial\lambda_T}\frac{\partial\lambda_T}{\partial M_b^L} \tag{188}$$

The derivatives of the variational parameters λ_S and λ_T with respect to $\vec{M}^L$ are obtained by solving the response equations

$$\frac{\partial^2G}{\partial\lambda_S\partial\lambda_S}\frac{\partial\lambda_S}{\partial M_a^L} = -\frac{\partial^2G}{\partial M_a^L\partial\lambda_S} \tag{189}$$

$$\frac{\partial^2G}{\partial\lambda_T\partial\lambda_T}\frac{\partial\lambda_T}{\partial M_a^L} = -\frac{\partial^2G}{\partial M_a^L\partial\lambda_T} \tag{190}$$

where the second derivatives on the left-hand sides are, respectively, the singlet and triplet electronic Hessians. The solution of the singlet linear response equation 189 gives the perturbing effect of the imaginary singlet paramagnetic spin−orbit (PSO) operator, whereas the solution of the triplet linear response equation 190 represents the perturbing effect of the real triplet Fermi contact (FC) and of the spin−dipole (SD) operator. The perturbing effect of the second-order real singlet diamagnetic spin−orbit (DSO) operators enters the reduced coupling constant via the first term of eq 188 and does not require solution of any response equation.

6.3.3. EPR Parameters

Electronparamagnetic resonance (EPR) is the leading magnetic technique for obtaining geometrical and electronic information about systems with unpaired electrons. EPR experimental results are commonly analyzed using a two-term spin Hamiltonian: the first term is the Zeeman term describing the interaction between the electronic spin $\vec{S}$ and the external magnetic field $\vec{B}$, through the Bohr magneton μ_B and the $\mathbf{g}$ tensor, whereas the second term describes the hyperfine interaction between $\vec{S}$ and the nuclear spin I through the hyperfine coupling (hc) tensor $\mathbf{A}$.

Compared to the state of the calculation of NMR properties, much less has been done on the first-principles calculation of EPR parameters. As a matter of fact, the treatment of EPR hyperfine coupling constants does have an appreciable history of first-principles theoretical treatments,[770,771] even if quan-

titative calculations of electronic $\mathbf{g}$ tensors have become possible only very recently, especially thanks to the developments of density functional theory.[742,772−775]

Between the $\mathbf{g}$ tensor and the hc tensor, the former is far more complex to evaluate through QM approaches. The $\mathbf{g}$ tensor is defined as a second-order derivative of the electronic energy E with respect to the external magnetic field and the electronic spin:

$$\mathbf{g}_{ab} = \frac{1}{\mu_B}\frac{\partial^2E}{\partial B_a\partial S_b} \tag{191}$$

As the $\mathbf{g}$ tensors may be affected significantly by small changes in electron density distribution, they are important probes of the environment around the molecule. Generally, environmental effects may influence the $\mathbf{g}$ tensor in two different ways: (a) indirectly, by modifying the structure of the radical (e.g., bond lengths or conformations), and (b) directly, by polarizing the electron density distribution and altering the ground state wave function at a given geometrical structure.

In the case of specific solvent−solute interactions, such as hydrogen bonding, supermolecule models may provide the most appropriate description even if the question remains as to what extent more long-range dielectric effects contribute in these cases. In contrast, nonspecific solvent−solute interactions, for example, in aprotic environments, might be described more efficiently by dielectric continuum models.

The first application of dielectric continuum models in the context of electronic $\mathbf{g}$ tensors has appeared only recently.[741] In this work, the performance of PCM within the framework of uncoupled DFT (UDFT) calculations is investigated for semiquinone radical anions in various solvents. Because the calculations involved a generalized gradient approximation functional and thus a UDFT approach, as well as a common gauge origin, no coupling terms due to the continuum have been computed during the perturbation treatment. In other words, the $\mathbf{g}$ tensor was computed in approximate way using a formula referring to isolated systems but with the Kohn−Sham wave function obtained in self-consistent reaction field (SCRF) calculations for a given solvent.

In contrast, a rigorous treatment of solvent effects should account for explicit solvent terms in the Hessian of the solvated molecule free energy functional and, thus, in the linear response equations determining the perturbed wave function exactly as done for nuclear shielding and/or spin−spin coupling constant. This has been achieved by Rinkevicius et al.[742] still within the PCM solvation approach.

Hyperfine splittings of free radicals are determined by the electron spin density at, or near, the position of any magnetic nucleus, and they are thus affected by the presence of the solvent. This has stimulated some attempts to apply a continuum solvation model to the calculation of the corresponding hyperfine tensor $\mathbf{A}$, which in liquid solutions reduces to the isotropic component only.[702,723−728,731] For each nucleus N of the solute molecule located at $\mathbf{r}_N$, the isotropic component of the hyperfine interaction tensor, $a(N)$,

is related to the local spin density through

$$a(N) = \frac{8\pi}{3}\beta_e\beta_N\gamma_N \sum_{\mu\nu} \mathbf{P}_{\mu\nu}^{\alpha-\beta}\langle\varphi_\mu|\delta(\mathbf{r} - \mathbf{r}_N)|\varphi_\nu\rangle \quad (192)$$

where β_e, β_N, and γ_N are the electronic and nuclear magnetons and the nuclear magnetogiric ratio, respectively, the indices μ and ν run over the basis functions, $\mathbf{P}$ is the difference between the density matrices of spin α and spin β electrons, and $\delta(\mathbf{r} - \mathbf{r}_N)$ is the Dirac delta. From the definition (eq 192), it appears evident that the evaluation of $a(N)$ does not require any response equation to be solved but only the knowledge of the density matrices for different spins. These are easily obtained from unrestricted Hartree–Fock (UHF) or Kohn–Sham (UKS) calculations.

6.4. Properties of Chiral Systems

In this section we present extensions of continuum models to describe chiral properties of solvated systems using QM approaches. These extensions are quite recent, whereas the problem of theoretically predicting chiral properties in solution is an old issue. Many empirical rules have been formulated to account for solvent effects on optical rotation (OR) and electronic circular dichroism (ECD) spectra, and classical continuum models have been used as well. Historically, solvent effects on properties related to optical activity have been described by including Lorentz local field factors in the expression for the specific property (see section 6.1.2). These local field factors are of the type

$$f = (n^2(\omega) + 2)/3 \quad (193)$$

where $n(\omega)$ is the refractive index of the solvent at the frequency ω of the external perturbation. However, the inclusion of such factors accounts for only the difference in the external and microscopic (the field acting on the molecule in solution) fields. It does *not* account for the effect of changes in the electronic wave function and in the property due to the presence of the solvent. In the following sections, we shall present models that overcome this limitation and introduce direct solvent effects on the property at a quantum mechanical level.

6.4.1. Electronic Circular Dichroism (ECD)

Circular dichroism (CD) is the most widely used form of chiroptical spectroscopy. The phenomenon of CD consists of the differential absorption of left- and right-circularly polarized light by a chiral molecule. CD due to electronic transitions is generally referred to as CD (also as ECD) and that due to vibrational transitions as VCD (see section 6.4.3).

The integrated intensity of a CD band gives a measure of the strength of CD, called the rotational strength. Rotational strength is defined theoretically, following Rosenfeld's treatment,[776] as the imaginary part of the scalar product of the electric and magnetic dipole transition moments of an electronic transition;

for a given transition $0 \rightarrow a$ it thus becomes[777]

$$R_{0a} = \text{Im}[\langle 0|\hat{\mu}|a\rangle\cdot\langle a|\hat{m}|0\rangle] \quad (194)$$

where $\hat{\mu}$ is the electric dipole transition moment operator, a measure of the linear displacement of charge upon excitation, and $\hat{m}$ is the magnetic dipole transition moment operator, a measure of the circular displacement of electron density upon excitation. The product of $\hat{\mu}$ and $\hat{m}$ results in a helical displacement of charge, which interacts differently with left- and right-circularly polarized light.

As previously noted for other spectroscopic properties, the presence of the solvent leads to different important effects on CD. First, solvent induces a local modification on the applied radiation, exactly as for IR and Raman spectra (see section 6.1.2). In addition, the solvent reaction field changes the electronic wave function and thereby the rotatory strengths. Finally, solvent may induce geometrical distortions in the molecules and indirectly change the rotatory strengths. In any case, even for rigid molecules the solvent dependence of CD spectra is found to vary significantly in different solvents, and a method that describes the direct solvent effects on the rotatory strength is therefore crucial, in particular when theory is invoked to assign absolute configurations of chiral molecules.

Despite this important role of solvation, only very recently have QM continuum methods been applied to the evaluation of solvents effects on ECD (although a first tentative attempt was presented by Ruiz-Lopez and Rinaldi[778] in the 1980s using a semiempirical approach). This delay was also due to the fact that the calculations of CD require large basis sets and electronic structure methods which account for electron correlation, especially dynamical correlation,[779–781] and thus only when continuum models have been extended to accurate QM approaches have applications to CD become possible. We can expect that many studies will appear soon as QM methods for ECD based on DFT are now becoming available in computational packages such as Gaussian,[103] Dalton,[135] TURBOMOLE,[135] or ADF.[64,65]

This first example in the literature of the application of QM continuum models to the calculation of rotational strengths is represented by the MPE method of Mikkelsen and collaborators (see section 2.3.2). The generalization of this method (both in the equilibrium and in the nonequilibrium version) to CD has been done using a coupled-cluster approach.[782,783] In this study, the solvent effects were found to have a significant influence on the transition properties, leading, in some cases, to a sign change of the rotatory strengths. In addition, the inadequacy of the Lorentz local field factors (see eq 193) to properly describe the solvent influence on this specific property is also shown. A subsequent example[784] of the use of continuum models to simulate CD spectra in solution has been presented by Pecul et al. using the PCM solvation model (see section 2.3.1).

6.4.2. Optical Rotation (OR)

The optical rotation (OR) and its variation with wavelength (optical rotatory dispersion, ORD) in

organic compounds in solutions were first observed by Biot, at the beginning of the 19th century. Biot also introduced the modern definition of "specific rotatory power" or "specific rotation," [α], of a liquid as $\alpha/\rho l$, where α is the measured optical rotation in degrees, l is the optical path length (or sample cell thickness) in decimeters, and ρ is the density of liquid. For an isotropic dilute solution of a chiral molecule, the specific rotation [α] (usually measured at the sodium D line of 589.3 nm) is generally written as[785−787]

$$[\alpha] = kf(\nu)\beta(\nu)\nu^2 M^{-1} \tag{195}$$

where k is a numerical constant, M is the molar mass in g mol^{-1}, and ν is in cm^{-1}. In eq 195, $f(\nu)$ indicates the local field factor of eq 193 calculated at the proper frequency ν, and $\beta(\nu)$ is equal to one-third the trace of the frequency-dependent electric dipole-magnetic dipole polarizability tensor having components defined as

$$\beta_{ab}(\nu) = \frac{c}{3\pi h} \, \mathrm{Im}\left[\sum_{k\neq 0} \frac{\langle 0|\mu_a^{\mathrm{el}}|k\rangle\langle k|\mu_b^{\mathrm{mag}}|0\rangle}{\nu_{k0}^2 - \nu^2} \right] \tag{196}$$

In eq 196, 0 and k label ground and excited electronic states and μ^{el} and μ^{mag} are the electronic electric and magnetic dipole moment operators. This sum-over-states has been cast in the framework of time-dependent linear response theory for SCF (either HF or DFT), multiconfigurational SCF, and coupled cluster wave functions. For SCF wave functions, the explicit evaluation of the sum-over-states can be avoided by rewriting $\beta_{\alpha\beta}$ in terms of electric and magnetic field derivatives of the ground state electronic wave function, namely[788−792]

$$\beta_{ab} = \frac{hc}{3\pi} \, \mathrm{Im}\left[\left\langle \frac{\partial\Psi_0}{\partial E_a} \Big| \frac{\partial\Psi_0}{\partial H_b} \right\rangle \right] \tag{197}$$

where $\partial\Psi_0/\partial E$ and $\partial\Psi_0/\partial H$ are frequency-dependent derivatives of the ground state electronic wave function with respect to the electric and magnetic fields, E and H, respectively.

In eq 195, the Lorentz local field factor $f(\nu)$ of eq 193 has been introduced to account for the solvent-induced changes in the microscopic (or local) electric field acting on the chiral molecule with respect to the macroscopic electric field of the light wave; $\beta(\nu)$ also depends on the solvent, exactly in the same way we have outlined in the previous section for the CD rotatory strength. Once more, to properly account for solvent effects on $\beta(\nu)$, a QM description is required.

The first QM study of the solvent effects on $\beta(\nu)$ has been presented by Mennucci et al.[600,793] within the framework of the IEF version of the PCM solvation model (see section 2.3.1.3). In this study, a frequency-dependent DFT/GIAO response approach has been used to compute the electric dipole−magnetic dipole polarizability: the mixed nature of $\beta(\nu)$, however, requires two response procedures containing an electric and a magnetic perturbation, respectively. For the electric perturbation, the inclusion of the additional solvent terms in the coupled perturbed equations is exactly equivalent to what was seen in the case of polarizabilities (see section 6.2.2). Due to the imaginary nature of the magnetic perturbation, solvent-induced terms do not appear explicitly but only contribute to the first-order expansion term of the Fock operator exactly as for the nuclear shielding (see section 6.3.1). In this study, solvent contributions to the electric perturbation were obtained in terms of solvent charges calculated using the value of the dielectric constant at the frequency of the external field (nonequilibrium solvation). In the general case, this is the sodium D line frequency, and thus the value for $\epsilon(\nu)$ coincides with the so-called optical dielectric constant, ϵ_{opt}, defined as the square of the refractive index.

The model was first applied to some conformationally rigid chiral organic molecules for a set of polar and apolar solvents. The predicted variation in specific rotation for polar solvents was found to be in excellent agreement with experiment for all of the molecules. For apolar solvents the agreement was much poorer and thus, because only electrostatic solute−solvent interactions were included in the model, it was concluded that nonelectrostatic effects may have some importance in determining specific rotation, at least for aromatic and chlorinated solvents such as carbon tetrachloride, benzene, and chloroform. As already noted for the ECD, the variations predicted by the classical Lorentz factor (eq 193) were found to be inconsistent, both qualitatively and quantitatively, with those calculated in terms of the QM IEF model. In subsequent papers, the same model was successfully applied to the study of optical rotation of more complex and flexible molecules such as glucose in aqueous solution[794] and paraconic acid in methanol;[795] in both cases it becomes fundamental to account for the solvent effects both in the property and in the relative population of the various conformers that contribute to the final OR value.

An alternative methodology to account for solvent effects on the OR has been presented by Mikkelsen and co-workers[796] using a coupled-cluster approach combined with a nonequilibrium version of the single-center multipole based on the spherical cavity dielectric continuum model described in section 2.3.2.

6.4.3. VCD and VROA

Chiral molecules exhibit optical activities also in their vibrational spectra. Specifically, vibrations associated with the chiral molecular structure produce spectral intensities that are dependent on the circular polarization direction of the excitation light and the detection optics. This optical activity can be observed in infrared spectra, as vibrational circular dichroism (VCD), and in Raman spectra, where it is referred to as Raman optical activity (ROA).

Both VCD and ROA were discovered in the early to mid-1970s (see refs 797, 798 and 799, 800, respectively), and since then, they have evolved into mature fields of research and application. Both can be used to determine the absolute configuration and solution conformation of chiral molecules. Each has advantages relative to the other that parallel the relative advantages of ordinary infrared absorption (IR) and Raman scattering.

Instrumentation for measuring VCD spectra and software for calculating VCD spectra from QM first principles have been commercially available since 1997. In contrast, commercial instrumentation for measuring ROA spectra became available only some years later, and user-friendly software for calculating ROA spectra is not yet available, even if it will become so very soon. As a result, there are many more publications describing the use of VCD for the determination of absolute configuration than there are for ROA and, therefore, this section will mainly focus on VCD.

Application of VCD to the assignment of absolute configuration and identification of dominant solution conformations entail comparison of observed spectra with spectra calculated for a specific configuration and conformation of the molecule or a suitable fragment of the molecule. Thanks to the work of Stephens and co-workers,[801−803] these calculations, which are typically obtained at the DFT level, are nowadays routinely performed for isolated molecules and exhibit an accuracy similar to that of other spectroscopic quantities (see, for example, ref 804). Less studied is the prediction of VCD spectra for solvated systems: only a few papers are present in the literature. These resort to the IEFPCM[714,715,805] of section 2.3.1.3 or to the simple Onsager continuum model (eventually with explicit solvent molecules)[806,807] to treat the solute−solvent electrostatic interaction.

To better understand how solvation models have been applied to the study of solvent effects on VCD we briefly present the general aspects of their QM formulation.

VCD intensity is proportional to the rotational or rotatory strength, the scalar product of the electric dipole and magnetic dipole transition moments. In the harmonic approximation, the rotational strength R is proportional to the scalar product between the derivative of the electric dipole moment of the molecule with respect to normal mode displacement (Q_a) and the derivative of the magnetic dipole moment of the molecule with respect to the nuclear velocities of the normal mode, expressed in terms of the conjugate momentum (P_a), namely

$$R^a = \frac{\hbar}{2}\left(\frac{\partial \vec{\mu}}{\partial Q_a}\right)\cdot\left(\frac{\partial \vec{m}}{\partial P_a}\right) \qquad (198)$$

Quantum chemistry programs calculate these intensities by taking derivatives of the energy of the molecule with respect to electric field or magnetic field and vibrational normal mode displacement or momentum. The calculations first require optimization of the geometry and determination of the normal modes of vibration. Coupled perturbed Hartree−Fock or Kohn−Sham methods are used to obtain the energy derivatives. In the case of the magnetic dipole derivatives, the method that is incorporated into commercial software such as Gaussian[17] utilizes the magnetic field perturbation method of Stephens et al.,[801] with GIAO orbitals to eliminate the origin dependence in the magnetic field derivatives.[808]

VCD spectra are affected by the solvent in different ways.

First, solvent can affect geometries and thus vibrational frequencies: for this effect the same comments reported in section 6.1.2 for IR spectra are valid here. Then, solvent can modify VCD intensities. The calculation of VCD intensities in the presence of a solvent still relies on the same equations formulated for isolated molecules, but with some refinements. As already remarked with regard to infrared intensities for molecules in solution (see section 6.1.2), the electric dipole in eq 198 has to be replaced by the sum of the dipole moment of the molecule and the dipole moment arising from the polarization induced by the molecule on the solvent. The latter takes into account effects due to the field generated from the solvent response to the probing field once the cavity has been created (the so-called "cavity field"). In principle, the magnetic dipole should be similarly reformulated. However, by assuming the response of the solvent to magnetic perturbations to be described only in terms of its magnetic permittivity (which is usually close to unity), it is reasonable to consider that the magnetic analogue of the electric "cavity field" gives minor contributions to the rotational strength. A formulation of this solvent-specific term has been given in ref 805 within the IEF version of the PCM model: in this case an additional set of charges spread on the solute cavity surface is introduced in addition to the PCM apparent charges representing the reaction field. These additional charges are those produced by the (Maxwell) electric field of the radiation in the medium, exactly as in the PCM treatment of the IR and Raman intensities shown in section 6.1.2.

A further important solvent effect on VD spectra is implicit, that is, through the possible changes in the relative energies of different conformers of the solute molecule when passing from gas phase to solution. In fact, if the solute can exist in different conformations that are differently stabilized by the solvent, the VCD spectra must be obtained by combining population-weighted spectra of all conformers where the weights are evaluated in solution.[805]

7. Continuum and Discrete Models

In section 1 we have anticipated one of the most important extensions that continuum solvation models have presented in recent years. This extension, which we denoted layering, has been propelled by two opposing reasons: namely, the necessity to reduce the complexity of calculations using discrete approaches on systems composed by a large number of molecules and the increasing accuracy required in the study of solvated systems (especially their molecular properties).

The layering can be considered a generalization of focusing. The material component of the models partitioned into several parts, or layers, and each layer is defined at a given level of accuracy in the description of the material system and with an appropriate reduction of the degrees of freedom. There are many possibilities for layering, which can be simply abbreviated as, for example, QM/QM/Cont or QM/MM/Cont for a couple of three-layer models in which the inner layer is treated at a given QM

level, the second to a lower QM or at a molecular mechanics level, respectively, and the third using a continuum approach.

In this section we present some examples of layering.

7.1. Continuum Methods within MD and MC Simulations

Continuum solvation models have been largely exploited in classical simulations, such as molecular dynamics (MD) or Monte Carlo (MC), to reduce computational efforts and to simplify two of the main difficulties of this kind of approach: the correct representation of the damping (or screening) of the electrostatic interactions between charges of the solute due to polarization of the medium, and the treatment of the solvent boundary conditions.

The most straightforward way to include effects of screening is to use a Coulomb law with a distance-dependent dielectric constant (see section 4.5). For a given interatomic distance, this model does not distinguish between atom pairs at the surface of the molecular system (generally a protein), where the solvent screening effect is large, and atom pairs in the core of the system, where the screening effect is small. A more physically correct model represents the solvent as a polarizable dielectric continuum surrounding the solute van der Waals surface, and the electrostatic potential is obtained by solving the Poisson−Boltzmann (PB) equation (see sections 2.3.4 and 2.3.5 and the references cited therein). However, for solving problems such as long-term protein dynamics or even protein folding, if PB electrostatics is used, even the fastest methods to solve the PB equation are too slow. To overcome this problem, a generalized Born approach such as those presented in section 2.3.3 can be used. For example, Schaefer and Karplus[151] developed the so-called analytical continuum electrostatics (ACE) potential, which approximates the potential given by solving the Poisson equation but needs much less computational effort. By adding a nonpolar free energy of solvation term, ACE has been extended to the analytical continuum solvent (ACS).[809]

Another continuum solvation method for use with MC and MD simulations is that known as "screened Coulomb potentials-based implicit solvent model" or SCP-ISM.[470,810,811] This model is based on the theory of polar liquids, originated in the works by Debye, Lorentz, and Sack and incorporates Onsager's reaction field effects. The SCP-ISM is derived using screening functions of sigmoidal behavior. The model yields an expression for the electric potential in the system (i.e., protein plus solvent treated as a combined, complex solvent medium with complex dielectric characteristics), an expression for the electrostatic energy of the solvated protein (that contains the free energy of the solvent), and an expression for the solvation free energy of the protein.

With regard to the boundary, several different treatments exist. The use of one instead of another depends strongly on the type of problem the simulation is to address. Periodic boundary conditions (PBC) enable a simulation to be performed using a relatively small number of particles in such a way that the particles experience forces as though they were in a bulk solution. In this scheme, a microscopic computational box is periodically replicated to form an infinite periodic system, which serves as a model for the macroscopic system. For all interactions with a range of action shorter than the size of the computational box (e.g., covalent and van der Waals interactions), artificial periodicity is not likely to be a problem. However, electrostatic interactions are effective at distances that typically go beyond the size of the computational box. There are two alternative practical approaches to handle electrostatic interactions in molecular simulations, which represent approximations of a different kind for the description of dilute solutions. The first approximation is to enforce the exact periodicity of the system in the context of Coulombic interactions, that is, to include all Coulombic interactions between any atom in the reference computational box and all atoms in the infinite periodic system. Methods relying on this approximation are called lattice-sum methods and include the Ewald summation and computationally more efficient grid-based methods.[812,813] The second approximation is to partially break the periodicity by truncating electrostatic interactions beyond a convenient cutoff distance, that is, include only interactions between any atom in the reference computational box and the closest (i.e., within the cutoff sphere) atoms in the infinite periodic system. Methods relying on this approximation are called cutoff-based methods and include (i) straight truncation of Coulombic interactions,[814,815] (ii) smooth truncation of Coulombic interactions by using a switching or shifting function,[815,816] and (iii) straight truncation of an effective interaction function including a Coulombic term and a reaction-field correction.[816−818]

The reaction-field approach has been used both for fixed boundary systems, as a correction for the absence of solvent outside a nonperiodic system of finite size,[193,819,820] and for multiple moving boundary systems, as a correction to the truncation of the Coulomb interaction beyond a given cutoff distance.[821,822] In the fixed boundary case, one considers a region around the system (formed by a distribution of charge possibly inside a solvent of permittivity ϵ_1) to behave as a dielectric continuum of permittivity ϵ_2. In the simple case of a spherical boundary, the correction to be applied will depend on the multipole expansion describing the charge distribution in the system (see section 2.2). Because molecular dynamics simulation requires only knowledge of interaction forces and possibly energies, only the reaction electric field and potential at any location r inside the boundary need to be considered. In the multiple moving boundary case, each charge, or charge group, is surrounded by a region (where the Coulomb interaction is calculated explicitly) of permittivity ϵ_1; in turn this region is embedded in a dielectric continuum of permittivity ϵ_2, which is assumed to compensate for the mean effect of the neglected interactions. For simplicity, the boundary to the continuum is approximated by a sphere around the central charge. Because each charge "sees" a different

part of space as a continuum, the electric reaction potential and field caused by the polarization of the continuum seen by a given charge i bear only a physical relationship to this particular charge. As shown by Hünenberger and van Gunsteren,[818] the reaction-field boundary conditions are simpler to implement and generally numerically faster than the Ewald sum method. They do not impose artificial periodicity on systems that are not inherently periodic and constitute a possible alternative to lattice sum methods, provided that their accuracy is comparable.

Despite the substantial use of concepts and tools of continuum models in MD/MC simulations we have mentioned so far, only recently have "real" continuum MD (or MC) approaches been formulated. Here we shall focus on a few.

In the method developed by Borgis and co-workers,[823] the interaction between the solvent and the solute degrees of freedom is described by means of a polarization density free energy functional which is minimum at electrostatic equilibrium. The approach is based on the electrostatic free energy functional for a charge distribution, the solute, in a polarizable medium, namely

$$G_{el}[\vec{P}(\vec{r}),\{\mathbf{r}_i\}^{N_\alpha}] = \frac{1}{2}\int \rho(\vec{r})\phi_0 \, d\vec{r} + G_{ex}[\vec{P}(\vec{r}),\{\mathbf{r}_i\}^{N_\alpha}] \tag{199}$$

where N_α is the number of smooth spherical charges defining the solute charge density $\rho(r)$ and generating the in vacuo potential ϕ_0 and $\vec{P}(\vec{r})$ is the polarization density field. The minimization of the functional in eq 199 with respect to $\vec{P}(\vec{r})$ for a fixed charged distribution leads to the constitutive equation of electrostatics

$$\vec{P}(\vec{r}) = \frac{\epsilon(\vec{r}) - 1}{4\pi}\vec{E}(\vec{r}) \tag{200}$$

with $\vec{E}(\vec{r})$ the Maxwell electrostatic field defined as

$$\vec{E}(\vec{r}) = -\vec{\nabla}\phi_0(\vec{r}) + \vec{\nabla}\int \frac{\nabla'\cdot\vec{P}(\vec{r})}{|\vec{r} - \vec{r}'|}\, d\vec{r}' \tag{201}$$

At its minimum the excess functional G_{ex} takes the value

$$G_{ex}[\vec{P}(\vec{r})_{min},\{\mathbf{r}_i\}^{N_\alpha}] = -\frac{1}{2}\int \vec{P}(\vec{r})\vec{E}_0(\vec{r})\, d\vec{r} \tag{202}$$

which is the usual expression for the electrostatic energy of a dielectric in an external electric field

$$\vec{E}_0(\vec{r}) = -\nabla\phi_0(\vec{r})$$

It is easy to show that eqs 200 and 201 are equivalent to the Poisson equation and, thus, that minimizing G_{el} with respect to $\vec{P}(\vec{r})$ provides an alternative way of solving the Poisson differential equation with respect to the techniques shown in section 2. The advantage of the functional formulation is that an analogy can be drawn with respect to DFT electronic structure calculations, and it can be

used in a dynamical context using "on-the-fly" Car-Parrinello-like minimization techniques (see section 7.2).

To solve numerically the electrostatic problem for a given charge distribution and a macroscopic dielectric, one has to expand the polarization field coordinates in some basis set. This will transform the functional in eq 199 into an ordinary function of the expansion coefficients which, in turn, become the variational parameters of a standard multidimensional optimization problem. This transformation is accomplished by using a Fourier pseudospectral (PS) approximation for the field variables, $\vec{P}(\vec{r})$. In this context, it is crucial that the position-dependent dielectric constant, $\epsilon(\vec{r})$, be continuous. To define such a continuous function, a model system is introduced with an internal permittivity, ϵ_i, in the proximity of each atom surrounded by a dielectric continuum of permittivity ϵ_s. Then, a computationally suitable form for the position dependent dielectric permittivity can be written as

$$\frac{1}{\epsilon(\vec{r})} = \frac{1}{\epsilon_i} - \left(\frac{1}{\epsilon_i} - \frac{1}{\epsilon_s}\right)H(\vec{r}) \tag{203}$$

where $H(\mathbf{r})$ is a proper volume exclusion function parametrized for each atomic radius.

The coupling of this electrostatic framework to the molecular dynamics method is achieved by treating the variational parameters $\vec{P}$ as virtual dynamical variables. A virtual mass of appropriate units is assigned to the $\vec{P}$s, and a fictitious polarization kinetic energy is included in the system Hamiltonian. The virtual dynamic variables $\vec{P}$s are treated in the same spirit as the electronic coordinates in the Car−Parrinello method. Unlike quantum systems in which electrons are always much faster than nuclei, the time scales of solvent and solute overlap in reality, and this allows us to choose a mass yielding a virtual dynamics much slower than that of electrons. During the simulation, the temperature of $\vec{P}$ must also be low enough for the particles to move adiabatically on a minimum of the surface of the polarization functional G_{el}. If this condition is satisfied, at each time step of a MD run the value of the computed functional G_{el} will fall very close to that obtained by reoptimization of the $\vec{P}$ for the instantaneous atomic coordinates.

The method has been programmed as an independent set of Fortran 90 routines and implemented in the MD program ORAC.[824]

The second example of continuum MD methods we analyze here is that proposed by Basilevsky and co-workers.[825−827] The main new feature is that the method combines the dielectric continuum approximation for treating fast electronic (inertialess) polarization effects arising from solvent electronic polarization modes and a MD simulation for the slow (inertial) polarization component, including orientational and translational solvent modes. This approach exploits the same idea of the previously cited "frequency-resolved cavity model" (FRCM)[412] in which the inertialess response of the medium was spatially distinguished from the inertial one (see section 5.3). According to this model, the solute is surrounded by

two surfaces, each of which is constructed as a collection of overlapping atomic spheres similar to the PCM method. For the first cavity, contained within the inner surface and representing the space occupied by the solute, the dielectric constant is taken as $\epsilon = 1$. Between the two surfaces the medium is represented by the inertialess dielectric constant $\epsilon = \epsilon_\infty$. This layer corresponds roughly to the first solvation shell. Outside the outer cavity the static dielectric constant is applied ($\epsilon = \epsilon_0$). The new aspect introduced in the method is that explicit solvent particles with mean dipoles and associated mean point charges assigned to the selected sites of the solvent molecules are immersed in the medium with $\epsilon = \epsilon_\infty$. The solute particle with charges q_i (taken as nonpolarizable vacuum charges) is placed at the center of the MD cell, and the electrostatic forces between solute and solvent charges as well as between solvent charges are scaled by the factor $1/\epsilon_\infty$. In combination with Lennard-Jones forces they form the effective force field for an MD simulation producing the equilibrium ensemble of solvent particles. We note that this simplistic screening of all electrostatic interactions by $1/\epsilon_\infty$ is not fully consistent with the dielectric model in which the dielectric constant in the solute region is not ϵ_∞, but unity; however, the authors found that the consequences of this discrepancy are negligible. This approach yields an ensemble of equilibrium solvent configurations adjusted to the electric field created by a charged or strongly polar solute. The electrostatic solvent response field is found as the solution of the Poisson equation including both solute and explicit solvent charges, with an accurate account of electrostatic boundary conditions at the surfaces separating spatial regions with different dielectric permittivities. This leads us to define two surface apparent charge densities spreading on the surfaces of the inner and outer layers.

This combined molecular−continuum approach comprises a contracted analogue of a conventional polarizable MD simulation. Despite obvious limitations, the present approach seems to provide several computational as well as conceptual advantages. An essentially related feature is that the MD-FRCM method is formulated in terms of "dressed" charges of solvent particles, whereas vacuum charges are used in conventional polarizable theories. This "dressing" makes an electronic contribution to the inertial response of the solvent particles. The mean charges comprise input parameters of the MD-FRCM scheme, and their explicit values are available either by rescaling the effective charges of some nonpolarizable solvent model or directly from a conventional polarizable computation of bulk solvent. Both equilibrium and nonequilibrium solvation effects can be studied by means of this model, and their inertial and inertialess contributions are naturally separated. The methodology has been coupled with the GROMOS96 MD program,[828] and it has been applied to compute charge transfer reorganization energies in a model two-site dipolar system in the water solvent.

We conclude this section by citing a further example of the coupling between ASC approaches and statistical methods. This algorithm has been devel-oped by Colominas, Luque, and Orozco,[52,829] by combining Monte Carlo (MC) calculation with a quasi-classical version of the DPCM (here called MST, see section 2.3.1.1). In the MC-MST approach, configurations are accepted or rejected following the Metropolis rules applied to an energy functional including the solvent electrostatic, van der Waals, and cavitation terms described in sections 2 and 3, respectively. In particular, the electrostatic term is obtained by assuming that solute moves in a fully equilibrated solvent represented by apparent surface charges determined by solute atomic charges following from a fitting of the electrostatic potential of a preliminary QM MST calculation. The method is especially useful in conformational studies of large molecules.[830]

7.2. Continuum Methods within ab Initio Molecular Dynamics

The term ab initio molecular dynamics (AIMD) is used to refer to a class of methods[831−834] that combines finite temperature dynamics with forces obtained from electronic structure calculations performed "on the fly" as the MD simulation. Currently, the most commonly used electronic structure theory in AIMD is the Kohn−Sham formulation of density functional theory (DFT), in which the electronic orbitals are expanded in a plane-wave basis set. This protocol provides a reasonably accurate description of the electronic structure for many types of chemical environment while maintaining an acceptable computational overhead and constitutes the original Car−Parrinello (CP) formulation of the method.[831] In this approach, the parameters in the electronic wave function are treated as dynamical variables (electron dynamics) and the electronic structure problem is solved by the application of the steepest descent method to the classical Newtonian equations of motions. The evolution of the electronic wave function and the forces acting on the atoms can be computed simultaneously, provided that the electronic state of the system is conserved (i.e., remains on the Born−Oppenheimer surface). This is achieved by the exploitation of the quantum mechanical adiabatic time scale separation of fast electronic and slow nuclear motion by transforming the electronic problem into classical mechanical adiabatic energy scale separation in the framework of dynamical systems theory. Hence, both the electronic structure problem and the dynamics of the atoms are solved concurrently by a set of Newton's equations. In contrast to the traditional approach, this theoretical breakthrough allows calculations of the fully dynamic time evolution of a structure (molecular dynamics) without resorting to a predefined potential energy surface.

The AIMD methods have been used to study a wide variety of chemically interesting and important problems in areas such as liquid structure, acid−base chemistry, industrial and biological catalysis, and materials (see, for example, refs 835 and 836). For condensed phases, AIMD methods have been extended to QM/MM[836,837] and combined (ONIOM-like) approaches[838,839] as well to continuum solvation models.

In particular, three different models to include a continuum model within the framework of AIMD are worth reviewing here.

An approach to introduce a continuum description within the framework of CP ab initio molecular dynamics has been presented by Ziegler and co-workers[100] using the conductor-like screening model (COSMO) described in section 2.3.1.2. In this implementation, the COSMO surface charges are treated as fictitious dynamic variables (with associated fictitious masses m_q) within the extended Lagrangian approach, solving the electrostatic problem determining the charges on the fly as the system evolves in time. The Lagrangian is also augmented by the fictitious kinetic energy of these charges and the additional potential energy terms due to solvation. The value of the fictitious masses m_q is chosen small enough that the charges are adiabatically decoupled from the other degrees of freedom.

From the Lagrangian, it is in principle straightforward to obtain the corresponding equations of motion that propagate the surface charges together with the nuclei and the wave functions. However, in practice this approach is nontrivial because of the implicit dependence of the solution energy terms on the nuclear positions. Both the electrostatic G_{diel} and the nonpolar G_{np} parts depend on the surface, which changes in area and shape as the nuclei move, and hence depend on the nuclear positions. This gives rise to additional forces acting on the nuclei, which need to be evaluated as derivatives of G_{diel} and G_{np}, respectively, with respect to the coordinates. We recall that in this approach G_{np}, which collects all nonelectrostatic contributions, notably the formation of the cavity in the solvent, in which the solute is placed, and the dispersion and exchange repulsion interactions between solute and solvent, is approximated as a linear function of the surface area of the cavity.

To perform energy-conserving dynamics, consistent, accurate forces are a fundamental prerequisite. To obtain such accurate forces, a steep but continuous surface function that effectively switches the surface charges off when they are not exposed on the molecular surface is used (see section 2.2. for more details).

The second example of coupling between continuum models and AIMD techniques we report in this section is that proposed by Fattebert and Gygi.[840,841] To carry out microcanonical total energy-conserving molecular dynamics simulation with a continuum solvation model, a density-based molecular cavity definition and a smooth solute−solvent transition are used. In this model the Poisson equation is solved directly in the form

$$-\vec{\nabla}\cdot(\epsilon[\rho]\vec{\nabla}V) = 4\pi\rho \qquad (204)$$

where the dielectric medium is now represented by a function ϵ of the electronic density, ρ, of the solute, and thus its effects can be easily integrated into a density functional. Using eq 204, one finds that the variation of electrostatic interaction energy with respect to ρ leads to the usual Hartree potential plus

an additional term

$$V_\epsilon(\vec{r}) = -\frac{1}{8\pi}|\vec{\nabla}V(\vec{r})|^2 \frac{\delta\epsilon}{\delta\rho}(\vec{r}) \qquad (205)$$

which is included in the Kohn−Sham equations to be solved.

Numerically, a finite difference (FD) approach (as that described in section 2.3.5) is exploited, and the Poisson equation is discretized by finite differences on a regular grid, which is the same used to compute the electronic density in terms of plane waves. For the dielectric function, a local model depending on three parameters is used, namely

$$\epsilon(\rho(\vec{r})) = 1 + \frac{\epsilon_\infty - 1}{2}\left(1 + \frac{1 - (\rho(\vec{r})/\rho_0)^{2\beta}}{1 + (\rho(\vec{r})/\rho_0)^{2\beta}}\right) \qquad (206)$$

where ϵ_∞ is the asymptotic value of ϵ for $\rho \rightarrow 0$, ρ_0 denotes the critical density in the middle of the interface solute−solvent, and β is related to the width of the interface. The parameters ρ_0 and β have been determined so that the continuum solvent effect on the total energy of a water molecule is the same as the average binding energy of an explicit solvent environment.

The introduction of the smooth dielectric function allows us to run constant-energy molecular dynamics that include the effects of a continuum solvent, and this is achieved by implementing the model in a CP molecular dynamics code.

7.3. Mixed Continuum/Discrete Descriptions

The large variety of techniques to represent the solvent by a macroscopic (polarizable) continuum surrounding the solute as well as those involving the explicit incorporation of many solvent molecules each present their particular weaknesses. For example, not all of the electronic aspects of hydrogen bonding between solvent and solute are correctly described by continuum models, whereas explicit descriptions, which are always size-limited, cannot fully take into account long-range (or bulk) effects. It follows that many of the approaches complement each other, and it is therefore worthwhile to investigate the possibility of combining different techniques in the same calculation. This has indeed been the topic of a number of recent studies in which the analysis is focused on the combination of complementary representations of the solvent, namely, explicitly by a small number of solvent molecules (microsolvation) and implicitly by a continuum.

This kind of generalized continuum model in which the solute includes a few explicit solvent molecules (namely, those belonging to the first solvation shell/s) will be here called "solvated supermolecules" to maintain a correspondence with the standard supermolecule approach in which gas phase clusters of interacting molecules are studied to account for the intermolecular interactions. It is important to specify that in this approach we include all methods in which both parts of the supermolecule (solute and the n solvent molecules) are described at the same level of quantum mechanical theory: possible hybrid or

combined approaches mixing different QM or QM and MM descriptions will be reviewed in the next sections.

7.3.1. Solvated Supermolecule

The coupling of the supermolecule approach with a continuum is an attractive technique that has proved to be extremely useful in studying solvent effects on electronic and vibrational spectra and response molecular properties as well in studying reaction mechanisms and energetics in solution; in section 6 we reported several references to which we add here a few more.[842−848]

One of the main reasons to explicitly treat some solvent molecules is to get an accurate description of strong specific interactions (e.g., hydrogen bonding); however, such an approach is not straightforward, and its correct realization requires a detailed analysis on the nature and the strength of such interactions.

In the case of very strong solute−solvent interactions such as solutes with strong H-bond acceptor centers in water or in alcohols, a sufficient description is often obtained by including all of the solvent molecules necessary to saturate such strong acceptor centers (in general, a few solvent molecules are enough) in the QM optimization procedure. The resulting structure is then used to compute the corresponding vibrational spectrum or the properties of interest or just to compute the thermal free energy necessary to get the energetics of a reaction. In all of the steps of this strategy an external continuum is used to account for long-range (or bulk) effects.

When we are in the presence of weaker interactions, however, a representation of the supermolecule in terms of a single rigid structure obtained as the minimum of the potential energy surface of the cluster cannot be adopted. The real situation is in fact dynamic and a variety of different representative structures can and do occur. A possible way to get such a picture is to consider structures derived from either classical or ab initio MD shots taken at different simulation times: for each of these selected structures the number of solvent molecules to be used in the supermolecule calculation is determined by a threshold imposed in the distance between the solute H-bond acceptor/donor center and the corresponding donor/acceptor center in the solvent molecules. Each of the resulting clusters (generally involving more than the solvent molecules really needed to saturate H-bonding centers) is then embedded in the external continuum and such a solvated supermolecule is studied at the proper QM level. In the most recent examples, the PCM method (either in the IEF or CPCM version, see section 2.3.1) is exploited to include bulk effects,[716,720−722,729,731,733] whereas older studies[849−852] adopted an image reaction field plus exclusion model to represent the polarization of the dielectric material embedding the clusters.[853]

In this approach, no geometry optimizations of the clusters are required; this of course makes the procedure easier from a computational point of view but not necessarily faster as an average among all of the selected structures has to be done to get a reliable description. A disadvantage of this procedure is that it cannot be used to directly compute vibrational spectra; more complex analyses are necessary as the structures do not correspond to real minima.

This approach combining (but not coupling) MD simulations and averaged QM calculations on selected clusters is not limited to the examples cited above, and they do not necessarily include an external continuum; indeed, it has been used in many different studies as an alternative to continuum models. The main difference is that without including the bulk effects through a continuum dielectric, very large clusters are required to get the complete picture of solvation, and thus the QM level of the theory is usually limited to semiempirical approaches or low-level ab initio methods.[854−862]

7.3.2. QM/MM/Continuum: ASC Version

Another example involving discrete and continuum approaches describes the solute at QM level, the first solvation shells with MM solvents, and the rest with a dielectric continuum. In such a way, both the first solvation shell effects (such as short-range repulsion and dispersion interactions and solvent entropic terms related to hydrophobic interactions) and long-range electrostatic effects in the bulk can be taken into account with modest computational cost. The small number of explicit solvent molecules makes the calculations of quantities that require configurational samplings much faster compared to a full-scale microscopic simulation.

In principle, all of the continuum models we have described in section 2.3 can be coupled with a QM/MM system. Here, however, we shall limit the exposition to those belonging to the ASC class of continuum models.

An example of this approach is the model developed by Cui,[863] in which the solute and a number of solvent molecules ("solute−solvent cluster") are described with QM/MM and the bulk solvent is treated with the IEFPCM model (see section 2.3.1.3). In this model, both the MM atoms, represented by fixed partial charges, and the QM atoms are contained in a generalized cavity embedded in the continuum. Following the same formalism used in section 2.4, the total electrostatic free energy of the "solvated" QM/MM system thus becomes

$$G_{el} = \text{tr } \mathbf{P}\Big[\tilde{\mathbf{h}} + \mathbf{h}^{QM/MM} + \frac{1}{2}(\mathbf{J}^{QM/MM} + \mathbf{Y}^{QM/MM})\Big] +$$
$$\frac{1}{2}\text{tr } \mathbf{P}\tilde{\mathbf{G}} + \Big(\tilde{V}_{NN} + E_{el}^{MM} + V_{NN}^{QM/MM} + \frac{1}{2}U_{NN}^{QM/MM} +$$
$$\frac{1}{2}U_{NN}^{MM/MM} + \frac{1}{2}U_{NN}^{MM}\Big) \quad (207)$$

where $\tilde{\mathbf{h}} = \mathbf{h} + \mathbf{J} + \mathbf{Y}$, $\tilde{\mathbf{G}} = \mathbf{G} + \mathbf{X}$, and $\mathbf{J}$, $\mathbf{Y}$, and $\mathbf{X}$ are the PCM matrices described in section 2.4.3 (see eqs 64−67). The terms $\mathbf{J}^{QM/MM}$, $\mathbf{Y}^{QM/MM}$, $U_{NN}^{QM/MM}$, $U_{NN}^{MM/QM}$, and U_{NN}^{MM} represent the additional electrostatic interactions between the QM/MM part and the induced surface charges. There are four types of interactions, namely, between QM electrons and MM-induced surface charges, between MM and QM electron-induced surface charges, between QM nuclei

and MM-induced surface charges, between MM and QM nuclei-induced surface charges, and between MM and MM-induced surface charges.

This QM/MM/PCM method has been implemented into the simulation package CHARMM,[864] which was previously interfaced with GAMESS for ab initio QM/MM calculations,[865] and it can be used for single-point solvation free energy calculations, Monte Carlo simulations, and geometry optimization as well as MD calculations for reactions in solution.

Another QM/MM/Cont approach is that of coupling continuum models with the QM/MM model developed by Gordon and co-workers, known as the effective fragment potential (EFP) method.[426,866,867] The basic idea behind this method is to replace the chemically inert part of a system by EFPs while performing a regular ab initio calculation on the chemically active part. A simple example of an active region might be a solute molecule, with a surrounding spectator region of solvent molecules represented by fragments. The charge distribution of the fragments is represented by an arbitrary number of charges, dipoles, quadrupoles, and octupoles, which interact with the ab initio Hamiltonian as well as with multipoles on other fragments. An arbitrary number of dipole polarizability tensors can be used to calculate the induced dipole on a fragment due to the electric field of the ab initio system as well as all other fragments. These induced dipoles interact with the ab initio system as well as the other EFPs, in turn changing their electric fields. All induced dipoles are therefore iterated to self-consistency. The combination of the EFP method with continuum solvation initially used an Onsager-like model[868] but subsequently has been extended to the IEF-PCM model.[869] Using the same formalism presented in section 2.4.2, the electrostatic component of the free energy of the solute (ab initio + EFP) continuum system can be written

$$G = \left[\mathrm{tr}\, \mathbf{P}\tilde{\mathbf{h}} + \frac{1}{2}\mathbf{P}\tilde{\mathbf{G}}(\mathbf{P}) + V_{NN} + \frac{1}{2}\,U_{NN} \right] +$$
$$\mathrm{tr}\, \mathbf{P}(\mathbf{J}_{stat}^{EFP} + \mathbf{J}_{pol}^{EFP}) + \frac{1}{2}\sum q_{stat}^{EFP}\, V_{stat}^{EFP} +$$
$$\frac{1}{2}\sum q_{pol}^{EFP}\, V_{pol}^{EFP} + \sum q_{stat}^{EFP}\, V_{pol}^{EFP} + \sum q^N V_{stat}^{EFP} +$$
$$\sum q^N V_{pol}^{EFP} \quad (208)$$

where for $\tilde{\mathbf{h}}$, $\tilde{\mathbf{G}}(\mathbf{P})$, V_{NN}, an U_{NN} we have used the same notation as that in eq 207. All of the other terms are due to the coupling between the EFP and PCM methods. In particular, $(\mathbf{J}_{stat}^{EFP})_{\mu\nu} = \sum q_{stat}^{EFP}\, V_{\mu\nu}^e$ and $(\mathbf{J}_{pol}^{EFP})_{\mu\nu} = \sum q_{pol}^{EFP} V_{\mu\nu}^e$, where $V_{\mu\nu}^e$ are the electrostatic potential integrals in the atomic orbital basis and $q_{stat}^{EFP})$ and q_{pol}^{EFP} are the ASC due to the static multipoles and the induced dipoles of the fragments, respectively. In the remaining terms, V^{EFP} denotes the electrostatic potential induced by the EFP fragments and the subscript indicates the source of such potential, namely, the static multipoles (stat) and the induced dipoles (pol).

Subsequently, the EFP/PCM approach has been reformulated[870] using a simultaneous iterative solution of the QM self-consistent field (SCF) and of the electrostatic equations (see also section 2.4.3): in this way, bulk solvation of large solutes can be efficiently modeled.

7.3.3. ONIOM/Continuum

An alternative formulation of the coupling of QM, MM, and continuum approaches is given by energy subtraction methods. The latter are a very general class of methods in which calculations are done on various regions of the molecule with various levels of theory, and the energies obtained at each level are finally added and subtracted to give suitable corrections. The introduction of continuum solvation into this kind of method has been realized by coupling the IEFPCM model we have described in section 2.3.1.3 with the class of subtraction methods developed by Morokuma and co-workers[871–875] and generally known by the acronym ONIOM. This acronym actually covers different techniques, combining either two (or more) different orbital-based techniques or orbital-based technique with an MM technique.

The concept of the ONIOM methods is extremely simple. The target calculation is the *high* level calculation for a large *real* system, E(high, real), which is prohibitively expensive. Instead of doing such a calculation, an inexpensive *low*-level calculation leading to the energy E(low, real) is performed together with two calculations (one at accurate *high* level and the other at the same *low* level) for a smaller part of the system, usually indicated as the *model* system, leading to the energies E(high, model) and E(low, model), respectively. Starting from E(low, model), if one assumes the correction for the high level, E(high, model) $-$ E(low, model), and the correction for the real system, E(low, real) $-$ E(low, model), to be additive, the energy of the real system at the high level can be estimated from three independent calculations as

$$E = E(\text{low, real}) + E(\text{high, model}) -$$
$$E(\text{low, model}) \quad (209)$$

Clearly this approach is completely general, and it can be straightforwardly extended to more than two layers. In addition, it has the advantage of not requiring a parametrized expression to describe the interaction of various regions. Any systematic errors in the way that the lower levels of theory describe the inner regions will be canceled out.

The combination of ONIOM with IEFPCM has been achieved in four alternative ways.[876] The resulting computational schemes differ mainly with respect to the level of coupling between the solute charge distribution and the continuum dielectric, which has important consequences for the computational efficiency. All of the schemes share the fact that only one cavity is defined, based on the geometry of the real system, which is subsequently used for all three subcalculations. Three of the four schemes can be placed in a hierarchy. In the highest method in the class (called ONIOM-PCM/A in the reference paper), all three subcalculations exploit the reaction field that is obtained self-consistently by employing the ONIOM *integrated density*. Obviously this is the

"correct" method, consistent with the philosophy of "integration" of the ONIOM method. The second method in the hierarchy (ONIOM-PCM/B) differs from the first one in the reaction field, which is now obtained from the (nonintegrated) density for the real system at the low level. In the lowest ONIOM-PCM scheme in this class (ONIOM-PCM/C), the solvation effect is included in only the low-level calculation on the real system, whereas the model system calculations are carried out in vacuo. The fourth method (ONIOM-PCM/X) is an approximation to the correct ONIOM-PCM/A but it does not fit in the hierarchy. The reaction field is in fact determined independently for each of the three subcalculations.

The ONIOM/PCM has been successfully applied to the study of magnetic properties of solvated systems,[716,730] and it has been used to describe solvated supermolecules (see section 7.3.1), being the model system represented by the solute.[716]

7.3.4. (Direct) Reaction Field Model

A further QM/MM approach is that developed by van Duijnen and co-workers,[876–878] known as direct reaction field (DRF).

The DRF model is an embedding technique enabling the computation of the interaction between a quantum mechanically described molecule and its classically described surroundings. The classical surroundings may be modeled in a number of ways: (i) by point charges to model the electrostatic field due to the surroundings, (ii) by polarizabilities to model the (electronic) response of the surroundings, (iii) by an enveloping dielectric to model bulk response of the surroundings, and (iv) by an enveloping ionic solution, characterized by its Debye screening length. The four representations may be combined freely.

The QM system may be described by a HF, DFT, GVB, CI, or MCSCF wave function. The static multipole moments of the MM part (charge, dipole, quadrupole, etc.) are represented by a point charge distribution at selected points.[879] The response moments (dipole polarizability only at present) are represented by a local (anisotropic) polarizability tensor located at the selected point or by distributed interacting atomic polarizabilities. Finally, the enveloping dielectric is assumed to be isotropic and homogeneous and the related Poisson–Boltzmann equation is solved numerically by defining a discretized surface that forms the boundary between the source and the dielectric. Solution of the equation provides a response potential inside the boundary. In DRF the surface is adaptable to the shape of the interior and local moments are used as the source, rather than the overall dipole moment.

These different partitions may be coupled self-consistently, enabling the computation of the energy of the entire system. To this end, potential and field operators are defined between the systems. In the DRF approach the self-consistency is not achieved by resorting to an iterative scheme but by writing out the coupling equations between the induced moments and deriving a coupling (or relay) matrix that, when inverted, solves the self-consistency problem formally and for any source field. This has great advantages

in combining classical descriptions of matter with QM electronic structure calculations.

The DRF model has been also extended to treat solvent nonequilibrium response,[880] by separating orientational and electronic components in the continuum dielectric. As described in section 5.2, this feature is important for spectroscopic applications, where the orientational response is not able to follow the electronic transition, so that the excited state is to be calculated in the orientational reaction field of the ground state, whereas the electronic response is allowed to adapt to the excited state. Recently, the DRF approach has been applied to the study of optical response properties (polarizabilities and hyperpolarizabilities) of solvated molecules.[881–883]

The DFR model has been implemented in different computational packages: the HONDO8.1,[884] GAMESS (UK),[885] ZINDO,[886] and a local version of the ADF.[64,65]

7.3.5. Langevin Dipole

The Langevin dipole (LD) solvation model developed by Warshel and co-workers[887–889] is based on the evaluation of interactions between the electrostatic field of the solute and point dipoles placed on a grid around the solute. This grid of dipoles is then surrounded by a dielectric continuum (the outer solvent region). The solute electrostatic field is generated from the point charges placed at the atomic nuclei. The total electrostatic field at a given dipole and the magnitude of this dipole are related via the Langevin function that exhibits saturation for large fields. The resulting electrostatic part of the solvation energy (ΔG_{ES}) is augmented by the solvation contribution from the outer continuum dielectric (ΔG_{bulk}), van der Waals (ΔG_{vdW}), hydrophobic (ΔG_{phob}), and solute polarization (ΔG_{relax}) terms to give the solvation free energy, ΔG_{solv}. The contributions (ΔG_{bulk}) to the solvation free energy from the outer solvent region are evaluated by a continuum approximation. This is done using Born's and Onsager's formulas for charges and dipoles. The hydrophobic free energy, ΔG_{phob}, is assumed to be related to the magnitude of the nonpolar molecular surface, which is proportional to the number of Langevin dipoles (grid points) that lie within 1.5 Å of the vdW surface of the solute. The van der Waals energy, ΔG_{vdW}, is calculated as the sum of r^{-9} repulsion and London dispersion terms.

Because ΔG_{ES} is evaluated from the gas phase charges, some correction is required to account for the increase in the solvation free energy due to the polarization of the solute electron density as it interacts with Langevin dipoles. This correction, which is denoted here ΔG_{relax}, is evaluated within the framework of the linear response approximation. Within this approximation, the energy invested in polarizing the solute is $-1/2$ the energy gained by the interaction between the polarizing potential and the induced changes in solute atomic charges (Δq_i). In some versions the factor of $1/2$ is replaced by an adjustable constant k_{relax}.

In the most recent implementation,[890–892] atomic charges are determined by fitting to the ab initio electrostatic potential. Because the atomic charges are not empirically adjustable (in contrast to the

previous versions of the model), other parameters of the LD solvation model had also to be reoptimized. These changes include introduction of the field-dependent grid points and surface-constrained dipoles on the outer solvent surface, the new relationship between magnitudes of dipoles placed at the inner and outer grid points, reparametrized van der Waals and hydrophobic terms, increased extent of dipole−dipole interactions, and a newly added solute-polarization term.

The LD model has been extended to study proteins, and the corresponding version of the model is known as protein dipoles Langevin dipoles (PDLD).[446,893]

The computational code of the LD model (called ChemSol[894]) has been also implemented in the Qchem quantum package.[894,895]

7.4. Other Methods

The electrostatic solvation methods examined in section 2 are all based on averaged solvent polarization, expressed in terms of a response function in which no use is made of the detailed microscopic description of the solvent. This definition of the solvent mean field greatly reduces the computational task but neglects the possible presence of specific solute−solvent interactions.

We pass now to examine other approaches in which some elements of the discreteness of solvent molecules are considered.

We shall limit our attention to two approaches that still use the mean solvent field approximations, but from a mean field obtained from a thermally averaged discrete description of the solvent. The two approaches are based on different formulations of this averaged description and will be separately treated. They will be indicated with the acronyms ASEP (averaged solvent electrostatic potential) and RISM-SCF (reference site model in a SCF version), but actually different versions of the two approaches have been elaborated, and we shall review all of the published versions to give a fuller idea of the work in progress in this specific field.

The problem both approaches are addressing is of finding a procedure able to reduce the strong computational burden due to the exceedingly large number of solvent freedom degrees a standard discrete description presents.

7.4.1. ASEP-MD

The method we shall consider here has been elaborated by Olivares del Valle and Aguilar, with co-workers, in Badajoz.

The starting point is a standard MD calculation: the solute and solvent coordinates were dumped at every N (with N properly defined) steps for further analysis. The resulting configurations are then translated and rotated in such a way that all of the solvent coordinates can be referred to a reference system centered on the solute mass center with the coordinate axis lying along the principal axes of inertia of the solute. This process is necessary to define a grid of points equal for all configurations.

For each stored configuration only those solvent molecules that are within a sphere centered on the solute molecule and radius equal to half the size of the simulation box are selected. The solute and the selected solvent molecules are then included in a dielectric continuum. The Laplace equation that gives the polarization of the continuum is solved numerically, making use of apparent charges (i.e., through the DPCM approach presented in section 2.3.1.1). The total electrostatic potential due to the permanent solvent charges, induced dipoles, and the surface charge density is calculated at each point of the grid defined inside the volume occupied by the solute molecule, and the averaged value of this solvent electrostatic potential (ASEP) is obtained by averaging over the configurations. The potential obtained in this way is a numerical potential and hence is not very suitable for use in quantum calculations; instead, a set of charges chosen in such a way that they reproduce the value of the ASEP inside the solute volume is introduced. The charges are usually arranged on spherical shells centered on the solute mass center (a solvent diameter apart), but shells adapted to the molecular shape of the solute and defined in terms of intersecting spheres centered on the solute atoms have also been used. Charges placed on two concentric shells (spherical or molecularly shaped) are generally sufficient to represent the effect of the total solvent electrostatic potential. The energy and the wave function of the solute molecule in the presence of this averaged solvent configuration are thus obtained by solving the Schrödinger equation associated with the perturbed Hamiltonian, namely

$$(H_{QM} + H_{QM-MM})|\Psi\rangle + E|\Psi\rangle \qquad (210)$$

where H_{QM} is the usual vacuum Hamiltonian of the solute molecule. The interaction term, H_{QM-MM}, takes the form

$$H_{QM-MM} = \int dr\, \rho\langle V(r)\rangle \qquad (211)$$

where ρ is the charge density operator associated with the solute molecule and $\langle V(r)\rangle$ is the value of ASEP at the point r.

There are different versions of the ASEP procedure. In the early versions a single QM calculation is performed with unpolarized MM descriptions of the solvent molecules[896] or with MM molecules including polarization.[897] More recent versions introduce iterations on the QM part, allowing solute polarization.[898] These versions have been called by the authors "coupled methods". There are two versions: the partial coupling (PC) in which the MM solvent molecules are kept unpolarized, and the complete coupling (CC) in which all of the molecules of the liquid specimen are polarized at the same level. The CC version is at present available for pure liquids only.

The computational efficiency of ASEP has been checked by comparisons with QM/MM codes;[899] the ASEP method turns out to be more efficient by some orders of magnitude. The most important advantage of ASEP-MD when compared with previous QM/MM calculations is that the number of quantum calculations is considerably less: around four to eight with

ASEP-MD versus several hundreds or even thousands with QM/MM. Although typical QM/MM methods have to make a quantum calculation for each solvent configuration selected, the number of calculations in the ASEP-MD method is independent of the number of solvent configurations. It depends on only the number of cycles necessary to find convergence in the process that couples the solute charge distribution and the solvent structure around it.

The robustness of ASEP has been demonstrated by the satisfactory results obtained in a sizable number of examples covering different types of solvation effects. We cite here a few: solvent shifts in electronic spectra,[900,901] anomeric equilibria,[902] multiple conformational equilibria,[903] structure and properties of pure liquids,[903,904] and Stark component of the interaction energy.[905]

More recently, the ASEP approach has been extended to study saddle points of reactions in solution[906] by using the free energy gradient (FEG) method,[907] in which the effective forces on the nuclei are taken as the average force over a set of equilibrium solvent−solute configurations. Once the molecular dynamics simulation has been made and the ASEP obtained, a geometry optimization calculation is performed. In this way, a new solute geometry is obtained, which is introduced into the next molecular dynamics simulation. The process is repeated until convergence. The gradient and Hessian, needed for the optimization process, are given by the quantum calculation program, but the appropriate van der Waals components have to be added. These components are calculated as an average over all of the solute−solvent configurations considered.

The ASEP method has been implemented by coupling the MOLDY code[908] for the MD part and GAUSSIAN[103] or HONDO[909] for the quantum calculations. A detailed description of the ASEP-MD code is also available.[910]

7.4.2. RISM-SCF

As we have pointed out, continuum solvation approaches cannot properly account for the average solvent structure caused by the granularity, packing, and hydrogen bonding. On the contrary, statistical mechanical theories based on distribution functions and integral equations can provide a rigorous framework for incorporating such effects into a description of solvation (see section 1.2).

One important class of integral equation theories is based on the reference interaction site model (RISM) proposed by Chandler and Andersen in 1972.[911] The theory is a natural extension of the Ornstein−Zernike equation of simple liquids to a mixture of atoms but with strong intramolecular correlation, which represents chemical bonds. The theory takes account of one of the two important chemical aspects of molecules, geometry, in terms of the site−site interactions between atoms. In its original form, however, it does not handle the other chemical aspect of molecules, electrostatics. The charge distribution in a molecule, which is a classical manifestation of the electronic structure, plays a

dominant role in determining the chemical specificity of the molecule. Therefore, without including the charge distribution in molecules, the description is incomplete in terms of chemical specificity. A complete chemical characterization of molecular liquids became possible at the beginning of 1980s due to the appearance of the extended RISM theory (also known as XRISM), which takes the charge distribution as well as the molecular geometry into account.[912,913] The extended RISM method was successfully used in the calculation of structural and thermodynamical properties of various chemical and biological systems and solutions,[914] but it was soon recognized that it poorly describes dielectric properties of polar liquids. At infinite dilution, a correction for a phenomenological dielectric constant can be introduced to the extended RISM integral equations, which allows one to obtain sensible results for ionic pairs in a polar molecular solvent and water. However, at finite salt concentrations the extended RISM theory fails due to an inherent dielectric inconsistency. To improve dielectric predictions of the RISM theory, Perkyns and Pettitt[915,916] introduced consistent corrections that are similar to a bridge function of molecular theories. This dielectrically consistent approach (DRISM) yielded accurate thermodynamics and structure in 1/1 salt aqueous solutions at finite concentrations.

A further improvement of the method was done by Kovalenko et al.[917−919] to introduce spatial distributions of liquid rather than radial correlation functions produced by the site−site RISM approach. Such generalization is known as three-dimensional RISM (3D-RISM) and it gives a detailed solvation structure in the form of three-dimensional correlation functions of interaction sites of solvent molecules near a solute particle of arbitrary shape.

More than 10 years after the original formulation of the extended RISM, Hirata's group proposed an extension to the ab initio electronic structure theory (SCF); such an extension was named RISM-SCF.[920−922] In the RISM-SCF theory, the total free energy A including solute and solvent is defined as

$$A = E_{\text{solute}} + \Delta\mu \qquad (212)$$

where E_{solute} represents the electronic energy of a solute molecule including the nuclear repulsion energy and $\Delta\mu$ is the excess chemical potential (solvation free energy) calculated from the RISM equation with the hypernetted-chain (HNC) closure.[913,922,923]

A can be seen as a functional of the site-density correlation functions between solute and solvent as well as of the wave function of the solute molecule. By solving these coupled equations, the mutually converged E_{solute} and $\Delta\mu$ give energies in the equilibrium state that include coupling of the solute electron and solvent.

As recently done by Sato and Sakaki,[924] it is interesting to directly compare standard continuum models (here in particular the PCM approach) and the RISM-SCF with regard to the terms to be added to the Fock operator so as to account for the solvent reaction field effects on the solute wave function. In section 2.3.1 we have shown that in the PCM

framework the operator has the form

$$V(\vec{r}) = \sum_i \frac{q_i}{|\vec{r} - \vec{s}_i|} \qquad (213)$$

where the sum runs over the solvent apparent charges. In the RISM-SCF approach the parallel operator has the form

$$V^{\mathrm{RISM}}(r) = \rho \sum_{\lambda,\alpha} b_\lambda q_\alpha \int 4\pi r^2 \frac{g_{\lambda,\alpha}(r)}{r} \, \mathrm{d}r \quad (214)$$

where ρ is the number density, b_λ is a population operator, $g_{\lambda\alpha}(r)$ is a pair correlation function between λ (solute) and α (solvent), and q_α is the partial charge on the solvent site α.

The main difference between the two operators (besides the obvious differences in the form) is that the RISM potential (also indicated as microscopic mean field V^{RISM}) includes molecular level information as well as bulk properties of the solvent. To better understand this point, we briefly summarize the RISM-SCF main computational strategy, which can be profitably presented as a sequence of steps.

In advance of the RISM-SCF cycle, the solvent correlation function is prepared by solving the RISM integral equations through a standard iterative scheme with a set of fixed intermolecular potential functions and with guess partial charges of the solute molecule as variables. Then using such a correlation function, the solute−solvent pair correlation functions are obtained. Immediately after the RISM convergence has been attained, the electrostatic solvent operator is calculated from eq 214 and inserted in the solvated Fock operator to calculate the solute wave function. Then the electrostatic contributions due to the nucleus and electronic cloud of the molecule are optimized independently with those due to partial charges assigned on each interaction site, using the least-squares fitting technique. Normalization constraints to preserve the total charge for each contribution are imposed during the fitting procedure. The RISM-SCF iteration is continued until both the electronic and solvent structures become self-consistent within given convergence criteria.

The RISM-SCF method has been extended to include analytical gradients for geometry optimizations and to the multiconfigurational self-consistent-field (MCSCF) method,[922] which can be used for exploring the excited state of a molecule in solution.

Sato et al.[925] have also reformulated the RISM-SCF/MCSCF for the 3D-RISM formalism to properly include the three-dimensional picture of the solvation structure necessary for complex solutes. The authors found that this reformulation allows one to reliably resolve locations and directions of hydrogen bonding in the hydration shells. At the same time, however, they also found that the results from the original RISM-SCF/MCSCF method are reasonably similar to those following from the 3D-RISM/SCF approach after reduction of the orientational dependence.

In recent years, applications of RISM-SCF to the calculation of NMR chemical shifts of solvated molecules have also been presented[926,927] as well as studies on the solvent reorganization energy associated with a charging process of organic compounds.[928,929] In the latter case both nonequilibrium solvation and nonelectrostatic effects were included.

In all of the above RISM-SCF versions the short-range interactions are described by site−site Lennard-Jones potentials, neglecting the solute−solvent short-range QM effects such as the exchange repulsion coming from the Pauli exclusion principle and the charge transfer interaction. To overcome these limitations, Yoshida and Kato[930] proposed an electronic structure theory in solution using the molecular Ornstein−Zernike equation, which is referred to as the MOZ-SCF method. In their treatment, the exchange repulsion/charge transfer interactions are incorporated for calculating the solute−solvent interactions by introducing an effective potential located on solvent molecule. Comparing the MOZ-SCF results with those from the RISM-SCF and PCM methods, it was found that the MOZ-SCF exerts an intermediate effect on the solute electronic state between the RISM-SCF and PCM.

Subsequently, Sato et al.[931] proposed a new approach to account for the quantum nature in the short-range interaction between solute and solvent in solution. Unlike the RISM-SCF theory, this approach describes not only the electronic structure of solute but also solute−solvent interactions in terms of a kind of model−potential method based on the Hartree−Fock frozen density formulation. In the treatment, the quantum effect due to solvent, including exchange repulsion, is projected onto the solute Hamiltonian using the spectral representation method, whereas the integral equation theory of liquids is employed to calculate the solvent distribution around solute.

8. Concluding Remarks

To conclude this review we express some considerations about the present state of the art of continuum models and about perspectives for the future.

The introductory remarks of section 1 represent a background for the whole review, which is centered on QM versions of the continuum solvation models. We shall comment later what this background means for the perspectives of development.

In section 2 and 3 we have examined, with abundant details, the elaboration of the models for solvation effects in very dilute solutions (discarding nonlinearities and time-dependent effects). Within this restrictive definition of solvation, we may consider the elaboration (computational as well as structural) of models given in these two sections as having reached maturity. By comparing the present exposition with that done in the 1994 review,[1] one notices a remarkable increase in the number of methods and computational codes, now far more efficient and accurate. Several new original procedures have also been formulated, almost all completely elaborated and introduced in distributed codes.

Most of the published applications of these methods (that we have only partially reported in this review) are about the energy of the focused subsystem and related quantities, such as solvent effects on the geometry. These studies address a large area of chemical applications: conformational changes, reaction mechanisms, dissociation/association equilibria, and solvent partition functions. The number of such applications, generally claiming success, is quite large; we are not able to give an estimate of their number, but we know of more than 1000 papers, and surely there are many more.

In contrast, less attention has been paid to extracting from the QM calculations elements for analysis and interpretation of solvent effects. Theoretical chemistry has elaborated a large number of concepts and computational tools in terms of submolecular units for the analysis and interpretation of structures and phenomena for systems in the gas phase; these tools are easily extended to solvated systems within a continuum representation. The inclusion of solvent effects adds a new dimension to the understanding of chemical structures and processes, which is rich in possible suggestions. We give an example drawn from a topic not treated in this review: the study of reaction mechanisms. Differential solvation forces related to the specific nature of chemical groups may accelerate or retard a chemical reaction. This has been shown in one of the first examples of a detailed ab initio study of an organic reaction,[932] in which the forces exerted by solvation on the reacting chemical groups (expressed in terms of localized orbitals) were explicitly derived and used to give a rationale for nuclear geometry and electron distribution changes near the transition state. This example, however, has not been followed by other researchers, perhaps because the necessary codes were not collected into a distributed package. The elaboration and distribution of easy-to-use interpretation packages is one of the aspects of conventional energy-based solvation methods for which a more decisive effort is called for and on which we encourage other researchers to intervene.

Section 4 collects under the heading "Nonuniformities in the Continuum Model" topics of different origins for which there is still the need of further methodological elaboration. For this reason we have given bibliographic references also related to the "history" of the subject. To do further development in an already considered field, it is in fact advisable to examine the sources; some ideas given in seminal papers are often neglected in the immediately following extensions and applications, but they can become valuable after some years. The spatial nonuniformities considered in that section are of local nature, occurring at some boundaries in the system. These characteristics prompted the extension of the review from the dielectric nonuniformities around ions, to which the "historical" exposition mainly refers, to other boundaries, enlarging the field of systems where continuum methods may be applied. Some among them are related to systems to which continuum methods, mostly in classical versions, have long been applied such as polyions and molec-

ular polymers in general; others involve heterogeneous systems in which the boundary involves a phase with a structure more stable in time than normal liquids.

We have given a few examples of successful applications of QM continuum methods to systems of this type, but clearly these examples simply indicate the beginning of methodological studies that still have to be developed. We have also indicated another field in which local nonuniformities may play a role, namely, that of the complex liquids, characterized by a mesoscopic length scale. This is a novel field to which the application of continuum models has not yet attempted, an attempt which seems to us possible and promising. In the same line of referring to material systems to which some basic methodological issues could be applied, we cite here the ionic liquids, and the isotropic solutions at finite rather than negligible concentration.

In conclusion, it may be said that for the topics of section 4 the state of the art indicates a situation in progress, not yet assessed, but with brilliant perspectives.

Time-dependent (TD) phenomena and response properties have been considered in sections 5 and 6, respectively. Remarkable advances have been registered in both areas in recent years. In particular, for TD phenomena, continuum methods have started to represent a valid alternative to simulation methods (historically the best suited for this kind of studies), and for response properties they are slowly but progressively acquiring the reliability of gas phase calculations. In both cases, an important discriminating factor has been the easy insertion of high-level QM descriptions of a molecule in continuum models. The computational advantage of a continuum approach with respect to simulation methods must be emphasized again: simulations have to dedicate a considerable portion of computational time to describe solvent degrees of freedom, and this, for example, makes almost impossible a serious study of response properties.

Concerning the description of molecular properties in condensed phases (both in continuum and in discrete approaches) some problems arise. Quantum mechanics gives a complete (in principle) description of the studied system which satisfies well-established rules: completeness of the set of eigenfunctions, complete orthogonality, expansion coefficients over the states directly related to the probability of finding that state in a measurement experiment, etc. These formal properties, however, are no longer valid when the molecule interacts with others. In other words, the molecular wave function has a different status in the presence or absence of molecular interactions. This fact is well-known to people trying to derive the value of a property of one of the molecular partners from calculations performed on a supermolecule. To obtain this value there is the need of additional assumptions, varying from case to case, because a universal protocol has never been established. It may be said that this protocol exists for continuum models, being the Hartree separation between the focused molecule and the continuum in general use.

This model can be good or bad, but in any case it is a common starting point on which additional refinements can be based.[336]

This, however, is not the only important issue to address. In condensed systems exhibiting rapid motions of the molecular components, such as liquids, other complications arise. There is, in fact, the need of an appropriate thermal average, which may change from property to property. For example, the calculation of electronic excitation energies in the simple model of vertical transitions gives poor results if based on the excited states of a molecule in equilibrium with the solvent. The inclusion in the model of changes in the fast component of the solvent polarization leads to excited states of better quality.

Other examples could be done, all indicating that the description of properties in condensed systems is more complex than for isolated molecules. This fact has been known for a long time, and experimental values of properties are always published with empirical corrections addressing the effect of the surrounding medium (namely, the local field factors introduced in section 6.2). These corrections, elaborated many years ago, are all based on quite simple continuum models. As shown in section 6.2.2, recently more precise expressions of these corrections, tailored on the single molecule, have been elaborated with the aid of modern solvation methods.

In parallel to this evolution, the number of properties for which there are available detailed and tested computational strategies has greatly increased, as a comparison of this review with the preceding ones shows. This rate of increase shows no tendency to level off, because there are many properties not yet examined in detail and because their number increases thanks to the ingenuity of experimentalists who continually devise new ways of probing the molecular matter.

The expansion of continuum methods in the descriptions of properties has now passed the divide between simple systems (such as homogeneous solutions) and complex systems, in which the whole system gives responses that cannot be reduced to those of the separate components. Even in this new field the positive results are numerous and give confidence in further rapid progresses. The realm of complex systems is quite interesting, being at the frontier of physical and chemical research and, for its variety, presenting a challenging variety of features each requiring an attentive analysis for its modeling.

We do not enter into an analysis of the role of the calculations of properties in the intrinsic context of theoretical chemistry and of its support to applications in academic and technological research, because our views have already been expressed in several papers.[336,933−935] For the scope of this section, it is sufficient to say that, in our opinion, the state of the art and the prospects for the topics considered in the section 6 are decidedly positive. The basic methodological elements have been established, the computational methods (now well documented) have been validated, and they can be safely employed, even if there is still a lot of work to refine.

Section 7 is focused on another aspect of the extension of continuum methods which is quite important and in progress, namely, the combination of continuum and discrete representations of the medium.

The admixture of continuum and discrete models (using a solute−solvent supermolecule) has been in use for a long time in different studies including the description of solute conformations and the analysis of the direct role of solvent molecules in chemical reaction mechanisms. We explicitly cite a paper[936] published the same year as the first PCM paper[8] to underscore that the use of supermolecules has been considered in QM continuum methods since their very beginning, and it has continued to the present. In that paper, a supermolecule approach plus continuum was used to compute solvent shifts in electronic absorption spectra. Nowadays, it is clear that small solute−solvent clusters can represent an important evolution of solvation methods to accurately describe spectroscopic properties (as also discussed in section 6). There is, howevet, the need to accompany this approach with others in which important aspects of the material model, such as the averages on the motions, are better described. There is a sizable variety of computational strategies addressing this mixing of continuum and discrete methods, and some protocols of use are in the process of refinement. In parallel, discrete simulations, in their struggle against computational costs, tend to exploit more extensively the computational advantages of continuum descriptions. This is an example of admixture of approaches from which our advancement in the description of matter may derive great benefits.

The perspective of a stronger admixture between continuum and discrete models is in line with what was pointed out in section 1.2 about distribution functions. In the present case, the main continuum distribution in question is the density distribution of massive particles, the molecules, interacting among themselves via the forces described by the intermolecular interaction theories. The dielectric function is one of the ancillary quantities related to the molecular density distribution; other functions, of different physical origin, exist, but they do not play a role in the present continuum solvation methods. The discrete molecule distribution can be replaced, partially or totally with continuum functions, as we have discussed in several points of this review. This change of description leads us to neglect a portion of the information carried by a discrete description. One needs to evaluate, problem by problem, whether this reduction in the information compromises the description of the phenomenon or whether the reduction in the computational burden is not accompanied by a loss of important details. In the case of solvation methods, as we have shown, the advantages of a continuum description are in general greater than the disadvantages. The topics considered in section 7 to a large extent address the area in which continuum methods require discrete corrections.

In section 1.2 we have considered another distribution, that of electrons in molecules interacting via

electrostatic forces. The discrete description of the single elements, given by the molecular orbital theory, may be replaced by a continuum distribution as it is given by the density functional theory, an approach that presents considerable advantages with respect to the basic MO theory (and some minor shortcomings). DFT has introduced some new concepts and techniques in the QM description of the molecules, some of which are now exploited in QM continuum solvent calculations.

Continuum solvation methods can be considered to reside at the separation between the realm of the electronic and molecular density distribution, receiving inputs and information from both sides. Other types of continuum/discrete pairs of descriptions exist for other aspects of the physical and chemical sciences. For some among them, describing the motion of electrons and of more massive particles both bound to some substrate (metal, dielectric solid body), a connection with the methods analyzed in this review has been already initiated. They actually represent the beginning of another chapter of continuum methods, in which the solvent is not compulsorily present.

To conclude this section, and the review, we may state that the part of the realm of applications of continuum methods in chemistry we have examined is vast and complex, with important sections arrived at maturity, others in rapid progress, and others still at the initial steps.

9. Acknowledgment

10. References

(1) Tomasi, J.; Persico, M. *Chem. Rev.* **1994**, *94*, 2027.
(2) Cramer, C. J.; Truhlar, D. G. *Chem. Rev.* **1999**, *99*, 2161.
(3) Orozco, M.; Luque, F. J. *Chem. Rev.* **2000**, *100*, 4187.
(4) Bonaccorsi, R.; Scrocco, E.; Tomasi, J. *J. Chem. Phys.* **1970**, *52*, 5270.
(5) Huron, M. J.; Claverie, P. *J. Phys. Chem.* **1972**, *76*, 2123.
(6) Rinaldi, D.; Rivail, J. L. *Theor. Chim. Acta* **1973**, *32*, 57.
(7) Tapia, O.; Goscinski, O. *Mol. Phys.* **1975**, *29*, 1653.
(8) Miertuš, S.; Scrocco, E.; Tomasi, J. *Chem. Phys.* **1981**, *55*, 117.
(9) Jensen, F. *Introduction to Computational Chemistry*; Wiley: Chichester, U.K., 1999.
(10) Levine, I. *Quantum Chemistry*, 5th ed.; Prentice Hall: Upper Saddle River, NJ, 1999.
(11) Leach, A. R. *Molecular Modelling: Principles and Applications*, 2nd ed.; Prentice Hall: Upper Saddle River, NJ, 2001.
(12) Cramer, C. J. *Essentials of Computational Chemistry: Theories and Models*, 2nd ed.; Wiley: Chichester, U.K., 2004.
(13) Onsager, L. *J. Am. Chem. Soc.* **1936**, *58*, 1486.
(14) Tomasi, J. *Theor. Chem. Acc.* **2000**, *103*, 196.
(15) Wong, M. W.; Wiberg, K. B.; Frisch, M. J. *J. Comput. Chem.* **1995**, *16*, 385.
(16) Foresman, J. B.; Keith, T. A.; Wiberg, K. B.; Snoonian, J.; Frisch, M. J. *J. Phys. Chem.* **1996**, *100*, 16098.
(17) Frisch, M. J.; Trucks, G. W.; Schlegel, H. B.; Scuseria, G. E.; Robb, M. A.; Cheeseman, J. R.; Montgomery, J. A. J.; Vreven, T.; Kudin, K. N.; Burant, J. C.; Millam, J. M.; Iyengar, S. S.; Tomasi, J.; Barone, V.; Mennucci, B.; Cossi, M.; Scalmani, G.; Rega, N.; Petersson, G. A.; Nakatsuji, H.; Hada, M.; Ehara, M.; Toyota, K.; Fukuda, R.; Hasegawa, J.; Ishida, M.; Nakajima, T. H.; Y.; Kitao, O.; Nakai, H.; Klene, M.; Li, X.; Knox, J. E.; Hratchian, H. P.; Cross, J. B.; Adamo, C.; Jaramillo, J.; Gomperts, R.; Stratmann, R. E.; Yazyev, O.; Austin, A. J.; Cammi, R.; Pomelli, C.; Ochterski, J. W.; Ayala, P. Y.; Morokuma, K.; Voth, G. A.; Salvador, P.; Dannenberg, J. J.; Zakrzewski, V. G.; Dapprich, S.; Daniels, A. D.; Strain, M. C.; Farkas, O.; Malick, D. K.; Rabuck, A. D.; Raghavachari, K.; Foresman, J. B.; Ortiz, J. V.; Cui, Q.; Baboul, A. G.; Clifford, S.; Cioslowski, J.; Stefanov,

B. B. L., G.;; Liashenko, A.; Piskorz, P.; Komaromi, I.; Martin, R. L.; Fox, D. J.; Keith, T.; Al-Laham, M. A.; Peng, C. Y.; Nanayakkara, A.; Challacombe, M.; Gill, P. M. W.; Johnson, B.; Chen, W.; Wong, M. W.; Gonzalez, C.; Pople, J. A. *Gaussian 03*, revision A.1; Pittsburgh, PA; 2003; http://www.Gaussian.com/.
(18) Amovilli, C.; McWeeny, R. *J. Mol. Struct. (THEOCHEM)* **1991**, *227*, 1.
(19) Yin, D. X.; MacKerell, A. D. *J. Phys. Chem.* **1996**, *100*, 2588.
(20) Hoshino, S.; Ohno, K. *J. Am. Chem. Soc.* **1997**, *119*, 8276.
(21) Bentley, J. *J. Phys. Chem. A* **1998**, *102*, 6043.
(22) Bentley, J. *J. Phys. Chem. A* **2000**, *104*, 9630.
(23) Bentley, J. *J. Chem. Phys.* **2003**, *119*, 5449.
(24) Malolepsza, E.; Piela, L. *J. Phys. Chem. A* **2003**, *107*, 5356.
(25) Bader, R. F. W. *Atoms in Molecules—A Quantum Theory*; Oxford University Press: Oxford, U.K., 1990.
(26) Bondi, A. *J. Phys. Chem.* **1964**, *68*, 441.
(27) Rowland, R. S.; Taylor, R. *J. Phys. Chem.* **1996**, *100*, 7384.
(28) Pauling, L. *The Nature of the Chemical Bond*, 3rd ed.; Cornell University Press: Ithaca, NY, 1960.
(29) http://www.hbcpnetbase.com/.
(30) Rappe, A. K.; Casewit, C. J.; Colwell, K. S.; Goddard, W. A.; Skiff, W. M. *J. Am. Chem. Soc.* **1992**, *114*, 10024.
(31) Connolly, M. L. *Science* **1983**, *221*, 709.
(32) Connolly, M. L. *J. Appl. Crystallogr.* **1983**, *16*, 548.
(33) Lee, B.; Richards, F. M. *J. Mol. Biol.* **1971**, *55*, 379.
(34) Richards, F. M. *Annu. Rev. Biophys. Bioeng.* **1977**, *6*, 151.
(35) Greer, J.; Bush, B. L. *Proc. Natl. Acad. Sci. U.S.A.* **1978**, *75*, 303.
(36) Connolly, M. L. *J. Mol. Graph.* **1993**, *11*, 139.
(37) http://www.netsci.org/Science/Compchem/feature14.html.
(38) Gogonea, V.; Osawa, E. *J. Mol. Struct. (THEOCHEM)* **1994**, *117*, 305.
(39) Gogonea, V.; Osawa, E. *J. Comput. Chem.* **1995**, *16*, 817.
(40) Sanner, M. F.; Olson, A. J.; Spehner, J. C. *Biopolymers* **1996**, *38*, 305.
(41) Sanner, M. F.; Olson, A. J.; Spehner, J. C.; MSMS; http://www.scripps.edu/~sanner/.
(42) Pascual-Ahuir, J. L.; Silla, E.; Tomasi, J.; Bonaccorsi, R. *J. Comput. Chem.* **1987**, *8*, 778.
(43) Pascual-Ahuir, J. L.; Silla, E. *J. Comput. Chem.* **1990**, *11*, 1047.
(44) Silla, E.; Villar, F.; Nilsson, O.; Pascual-Ahuir, J. L.; Tapia, O. *J. Mol. Graph.* **1990**, *8*, 168.
(45) Silla, E.; Tunon, I.; Pascual-Ahuir, J. L. *J. Comput. Chem.* **1991**, *12*, 1077.
(46) Pomelli, C. S.; Tomasi, J. *J. Comput. Chem.* **1998**, *19*, 1758.
(47) Pomelli, C. S.; Tomasi, J.; Cossi, M.; Barone, V. *J. Comput. Chem.* **1999**, *20*, 1693.
(48) Amovilli, C.; Barone, V.; Cammi, R.; Cancès, E.; Cossi, M.; Mennucci, B.; Pomelli, C. S.; Tomasi, J. *Adv. Quant. Chem.* **1998**, *32*, 227.
(49) Cossi, M.; Barone, V. *J. Chem. Phys.* **1998**, *109*, 6246.
(50) Cammi, R.; Tomasi, J. *J. Comput. Chem.* **1995**, *16*, 1449.
(51) Luque, F. J.; Bofill, J. M.; Orozco, M. *J. Chem. Phys.* **1995**, *103*, 10183.
(52) Colominas, C.; Luque, F. J.; Orozco, M. *J. Comput. Chem.* **1999**, *20*, 665.
(53) Luque, F. J.; Curutchet, C.; Munoz-Muriedas, J.; Bidon-Chanal, A.; Soteras, I.; Morreale, A.; Gelpi, J. L.; Orozco, M. *Phys. Chem. Chem. Phys.* **2003**, *5*, 3827.
(54) Morreale, A.; Gelpi, J. L.; Luque, F. J.; Orozco, M. *J. Comput. Chem.* **2003**, *24*, 1610.
(55) Curutchet, C.; Cramer, C. J.; Truhlar, D. G.; Ruiz-Lopez, M. F.; Rinaldi, D.; Orozco, M.; Luque, F. J. *J. Comput. Chem.* **2003**, *24*, 284.
(56) Basilevsky, M. V.; Chudinov, G. E. *Chem. Phys.* **1991**, *157*, 327.
(57) Wiberg, K. B.; Keith, T. A.; Frisch, M. J.; Murcko, M. *J. Phys. Chem.* **1995**, *99*, 9072.
(58) Klamt, A.; Schüürmann, G. *J. Chem. Soc., Perkin Trans. 2* **1993**, 799.
(59) Stefanovich, E. V.; Truong, T. N. *Chem. Phys. Lett.* **1995**, *244*, 65.
(60) Truong, T. N.; Stefanovich, E. V. *Chem. Phys. Lett.* **1995**, *240*, 253.
(61) Barone, V.; Cossi, M. *J. Phys. Chem. A* **1998**, *102*, 1995.
(62) Cossi, M.; Rega, N.; Scalmani, G.; Barone, V. *J. Comput. Chem.* **2003**, *24*, 669.
(63) Pye, C. C.; Ziegler, T. *Theor. Chem. Acc.* **1999**, *101*, 396.
(64) Velde, G. T.; Bickelhaupt, F. M.; Baerends, E. J.; Guerra, C. F.; Van Gisbergen, S. J. A.; Snijders, J. G.; Ziegler, T. *J. Comput. Chem.* **2001**, *22*, 931.
(65) *ADF, 2004.01*; Vrije Universiteit: Amsterdam, The Netherlands, 2004; http://www.scm.com.
(66) Chipman, D. N. *Theor. Chem. Acc.* **2002**, *107*, 80.
(67) Klamt, A. *J. Phys. Chem,* **1995**, *99*, 2224.
(68) Klamt, A.; Jonas, V.; Burger, T.; Lohrenz, J. C. W. *J. Phys. Chem. A* **1998**, *102*, 5074.
(69) Klamt, A.; Eckert, F. *Fluid Phase Equilib.* **2000**, *172*, 43.
(70) Mehler, C.; Klamt, A.; Peukert, W. *AIChE J.* **2002**, *48*, 1093.

(71) Klamt, A.; Eckert, F.; Hornig, M. *J. Comput.-Aided Mol. Des.* **2001**, *15*, 355.
(72) Putnam, R.; Taylor, R.; Klamt, A.; Eckert, F.; Schiller, M. *Ind. Eng. Chem. Res.* **2003**, *42*, 3635.
(73) GmbH&CoKG, C. *COSMOtherm*, release C1.2; Leverkusen, Germany, 2003; http://www.cosmologic.de.
(74) Cancès, E.; Mennucci, B.; Tomasi, J. *J. Chem. Phys.* **1997**, *107*, 3032.
(75) Mennucci, B.; Cancès, E.; Tomasi, J. *J. Phys. Chem. B* **1997**, *101*, 10506.
(76) Cancès, E.; Mennucci, B. *J. Math. Chem.* **1998**, *23*, 309.
(77) Hackbusch, W. *Integral Equations: Theory and Numerical Treatment*; Birkhauser: Basel, Switzerland, 1995.
(78) Mennucci, B.; Cammi, R.; Tomasi, J. *J. Chem. Phys.* **1998**, *109*, 2798.
(79) Corni, S.; Tomasi, J. *J. Chem. Phys.* **2001**, *114*, 3739.
(80) Frediani, L.; Cammi, R.; Corni, S.; Tomasi, J. *J. Chem. Phys.* **2004**, *120*, 3893.
(81) Chipman, D. M. *J. Chem. Phys.* **1997**, *106*, 10194.
(82) Zhan, C. G.; Bentley, J.; Chipman, D. M. *J. Chem. Phys.* **1998**, *108*, 177.
(83) Chipman, D. M. *J. Chem. Phys.* **1999**, *110*, 8012.
(84) Chipman, D. M. *J. Chem. Phys.* **2000**, *112*, 5558.
(85) Chipman, D. M. *J. Chem. Phys.* **2002**, *116*, 10129.
(86) Mennucci, B.; Tomasi, J. *J. Chem. Phys.* **1997**, *106*, 5151.
(87) Cancès, E.; Mennucci, B. *J. Chem. Phys.* **2001**, *114*, 4744.
(88) Cossi, M.; Rega, N.; Scalmani, G.; Barone, V. *J. Chem. Phys.* **2001**, *114*, 5691.
(89) Cossi, M.; Scalmani, G.; Rega, N.; Barone, V. *J. Chem. Phys.* **2002**, *117*, 43.
(90) Brebbia, C. A.; Dominguez, J. *Appl. Math. Mod.* **1977**, *1*, 372.
(91) http://www.wessex.ac.uk/conferences/2005/bem05/index.html.
(92) Pascual-Ahuir, J. L.; Silla, E.; Tunon, I. *J. Comput. Chem.* **1994**, *15*, 1127.
(93) Cossi, M.; Mennucci, B.; Cammi, R. *J. Comput. Chem.* **1996**, *17*, 57.
(94) Pomelli, C. S.; Tomasi, J. *Theor. Chem. Acc.* **1998**, *99*, 34.
(95) Pomelli, C. S.; Tomasi, J.; Cammi, R. *J. Comput. Chem.* **2001**, *22*, 1262.
(96) Frediani, L.; Cammi, R.; Pomelli, C. S.; Tomasi, J.; Ruud, K. *J. Comput. Chem.* **2004**, *25*, 375.
(97) Schmidt, M. W.; Baldridge, K. K.; Boatz, J. A.; Elbert, S. T.; Gordon, M. S.; Jensen, J. H.; Koseki, S.; Matsunaga, N.; Nguyen, K. A.; Su, S. J.; Windus, T. L.; Dupuis, M.; Montgomery, J. A. *J. Comput. Chem.* **1993**, *14*, 1347.
(98) http://www.msg.ameslab.gov/GAMESS/GAMESS.html.
(99) Scalmani, G.; Rega, N.; Cossi, M.; Barone, V. *J. Comput. Methods Sci. Eng.* **2002**, *2*, 469.
(100) Senn, H. M.; Margl, P. M.; Schmid, R.; Ziegler, T.; Blochl, P. E. *J. Chem. Phys.* **2003**, *118*, 1089.
(101) Pomelli, C. *J. Comput. Chem.* **2004**, *25*, 1532.
(102) Mennucci, B.; Cammi, R. *Int. J. Quantum Chem.* **2003**, *93*, 121.
(103) http://www.Gaussian.com/index.html.
(104) Zhan, C. G.; Chipman, D. M. *J. Chem. Phys.* **1999**, *110*, 1611.
(105) Chipman, D. M. *J. Chem. Phys.* **1996**, *104*, 3276.
(106) Purisima, E. O.; Nilar, S. H. *J. Comput. Chem.* **1995**, *16*, 681.
(107) Purisima, E. O. *J. Comput. Chem.* **1998**, *19*, 1494.
(108) Greengard, L. F.; Rokhlin, A. *J. Comput. Phys.* **1987**, *73*, 325.
(109) Strain, M. C.; Scuseria, G. E.; Frisch, M. J. *Science* **1996**, *271*, 51.
(110) White, C. A.; Johnson, B. G.; Gill, P. M. W.; Head-Gordon, M. *Chem. Phys. Lett.* **1996**, *253*, 268.
(111) Challacombe, M.; Schwegler, E. *J. Chem. Phys.* **1997**, *106*, 5526.
(112) Scalmani, G.; Barone, V.; Kudin, K. N.; Pomelli, C. S.; Scuseria, G. E.; Frisch, M. J. *Theor. Chem. Acc.* **2004**, *111*, 90.
(113) York, D. M.; Karplus, M. *J. Phys. Chem. A* **1999**, *103*, 11060.
(114) Scalmani, G.; Frisch, M. J. **2005**, in preparation.
(115) Kirkwood, J. G. *J. Chem. Phys.* **1934**, *2*, 767.
(116) Cossi, M.; Barone, V.; Mennucci, B.; Tomasi, J. *Chem. Phys. Lett.* **1998**, *286*, 253.
(117) Chipman, D. M. *J. Chem. Phys.* **2004**, *120*, 5566.
(118) Yoon, B. J.; Lenhoff, A. M. *J. Comput. Chem.* **1990**, *11*, 1080.
(119) Zauhar, R. J.; Morgan, R. S. *J. Comput. Chem.* **1990**, *11*, 603.
(120) Zauhar, R. J. *J. Comput. Chem.* **1991**, *12*, 575.
(121) Juffer, A. H.; Botta, E. F. F.; Vankeulen, B. A. M.; Vanderploeg, A.; Berendsen, H. J. C. *J. Comput. Chem.* **1991**, *97*, 144.
(122) Yoon, B. J.; Lenhoff, A. M. *J. Phys. Chem.* **1992**, *96*, 3130.
(123) Zauhar, R. J. *J. Comput.-Aided Mol. Des.* **1995**, *9*, 149.
(124) Juffer, A. H.; Argos, P.; Vogel, H. J. *J. Phys. Chem. B* **1997**, *101*, 7664.
(125) Zhou, H. X. *Biophys. J.* **1993**, *65*, 955.
(126) Liang, J.; Subramaniam, S. *Biophys. J.* **1997**, *73*, 1830.
(127) Zauhar, R. J.; Varnek, A. *J. Comput. Chem.* **1996**, *17*, 864.
(128) Boschitsch, A. H.; Fenley, M. O.; Zhou, H. X. *J. Phys. Chem. B* **2002**, *106*, 2741.
(129) Xiang, Z. X.; Huang, F. H.; Shi, Y. Y. *J. Phys. Chem.* **1994**, *98*, 12782.
(130) Kirkwood, J. G. *J. Chem. Phys.* **1939**, *7*, 911.
(131) Onsager, L. *J. Am. Chem. Soc.* **1936**, *58*, 1486.
(132) Wong, M. A.; Frisch, M. J.; Wiberg, K. B. *J. Am. Chem. Soc.* **1991**, *113*, 4776.
(133) Wong, M. A.; Frisch, M. J.; Wiberg, K. B. *J. Am. Chem. Soc.* **1992**, *114*, 523.
(134) Mikkelsen, K. V.; Agren, H.; Jensen, H. J. A.; Helgaker, T. *J. Chem. Phys.* **1988**, *89*, 3086.
(135) Helgaker, H.; Jensen, H. J. A.; Jørgensen, P.; Olsen, J.; Ruud, K.; Ågren, H.; Auer, A. A.; Bak, K. L.; Bakken, V.; Christiansen, O.; Coriani, S.; Dahle, P.; Dalskov, E. K.; Enevoldsen, T.; Fernandez, B.; Hättig, C.; Hald, K.; Halkier, A.; Heiberg, H.; Hettema, H.; Jonsson, D.; Kirpekar, S.; Kobayashi, R.; Koch, H.; Mikkelsen, K. V.; Norman, P.; Packer, M. J.; Pedersen, T. B.; Ruden, T. A.; Sanchez, J.; Saue, T.; Sauer, S. P. A.; Schimmelpfennig, B.; Sylvester-Hvid, K. O.; Taylor, P. R.; Vahtras, O.; *Dalton*, release 1.2; Oslo, Norway, 2001; http://www.kjemi-.uio.no/software/dalton/.
(136) Mikkelsen, K. V.; Jorgensen, P.; Jensen, H. J. A. *J. Chem. Phys.* **1994**, *100*, 6597.
(137) Mikkelsen, K. V.; Cesar, A.; Agren, H.; Jensen, H. J. A. *J. Chem. Phys.* **1995**, *103*, 9010.
(138) Mikkelsen, K. V.; Sylvester-Hvid, K. O. *J. Phys. Chem.* **1996**, *100*, 9116.
(139) Sylvester-Hvid, K. O.; Mikkelsen, K. V.; Jonsson, D.; Norman, P.; Agren, H. *J. Chem. Phys.* **1998**, *109*, 5576.
(140) Christiansen, O.; Mikkelsen, K. V. *J. Chem. Phys.* **1999**, *110*, 8348.
(141) Christiansen, O.; Mikkelsen, K. V. *J. Chem. Phys.* **1999**, *110*, 1365.
(142) Osted, A.; Kongsted, J.; Mikkelsen, K. V.; Christiansen, O. *Mol. Phys.* **2003**, *101*, 2055.
(143) Kongsted, J.; Osted, A.; Mikkelsen, K. V.; Christiansen, O. *J. Chem. Phys.* **2004**, *120*, 3787.
(144) Rivail, J. L.; Rinaldi, D. *Chem. Phys.* **1976**, *18*, 233.
(145) Rinaldi, D.; Bouchy, A.; Rivail, J. L.; Dillet, V. *J. Chem. Phys.* **2004**, *120*, 2343.
(146) Bottcher, C. J. F. *Theory of Electric Polarization*, 2nd ed.; Elsevier: Amsterdam, The Netherlands, 1973.
(147) Dillet, V.; Rinaldi, D.; Bertran, J.; Rivail, J. L. *J. Chem. Phys.* **1996**, *104*, 9437.
(148) Born, M. *Z. Phys.* **1920**, *1*, 45.
(149) Still, W. C.; Tempczyk, A.; Hawley, R. C.; Hendrickson, T. *J. Am. Chem. Soc.* **1990**, *112*, 6127.
(150) Bashford, D.; Case, D. A. *Annu. Rev. Phys. Chem.* **2000**, *51*, 129.
(151) Schaefer, M.; Karplus, M. *J. Phys. Chem.* **1996**, *100*, 1578.
(152) Hsu, C. P.; Head-Gordon, M.; Head-Gordon, T. *J. Chem. Phys.* **1999**, *111*, 9700.
(153) Babu, C. S.; Lim, C. *J. Chem. Phys.* **2001**, *114*, 889.
(154) Lee, M. S.; Salsbury, F. R.; Brooks, C. L. *J. Chem. Phys.* **2002**, *116*, 10606.
(155) Lee, M. S.; Feig, M.; Salsbury, F. R.; Brooks, C. L. *J. Comput. Chem.* **2003**, *24*, 1348.
(156) Qiu, D.; Shenkin, P. S.; Hollinger, F. P.; Still, W. C. *J. Phys. Chem. A* **1997**, *101*, 3005.
(157) MacKerell, A. D.; Bashford, D.; Bellott, M.; Dunbrack, R. L.; Evanseck, J. D.; Field, M. J.; Fischer, S.; Gao, J.; Guo, H.; Ha, S.; Joseph-McCarthy, D.; Kuchnir, L.; Kuczera, K.; Lau, F. T. K.; Mattos, C.; Michnick, S.; Ngo, T.; Nguyen, D. T.; Prodhom, B.; Reiher, W. E.; Roux, B.; Schlenkrich, M.; Smith, J. C.; Stote, R.; Straub, J.; Watanabe, M.; Wiorkiewicz-Kuczera, J.; Yin, D.; Karplus, M. *J. Phys. Chem. B* **1998**, *102*, 3586.
(158) Dominy, B. N.; Brooks, C. L. *J. Phys. Chem. B* **1999**, *103*, 3765.
(159) Cheng, A.; Best, S. A.; Merz, K. M.; Reynolds, C. H. *J. Mol. Graphics Modell.* **2000**, *18*, 273.
(160) Zagrovic, B.; Sorin, E. J.; Pande, V. *J. Mol. Biol.* **2001**, *313*, 151.
(161) Hawkins, G. D.; Cramer, C. J.; Truhlar, D. G. *Chem. Phys. Lett.* **1995**, *246*, 122.
(162) Hawkins, G. D.; Cramer, C. J.; Truhlar, D. G. *J. Phys. Chem.* **1996**, *100*, 19824.
(163) Onufriev, A.; Bashford, D.; Case, D. A. *J. Phys. Chem. B* **2000**, *104*, 3712.
(164) Sheinerman, F. B.; Norel, R.; Honig, Barry *Curr. Opin. Struct. Biol.* **2000**, *10*, 153.
(165) Tsui, V.; Case, D. A. *Biopolymers* **2001**, *56*, 275.
(166) Cramer, C. J.; Truhlar, D. G. *Chem. Rev.* **1999**, *99*, 2161.
(167) Thompson, J. D.; Cramer, C. J.; Truhlar, D. G. *J. Phys. Chem. A* **2004**, *108*, 6532.
(168) http://comp.chem.umn.edu/amsol/.
(169) Zhu, T. H.; Li, J. B.; Hawkins, G. D.; Cramer, C. J.; Truhlar, D. G. *J. Chem. Phys.* **1998**, *109*, 9117.
(170) Li, J. B.; Hawkins, G. D.; Cramer, C. J.; Truhlar, D. G. *Chem. Phys. Lett.* **1998**, *288*, 293.
(171) Zhu, T. H.; Li, J. B.; Liotard, D. A.; Cramer, C. J.; Truhlar, D. G. *J. Chem. Phys.* **1999**, *110*, 5503.
(172) Li, J. B.; Zhu, T. H.; Hawkins, G. D.; Winget, P.; Liotard, D. A.; Cramer, C. J.; Truhlar, D. G. *Theor. Chem. Acc.* **1999**, *103*, 9.
(173) Pu, J. T.; Xidos, J. D.; Li, J.; Zhu, T.; Hawkins, G. D.; Chuang, Y.-Y.; Fast, P. L.; Liotard, D. A.; Rinaldi, D.; Cramer, C. J.; Truhlar, D. G.; *GAMESSPLUS*, 4.2; University of Minnesota: Minneapolis, MN, 2004; http://comp.chem.umn.edu/gamessplus/.

(174) Nakamura, H. X.; Thompson, J. D.; Li, J.; Hawkins, G. D.; Zhu, T.; Lynch, B. J.; Volobuev, Y.; Rinaldi, D.; Liotard, D. A.; Cramer, C. J.; Truhlar, D. G. *HONDOPLUS*, 4.5; University of Minnesota: Minneapolis, MN, 2004; http://t1.chem.umn.edu/hondoplus/.
(175) http://t1.chem.umn.edu/hondoplus/.
(176) Thompson, J. D.; Lynch, B. J.; Xidos, J. D.; Li, J.; Hawkins, G. D.; Zhu, T.; Volobuev, Y.; Dupuis, M.; Rinaldi, D.; Liotard, D. A.; Cramer, C. J.; Truhlar, D. G. *SMxGAUSS*, 1.0; University of Minnesota: Minneapolis, MN, 2004; http://comp.chem.umn-.edu/smxgauss/.
(177) Storer, J. W.; Giesen, D. J.; Cramer, C. J.; Truhlar, D. G. *J. Comput.-Aided Mol. Des.* **1995**, *9*, 87.
(178) Giesen, D. J.; Storer, J. W.; Cramer, C. J.; Truhlar, D. G. *J. Am. Chem. Soc.* **1995**, *117*, 1057.
(179) Cortis, C. M.; Langlois, J. M.; Beachy, M. D.; Friesner, R. A. *J. Chem. Phys.* **1996**, *105*, 5472.
(180) Cortis, C. M.; Friesner, R. A. *J. Comput. Chem.* **1997**, *18*, 1570.
(181) Cortis, C. M.; Friesner, R. A. *J. Comput. Chem.* **1997**, *18*, 1591.
(182) http://www.schrodinger.com/Products/maestro.html.
(183) Baker, N. A.; Sept, D.; Joseph, S.; Holst, M. J.; McCammon, J. A. *Proc. Natl. Acad. Sci. U.S.A.* **2001**, *98*, 10037.
(184) Klapper, I.; Hagstrom, R.; Fine, R.; Sharp, K.; Honig, B. *Proteins: Struct., Funct. Genet.* **1986**, *1*, 47.
(185) Warwicker, J. *J. Theor. Biol.* **1986**, *121*, 199.
(186) Bashford, D.; Karplus, M. *Biochemistry* **1990**, *29*, 10219.
(187) Briggs, J. M.; Madura, J. D.; Davis, M. E.; Gilson, M. K.; Antosiewicz, J.; Luty, B. A.; Wade, R. C.; Bagheri, B.; Ilin, A.; Tan, R. C.; McCammon, J. A. *UHBD*; University of California: San Diego, CA; http://mccammon.ucsd.edu/uhbd.html.
(188) Davis, M. E.; Madura, J. D.; McCammon, J. A. *Biophys. J.* **1990**, *57*, A415.
(189) Davis, M. E.; Madura, J. D.; Luty, B. A.; McCammon, J. A. *Comput. Phys. Commun.* **1991**, *62*, 187.
(190) Madura, J. D.; Briggs, J. M.; Wade, R. C.; Davis, M. E.; Luty, B. A.; Ilin, A.; Antosiewicz, J.; Gilson, M. K.; Bagheri, B.; Scott, L. R.; McCammon, J. A. *Comput. Phys. Commun.* **1995**, *91*, 57.
(191) http://www.accelrys.com/insight/DelPhi_page.html.
(192) Nicholls, A.; Honig, B. *J. Comput. Chem.* **1991**, *12*, 435.
(193) Honig, B.; Nicholls, A. *Science* **1995**, *268*, 1144.
(194) Holst, M.; Saied, F. *J. Comput. Chem.* **1993**, *14*, 105.
(195) Bashford, D.; MEAD (Macroscopic Electrostatics with Atomic Detail); http://www.scripps.edu/mb/bashford/.
(196) Li, J.; Nelson, M. R.; Peng, C.-Y.; Bashford, D.; Noodleman, L. *J. Phys. Chem. A* **1998**, *102.*, 6311.
(197) Dillet, V.; Dyson, H. J.; Bashford, D. *Biochemistry* **1998**, *37*, 10298.
(198) Holst, M.; Baker, N.; Wang, F. *J. Comput. Chem.* **2000**, *21*, 1319.
(199) Baker, N.; Holst, M.; Wang, F. *J. Comput. Chem.* **2000**, *21*, 1343.
(200) McWeeny, R. *Methods of Molecular Quantum Mechanics*; Academic Press: London, U.K., 1992.
(201) Klamt, A.; Jonas, V. *J. Chem. Phys.* **1996**, *105*, 9972.
(202) Cancès, E.; Mennucci, B. *J. Chem. Phys.* **2001**, *115*, 6130.
(203) Chipman, D. M. *J. Phys. Chem. A* **2000**, *104*, 11816.
(204) Medeiros, L. A. *J. Math. Anal. Appl.* **1979**, *69*, 252.
(205) Yomosa, S. *J. Phys. Soc. Jpn.* **1973**, *35*, 1738.
(206) Sanhueza, J. E.; Tapia, O.; Laidlaw, W. G.; Trsic, M. *J. Chem. Phys.* **1979**, *70*, 3096.
(207) Tapia, O.; Johannin, G. *J. Chem. Phys.* **1981**, *91*, 3624.
(208) Sanhueza, J. E.; Tapia, O. *J. Mol. Struct. (THEOCHEM)* **1982**, *6*, 131.
(209) Cioslowski, J. *Phys. Rev. A* **1987**, *36*, 374−376.
(210) Heimsoeth, B. *Int. J. Quantum Chem.* **1990**, *37*, 85.
(211) Amovilli, C.; Mennucci, B.; Floris, F. M. *J. Phys. Chem. B* **1998**, *102*, 3023.
(212) Cossi, M.; Barone, V.; Robb, M. A. *J. Chem. Phys.* **1999**, *111*, 5295.
(213) Aguilar, M. A.; Olivares Del Valle, F. J.; Tomasi, J. *J. Chem. Phys.* **1993**, *98*, 7375.
(214) Cammi, R.; Frediani, L.; Mennucci, B.; Tomasi, J.; Ruud, K.; Mikkelsen, K. V. *J. Chem. Phys.* **2002**, *117*, 13.
(215) Cammi, R.; Frediani, L.; Mennucci, B.; Ruud, K. *J. Chem. Phys.* **2003**, *119*, 5818.
(216) Bonaccorsi, R.; Cimiraglia, R.; Tomasi, J. *J. Comput. Chem.* **1983**, *4*, 567.
(217) Yomosa, S. *J. Phys. Soc. Jpn.* **1974**, *36*, 1655.
(218) Basilevsky, M. V.; Chudinov, G. E. *J. Mol. Struct. (THEOCHEM)* **1992**, *92*, 223.
(219) Houjou, H.; Sakurai, M.; Inoue, Y. *J. Chem. Phys.* **1997**, *107*, 5652.
(220) Karelson, M.; Zerner, M. C. *J. Phys. Chem.* **1992**, *96*, 6949.
(221) Klamt, A. *J. Phys. Chem.* **1996**, *100*, 3349.
(222) Mennucci, B.; Toniolo, A.; Cappelli, C. *J. Chem. Phys.* **1999**, *111*, 7197.
(223) Huron, B.; Malrieu, J.-P.; Rancurel, P. *J. Chem. Phys.* **1973**, *58*, 5745.
(224) Evangelisti, E.; Daudey, J.-P.; Malrieu, J.-P. *Chem. Phys.* **1983**, *75*, 91.
(225) Cimiraglia, R.; Persico, M. *J. Comput. Chem.* **1987**, *8*, 39.
(226) Olivares del Valle, F. J.; Tomasi, J. *Chem. Phys.* **1991**, *150*, 139.
(227) Aguilar, M. A.; Olivares del Valle, F. J.; Tomasi, J. *Chem. Phys.* **1991**, *150*, 151.
(228) Olivares del Valle, F. J.; Bonaccorsi, R.; Cammi, R.; Tomasi, J. *THEOCHEM* **1991**, *76*, 295.
(229) Olivares del Valle, F. J.; Aguilar, M. A. *J. Comput. Chem.* **1992**, *13*, 115.
(230) Olivares del Valle, F. J.; Aguilar, M. A.; Tolosa, S. *J. Mol. Struct. (THEOCHEM)* **1993**, *279*, 223.
(231) Olivares del Valle, F. J.; Aguilar, M. A. *J. Mol. Struct. (THEOCHEM)* **1993**, *280*, 25.
(232) Angyan, J. G. *Int. J. Quantum Chem.* **1993**, *47*, 469.
(233) Angyan, J. G. *Chem. Phys. Lett.* **1995**, *241*, 51.
(234) Cammi, R.; Mennucci, B.; Tomasi, J. *J. Phys. Chem. A* **1999**, *103*, 9100.
(235) Nielsen, C. B.; Mikkelsen, K. V.; Sauer, S. P. A. *J. Chem. Phys.* **2001**, *114*, 7753.
(236) Cammi, R.; Mennucci, B.; Pomelli, C.; Cappelli, C.; Corni, S.; Frediani, L.; Trucks, G. W.; Frisch, M. J. *Theor. Chem. Acc.* **2004**, *111*, 66.
(237) Warshel, A.; Weiss, R. M. *J. Am. Chem. Soc.* **1980**, *102*, 6218.
(238) Kim, H. J.; Hynes, J. T. *J. Chem. Phys.* **1990**, *93*, 5194.
(239) Kim, H. J.; Hynes, J. T. *J. Chem. Phys.* **1990**, *93*, 5211.
(240) Kim, H. J.; Hynes, J. T. *J. Chem. Phys.* **1992**, *96*, 5088.
(241) Song, L.; Wu, W.; Zhang, Q.; Shaik, S. *J. Phys. Chem. A* **2004**, *108*, 6017.
(242) Abraham, M. H. Quantitative treatment of solute/solvent interactions. In *Theoretical and Computational Chemistry Series*; Politzer, P., Murray, J. S., Eds.; Elsevier: Amsterdam, The Netherlands, 1994; Vol. 1.
(243) Uhlig, H. H. *J. Phys. Chem.* **1937**, *41*, 1215.
(244) Margulis, M. A. *High Energy Chem.* **2004**, *38*, 135.
(245) Yang, J. W.; Duan, J. M.; Fornasiero, D.; Ralston, J. *J. Phys. Chem. B* **2003**, *107*, 6139.
(246) Lee, B. *J. Chem. Phys.* **1985**, *83*, 2421.
(247) Straatsma, T. P.; Berendsen, H. J. C.; Postma, J. P. M. *J. Chem. Phys.* **1986**, *85*, 6720.
(248) Tanaka, H. *J. Chem. Phys.* **1987**, *86*, 1512.
(249) Pohorille, A.; Pratt, L. R. *J. Am. Chem. Soc.* **1990**, *112*, 5066.
(250) Pratt, L. R.; Pohorille, A. *Proc. Natl. Acad. Sci. U.S.A.* **1992**, *89*, 2995.
(251) Madan, B.; Lee, B. *Biophys. Chem.* **1994**, *51*, 279.
(252) Wolfenden, R.; Radzicka, A. *Science* **1994**, *265*, 936.
(253) Beutler, T. C.; Beguelin, D. R.; Vangunsteren, W. F. *J. Chem. Phys.* **1995**, *102*, 3787.
(254) Wallqvist, A.; Berne, B. J. *J. Phys. Chem.* **1995**, *99*, 2885.
(255) Prevost, M.; Oliveira, I. T.; Kocher, J. P.; Wodak, S. J. *J. Phys. Chem.* **1996**, *100*, 2738.
(256) Re, M.; Laria, D.; FernandezPrini, R. *Chem. Phys. Lett.* **1996**, *250*, 25.
(257) Crooks, G. E.; Chandler, D. *Phys. Rev. E* **1997**, *56*, 4217.
(258) Floris, F. M.; Selmi, M.; Tani, A.; Tomasi, J. *J. Chem. Phys.* **1997**, *107*, 6353.
(259) Ikeguchi, M.; Shimizu, S.; Nakamura, S.; Shimizu, K. *J. Phys. Chem. B* **1998**, *102*, 5891.
(260) Tomas-Oliveira, I.; Wodak, S. J. *J. Chem. Phys.* **1999**, *111*, 8576.
(261) Ashbaugh, H. S.; Garde, S.; Hummer, G.; Kaler, E. W.; Paulaitis, M. E. *Biophys. J.* **1999**, *77*, 645.
(262) Gallicchio, E.; Kubo, M. M.; Levy, R. M. *J. Phys. Chem. B* **2000**, *104*, 6271.
(263) In't Veld, P. J.; Stone, M. T.; Truskett, T. M.; Sanchez, I. C. *J. Phys. Chem. B* **2000**, *104*, 12028.
(264) Southall, N. T.; Dill, K. A. *J. Phys. Chem. B* **2000**, *104*, 1326.
(265) Pratt, L. R.; LaViolette, R. A.; Gomez, M. A.; Gentile, M. E. *J. Phys. Chem. B* **2001**, *105*, 11662.
(266) Huang, D. M.; Geissler, P. L.; Chandler, D. *J. Phys. Chem. B* **2001**, *105*, 6704.
(267) Garde, S.; Ashbaugh, H. S. *J. Chem. Phys.* **2001**, *115*, 977.
(268) Stone, M. T.; In't Veld, P. J.; Lu, Y.; Sanchez, I. C. *Mol. Phys.* **2002**, *100*, 2773.
(269) Hofinger, S.; Zerbetto, F. *Chem.-Eur. J.* **2003**, *9*, 566.
(270) Hofinger, S.; Zerbetto, F. *J. Phys. Chem. A* **2003**, *107*, 11253.
(271) Hofinger, S.; Zerbetto, F. *Theor. Chem. Acc.* **2004**, *112*, 240.
(272) Levy, R. M.; Gallicchio, E. *Annu. Rev. Phys. Chem.* **1998**, *49*, 531.
(273) Colominas, C.; Luque, F. J.; Teixido, J.; Orozco, M. *Chem. Phys.* **1999**, *240*, 253.
(274) Bonaccorsi, R.; Ghio, C.; Tomasi, J. The effect of the solvent on electronic transitions and other properties of molecular solutes. In *Current Aspects of Quantum Chemistry 1981*; Carbò, R., Ed.; Elsevier: Amsterdam, The Netherlands, 1982.
(275) Reiss, H.; Frisch, H. L.; Lebowitz, J. L. *J. Chem. Phys.* **1959**, *31*, 369.
(276) Reiss, H.; Frisch, H. L.; Helfand, E.; Lebowitz, J. L. *J. Chem. Phys.* **1960**, *32*, 119.
(277) Pierotti, R. A. *J. Phys. Chem.* **1963**, *67*, 1840.
(278) Pierotti, R. A. *J. Phys. Chem.* **1965**, *69*, 281.
(279) Pierotti, R. A. *Chem. Rev.* **1976**, *76*, 712.
(280) Miertus, S.; Tomasi, J. *Chem. Phys.* **1982**, *65*, 239.

(281) Tang, K. E. S.; Bloomfield, V. A. *Biophys. J.* **2000**, *79*, 2222.
(282) Ben-Amotz, D.; Herschbach, D. R. *J. Phys. Chem.* **1990**, *94*, 1038.
(283) Cole, R. H. *J. Chem. Phys.* **1957**, *27*, 33.
(284) Mayer, S. W. *J. Phys. Chem.* **1963**, *67*, 2160.
(285) Wilhelm, E.; Battino, R. *J. Chem. Phys.* **1971**, *55*, 4012.
(286) Salsburg, Z. W.; Kirkwood, J. G. *J. Chem. Phys.* **1953**, *21*, 2169.
(287) Boublik, T. *J. Chem. Phys.* **1970**, *53*, 471.
(288) Mansoori, G. A.; Carnahan, N. F.; Starling, K. E.; Leland, T. W., Jr. *J. Chem. Phys.* **1971**, *54*, 1523.
(289) Carnahan, N. F.; Starling, K. E. *J. Chem. Phys.* **1969**, *51*, 635.
(290) Matyushov, D. V.; Schmid, R. *J. Chem. Phys.* **1996**, *104*, 8627.
(291) Ben-Amotz, D.; Willis, K. G. *J. Phys. Chem.* **1993**, *97*, 7736.
(292) Marcus, Y. *Ion Solvation*; Wiley: Chichester, U.K., 1985.
(293) Marcus, Y. *Ion Properties*; Dekker: New York, 1997.
(294) Lucas, M. *J. Phys. Chem.* **1976**, *80*, 359.
(295) Cabani, S. *Advances in Solution Chemistry*; Bertini, I., Lunazzi, L., Eds.; Plenum: New York, 1981.
(296) Morel-Desrosiers, N.; Morel, J.-P. *Can. J. Chem.* **1981**, *59*, 1.
(297) Irisa, M.; Nagayama, K.; Hirata, F. *Chem. Phys. Lett.* **1993**, *207*, 430.
(298) Langlet, J.; Claverie, P.; Caillet, J.; Pullman, A. *J. Phys. Chem.* **1988**, *92*, 1617.
(299) Huang, D. M.; Chandler, D. *J. Phys. Chem. B* **2002**, *106*, 2047.
(300) Gibbons, W. M. *Mol. Phys.* **1969**, *17*, 81.
(301) Cotter, M. A.; Martire, D. E. *J. Chem. Phys.* **1970**, *52*, 1902.
(302) Cotter, M. A.; Martire, D. E. *J. Chem. Phys.* **1970**, *52*, 1909.
(303) Lasher, G. *J. Chem. Phys.* **1970**, *53*, 4141.
(304) Boublik, T. *Mol. Phys.* **1976**, *32*, 732.
(305) Boublik, T. *Mol. Phys.* **1988**, *63*, 685.
(306) Mennucci, B.; Cossi, M.; Tomasi, J. *J. Phys. Chem.* **1996**, *100*, 1807.
(307) Hummer, G.; Garde, S.; Garcia, A. E.; Pohorille, A.; Pratt, L. R. *Proc. Natl. Acad. Sci. U.S.A.* **1996**, *93*, 8951.
(308) Hummer, G.; Garde, S.; Garcia, A. E.; Paulaitis, M. E.; Pratt, L. R. *J. Phys. Chem. B* **1998**, *102*, 10469.
(309) Pratt, L. R. *Annu. Rev. Phys. Chem.* **2002**, *53*, 409.
(310) Alexandrovsky, V. V.; Basilevsky, M. V.; Leontyev, I. V.; Mazo, M. A.; Sulimov, V. B. *J. Phys. Chem. B* **2004**, *108*, 15830.
(311) Basilevsky, M. V.; Grigoriev, F. V.; Leontyev, I. V.; Sulimov, V. B. *J. Phys. Chem. B* **2005**, in press.
(312) Tolman, R. C. *J. Chem. Phys.* **1948**, *16*, 758.
(313) Kirkwood, J. G.; Buff, F. P. *J. Chem. Phys.* **1949**, *17*, 338.
(314) Sinanoglu, O. *Chem. Phys. Lett.* **1967**, *1*, 340.
(315) Sinanoglu, O. *Theor. Chim. Acta* **1974**, *33*, 279.
(316) Sinanoglu, O. *J. Chem. Phys.* **1981**, *75*, 463.
(317) Sinanoglu, O. Molecular interactions within liquids—the solvophobic force and molecular surface areas. In *Molecular Interactions*; Orville-Thomas, W. J., Ratajczak, H., Eds.; Wiley: New York, 1982; Vol. III.
(318) Tunon, I.; Silla, E.; Pascual-Ahuir, J. L. *Chem. Phys. Lett.* **1993**, *203*, 289.
(319) Tortonda, F. R.; Pascual Ahuir, J. L.; Silla, E.; Tunon, I. *J. Phys. Chem.* **1995**, *99*, 12525.
(320) Tunon, I.; Ruiz Lopez, M. F.; Rinaldi, D.; Bertran, J. *J. Comput. Chem.* **1996**, *17*, 148.
(321) Pitarch, J.; Moliner, V.; Pascual-Ahuir, J. L.; Silla, E.; Tunon, I. *J. Phys. Chem.* **1996**, *100*, 9955.
(322) Luque, F. J.; Bachs, M.; Aleman, C.; Orozco, M. *J. Comput. Chem.* **1996**, *17*, 806.
(323) Floris, F. M.; Tani, A.; Tomasi, J. *Chem. Phys.* **1993**, *169*, 11.
(324) Amovilli, C.; Mennucci, B. *J. Phys. Chem. B* **1997**, *101*, 1051.
(325) Amovilli, C.; McWeeny, R. *Chem. Phys.* **1990**, *140*, 243.
(326) Floris, F. M.; Tomasi, J.; Pascual-Ahuir, J. L. *J. Comput. Chem.* **1991**, *12*, 784.
(327) Linder, B. *Adv. Chem. Phys.7* **1967**, *12*, 225.
(328) Hunt, K. L. C. *J. Chem. Phys.* **1990**, *92*, 1180.
(329) Li, X.; Hunt, K. L. C. *J. Chem. Phys.* **1996**, *105*, 4076.
(330) Hunt, K. L. C. *J. Chem. Phys.* **2002**, *116*, 5440.
(331) Jenkins, O. S.; Hunt, K. L. C. *J. Chem. Phys.* **2003**, *119*, 8250.
(332) Feynman, R. P. *Phys. Rev.* **1939**, *56*, 340.
(333) Hirschfelder, J. O.; Eliason, M. A. *J. Chem. Phys.* **1967**, *47*, 1164.
(334) Amovilli, C. *Chem. Phys. Lett.* **1994**, *229*, 244.
(335) Pertsin, A. J.; Kitaigorodsky, A. I. *The Atom-Atom Potential Method*; Springer-Verlag: Berlin, Germany, 1986.
(336) Tomasi, J. *Theor. Chem. Acc.* **2004**, *112*, 184.
(337) Gogonea, V.; Merz, K. M. *J. Chem. Phys.* **2000**, *112*, 3227.
(338) Gogonea, V.; Merz, K. M. *J. Phys. Chem. B* **2000**, *104*, 2117.
(339) Jalbout, A. F.; Adamowicz, L. *J. Phys. Chem. A* **2001**, *105*, 1033.
(340) Jordan, K. D.; Wang, F. *Annu. Rev. Phys. Chem.* **2003**, *54*, 367.
(341) Tomasi, J.; Mennucci, B.; Cammi, R. MEP: a tool for interpretation and prediction. From molecular structure to solvation effects. In *Molecular Electrostatic Potentials. Concepts and Applications*; Murray, J. S., Sen, K., Eds.; Elsevier: Amsterdam, The Metherlands, 1996.
(342) Olivares del Valle, F. J.; Aguilar, M. A.; Contador, J. C. *Chem. Phys.* **1993**, *170*, 161.
(343) Nanu, D. E.; Mennucci, B.; de Loos, T. W. *Fluid Phase Equilib.* **2004**, *221*, 127.
(344) Bachs, M.; Luque, F. J.; Orozco, M. *J. Comput. Chem.* **1994**, *15*, 446.
(345) Curutchet, C.; Orozco, M.; Luque, F. J. *J. Comput. Chem.* **2001**, *22*, 1180.
(346) Luque, F. J.; Zhang, Y.; Aleman, C.; Bachs, M.; Gao, J.; Orozco, M. *J. Phys. Chem.* **1996**, *100*, 4269.
(347) Orozco, M.; Luque, F. J. *Chem. Phys.* **1994**, *182*, 237.
(348) Curutchet, C.; Bidon-Chanal, B.; Soteras, I.; Orozco, M.; Luque, F. J. *Chem. Phys. Lett.* **2004**, *384*, 299.
(349) Barone, V.; Cossi, M.; Tomasi, J. *J. Chem. Phys.* **1997**, *107*, 3210.
(350) Camaioni, D. M.; Dupuis, D.; Bentley, J. *J. Phys. Chem. A* **2003**, *107*, 5778.
(351) Marcus, R. A. E. H. *Annu. Rev. Phys. Chem.* **1964**, *15*, 155.
(352) Hynes, J. T. *Annu. Rev. Phys. Chem.* **1985**, *36*, 573.
(353) Tomasi, J.; Mennucci, B.; Cammi, R.; Cossi, M. Quantum mechanical models for reactions in solution. In *Computational Approaches to Biochemical Reactivity*; Naray-Szabo, G., Warshel, A., Eds.; Kluwer Academic Publishers: Dordrecht, The Netherlands, 1997; Vol. 19.
(354) Ruiz-Lopez, M. F.; Oliva, A.; Tunon, I.; Bertran, J. *J. Phys. Chem. A* **1998**, *102*, 10728.
(355) Soudackov, A.; Hammes-Schiffer, S. *J. Chem. Phys.* **1999**, *111*, 4672.
(356) Warshel, A.; Bentzien, J. *ACS Symp. Ser.* **1999**, *No. 721*, 489.
(357) Schenter, G. K.; Garrett, B. C.; Truhlar, D. G. *J. Phys. Chem. B* **2001**, *105*, 9672.
(358) Ben-Naim, A. *Solvation Thermodynamics*; Plenum Press: New York, 1987.
(359) Ben-Naim, A. *Statistical Thermodynamics for Chemists and Biochemists*; Plenum Press: New York, 1992.
(360) Fuller Brown, W. *Handb. Phys.* **1956**, *17*.
(361) Debye, P. *Z. Phys.* **1912**, *13*, 97.
(362) Debye, P. *Handb. Radiol.* **1926**, *6*, 619.
(363) Lorentz, H. A. *The Theory of Electrons*; Teubner: Leipzig, Germany, 1909.
(364) Webb, T. J. *J. Am. Chem. Soc.* **1926**, *48*, 2589.
(365) Sack, V. H. *Phys. Z.* **1926**, *27*, 206.
(366) Sack, V. H. *Phys. Z.* **1927**, *28*, 199.
(367) Ingold, C. K. *J. Chem. Soc.* **1931**, 2179.
(368) Frölich, H. *Trans. Faraday Soc.* **1948**, *44*, 238.
(369) Booth, F. *J. Chem. Phys.* **1951**, *19*, 391.
(370) Buckingham, A. D. *J. Chem. Phys.* **1956**, *25*, 428.
(371) Harris, F. E.; Alder, B. J. *J. Chem. Phys.* **1953**, *21*, 1031.
(372) Dogonadze, R. R.; Kornyshev, A. A. *J. Chem. Soc., Faraday Trans. 2* **1974**, *70*, 1121.
(373) Dogonadze, R. R.; Kalman, E.; Kornyshev, A. A.; Ulstrup, J. *The Chemical Physics of Solvation, Part A*; Elsevier: Amsterdam, The Netherlands, 1985.
(374) Bopp, P. A.; Kornyshev, A. A.; Sutmann, G. *Phys. Rev. Lett.* **1996**, *76*, 1280.
(375) Kornyshev, A. A.; Sutmann, G. *Phys. Rev. Lett.* **1997**, *79*, 3435.
(376) Kornyshev, A. A.; Sutmann, G. *J. Mol. Liq.* **1999**, *82*, 151.
(377) Basilevsky, M. V.; Parsons, D. F. *J. Chem. Phys.* **1996**, *105*, 3734.
(378) Basilevsky, M. V.; Parsons, D. F. *J. Chem. Phys.* **1998**, *108*, 9107.
(379) Basilevsky, M. V.; Parsons, D. F. *J. Chem. Phys.* **1998**, *108*, 9114.
(380) Voet, A. *Trans. Faraday Soc.* **1936**, *2*, 1301.
(381) Latimer, W. M.; Pitzer, K. S.; Slansky, C. L. *J. Chem. Phys.* **1939**, *7*, 108.
(382) Hush, N. *Aust. J. Sci. Res.* **1948**, *1*, 1948.
(383) Grahame, D. C. *J. Chem. Phys.* **1950**, *18*, 903.
(384) Powell, R. E.; Latimer, W. M. *J. Chem. Phys.* **1951**, *19*, 1139.
(385) Debye, P. *Polar Molecules*; Dover: New York, 1929.
(386) Ritson, D. Y.; Harted, J. B. *J. Chem. Phys.* **1948**, *16*, 11.
(387) Haggins, G. H.; Hasted, J. B.; Buchanan, J. T. B. *J. Chem. Phys.* **1952**, *20*, 1452.
(388) Tanford, C.; Kirkwood, J. G. *J. Am. Chem. Soc.* **1957**, *79*, 5333.
(389) Millen, W. A.; Watts, D. W. *J. Am. Chem. Soc.* **1967**, *89*, 6051.
(390) Muirhead-Gould, J. S. L.; K. J. *Trans. Faraday Soc.* **1967**, *63*, 944.
(391) Block, H.; Walker, S. M. *Chem. Phys. Lett.* **1973**, *19*, 363.
(392) Franks, F. *Water. A Comprehensive Treatise*; Plenum: New York, 1976.
(393) Stiles, P. J. *Aust. J. Chem.* **1980**, *33*, 1389.
(394) Bucher, M.; Porter, T. L. *J. Phys. Chem.* **1986**, *90*, 3406.
(395) Lavery, R.; Sklenar, H.; Zakrzewska, K.; Pullman, B. *J. Biomol. Struct. Dyn.* **1986**, *3*, 989.
(396) Abe, T. *J. Phys. Chem.* **1986**, *90*, 713.
(397) Hyun, J.-K.; Babu, C. S.; Ichiye, T. *J. Phys. Chem.* **1995**, *99*, 5187.
(398) Sandberg, L.; Edholm, O. *J. Chem. Phys.* **2002**, *116*, 2936.
(399) Ehrenson, S. *J. Comput. Chem.* **1981**, *2*, 41.
(400) Ehrenson, S. *J. Comput. Chem.* **1984**, *5*, 56.
(401) Ehrenson, S. *J. Comput. Chem.* **1986**, *7*, 648.
(402) Oster, G. *J. Am. Chem. Soc.* **1944**, *66*, 948.
(403) Beveridge, D. L.; Schnuelle, G. W. *J. Phys. Chem.* **1975**, *79*, 2562.
(404) Abraham, M. H.; Liszi, J.; Meszaros, L. *J. Chem. Phys.* **1979**, *70*, 2491.
(405) Abraham, M. H.; Liszi, J. *J. Chem. Soc., Faraday 1* **1978**, *74*, 1604.

(406) Abraham, M. H.; Liszi, J. *J. Chem. Soc., Faraday 1* **1978**, *74*, 2858.
(407) Abraham, M. H.; Liszi, J. *J. Chem. Soc., Faraday 1* **1980**, *76*, 1219.
(408) Abraham, M. H.; Liszi, J.; Papp, E. *J. Chem. Soc., Faraday 1* **1982**, *78*, 197.
(409) Abraham, M. H.; Liszi, J.; Kristóf, E. *Aust. J. Chem.* **1982**, *35*, 1273.
(410) Abraham, M. H.; Matteoli, E.; Liszi, J. *J. Chem. Soc., Faraday 1* **1983**, *79*, 2781.
(411) Basilevsky, M. V.; Soudackov, A. V.; Voronin, A. I. *Chem. Phys.* **1998**, *235*, 281.
(412) Basilevsky, M. V.; Rostov, I. V.; Newton, M. D. *Chem. Phys.* **1998**, *232*, 189.
(413) Leontyev, I. V.; Basilevsky, M. V.; Newton, M. D. *Theor. Chem. Acc.* **2004**, *111*, 110.
(414) Buckingham, A. D. *Discuss. Faraday Soc.* **1957**, *21*, 151.
(415) Frank, H. S.; Wen, W. Y. *Discuss. Faraday Soc.* **1957**, *24*, 133.
(416) Goldman, S.; Bates, R. G. *J. Am. Chem. Soc.* **1972**, *94*, 1476
(417) Tremaine, P. R.; Goldman, S. *J. Phys. Chem.* **1978**, *82*, 2317.
(418) Pitzer, K. S. *J. Phys. Chem.* **1983**, *87*, 1120.
(419) Tanger, J. C.; Pitzer, K. S. *J. Phys. Chem.* **1989**, *93*, 4941.
(420) Floris, F.; Persico, M.; Tani, A.; Tomasi, J. *Chem. Phys. Lett.* **1992**, *199*, 518.
(421) Floris, F. M.; Persico, M.; Tani, A.; Tomasi, J. *Chem. Phys. Lett.* **1994**, *227*, 126.
(422) Floris, F.; Persico, M.; Tani, A.; Tomasi, J. *Chem. Phys.* **1995**, *195*, 207.
(423) Floris, F. M.; Martinez, J. M.; Tomasi, J. *J. Chem. Phys.* **2002**, *116*, 5448.
(424) Floris, F. M.; Martinez, J. M.; Tomasi, J. *J. Chem. Phys.* **2002**, *116*, 5460.
(425) Chillemi, G.; Barone, V.; D'Angelo, P.; Mancini, G.; Persson, I.; Sanna, N. *J. Phys. Chem. B* **2005**, *109*, 9186.
(426) Jensen, J. H.; Day, P. N.; Gordon, M. S.; Basch, H.; Cohen, D.; Garmer, D. R.; Kraus, M.; Stevens, W. J. Effective fragment method for modeling intermolecular hydrogen-bonding effects on quantum-mechanical calculations. In *Modeling the Hydrogen Bond*; ACS Symposium Series 569; American Chemical Society: Washington, DC, 1994.
(427) Merrill, G. N.; Webb, S. P. *J. Phys. Chem. A* **2003**, *107*, 7852.
(428) Merrill, G. N.; Webb, S. P.; Bivin, D. B. *J. Phys. Chem. A* **2003**, *107*, 386.
(429) Lee, S.; Kim, J.; Park, J. K.; Kim, K. S. *J. Phys. Chem.* **1996**, *100*, 14329.
(430) Katz, A. K.; Bock, C. W.; Glusker, J. P. *J. Am. Chem. Soc.* **1996**, *118*, 5752.
(431) Pavlov, M.; Siegbahn, P. E. M.; Sandström, M. *J. Phys. Chem. A* **1998**, *102*, 219.
(432) Pye, C. C.; Rudolph, W. W. *J. Phys. Chem. A* **1998**, *102*, 9933.
(433) Rudolph, W. W.; Mason, R.; Pye, C. C. *Phys. Chem. Chem. Phys.* **2000**, *2*, 5030.
(434) Richens, D. T. *The Chemistry of Aqua Ions*; Wiley: Chichester, U.K., 1997.
(435) Tunon, I.; Rinaldi, D.; Ruiz-Lopez, M. F.; Rivail, J. L. *J. Phys. Chem.* **1995**, *99*, 3798.
(436) Martinez, J. M.; Pappalardo, R. R.; Sanchez Marcos, E.; Mennucci, B.; Tomasi, J. *J. Phys. Chem. B* **2002**, *106*, 1118.
(437) Sandberg, L.; Casemyr, R.; Edholm, O. *J. Phys. Chem. B* **2002**, *106*, 7889.
(438) Sandberg, L.; Edholm, O. *J. Chem. Phys.* **2002**, *116*, 2936.
(439) Jorgensen, W. L.; Maxwell, D. S.; TiradoRives, J. *J. Am. Chem. Soc.* **1996**, *118*, 11225.
(440) Rizzo, R. C.; Jorgensen, W. L. *J. Am. Chem. Soc.* **1999**, *121*, 4827.
(441) Sandberg, L.; Edholm, O. *J. Phys. Chem. B* **2001**, *105*, 273.
(442) Berendsen, H. J. C.; van der Spoel, D.; van Drunen, R. *Comput. Phys. Commun.* **1995**, *91*, 43.
(443) Gilson, M. K.; Rashin, A.; Fine, R.; Honig, B. *J. Mol. Biol.* **1985**, *183*, 503.
(444) Harvey, S. C. *Proteins* **1989**, *5*, 78.
(445) Antosiewicz, J.; McCammon, J. A.; Gilson, M. K. *J. Mol. Biol.* **1994**, *238*, 415.
(446) Schutz, C. N.; Warshel, A. *Proteins* **2001**, *44*, 400.
(447) Bjerrum, N. Z. *Phys. Chem. Stoechiom. Verwandschaftsl* **1923**, *106*, 219.
(448) Kirkwood, J. G.; Westheimer, F. H. *J. Chem. Phys.* **1938**, *6*, 506.
(449) Simonson, T.; Perahia, D. *Comput. Phys. Commun.* **1995**, *91*, 291.
(450) Simonson, T.; Brooks, C. L. *J. Am. Chem. Soc.* **1996**, *118*, 8452.
(451) Lamm, G.; Pack, G. R. *J. Phys. Chem. B* **1997**, *101*, 959.
(452) Voges, D.; Karshikoff, A. *J. Chem. Phys.* **1998**, *108*, 2219.
(453) Jayaram, B.; Liu, Y.; Beveridge, D. L. *J. Chem. Phys.* **1998**, *109*, 1465.
(454) Liu, Y.; Ichiye, T. *Biophys. Chem.* **1999**, *78*, 97.
(455) Roux, B.; Simonson, T. *Biophys. Chem.* **1999**, *78*, 1.
(456) Mallik, B.; Masunov, A.; Lazaridis, T. *J. Comput. Chem.* **2002**, *23*, 1090.
(457) Takahashi, T.; Sugiura, J.; Nagayama, K. *J. Chem. Phys.* **2002**, *116*, 8232.
(458) Vasilyev, V. *J. Comput. Chem.* **2002**, *23*, 1254.
(459) Haberthur, U.; Majeux, N.; Werner, P.; Caflisch, A. *J. Comput. Chem.* **2003**, *24*, 1936.
(460) Kundu, S.; Gupta-Bhaya, P. *J. Mol. Struct. (THEOCHEM)* **2003**, *639*, 21.
(461) Simonson, T. *Rep. Prog. Phys.* **2003**, *66*, 737.
(462) Patel, S.; Mackerell, A. D.; Brooks, C. L. *J. Comput. Chem.* **2004**, *25*, 1504.
(463) Warshel, A. R., S. T.; Churg, A. K. *Proc. Natl. Acad. Sci. U.S.A.* **1984**, *81*, 4785.
(464) Mehler, E. L.; Eichele, G. *Biochemistry* **1984**, *23*, 3887.
(465) Mehler, E. L. *J. Phys. Chem.* **1996**, *100*, 16006.
(466) Hingerty, B. E.; Ritchie, R. H.; Ferrel, T. L.; Turner, J. E. *Biopolymers* **1985**, *24*, 427.
(467) Ramstein, J.; Lavery, R. *Proc. Natl. Acad. Sci. U.S.A.* **1988**, *85*, 7231.
(468) Guarnieri, F.; Schmidt, A. B.; Mehler, E. L. *Int. J. Quantum Chem.* **1998**, *69*, 57.
(469) Sandberg, L.; Edholm, O. *Proteins* **1999**, *36*, 474.
(470) Hassan, S. A.; Guarnieri, F.; Mehler, E. L. *J. Phys. Chem. B* **2000**, *104*, 6478.
(471) Bucher, M.; Porter, T. L. *J. Phys. Chem.* **1986**, *90*, 3406.
(472) Ehrenson, S. *J. Comput. Chem.* **1989**, *10*, 77.
(473) Mehler, E. L. The Lorenz–Debye–Sack theory and dielectric screening electrostatic effects in proteins and nucleic acids. In *Molecular Electrostatic Potentials; Concepts and Applications*; Murray, J. S., Sen, K., Eds.; Elsevier: Amsterdam, The Netherlands, 1996.
(474) Gelwart, W. M.; Ben-Shaul, A. *J. Phys. Chem.* **1996**, *100*, 13169.
(475) Hoshi, H.; Sakurai, M.; Inoue, Y.; Chujo, R. *J. Chem. Phys.* **1987**, *87*, 1107.
(476) Hoshi, H.; Sakurai, M.; Inoue, Y.; Chujo, R. *J. Mol. Struct. (THEOCHEM)* **1988**, *180*, 267.
(477) Furuki, T.; Umeda, A.; Sakurai, M.; Inoue, Y.; Chujo, R.; Harata, K. *J. Comput. Chem.* **1994**, *15*, 90.
(478) Houjou, H.; Inoue, Y.; Sakurai, M. *J. Am. Chem. Soc.,* **1998**, *120*, 4459.
(479) Furuki, T.; Hosokawa, F.; Sakurai, M.; Inoue, Y.; Chujo, R. *J. Am. Chem. Soc.* **1993**, *115*, 2903.
(480) Furuki, T.; Sakurai, M.; Inoue, Y. *J. Phys. Chem.* **1995**, *99*, 12047.
(481) Sakurai, M.; Furuki, T.; Inoue, Y. *J. Phys. Chem.* **1995**, *99*, 17789.
(482) Sakurai, M.; Tamagawa, H.; Inoue, Y.; Ariga, K.; Kunitake, T. *J. Phys. Chem. B* **1997**, *101*, 4810.
(483) Tamagawa, H.; Sakurai, M.; Inoue, Y.; Ariga, K.; Kunitake, T. *J. Phys. Chem. B* **1997**, *101*, 4817.
(484) Houjou, H.; Inoue, Y.; Sakurai, M. *J. Phys. Chem. B* **2001**, *105*, 867.
(485) Sakurai, M.; Sakata, K.; Saito, S.; Nakajima, S.; Inoue, Y. *J. Am. Chem. Soc.* **2003**, *125*, 3108.
(486) Bonaccorsi, R.; Scrocco, E.; Tomasi, J. *Int. J. Quantum Chem.* **1986**, *29*, 717.
(487) Bonaccorsi, R.; Hodoscek, M.; Tomasi, J. *THEOCHEM* **1988**, *41*, 105.
(488) Bonaccorsi, R.; Ojalvo, E.; Tomasi, J. *Collect. Czech. Chem. Commun.* **1988**, *53*, 2320.
(489) Bonaccorsi, R.; Floris, F.; Palla, P.; Tomasi, J. *Thermochim. Acta* **1990**, *162*, 213.
(490) Bonaccorsi, R.; Ojalvo, E.; Palla, P.; Tomasi, J. *Chem. Phys.* **1990**, *143*, 245.
(491) Frediani, L.; Pomelli, C. S.; Tomasi, J. *Phys. Chem. Chem. Phys.* **2000**, *2*, 4876.
(492) Frediani, L.; Mennucci, B.; Cammi, R. *J. Phys. Chem. B* **2004**, *108*, 13796.
(493) Benjamin, I. *Chem. Phys. Lett.* **1998**, *287*, 480.
(494) Benjamin, I. *Chem. Rev.* **1996**, *96*, 1449.
(495) Benjamin, I.; Kharkats, Y. I. *Electrochim. Acta* **1998**, *44*, 133.
(496) Michael, D.; Benjamin, I. *J. Electroanal. Chem.* **1998**, *450*, 335.
(497) Vieceli, J. C.; Benjamin, I. *J. Chem. Phys.* **2002**, *117*, 4532.
(498) Benjamin, I. *Chem. Phys. Lett.* **2004**, *393*, 453.
(499) Vieceli, J.; Benjamin, I. *Chem. Phys. Lett.* **2004**, *385*, 79.
(500) King, G.; Lee, F. S.; Warshel, A. *J. Chem. Phys.* **1991**, *95*, 4366.
(501) Simonson, T.; Perahia, D. *Proc. Natl. Acad. Sci. U.S.A.* **1995**, *92*, 1082.
(502) Zhou, F.; Schulten, K. *J. Phys. Chem.* **1995**, *99*, 2194
(503) Stern, H. A.; Feller, S. E. *J. Chem. Phys.* **2003**, *118*, 3401.
(504) Corni, S.; Tomasi, J. *Chem. Phys. Lett.* **2001**, *342*, 135.
(505) Corni, S.; Cappelli, C.; Cammi, R.; Tomasi, J. *J. Phys. Chem. A* **2001**, *105*, 8310.
(506) Corni, S.; Tomasi, J. *J. Chem. Phys.* **2002**, *117*, 7266.
(507) Corni, S.; Tomasi, J. *J. Chem. Phys.* **2002**, *116*, 1156.
(508) Corni, S.; Tomasi, J. *J. Chem. Phys.* **2003**, *118*, 6481.
(509) Andreussi, O.; Corni, S.; Mennucci, B.; Tomasi, J. *J. Chem. Phys.* **2004**, *121*, 10190.
(510) Ashcroft, N. W.; Mermin, N. D. *Solid State Physics*; Saunders College Publishing: Fort Worth, TX, 1976.

(511) Lundqvist, S. In *Theory of the Inhomogeneous Electron Gas*; Lundqvist, S., March, N. H., Eds.; Plenum Press: New York, 1983.
(512) Lindhard, J. *K. Danske Vidensk. Selsk. Mat.-Fys. Medd.* **1954**, *28*.
(513) Kliewer, K. L.; Fuchs, R. *Phys. Rev.* **1969**, *181*, 552.
(514) Rahman, T. S.; Maradudin, A. A. *Phys. Rev. B* **1980**, *21*, 504.
(515) Jorgensen, S.; Ratner, M. A.; Mikkelsen, K. V. *J. Chem. Phys.* **2001**, *115*, 3792.
(516) Jorgensen, S.; Ratner, M. A.; Mikkelsen, K. V. *J. Chem. Phys.* **2002**, *116*, 10902.
(517) Jorgensen, S.; Ratner, M. A.; Mikkelsen, K. V. *Chem. Phys.* **2002**, *278*, 53.
(518) Bottcher, C. J. F.; Bordewijk, P. *Theory of Electric Polarization*, 2nd ed.; Elsevier: Amsterdam, The Netherlands, 1978.
(519) Landau, L. D.; Lifshitz, E. M. *Electrodynamics of Continuous Media*; Butterworth-Heinemann: Boston, MA, 1999.
(520) Georgievskii, Y.; Hsu, C.-P.; Marcus, R. A. *J. Chem. Phys.* **1999**, *110*, 5307.
(521) Marcus, R. A. *J. Chem. Phys.* **1956**, *24*, 966.
(522) Cammi, R.; Tomasi, J. *Int. J. Quantum Chem. Symp.* **1995**, *29*, 465.
(523) Jortner, J. *Mol. Phys.* **1962**, *5*, 257.
(524) Basilevsky, M. V.; Chudinov, G. E. *Chem. Phys.* **1991**, *157*, 345.
(525) Cossi, M.; Barone, V. *J. Phys. Chem. A* **2000**, *104*, 10614.
(526) Aguilar, M. A. *J. Phys. Chem. A* **2001**, *105*, 10393.
(527) Cammi, R.; Mennucci, B. *J. Chem. Phys.* **1999**, *110*, 9877.
(528) Cossi, M.; Barone, V. *J. Chem. Phys.* **2001**, *115*, 4708.
(529) Caricato, M.; Mennucci, B.; Tomasi, J. *J. Phys. Chem. A* **2004**, *108*, 6248.
(530) Cammi, R.; Corni, S.; Mennucci, B.; Tomasi, J. *J. Chem. Phys.* **2005**, *122*, 104513.
(531) Chandler, D.; Schweizer, K. S.; Wolynes, P. G. *Phys. Rev. Lett.* **1982**, *49*.
(532) Chen, Y.-C.; Lebowitz, J. L.; Nielaba, P. *J. Chem. Phys.* **1989**, *91*, 340.
(533) Wolynes, P. G. *J. Chem. Phys.* **1987**, *86*, 5133.
(534) Nichols, I. A. L.; Calef, D. F. *J. Chem. Phys.* **1988**, *89*, 3783.
(535) Rips, I.; Klafter, J.; Jortner, J. *J. Chem. Phys.* **1988**, *89*, 4288.
(536) Bagchi, B.; Chandra, A. *J. Chem. Phys.* **1989**, *90*, 7338.
(537) Fried, L. E.; Mukamel, S. *J. Chem. Phys.* **1990**, *93*, 932.
(538) Raineri, F. O.; Zhou, Y. Q.; Friedman, H. L. *Chem. Phys.* **1991**, *152*, 201.
(539) Raineri, F. O.; Resat, H.; Perng, B. C.; Hirata, F.; Friedman, H. L. *J. Chem. Phys.* **1994**, *100*, 1477.
(540) Biswas, R.; Bagchi, B. *J. Phys. Chem.* **1996**, *100*, 4261.
(541) Hsu, C. P.; Song, X. Y.; Marcus, R. A. *J. Phys. Chem. B* **1997**, *101*, 2546.
(542) Song, X. Y.; Chandler, D. *J. Chem. Phys.* **1998**, *108*, 2594.
(543) Song, X. Y.; Chandler, D.; Marcus, R. A. *J. Phys. Chem.* **1996**, *100*, 11954.
(544) Ingrosso, F.; Mennucci, B.; Tomasi, J. *J. Mol. Liq.* **2003**, *108*, 21.
(545) Caricato, M.; Ingrosso, F.; Mennucci, B.; Tomasi, J. *J. Chem. Phys.* **2005**, *122*, 154501.
(546) Mennucci, B. *Theor. Chem. Acc.* **2005**, submitted for publication.
(547) Parsons, D. F.; Vener, M. V.; Basilevsky, M. V. *J. Phys. Chem. A* **1999**, *103*, 1171.
(548) Berg, M. *Chem. Phys. Lett.* **1994**, *228*, 317.
(549) Fourkas, J. T.; Benigno, A.; Berg, M. *J. Chem. Phys.* **1993**, *99*, 8552.
(550) Fourkas, J. T.; Berg, M. *J. Chem. Phys.* **1993**, *98*, 7773.
(551) Gardecki, J.; Horng, M. L.; Papazyan, A.; Maroncelli, M. *J. Mol. Liq.* **1995**, *65−6*, 49.
(552) Reynolds, L.; Gardecki, J. A.; Frankland, S. J. V.; Horng, M. L.; Maroncelli, M. *J. Phys. Chem.* **1996**, *100*, 10337.
(553) Berg, M. A.; Hubble, H. W. *Chem. Phys.* **1998**, *233*, 257.
(554) Berg, M. A. *J. Chem. Phys.* **1999**, *110*, 8577.
(555) Fleming, G. R.; Cho, M. *Annu. Rev. Phys. Chem.* **1996**, *47*, 109.
(556) Yan, Y. J.; Mukamel, S. *J. Chem. Phys.* **1988**, *89*, 5160.
(557) Mukamel, S. *Principles of Nonlinear Optical Spectroscopy*; Oxford University Press: New York, 1995.
(558) Li, B. L.; Johnson, A. E.; Mukamel, S.; Myers, A. B. *J. Am. Chem. Soc.* **1994**, *116*, 11039.
(559) Kelley, A. M. *J. Phys. Chem. A* **1999**, *103*, 6891.
(560) Marcus, R. A. *J. Chem. Phys.* **1965**, *43*, 679.
(561) Hush, N. *Prog. Inorg. Chem.* **1967**, *8*, 391.
(562) Marcus, R. A. *J. Phys. Chem.* **1989**, *93*, 3078.
(563) Marcus, R. A. *Rev. Mod. Phys.* **1993**, *65*, 599.
(564) Newton, M. D. *Adv. Chem. Phys.* **1999**, *106*, 303.
(565) Liu, Y.-P.; Newton, M. D. *J. Phys. Chem.* **1995**, *99*, 9.
(566) Bursulaya, B. D.; Zichi, D. A.; Kim, H. J. *J. Phys. Chem.* **1995**, *99*, 10069.
(567) Kim, H. J. *J. Chem. Phys.* **1996**, *105*, 6818.
(568) Schmitt, U. W.; Voth, G. A. *J. Phys. Chem. B* **1998**, *102*, 5547.
(569) Matyushov, D. V.; Voth, G. A. *J. Phys. Chem. A* **1999**, *103*, 10981.
(570) Matyushov, D. V.; Voth, G. A. *J. Phys. Chem. A* **2000**, *104*, 6470.
(571) Matyushov, D. V.; Voth, G. A. *J. Phys. Chem. A* **2000**, *104*, 6485.
(572) Naka, K.; Morita, A.; Kato, S. *J. Chem. Phys.* **1999**, *110*, 3484.
(573) Kim, H. J. *J. Chem. Phys.* **1996**, *105*, 6833.
(574) Scholes, G. D. *Annu. Rev. Phys. Chem.* **2003**, *54*, 57.
(575) Forster, T. *Ann. Phys.* **1948**, *2*, 55.
(576) Dexter, D. L. *J. Chem. Phys.* **1953**, *21*, 836.
(577) Knox, R. S.; van Amerongen, H. *J. Phys. Chem. B* **2002**, *106*, 5289.
(578) Juzeliunas, G.; Andrews, D. L. *J. Chem. Phys. B* **1994**, *106*, 5289.
(579) Agranovich, V. M.; Galanin, M. D. *Electronic Excitation Energy Transfer in Condensed Matter*; North-Holland: Amsterdam, The Netherlands, 1982.
(580) Tretiak, S.; Middleton, C.; Chernyak, V.; Mukamel, S. *J. Phys. Chem. B* **2000**, *104*, 4519.
(581) Tretiak, S.; Middleton, C.; Chernyak, V.; Mukamel, S. *J. Phys. Chem. B* **2000**, *104*, 9540.
(582) Hsu, C.-P.; Fleming, G. R.; Head-Gordon, M.; Head-Gordon, T. *J. Chem. Phys.* **2001**, *114*, 3065.
(583) Iozzi, M. F.; Mennucci, B.; Tomasi, J.; Cammi, R. *J. Chem. Phys.* **2004**, *120*, 7029.
(584) Bauernschmitt, R.; Haser, M.; Treutler, O.; Ahlrichs, R. *Chem. Phys. Lett.* **1997**, *264*, 573.
(585) Casida, M. E.; Jamorski, C.; Casida, K. C.; Salahub, D. R. *J. Chem. Phys.* **1998**, *108*, 4439.
(586) Stratmann, R. E.; Scuseria, G. E.; Frisch, M. J. *J. Chem. Phys.* **1998**, *109*, 8218.
(587) van Gisbergen, S. J. A.; Kootstra, F.; Schipper, P. R. T.; Gritsenko, O. V.; Snijders, J. G.; Baerends, E. J. *Phys. Rev. A* **1998**, *57*, 2556.
(588) Tozer, D. J.; Handy, N. C. *Phys. Chem. Chem. Phys.* **2000**, *2*, 2117.
(589) Marques, M. A. L.; Gross, E. K. U. *Annu. Rev. Phys. Chem.* **2004**, *55*, 427.
(590) Davydov, A. S. *Theory of Molecular Excitons*; McGraw Hill: New York, 1962.
(591) Mennucci, B.; Tomasi, J.; Cammi, R. *Phys. Rev. B* **2004**, *70*, 205212.
(592) Gersten, J.; Nitzan, A. *J. Chem. Phys.* **1981**, *75*, 1139.
(593) Eckardt, W.; Penzar, Z. *Phys. Rev. B* **1986**, *34*, 8444.
(594) Leung, P. T.; Hider, M. H. *J. Chem. Phys.* **1993**, *98*, 5019.
(595) Girard, C.; Martin, O. J. F.; Dereux, A. *Phys. Rev. Lett.*. **1995**, *75*, 17.
(596) Basilevsky, M. V.; Parsons, D. F.; Vener, M. V. *J. Chem. Phys.* **1998**, *108*, 1103.
(597) Cammi, R.; Tomasi, J. *Int. J. Quantum Chem.* **1996**, *60*, 297.
(598) Nielsen, C. B.; Sauer, S. P. A.; Mikkelsen, K. V. *J. Chem. Phys.* **2003**, *119*, 3849.
(599) Cammi, R.; Cossi, M.; Mennucci, B.; Tomasi, J. *J. Chem. Phys.* **1996**, *105*, 10556.
(600) Mennucci, B.; Tomasi, J.; Cammi, R.; Cheeseman, J. R.; Frisch, M. J.; Devlin, F. J.; Gabriel, S.; Stephens, P. J. *J. Phys. Chem. A* **2002**, *106*, 6102.
(601) Kramer, P.; Saraceno, M. *Geometry of the Time-Dependent Variational Principle in Quantum Mechanics*; Springer-Verlag: Berlin, Germany, 1981.
(602) Moccia, R. *Int. J. Quantum Chem.* **1973**, *7*, 779.
(603) Moccia, R. *Int. J. Quantum Chem.* **1974**, *8*, 293.
(604) Arickx, F.; Broeckhove, J.; Kesteloot, E.; Lathouwers, L.; Van Leuven, P. *Chem. Phys. Lett.* **1986**, *128*, 310.
(605) Broeckhove, J.; Lathouwers, L.; Kesteloot, E.; Van Leuven, P. *Chem. Phys. Lett.* **1988**, *149*, 547.
(606) Broeckhove, J.; Lathouwers, L.; van Leuven, P. *J. Mol. Struct. (THEOCHEM)* **1989**, *199*, 245.
(607) McLachlan, A. D.; Ball, M. A. *Rev. Mod. Phys.* **1964**, *36*, 844.
(608) Dalgarno, A. In *Perturbation Theory and its Application in Quantum Mechanics*; Wilcox, C. H., Ed.; Wiley: New York, 1967.
(609) Langhoff, P. W.; Epstein, S. T.; Karplus, M. *Rev. Mod. Phys.* **1972**, *44*, 602.
(610) Lowdin, P. O.; Mukerjee, P. K. *Chem. Phys. Lett.* **1972**, *14*, 1.
(611) Olsen, J.; Jorgensen, P., Time-dependent response theory with applications to SCF and MCSCF wavefunctions. In *Modern Electronic Structure Theory*; Yarkony, D. R., Ed.; World Scientific: Singapore, 1995; Vol. 2.
(612) Lavenda, B. H. *Nuovo Cimento Soc. Ital. Fis. B* **2003**, *118*, 143.
(613) Christiansen, O.; Jorgensen, P.; Hattig, C. *Int. J. Quantum Chem.* **1998**, *68*, 1.
(614) Cammi, R.; Mennucci, B.; Tomasi, J. *J. Phys. Chem. A* **2000**, *104*, 5631.
(615) Casida, M. E. In *Recent Advances in Computational Chemistry*; Chong, D. P., Ed.; World Scientific: Singapore, 1995; Vol. 1.
(616) Bauernschmitt, R.; Ahlrichs, R. *Chem. Phys. Lett.* **1996**, *256*, 454.
(617) Hirata, S.; Head-Gordon, M. *Chem. Phys. Lett.* **1999**, *314*, 291.
(618) Fonseca, T.; Kim, H. J.; Hynes, J. T. *J. Photochem. Photobiol., A: Chem.* **1994**, *82*, 67.
(619) Gedeck, P.; Schneider, S. *J. Photochem. Photobiol., A: Chem.* **1997**, *105*, 165.
(620) Kim, H. J.; Hynes, J. T. *J. Photochem. Photobiol., A: Chem.* **1997**, *105*, 337.
(621) Gedeck, P.; Schneider, S. *J. Photochem. Photobiol., A: Chem.* **1999**, *121*, 7.

(622) Shukla, M. K.; Leszczynski, J. *Int. J. Quantum Chem.* **2000**, *77*, 240.

(623) Shukla, M. K.; Mishra, S. K.; Kumar, A.; Mishra, P. C. *J. Comput. Chem.* **2000**, *21*, 826.

(624) Mennucci, B.; Toniolo, A.; Tomasi, J. *J. Phys. Chem. A* **2001**, *105*, 7126.

(625) Mennucci, B.; Toniolo, A.; Tomasi, J. *J. Phys. Chem. A* **2001**, *105*, 4749.

(626) Improta, R.; Barone, V. *J. Am. Chem. Soc.* **2004**, *126*, 14320.

(627) Duan, X.-H.; Li, X.-Y.; He, R.-X.; Cheng, X.-M. *J. Chem. Phys.* **2005**, *122*, 084314.

(628) Aquilante, F.; Barone, V.; Roos, B. O. *J. Chem. Phys.* **2003**, *119*, 12323.

(629) Mennucci, B.; Toniolo, A.; Tomasi, J. *J. Am. Chem. Soc.* **2000**, *122*, 10621.

(630) Jonsson, D.; Norman, P.; Agren, H.; Luo, Y.; Syvester-Hvid, K. O.; Mikkelsen, K. V. *J. Chem. Phys.* **1998**, *109*, 6351.

(631) Poulsen, T. D.; Ogilby, P. R.; Mikkelsen, K. V. *J. Phys. Chem. A* **1998**, *102*, 8970.

(632) Ingrosso, F.; Ladanyi, B. M.; Mennucci, B.; Elola, M. D.; Tomasi, J. *J. Phys. Chem. B* **2005**, *109*, 3553.

(633) Yamaguchi, Y.; Osamura, Y.; Goddard, J. D.; Schaefer, H. F. *A New Dimension to Quantum Chemistry: Analytic Derivative Methods in Ab initio Molecular Electronic Structure*; Oxford University Press: New York, 1994.

(634) Wong, M. W.; Wiberg, K. B.; Frisch, M. *J. Chem. Phys.* **1991**, *95*, 8991.

(635) Li, H.; Jensen, J. H. *J. Comput. Chem.* **2004**, *25*, 1449.

(636) Cammi, R.; Tomasi, J. *J. Chem. Phys.* **1994**, *101*, 3888.

(637) Cammi, R.; Tomasi, J. *J. Chem. Phys.* **1994**, *100*, 7495.

(638) Cances, E.; Mennucci, B. *J. Chem. Phys.* **1998**, *109*, 249.

(639) Cances, E.; Mennucci, B.; Tomasi, J. *J. Chem. Phys.* **1998**, *109*, 260.

(640) Mennucci, B.; Cammi, R.; Tomasi, J. *J. Chem. Phys.* **1999**, *110*, 6858.

(641) Andzelm, J.; Kolmel, C.; Klamt, A. *J. Chem. Phys.* **1995**, *103*, 9312.

(642) Truong, T. N.; Stefanovich, E. V. *J. Chem. Phys.* **1995**, *103*, 3709.

(643) Rinaldi, D.; Rivail, J. L.; Rguini, N. *J. Comput. Chem.* **1992**, *13*, 675.

(644) Reguero, M.; Pappalardo, R. R.; Robb, M. A.; Rzepa, H. S. *J. Chem. Soc., Perkin Trans. 2* **1993**, 1499.

(645) Mirone, P. *Spectrochim. Acta* **1966**, *22*, 1897.

(646) Buckingham, A. D. *Proc. R. Soc. (London)* **1960**, *A255*, 32.

(647) Buckingham, A. D. *Proc. R. Soc. (London)* **1958**, *A248*, 169.

(648) Polo, S. R.; Wilson, M. K. *J. Chem. Phys.* **1955**, *23*, 2376.

(649) Chako, N. Q. *J. Chem. Phys.* **1934**, *2*, 644.

(650) Eckhardt, G.; Wagner, W. *J. Mol. Spectrosc.* **1966**, *19*, 407.

(651) Pivorov, V. M. *Opt. Spectrosc.* **1960**, *9*, 139.

(652) Cammi, R.; Cappelli, C.; Corni, S.; Tomasi, J. *J. Phys. Chem. A* **2000**, *104*, 9874.

(653) Cappelli, C.; Corni, S.; Cammi, R.; Mennucci, B.; Tomasi, J. *J. Chem. Phys.* **2000**, *113*, 11270.

(654) Cappelli, C.; Corni, S.; Tomasi, J. *J. Chem. Phys.* **2001**, *115*, 5531.

(655) Cammi, R.; Mennucci, B.; Tomasi, J. *J. Phys. Chem. A* **1998**, *102*, 870.

(656) Cammi, R.; Mennucci, B.; Tomasi, J. *J. Phys. Chem. A* **2000**, *104*, 4690.

(657) Olivares Del Valle, F. J.; Tomasi, J. *Chem. Phys.* **1987**, *114*, 231.

(658) Olivares Del Valle, F. J.; Aguilar, M.; Tolosa, S.; Contador, J. C.; Tomasi, J. *Chem. Phys.* **1990**, *143*, 371.

(659) Rivail, J. L.; Rinaldi, D.; Dillet, V. *Mol. Phys.* **1996**, *89*, 1521.

(660) Corni, S.; Cappelli, C.; Del Zoppo, M.; Tomasi, J. *J. Phys. Chem. A* **2003**, *107*, 10261.

(661) Kellner, R.; Mizaikoff, B.; Jakusch, M.; Wanzenböck, H. D. W. N. *Appl. Spectrosc.* **1997**, *51*, 495.

(662) Osawa, M. *Top. Appl. Phys.* **2001**, *81*, 163.

(663) Nie, S. M.; Emery, S. R. *Science* **1997**, *275*, 1102.

(664) Kneipp, K.; Kneipp, H.; Itzkan, I.; Dasari, R. R.; Feld, M. S. *Chem. Rev.* **1999**, *99*, 2957.

(665) Kneipp, K.; Kneipp, H.; Itzkan, I.; Dasari, R. R.; Feld, M. S. *J. Phys. Condens. Matter* **2002**, *14*, R597.

(666) Moskovits, M.; Tay, L. L.; Yang, J.; Haslett, T. *Top. Appl. Phys.* **2002**, *82*, 215.

(667) Schatz, G. C.; Van Duyne, R. P. In *Handbook of Vibrational Spectroscopy*; Chalmers, J., Griffiths, P. R., Eds.; Wiley: New York, 2002.

(668) Girard, C.; Hache, F. *Chem. Phys.* **1987**, *118*, 249.

(669) Pandey, P. K. K.; Schatz, G. C. *Chem. Phys. Lett.* **1982**, *88*, 193.

(670) Nakai, H.; Nakatsuji, H. *J. Chem. Phys.* **1995**, *103*, 2286.

(671) Cammi, R.; Mennucci, B.; Tomasi, J. *J. Am. Chem. Soc.* **1998**, *120*, 8834.

(672) Cammi, R.; Mennucci, B.; Tomasi, J., On the calculation of nonlinear optical macroscopic susceptibilities in solution within the Polarizable Continuum Model approach. In *Nonlinear Optical Responses of Molecules, Solids and Liquids: Methods and Applications*; Papadopoulos, M. G., Ed.; Research Signpost: Kerala, India, 2003.

(673) Bishop, D. M.; Kirtman, B. *J. Chem. Phys.* **1991**, *95*, 2646.

(674) Bishop, D. M.; Kirtman, B. *J. Chem. Phys.* **1992**, *97*, 5255.

(675) Bishop, D. M.; Hasan, M.; Kirtman, B. *J. Chem. Phys.* **1995**, *103*, 4157.

(676) Kirtman, B.; Luis, J. M.; Bishop, D. M. *J. Chem. Phys.* **1998**, *108*, 10008.

(677) Norman, P.; Macak, P.; Luo, Y.; Agren, H. *J. Chem. Phys.* **1999**, *110*, 7960.

(678) Willetts, A.; Rice, J. E. *J. Chem. Phys.* **1993**, *99*, 426.

(679) Yu, J.; Zerner, M. C. *J. Chem. Phys.* **1994**, *100*, 7487.

(680) Luo, Y.; Norman, P.; Agren, H.; Sylvester-Hvid, K. O.; Mikkelsen, K. V. *Phys. Rev. E* **1998**, *57*, 4778.

(681) Sylvester-Hvid, K. O.; Mikkelsen, K. V.; Jonsson, D.; Norman, P.; Agren, H. *J. Phys. Chem. A* **1999**, *103*, 8375.

(682) Poulsen, T. D.; Ogilby, P. R.; Mikkelsen, K. V. *J. Chem. Phys.* **2001**, *115*, 7843.

(683) Jorgensen, S.; Ratner, M. A.; Mikkelsen, K. V. *J. Chem. Phys.* **2001**, *115*, 8185.

(684) Kongsted, J.; Osted, A.; Mikkelsen, K. V.; Christiansen, O. *J. Chem. Phys.* **2003**, *119*, 10519.

(685) Cammi, R.; Cossi, M.; Tomasi, J. *J. Chem. Phys.* **1996**, *104*, 4611.

(686) Cammi, R.; Cossi, M.; Mennucci, B.; Tomasi, J. *J. Mol. Struct.* **1997**, *437*, 567.

(687) Champagne, B.; Mennucci, B.; Cossi, M.; Cammi, R.; Tomasi, J. *Chem. Phys.* **1998**, *238*, 153.

(688) Mennucci, B.; Cammi, R.; Cossi, M.; Tomasi, J. *J. Mol. Struct. (THEOCHEM)* **1998**, *426*, 191.

(689) Cappelli, C.; Rizzo, A.; Mennucci, B.; Tomasi, J.; Cammi, R.; Rikken, G. L. J. A.; Mathevet, R.; Rizzo, C. *J. Chem. Phys.* **2003**, *118*, 10712.

(690) Prasad, P. N.; Williams, D. J. *Introduction to Nonlinear Optical Effects in Molecules and Polymers*; Wiley: New York, 1991.

(691) Wortmann, R.; Bishop, D. M. *J. Chem. Phys.* **1998**, *108*, 1001.

(692) Norman, P.; Luo, Y.; Agren, H. *J. Chem. Phys.* **1997**, *107*, 9535.

(693) Luo, Y.; Norman, P.; Agren, H. *J. Chem. Phys.* **1998**, *109*, 3589.

(694) Macak, P.; Norman, P.; Luo, Y.; Agren, H. *J. Chem. Phys.* **2000**, *112*, 1868.

(695) Luo, Y.; Norman, P.; Macak, P.; Agren, H. *J. Chem. Phys.* **1999**, *111*, 9853.

(696) Wortmann, R.; Krämer, P.; Glania, C.; Lebus, S.; Detzer, N. *Chem. Phys.* **1993**, *173*, 99.

(697) Liptay, W.; Becker, J.; Wehning, D.; Lang, W.; Burkhard, O. *Z. Naturforsch. A* **1982**, *37*, 1396.

(698) Liptay, W.; Wehning, D.; Becker, J.; Rehm, T. *Z. Naturforsch. A* **1982**, *37*, 1369.

(699) Singer, K. D.; Garito, A. F. *J. Chem. Phys.* **1981**, *75*, 3572.

(700) Cammi, R.; Frediani, L.; Mennucci, B.; Tomasi, J. *J. Mol. Struct. (THEOCHEM)* **2003**, *633*, 209.

(701) Pavanello, M.; Mennucci, B.; Ferrarini, A. *J. Chem. Phys.* **2005**, *122*, 064906.

(702) Fernandez, B.; Christiansen, O.; Bludsky, O.; Jorgensen, P.; Mikkelsen, K. V. *J. Chem. Phys.* **1996**, *104*, 629.

(703) Mikkelsen, K. V.; Ruud, K.; Helgaker, T. *Chem. Phys. Lett.* **1996**, *253*, 443.

(704) Astrand, P.; Mikkelsen, K. V.; Ruud, K.; Helgaker, T. *J. Phys. Chem.* **1996**, *100*, 19771.

(705) Mikkelsen, K. V.; Jorgensen, P.; Ruud, K.; Helgaker, T. *J. Chem. Phys.* **1997**, *106*, 1170.

(706) Astrand, P. O.; Mikkelsen, K. V.; Jorgensen, P.; Ruud, K.; Helgaker, T. *J. Chem. Phys.* **1998**, *108*, 2528.

(707) Mikkelsen, K. V.; Ruud, K.; Helgaker, T. *J. Comput. Chem.* **1999**, *20*, 1281.

(708) Jaszunski, M.; Mikkelsen, K. V.; Rizzo, A.; Witanowski, M. *J. Phys. Chem. A* **2000**, *104*, 1466.

(709) Pecul, M.; Sadlej, J. *Chem. Phys.* **1998**, *234*, 111.

(710) Pecul, M.; Sadlej, J. *Chem. Phys.* **2000**, *255*, 137.

(711) Pennanen, T. S.; Vaara, J.; Lantto, P.; Sillanpää, A. J.; Laasonen, K.; Jokisaari, J. *J. Am. Chem. Soc.* **2004**, *126*, 11093.

(712) Cammi, R. *J. Chem. Phys.* **1998**, *109*, 3185.

(713) Cammi, R.; Mennucci, B.; Tomasi, J. *J. Chem. Phys.* **1999**, *110*, 7627.

(714) Mennucci, B.; Cammi, R.; Tomasi, J. *Int. J. Quantum Chem.* **1999**, *75*, 767.

(715) Gontrani, L.; Mennucci, B.; Tomasi, J. *J. Mol. Struct. (THEOCHEM)* **2000**, *500*, 113.

(716) Mennucci, B.; Martinez, J. M.; Tomasi, J. *J. Phys. Chem. A* **2001**, *105*, 7287.

(717) Mennucci, B. *J. Am. Chem. Soc.* **2002**, *124*, 1506.

(718) Ruud, K.; Frediani, L.; Cammi, R.; Mennucci, B. *Int. J. Mol. Sci.* **2003**, *4*, 119.

(719) Klein, R.; Mennucci, B.; Tomasi, J. *J. Phys. Chem. A* **2004**, *108*, 5851.

(720) Cappelli, C.; Monti, S.; Mennucci, B. *J. Phys. Chem. A* **2005**, *109*, 1933.

(721) Mennucci, B.; Martinez, J. M. *J. Phys. Chem. B* **2005**, *109*, 9818.

(722) Mennucci, B.; Martinez, J. M. *J. Phys. Chem. B* **2005**, *109*, 9830.

(723) Rega, N.; Cossi, M.; Barone, V. *J. Chem. Phys.* **1996**, *105*, 11060.

(724) Rega, N.; Cossi, M.; Barone, V. *J. Am. Chem. Soc.* **1997**, *119*, 12962.

(725) Rega, N.; Cossi, M.; Barone, V. *J. Am. Chem. Soc.* **1998**, *120*, 5723.
(726) Jolibois, F.; Cadet, J.; Grand, A.; Subra, R.; Rega, N.; Barone, V. *J. Am. Chem. Soc.* **1998**, *120*, 1864.
(727) Adamo, C.; Heitzmann, M.; Meilleur, F.; Rega, N.; Scalmani, G.; Grand, A.; Cadet, J.; Barone, V. *J. Am. Chem. Soc.* **2001**, *123*, 7113.
(728) Saracino, G. A. A.; Tedeschi, A.; D'Errico, G.; Improta, R.; Franco, L.; Ruzzi, M.; Corvaia, C.; Barone, V. *J. Phys. Chem. A* **2002**, *106*, 10700.
(729) Cossi, M.; Crescenzi, O. *J. Chem. Phys.* **2003**, *118*, 8863.
(730) D'Amore, M.; Improta, R.; Barone, V. *J. Phys. Chem. A* **2003**, *107*, 6264.
(731) Pavone, M.; Benzi, C.; De Angelis, F.; Barone, V. *Chem. Phys. Lett.* **2004**, *395*, 120.
(732) Cossi, M.; Crescenzi, O. *Theor. Chem. Acc.* **2004**, *111*, 162.
(733) Crescenzi, O.; Pavone, M.; De Angelis, F.; Barone, V. *J. Phys. Chem. B* **2005**, *109*, 445.
(734) Benzi, C.; Cossi, M.; Barone, V.; Tarroni, R.; Zannoni, C. *J. Phys. Chem. B* **2005**, *109*, 2584.
(735) Manalo, M. N.; de Dios, A. C.; Cammi, R. *J. Phys. Chem. A* **2000**, *104*, 9600.
(736) Manalo, M. N.; de Dios, A. C. *Magn. Reson. Chem.* **2002**, *40*, 781.
(737) Wu, A. A.; Cremer, D.; Gauss, J. *J. Phys. Chem. A* **2003**, *107*, 8737.
(738) Tuttle, T.; Kraka, E.; Wu, A.; Cremer, D. *J. Am. Chem. Soc.* **2004**, *126*, 5093.
(739) Zaccari, D. G.; Snyder, J. P.; Peralta, J. E.; Taurian, O. E.; Contreras, R. H.; Barone, V. *Mol. Phys.* **2002**, *100*, 705.
(740) Zaccari, D. G.; Barone, V.; Peralta, J. E.; Contreras, R. H.; Taurian, O. E.; Diez, E.; Esteban, A. *Int. J. Mol. Sci.* **2003**, *4*, 93.
(741) Ciofini, I.; Reviakine, R.; Arbuznikov, A.; Kaupp, M. *Theor. Chem. Acc.* **2004**, *111*, 132.
(742) Rinkevicius, Z.; Telyatnyk, L.; Vahtras, O.; Ruud, K. *J. Chem. Phys.* **2004**, *121*, 5051.
(743) Buckingham, A. D.; Schafer, T.; Schneider, W. G. *J. Chem. Phys.* **1960**, *32*, 1227.
(744) Kamlet, M. J.; Abboud, J. L. M.; Taft, R. W. *Prog. Phys. Org. Chem.* **1980**, *13*, 485.
(745) Witanowski, M.; Biedrzycka, Z.; Sicinska, W.; Grabowski, Z. *J. Magn. Reson.* **1998**, *131*, 54.
(746) Witanowski, M.; Sicinska, W.; Biedrzycka, Z.; Webb, G. A. *J. Mol. Struct.* **1999**, *476*, 133.
(747) Witanowski, M.; Biedrzycka, Z.; Sicinska, W.; Webb, G. A. *J. Mol. Struct.* **2000**, *516*, 107.
(748) Witanowski, M.; Biedrzycka, Z.; Sicinska, W.; Grabowski, Z. *J. Mol. Struct.* **2002**, *602*, 199.
(749) Witanowski, M.; Biedrzycka, Z.; Sicinska, W.; Grabowski, Z. *J. Magn. Reson.* **2003**, *164*, 212.
(750) Ramsey, N. F. *Phys. Rev.* **1950**, *78*, 699.
(751) Ramsey, N. F. *Phys. Rev.* **1953**, *91*, 303.
(752) Ditchfield, R. *Mol. Phys.* **1974**, *27*, 789.
(753) Wolinski, K.; Hinton, J. F.; Pulay, P. *J. Am. Chem. Soc.* **1990**, *112*, 8251.
(754) Gauss, J. *J. Chem. Phys.* **1993**, *99*, 3629.
(755) Gauss, J.; Stanton, J. F. *J. Chem. Phys.* **1995**, *102*, 251.
(756) Gauss, J.; Stanton, J. F. *J. Chem. Phys.* **1996**, *104*, 2574.
(757) Cheeseman, J. R.; Trucks, G. W.; Keith, T. A.; Frisch, M. J. *J. Chem. Phys.* **1996**, *104*, 5497.
(758) Helgaker, T.; Wilson, P. J.; Amos, R. D.; Handy, N. C. *J. Chem. Phys.* **2000**, *113*, 2983.
(759) Höller, R. L. L. *Chem. Phys. Lett.* **1981**, *84*, 94.
(760) Hinton, J. F.; Guthrie, P.; Pulay, P.; Wolinski, K. *J. Am. Chem. Soc.* **1992**, *114*, 1604.
(761) Chesnut, D. B.; Rusidoski, B. E. *J. Mol. Struct. (THEOCHEM)* **1994**, *314*, 19.
(762) Pecul, M. J. S. *Chem. Phys.* **1998**, *234*, 111.
(763) Benedict, H.; Shenderovich, I. G.; Malkina, O. L.; Malkin, V. G.; Denisov, G. S.; Golubev, N. S.; Limbach, H. H. *J. Am. Chem. Soc.* **2000**, *122*, 1979.
(764) Pecul, M.; Leszczynski, J.; Sadlej, J. *J. Phys. Chem. A* **2000**, *104*, 8105.
(765) Pecul, M.; Leszczynski, J.; Sadlej, J. *J. Chem. Phys.* **2000**, *112*, 7930.
(766) Pecul, M.; Sadlej, J.; Leszczynski, J. *J. Chem. Phys.* **2001**, *115*, 5498.
(767) Del Bene, J. E.; Jordan, M. J. T. *J. Phys. Chem. A* **2002**, *106*, 5385.
(768) Del Bene, J. E.; Elguero, J.; Alkorta, I.; Yanez, M.; Mo, O. *J. Chem. Phys.* **2004**, *120*, 3237.
(769) Helgaker, T.; Watson, M.; Handy, N. C. *J. Chem. Phys.* **2000**, *113*, 9402.
(770) Engels, B.; Eriksson, L. A.; Lunell, S. *Adv. Quantum Chem.* **1996**, *27*, 297.
(771) Improta, R.; Barone, V. *Chem. Rev.* **2004**, *104*, 1231.
(772) Schreckenbach, G.; Ziegler, T. *J. Phys. Chem. A* **1997**, *101*, 3388.

(773) vanLenthe, E.; Wormer, P. E. S.; vanderAvoird, A. *J. Chem. Phys.* **1997**, *107*, 2488.
(774) Kaupp, M.; Remenyi, C.; Vaara, J.; Malkina, O. L.; Malkin, V. G. *J. Am. Chem. Soc.* **2002**, *124*, 2709.
(775) Kaupp, M.; Reviakine, R.; Malkina, O. L.; Arbuznikov, A.; Schimmelpfennig, B.; Malkin, V. G. *J. Comput. Chem.* **2002**, *23*, 794.
(776) Rosenfeld, L. *Z. Phys.* **1928**, *52*, 161.
(777) Hansen, A. E.; Bouman, T. D. *Adv. Chem. Phys.* **1980**, *44*, 545.
(778) Ruiz Lopez, M. F.; Rinaldi, D. *J. Mol. Struct. (THEOCHEM)* **1983**, *93*, 277.
(779) Furche, F.; Ahlrichs, R.; Wachsmann, C.; Weber, E.; Sobanski, A.; Vogtle, F.; Grimme, S. *J. Am. Chem. Soc.* **2000**, *122*, 1717.
(780) Autschbach, J.; Ziegler, T.; Gisbergen, S. J. A. v.; Baerends, E. J. *J. Chem. Phys.* **2002**, *116*, 6930.
(781) Diedrich, C.; Grimme, S. *J. Phys. Chem. A* **2003**, *107*, 2524.
(782) Kongsted, J.; Hansen, A. E.; Pedersen, T. B.; Osted, A.; Mikkelsen, K. V.; Christiansen, O. *Chem. Phys. Lett.* **2004**, *391*, 259.
(783) Kongsted, J.; Pedersen, T. B.; Osted, A.; Hansen, A. E.; Mikkelsen, K. V.; Christiansen, O. *J. Phys. Chem. A* **2004**, *108*, 3632.
(784) Pecul, M.; Marchesan, D.; Ruud, K.; Coriani, S. *J. Chem. Phys.* **2005**, *122*, 024106.
(785) Moffitt, W.; Moscowitz, A. *J. Chem. Phys.* **1959**, *30*, 648.
(786) Condon, E. U. *Rev. Mod. Phys.* **1937**, *9*, 432.
(787) Eyring, H.; Walter, J.; Kimball, G. E. *Quantum Chemistry*; Wiley: New York, 1944.
(788) Amos, R. D. *Chem. Phys. Lett.* **1982**, *87*, 23.
(789) Bak, K. L.; Jorgensen, P.; Helgaker, T.; Ruud, K. *Faraday Discuss.* **1994**, 121.
(790) Cheeseman, J. R.; Frisch, M. J.; Devlin, F. J.; Stephens, P. J. *J. Phys. Chem. A* **2000**, *104*, 1039.
(791) Stephens, P. J.; Devlin, F. J.; Cheeseman, J. R.; Frisch, M. J. *J. Phys. Chem. A* **2001**, *105*, 5356.
(792) Polavarapu, P. L. *Chirality* **2002**, *14*, 768−781.
(793) Stephens, P. J.; Devlin, F. J.; Cheeseman, J. R.; Frisch, M. J.; Mennucci, B.; Tomasi, J. *Tetrahedron−Asymmetry* **2000**, *11*, 2443.
(794) da Silva, C. O.; Mennucci, B.; Vreven, T. *J. Org. Chem.* **2004**, *69*, 8161.
(795) Marchesan, D.; Coriani, S.; Forzato, C.; Nitti, P.; Pitacco, G.; Ruud, K. *J. Phys. Chem. A* **2005**, *109*, 1449.
(796) Kongsted, J.; Pedersen, T. B.; Strange, M.; Osted, A.; Hansen, A. E.; Mikkelsen, K. V.; Pawlowski, F.; Jorgensen, P.; Hattig, C. *Chem. Phys. Lett.* **2005**, *401*, 385.
(797) Holzwarth, G.; Hsu, E. C.; Mosher, H. S.; Faulkner, T. R.; Moscowitz, A. *J. Am. Chem. Soc.* **1974**, *96*, 251.
(798) Nafie, L. A.; Cheng, J. C.; Stephens, P. J. *J. Am. Chem. Soc.* **1975**, *97*, 3842.
(799) Barron, L. D.; Bogaard, M. P.; Buckingham, A. D. *J. Am. Chem. Soc.* **1973**, *95*, 603.
(800) Hug, W.; Kint, S.; Bailey, G. F.; Scherer, J. R. *J. Am. Chem. Soc.* **1975**, *97*, 5589.
(801) Stephens, P. J.; Ashvar, C. S.; Devlin, F. J.; Cheeseman, J. R.; Frisch, M. J. *Mol. Phys.* **1996**, *89*, 579.
(802) Devlin, F. J.; Stephens, P. J.; Cheeseman, J. R.; Frisch, M. J. *J. Phys. Chem. A* **1997**, *101*, 9912.
(803) Stephens, P. J.; Chabalowski, C. F.; Devlin, F. J.; Jalkanen, K. J. *Chem. Phys. Lett.* **1994**, *225*, 247.
(804) Stephens, P. J.; Devlin, F. J. *Chirality* **2000**, *12*, 172.
(805) Cappelli, C.; Corni, S.; Mennucci, B.; Cammi, R.; Tomasi, J. *J. Phys. Chem. A* **2002**, *106*, 12331.
(806) Frimand, K.; Bohr, H.; Jalkanen, K. J.; Suhai, S. *Chem. Phys.* **2000**, *255*, 165.
(807) Abdali, S.; Jalkanen, K. J.; Bohr, H.; Suhai, S.; Nieminen, R. M. *Chem. Phys.* **2002**, *282*, 219.
(808) Stephens, P. J.; Devlin, F. J. *Chirality* **2000**, *12*, 172.
(809) Schaefer, M.; Bartels, C.; Karplus, M. *J. Mol. Biol.* **1998**, *284*, 835.
(810) Hassan, S. A.; Guarnieri, F.; Mehler, E. L. *J. Phys. Chem. B* **2000**, *104*, 6490.
(811) Hassan, S. A.; Mehler, E. L.; Zhang, D. Q.; Weinstein, H. *Proteins* **2003**, *51*, 109.
(812) Hockney, R. W.; Eastwood, J. W. *Computer Simulation Using Particles*, 2nd ed.; IOP: Bristol, U.K., 1988.
(813) Essmann, U.; Perera, L.; Berkowitz, M. L.; Darden, T.; Lee, H.; Pedersen, L. G. *J. Chem. Phys.* **1995**, *103*, 8577.
(814) Allen, M. P.; Tildesley, D. J. *Computer Simulation of Liquids*; Oxford University Press: New York, 1989.
(815) van Gunsteren, W. F.; Berendsen, H. J. C. *Angew. Chem.-Int. Ed.* **1990**, *29*, 992.
(816) Steinbach, P. J.; Brooks, B. R. *J. Comput. Chem.* **1994**, *15*, 667.
(817) Hummer, G.; Soumpasis, D. M.; Neumann, M. *J. Phys.-Condens. Matter* **1994**, *6*, A141.
(818) Hünenberger, P. H.; van Gunsteren, W. F. *J. Chem. Phys.* **1998**, *108*, 6117.
(819) Alper, H.; Levy, R. M. *J. Chem. Phys.* **1993**, *99*, 9847.
(820) Wang, L.; Hermans, J. *J. Phys. Chem.* **1995**, *99*, 12001.
(821) Barker, J. A. *Mol. Phys.* **1994**, *83*, 1057.

(822) Tironi, I. G.; Sperb, R.; Smith, P. E.; van Gunsteren, W. F. *J. Chem. Phys.* **1995**, *102*, 5451.
(823) Marchi, M.; Borgis, D.; Levy, N.; Ballone, P. *J. Chem. Phys.* **2001**, *114*, 4377.
(824) Procacci, P.; Darden, T. A.; Paci, E.; Marchi, M. *J. Comput. Chem.* **1997**, *18*, 1848.
(825) Vener, M. V.; Leontyev, I. V.; Dyakov, Y. A.; Basilevsky, M. V.; Newton, M. A. *J. Phys. Chem. B* **2002**, *106*, 13078.
(826) Leontyev, I. V.; Vener, M. V.; Rostov, I. V.; Basilevsky, M. V.; Newton, M. D. *J. Chem. Phys.* **2003**, *119*, 8024.
(827) Vener, M. V.; Leontyev, I. V.; Basilevsky, M. V. *J. Chem. Phys.* **2003**, *119*, 8038.
(828) http://www.igc.ethz.ch/gromos.
(829) Colominas, C.; Luque, F. J.; Orozco, M. MC-MST computer program; University of Barcelona, Barcelona, Spain, 1998.
(830) Hernandez, B.; Curutchet, C.; Colominas, C.; Orozco, M.; Luque, F. J. *Mol. Simul.* **2002**, *28*, 153.
(831) Car, R.; Parrinello, M. *Phys. Rev. Lett.* **1985**, *55*, 2471.
(832) Remler, D. K.; Madden, P. A. *Mol. Phys.* **1990**, *70*, 921.
(833) Payne, M. C.; Teter, M. P.; Allan, D. C.; Arias, T. A.; Joannopoulos, J. D. *Rev. Mod. Phys.* **1992**, *64*, 1045.
(834) Tuckerman, M. E.; Ungar, P. J.; vonRosenvinge, T.; Klein, M. L. *J. Phys. Chem.* **1996**, *100*, 12878.
(835) Tuckerman, M. E. *J. Phys.: Condens. Matter* **2002**, *14*, R1297.
(836) Tse, J. S. *Annu. Rev. Phys. Chem.* **2002**, *53*, 249.
(837) Laio, A.; VandeVondele, J.; Rothlisberger, U. *J. Chem. Phys.* **2002**, *116*, 6941.
(838) Woo, T. K.; Cavallo, L.; Ziegler, T. *Theor. Chem. Acc.* **1998**, *100*, 1432.
(839) Rega, N.; Iyengar, S. S.; Voth, G. A.; Schlegel, H. B.; Vreven, T.; Frisch, M. J. *J. Phys. Chem. B* **2004**, *108*, 4210.
(840) Fattebert, J. L.; Gygi, F. *J. Comput. Chem.* **2002**, *23*, 662.
(841) Fattebert, J. L.; Gygi, F. *Int. J. Quantum Chem.* **2003**, *93*, 139.
(842) Cappelli, C.; Mennucci, B.; Silva, C. O. d.; Tomasi, J. *J. Chem. Phys.* **2000**, *112*, 5382.
(843) Pliego, J. R., Jr.; Riveros, J. M. *J. Phys. Chem. A* **2001**, *105*, 7241.
(844) Pliego, J. R., Jr.; Riveros, J. M. *J. Phys. Chem. A* **2002**, *106*, 7434.
(845) Sicinska, D.; Paneth, P.; Truhlar, D. G. *J. Phys. Chem. B* **2002**, *106*, 2708.
(846) Langella, E.; Rega, N.; Improta, R.; Crescenzi, O.; Barone, V. *J. Comput. Chem.* **2002**, *23*, 650.
(847) da Silva, C. O.; Mennucci, B.; Vreven, T. *J. Phys. Chem. A* **2003**, *107*, 6630.
(848) Mo, S. J.; Vreven, T.; Mennucci, B.; Morokuma, K.; Tomasi, J. *Theor. Chem. Acc.* **2004**, *111*, 154.
(849) Zeng, J.; Hush, N. S.; Reimers, J. R. *J. Chem. Phys.* **1993**, *99*, 1496.
(850) Zeng, J.; Hush, N. S.; Reimers, J. R. *J. Chem. Phys.* **1993**, *99*, 1508.
(851) Zeng, J.; Woywod, C.; Hush, N. S.; Reimers, J. R. *J. Am. Chem. Soc.* **1995**, *117*, 8618.
(852) Zeng, J.; Hush, N. S.; Reimers, J. R. *J. Phys. Chem.* **1996**, *100*, 9561.
(853) Friedman, H. *Mol. Phys.* **1975**, *29*, 1533.
(854) Rocha, W. R.; De Almeida, K. J.; Coutinho, K.; Canuto, S. *Chem. Phys. Lett.* **2001**, *345*, 171.
(855) Rocha, W. R.; Coutinho, K.; de Almeida, W. B.; Canuto, S. *Chem. Phys. Lett.* **2001**, *335*, 127.
(856) de Almeida, K. J.; Coutinho, K.; de Almeida, W. B.; Rocha, W. R.; Canuto, S. *Phys. Chem. Chem. Phys.* **2001**, *3*, 1583.
(857) Coutinho, K.; Saavedra, N.; Serrano, A.; Canuto, S. *J. Mol. Struct. (THEOCHEM)* **2001**, *539*, 171.
(858) Rivelino, R.; Coutinho, K.; Canuto, S. *J. Phys. Chem. B* **2002**, *106*, 12317.
(859) Rocha, W. R.; Martins, V. M.; Coutinho, K.; Canuto, S. *Theor. Chem. Acc.* **2002**, *108*, 31.
(860) Canuto, S.; Coutinho, K.; Trzesniak, D. *Adv. Quantum Chem.* **2002**, *41*, 161.
(861) Coutinho, K.; Guedes, R. C.; Cabral, B. J. C.; Canuto, S. *Chem. Phys. Lett.* **2003**, *369*, 345.
(862) Coutinho, K.; Canuto, S. *J. Mol. Struct. (THEOCHEM)* **2003**, *632*, 235.
(863) Cui, Q. *J. Chem. Phys.* **2002**, *117*, 4720.
(864) Brooks, B. R.; Bruccoleri, R. E.; Olafson, B. D.; States, D. J.; Swaminathan, S.; Karplus, M. *J. Comput. Chem.* **1983**, *4*, 187.
(865) Lyne, P. D.; Hodoscek, M.; Karplus, M. *J. Phys. Chem. A* **1999**, *103*, 3462.
(866) Chen, W.; Gordon, M. S. *J. Chem. Phys.* **1996**, *105*, 11081.
(867) Gordon, M. S.; Freitag, M. A.; Bandyopadhyay, P.; Jensen, J. H.; Kairys, V.; Stevens, W. J. *J. Phys. Chem. A* **2001**, *105*, 293.
(868) Bandyopadhyay, P.; Gordon, M. S. *J. Chem. Phys.* **2000**, *113*, 1104.
(869) Bandyopadhyay, P.; Gordon, M. S.; Mennucci, B.; Tomasi, J. *J. Chem. Phys.* **2002**, *116*, 5023.
(870) Li, H.; Pomelli, C. S.; Jensen, J. H. *Theor. Chem. Acc.* **2003**, *109*, 71.
(871) Svensson, M.; Humbel, S.; Froese, R. D. J.; Matsubara, T.; Sieber, S.; Morokuma, K. *J. Phys. Chem.* **1996**, *100*, 19357.
(872) Froese, R. D. J.; Morokuma, K. In *The Encyclopedia of Computational Chemistry*; Schleyer, P. v. R., Allinger, N. L., Clark, T., Gasteiger, J., Kollman, P. A., Schaefer III, H. F., Schreiner, P. R., Eds.; Wiley: Chichester, U.K., 1998.
(873) Dapprich, S.; Komaromi, I.; Byun, K. S.; Morokuma, K.; Frisch, M. J. *J. Mol. Struct. (THEOCHEM)* **1999**, *462*, 1.
(874) Karadakov, P. B.; Morokuma, K. *Chem. Phys. Lett.* **2000**, *317*, 589.
(875) Vreven, T.; Morokuma, K. *J. Comput. Chem.* **2000**, *21*, 1419.
(876) Vreven, T.; Mennucci, B.; Silva, C. O. d.; Morokuma, K.; Tomasi, J. *J. Chem. Phys.* **2001**, *115*, 62.
(877) Thole, B. T.; Van Duijnen, P. T. *Chem. Phys.* **1982**, *71*, 211.
(878) Van Duijnen, P. T.; Juffer, A. H.; Dijkman, H. P. *THEOCHEM* **1992**, *92*, 195.
(879) Thole, B. T.; Van Duijnen, P. T. *Theor. Chim. Acta* **1983**, *63*, 209.
(880) Grozema, F. C.; van Duijnen, P. T. *J. Phys. Chem. A* **1998**, *102*, 7984.
(881) van Duijnen, P. T.; de Vries, A. H.; Swart, M.; Grozema, F. *J. Chem. Phys.* **2002**, *117*, 8442.
(882) Jensen, L.; van Duijnen, P. T.; Snijders, J. G. *J. Chem. Phys.* **2003**, *119*, 3800.
(883) Jensen, L.; van Duijnen, P. T.; Snijders, J. G. *J. Chem. Phys.* **2003**, *119*, 12998.
(884) Dupuis, D.; Farazdel, A.; Karma, S. P.; Maluendes, S. A. In *MOTECC-90, ESCOM*; Clementi, E., Ed.; ESCOM: Leiden, The Netherlands, 1990; Vol. 277.
(885) GAMESS (UK). http://www.cse.clrc.ac.uk/qcg/gamess-uk/.
(886) Zerner, M. C.; *ZINDO; Quantum Theory Project*, University of Florida, Gainesville, FL; http://www.accelrys.com/cerius2/zindo.html.
(887) Warshel, A.; Levitt, M. *Nature* **1975**, *253*, 694.
(888) Warshel, A.; Levitt, M. *J. Mol. Biol.* **1976**, *103*, 227.
(889) Warshel, A.; Russell, S. T. *Q. Rev. Biophys.* **1984**, *17*, 283.
(890) Florian, J.; Warshel, A. *J. Phys. Chem. B* **1997**, *101*, 5583.
(891) Florian, J.; Sponer, J.; Warshel, A. *J. Phys. Chem. B* **1999**, *103*, 884.
(892) Florian, J.; Warshel, A. *J. Phys. Chem. B* **1999**, *103*, 10282.
(893) Lee, F. S.; Chu, Z. T.; Warshel, A. *J. Comput. Chem.* **1993**, *14*, 161.
(894) http://www-rcf.usc.edu/~florian/chemsol.html.
(895) http://www.q-chem.com/.
(896) Sanchez, M. L.; Aguilar, M. A.; Olivares del Valle, F. J. *J. Comput. Chem.* **1997**, *18*, 313.
(897) Mendoza, M. L. S.; Aguilar, M. A.; Olivares del Valle, F. J. *J. Mol. Struct. (THEOCHEM)* **1998**, *426*, 181.
(898) Sanchez, M. L.; Martin, M. E.; Aguilar, M. A.; Olivares del Valle, F. J. *J. Comput. Chem.* **2000**, *21*, 705.
(899) Martin, M. E.; Aguilar, M. A.; Chalmet, S.; Ruiz-Lopez, M. *Chem. Phys. Lett.* **2001**, *344*, 107.
(900) Martin, M. E.; Sanchez, M. L.; Olivares del Valle, F. J.; Aguilar, M. A. *J. Chem. Phys.* **2000**, *113*, 6308.
(901) Martin, M. E.; Munoz Losa, A.; Fdez. Galvan, I.; Aguilar, M. A. *J. Chem. Phys.* **2004**, *121*, 3710.
(902) Fdez. Galvan, I.; Olivares del Valle, F. J.; Martin, M. E.; Aguilar, M. A. *Theor. Chem. Acc.* **2004**, *111*, 196.
(903) Corchado, J. C.; Sanchez, M. L.; Aguilar, M. A. *J. Am. Chem. Soc.* **2004**, *126*, 7311.
(904) Munoz-Losa, A.; Fdez. Galvan, I.; Martin, M. E.; Aguilar, M. A. *J. Phys. Chem. B* **2003**, *107*, 5043.
(905) Sanchez, M. L.; Martin, M. E.; Fdez. Galvan, I.; Olivares del Valle, F. J.; Aguilar, M. A. *J. Phys. Chem. B* **2002**, *106*, 4813.
(906) Fdez. Galvan, I.; Martin, M. E.; Aguilar, M. A. *J. Comput. Chem.* **2004**, *25*, 1227.
(907) Okuyama-Yoshida, N.; Nagaoka, M.; Yamabe, T. *Int. J. Quantum Chem.* **1998**, *70*, 95.
(908) Refson, K. *MOLDY User's Manual*, rev. 2.10; MOLDY; http://www.earth.ox.ac.uk/~keithr/moldy.html.
(909) Dupuis, M.; Marquez, A.; Davidson, E. R. *HONDO 2000*, based on HONDO 95.3; Indiana University, Bloomington, IN, 2000.
(910) Fdez. Galvan, I.; Sanchez, M. L.; Martin, M. E.; Olivares del Valle, F. J.; Aguilar, M. A. *Comput. Phys. Commun.* **2003**, *155*, 244.
(911) Chandler, D.; Andersen, H. C. *J. Chem. Phys.* **1972**, *57*, 1930.
(912) Hirata, F.; Rossky, P. J. *Chem. Phys. Lett.* **1981**, *83*, 329.
(913) Hirata, F.; Pettitt, B. M.; Rossky, P. J. *J. Chem. Phys.* **1982**, *77*, 509.
(914) Hirata, F. *Bull. Chem. Soc. Jpn.* **1998**, *71*, 1483.
(915) Perkyns, J.; Pettitt, B. M. *J. Chem. Phys.* **1992**, *97*, 7656.
(916) Perkyns, J. S.; Pettitt, B. M. *Chem. Phys. Lett.* **1992**, *190*, 626.
(917) Kovalenko, A.; Ten-No, S.; Hirata, F. *J. Comput. Chem.* **1999**, *20*, 928.
(918) Kovalenko, A.; Hirata, F. *J. Chem. Phys.* **2000**, *112*, 10391.
(919) Kovalenko, A.; Hirata, F. *J. Chem. Phys.* **2000**, *113*, 2793.
(920) Ten-no, S.; Hirata, F.; Kato, S. *Chem. Phys. Lett.* **1993**, *214*, 391.
(921) Ten-no, S.; Hirata, F.; Kato, S. *J. Chem. Phys.* **1994**, *100*, 7443.
(922) Sato, H.; Hirata, F.; Kato, S. *J. Chem. Phys.* **1996**, *105*, 1546.

(923) Hirata, F.; Rossky, P. J.; Pettitt, B. M. *J. Chem. Phys.* **1983**, *78*, 4133.
(924) Sato, H.; Sakaki, S. *J. Phys. Chem. A* **2004**, *108*, 1629.
(925) Sato, H.; Kovalenko, A.; Hirata, F. *J. Chem. Phys.* **2000**, *112*, 9463.
(926) Yamazaki, T.; Sato, H.; Hirata, F. *Chem. Phys. Lett.* **2000**, *325*, 668.
(927) Yamazaki, T.; Sato, H.; Hirata, F. *J. Chem. Phys.* **2001**, *115*, 8949.
(928) Sato, H.; Kobori, Y.; Tero-Kubota, S.; Hirata, F. *J. Chem. Phys.* **2003**, *119*, 2753.
(929) Sato, H.; Kobori, Y.; Tero-Kubota, S.; Hirata, F. *J. Phys. Chem. B* **2004**, *108*, 11709.
(930) Yoshida, N.; Kato, S. *J. Chem. Phys.* **2000**, *113*, 4974.
(931) Yamazaki, T.; Sato, H.; Hirata, F. *J. Chem. Phys.* **2003**, *119*, 6663.

(932) Coitino, E. L.; Tomasi, J.; Ventura, O. N. *J. Chem. Soc., Faraday Trans.* **1994**, *90*, 1745.
(933) Tomasi, J.; Cammi, R.; Mennucci, B. *Int. J. Quantum Chem.* **1999**, *75*, 783.
(934) Tomasi, J.; Cammi, R.; Mennucci, B.; Cappelli, C.; Corni, S. *Phys. Chem. Chem. Phys.* **2002**, *4*, 5697.
(935) Cammi, R.; Mennucci, B.; Tomasi, J. Computational Modelling of the Solvent Effects on Molecular Properties: An Overview of the Polarizable Continuum Model (PCM) Approach. In *Computational Chemistry: Reviews of Current Trends*; Leszczynski, J., Ed.; World Scientific: Singapore, 2003; Vol. 8.
(936) Cimiraglia, R.; Miertus, S.; Tomasi, J. *Chem. Phys. Lett.* **1981**, *80*, 286.